Quantifying isoprene and monoterpenes in the remote marine environment

Sina Corinna Hackenberg

PhD

University of York

Chemistry

September 2015

Abstract

Measurements of isoprene and six monoterpenes (α- and β-pinene, myrcene, δ3-carene, ocimene and limonene) were made during research cruises in the Atlantic Ocean and Arctic (80 °N - 50 °S). The trace gas species were quantified in the surface ocean, in depth profiles and in the marine boundary layer (MBL).

Atmospheric mixing ratios of the analytes were typically below the detection limit (DL) to a few pptv over the Atlantic and mostly <DL (sub-pptv) in the Arctic, after careful quality control to exclude influence from contaminated air. Isoprene mixing ratios were similar to published observations in oligotrophic regions, but monoterpene levels much lower than previously reported. It is unclear whether this discrepancy is caused by sampling over lower-productivity waters, or by analytical differences including potential contamination.

Isoprene concentrations in the surface ocean varied from *ca.* 1 to 70 pmol L^{-1}, similar to the majority of previous studies, and correlated reasonably with several supporting biological parameters available for the cruises. Chlorophyll-a, various pigments including photoprotective carotenoids and Fucoxanthin, cyanobacterial cell counts and primary production yielded significant linear regressions (with R^2 = 0.4 - 0.6), which improved when separated into two temperature regimes with a threshold at 20 °C.

Monoterpene concentrations in seawater are reported for the first time, varying from <DL (sub-pmol L^{-1}) to up to several pmol L^{-1} with no clear trends or relationships with biological data. The monoterpene generally showing the highest levels in water and air was limonene; however this was attributed mostly to contamination.

The impacts of emissions derived from this new data on global atmospheric chemistry and secondary organic aerosol formation in the MBL were estimated to be small in light of recent literature and previously published marine terpene data; however they may play a role in nucleation processes as recently suggested, even at low concentrations.

Contents

List of Figures

List of Tables

Acknowledgements

First of all, I would like to thank my supervisors Lucy Carpenter and Ally Lewis who have made this PhD possible and supported me through it – I have learned so much and really enjoyed it, and you have given me the opportunity to be involved in some very interesting science in amazing environments.

Of course, a huge thanks to Steve who was always there to patiently help, explain and encourage, and for the discussions to find solutions for all those issues that are invariably part of a scientific research project. Thank you also to Rosie for *always* being happy to listen and help, with both theoretical and practical problems. Jamie, for his cruise work and generally being cheerful.

The atmospheric research group as a whole are great to work with and I have very much appreciated their positive attitude, willingness to help one another and ability have fun.

I would like to thank the crew and scientists involved in my ship campaigns, especially the friends I made on the cruises, for making them possible, interesting and simply brilliant.

Finally, I am very grateful to all my friends and family, who have encouraged me throughout and let me spend a lot of time on my project (and not always enough with them) without complaining too much.

Declaration

The research described in this thesis is original work, which I undertook at the University of York during 2011-2015 and which has not been presented for a research degree at this or any other university. Except where stated and with the exceptions stated explicitly below, all of the work contained within this thesis represents the original contribution of the author. All sources are acknowledged as references.

Water sampling tasks on ACCACIA 2 were shared between myself, Stephen Andrews, Rosie Chance and Lucy Carpenter, and between myself and Jamie Minaeian on AMT 23. I was responsible for the general instrument operation during the cruises except for half of ACCACIA 2, when responsibility was shared with Stephen Andrews. Stephen Andrews performed all practical work during ACCACIA 1. All subsequent hydrocarbon data analysis was performed by myself.

Some aspects of work described in this thesis have been published in (also listed at the beginning of chapter 2, to which it relates):

Andrews, S. J., Hackenberg, S. C., and Carpenter, L. J.: Technical Note: A fully automated purge and trap GC-MS system for quantifcation of volatile organic compound (VOC) fluxes between the ocean and atmosphere, Ocean Science, 11, 313-321, doi: 10.5194/os-11-313-2015.

I contributed to the development of the system that was designed and built by S. Andrews, and provided data for the described performance characteristics.

This study was supported by the UK Natural Environment Research Council National Capability funding to Plymouth Marine Laboratory and the National Oceanography Centre, Southampton. This a contribution of the AMT programme.

Chapter 1

Introduction

This introductory chapter will explore various aspects of the systems and processes that govern the atmospheric and oceanic abundances of isoprene and monoterpenes. It includes an overview of terrestrial production and emissions of isoprene and monoterpenes, which is a much more established research area than oceanic production; atmospheric reactions, including aerosol formation and the consequent impact on clouds and climate; oceanic emissions of volatile organic compounds and their potential to impact marine organic aerosol; and a description of the current models and approaches used to estimate global marine isoprene emissions. Finally, an overview of the aims of this thesis is presented.

1.1 Background

Isoprene (C_5H_8) is one of the most extensively studied volatile organic compounds (VOCs) in the atmosphere, constituting approximately one third of the global VOC emissions (biogenic and anthropogenic) or half of the total biogenic non-methane hydrocarbon (NMHC) emissions (Guenther et al., 2012). Estimates of the global source strength converge around 500 Tg yr^{-1} (Arneth et al., 2008; Guenther et al., 2012, and references therein), but range from 350 to 800 Tg yr^{-1} as there are still substantial uncertainties associated with these results due to uncertainties in landscape types, meteorological drivers and model algorithms in addition to uncertainties in biogenic VOC (BVOC) emissions (Guenther et al., 2012). Arneth et al. (2008) even argue that there may be a false sense of having reached a point at which understanding of the system is sufficient for models to converge, when this is in fact achieved by most schemes being based on the same parameterisations. The importance of isoprene for atmospheric chemistry is well established: it is highly reactive due to its two double bonds and can affect the oxidative capacity of the atmosphere as well as contribute to secondary organic aerosol (SOA) formation (discussed in detail in section 1.3), thus also influencing air quality and climate (Carlton et al., 2009).

Monoterpenes ($C_{10}H_{16}$) are also emitted at significant levels from nature, accounting for around 15 % of the global BVOC emissions, however with estimates ranging from 32 to 177 Tg yr^{-1} (Guenther et al., 2012). Their reactivity is much higher than that of isoprene and atmospheric oxidation results in significantly higher SOA yields, albeit with considerable variations between the different monoterpenes (see section 1.3). The large SOA formation potential also leads to substantial impacts on air quality and climate, but with extensive uncertainties associated with the distribution and magnitude of these effects (Goldstein and Galbally, 2007; Hallquist et al., 2009).

While much research has focused on the terrestrial environment due to its large source strength for BVOCs, recent studies suggest that isoprene and monoterpene emissions from the ocean may also play a significant role in the global atmospheric chemistry (Shaw et al., 2010, and references therein; sections 1.6 and 1.7).

1.2 Terrestrial terpenoids

Isoprene emission from plants was first discovered in the 1950s by Sanadze and Kursunov, who also showed a light and temperature dependence in their measurements early on, and independently around the same time by Rasmussen and Went, but it was not accepted for some time that the observed species was indeed isoprene (Sanadze, 2004; Sharkey and Yeh, 2001, and references therein). It was known that the so-called isoprenoids (or terpenoids, as they were originally produced by heating turpentine) were made up of isoprene units, i.e. C_5H_8 ("isoprene rule"), but they are not in fact made from isoprene itself. Initially, some researchers believed isoprene did not occur in nature in its "free" form because it was not an intermediate in terpene production and had low atmospheric concentrations (Sharkey and Yeh, 2001; Sanadze, 2004).

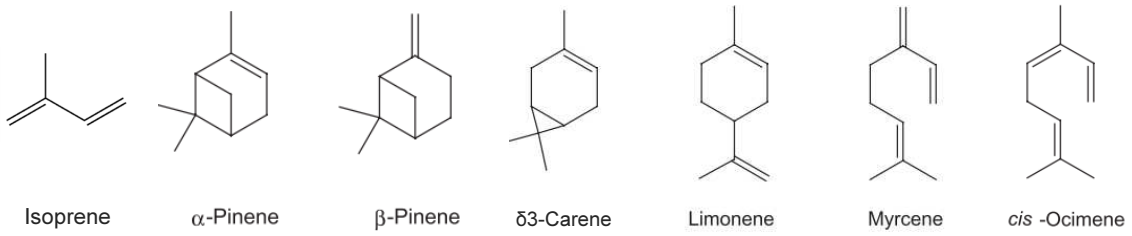

Figure 1.1 – Structures of isoprene and monoterpenes studied during this project.

Monoterpene emissions were noted for the first time by Went (1960) who attributed observed blue hazes in forested areas to these biogenic compounds (this was also the first indication of their aerosol formation potential, see section 1.3). Monoterpenes are a diverse range of compounds including acyclic, mono- and bi-cyclic isomers with one or more C-C double bonds that may be exo- or endocyclic (outside or inside a ring structure, respectively). Oxygenated monoterpenes are also often referred to as monoterpenes, but do not strictly belong to this group due to their different molecular formula.

An understanding of the biological, evolutionary and biochemical backgrounds of terpenoid emission is relevant to atmospheric chemistry, as it is necessary in order to correctly represent these processes in emission parameterisations required for larger-scale chemical transport models, or even to make more accurate predictions regarding the future development of emissions in climate models (e.g. Harrison et al., 2013).

1.2.1 Biosynthesis

Isoprene is made inside chloroplasts from its precursor DMAPP (dimethylallyl pyrophosphate), which comes from the MEP (2-methylerythritol 4-phosphate) pathway, by the enzyme isoprene synthase (IspS; schematic biosynthetic pathway shown in Figure 1.2; Sharkey and Yeh (2001) and references therein). It is now generally accepted that the mevalonic acid (MVA) pathway is not involved in isoprene biosynthesis (Sharkey and Yeh, 2001; Lichtenthaler, 2009). Plants without the *IspS* gene do not emit isoprene, and various studies, including genetic modification of some species to express the gene, have been able to link IspS activity to isoprene emission and benefits to the plant attributed to isoprene emission (Sharkey et al., 2008, and references therein). Monoterpenes are made by a monoterpene synthase via geranyl pyrophosphate (GPP) from the same pathway by adding an IPP (isopentenyl pyrophosphate, an isomer of DMAPP) unit to DMAPP (Figure 1.2). The MEP pathway is also responsible for the synthesis of many of the compounds vital to plant life (function and reproduction) such as hormones (C_{20} and C_{30}) and carotenoids (C_{40}, including photosynthetic pigments), termed "essential" isoprenoids (Owen and Peñuelas, 2005).

Isoprene and monoterpenes are produced using typically around 2-5 % of the carbon fixed by photosynthesis, but isoprene production can account for up to 50 % under stress, when photosynthesis is reduced while isoprene emission as a stress response remains constant (Harrison et al., 2013; Loreto and Fineschi, 2015; see section 1.2.2 below for the role of isoprene emission in abiotic stress response). Carbon can also be obtained from other sources, often in higher proportions if that available from *de novo* photosynthesis becomes limited; this may however not be unique to isoprene synthesis (Vickers et al., 2009; Sharkey et al., 2008; and references therein). Isoprene is emitted from the leaf almost instantaneously upon formation (unlike most monoterpenes, which are stored in the plant), and as a consequence of its synthetic pathway, isoprene emission is regulated by a number of factors that affect IspS and the MEP pathway, including temperature and available energy and carbon (Sharkey et al., 2008). It is not controlled by the stomatal conductance, as the emission is determined by the gradient between the isoprene mixing ratio in the intercellular air space of the leaf and that in ambient air as well as the stomatal conductance, so that a decrease in conductance is quickly balanced by a change in the concentration gradient (Niinemets et al., 2014, and references therein). A number of monoterpenes behave in an identical

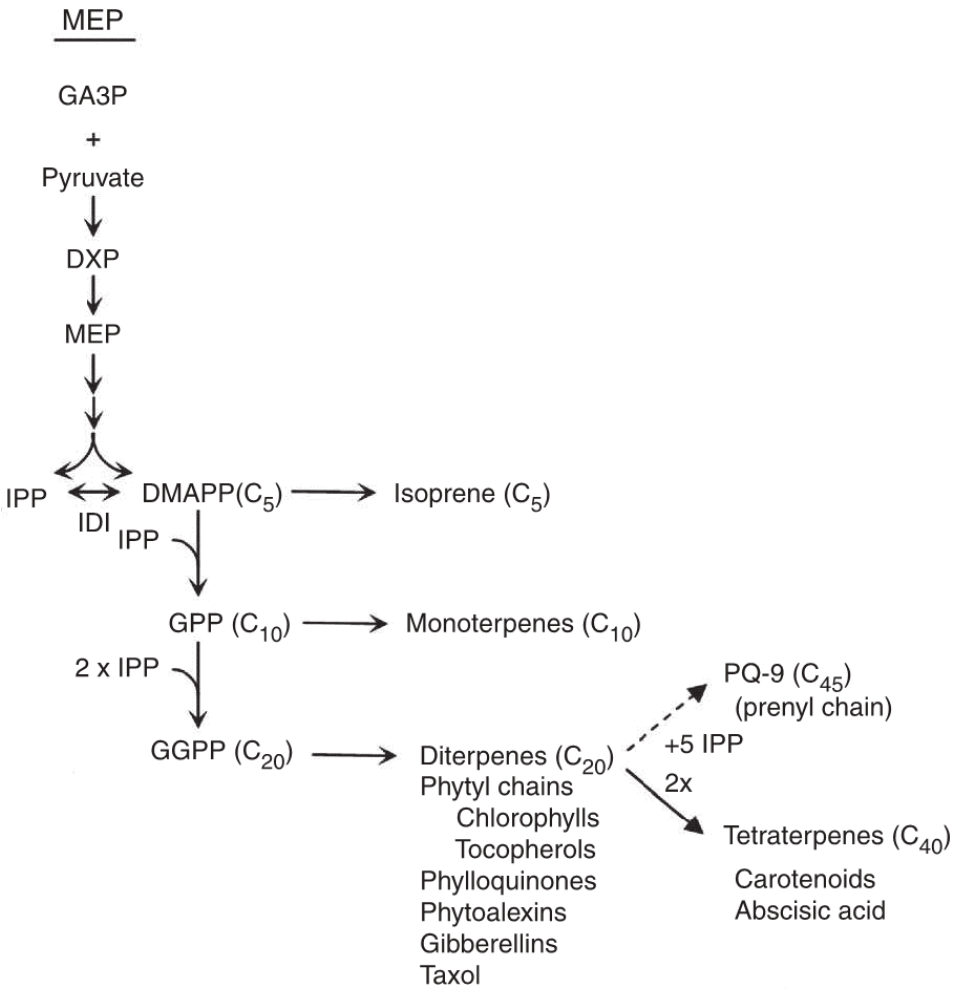

Figure 1.2 – Isoprenoid biosynthetic pathway in the chloroplast. MEP = 2-methylerythritol 4-phosphate, GA3P = glyceraldehyde 3-phosphate, DXP = 1-deoxy-D-xylulose 5-phosphate, IPP = isopentenyl pyrophosphate, DMAPP = dimethylallyl pyrophosphate, IDI = isopentyl pyrophosphate isomerase, GPP = geranyl pyrophosphate, GGPP = geranylgeranyl pyrophosphate, PQ = plastoquinone. Adapted from Vickers et al. (2009).

fashion (immediate emission), while others are stored in various parts of the plant and emitted as a result of warming or mechanical stress at other times (Harrison et al., 2013).

1.2.2 Functions

It has been argued by many authors (e.g. Pichersky et al., 2006; Vickers et al., 2009) that volatile terpenoid emission very probably confers benefits to the emitting plant, simply because it is unlikely that such a costly (in terms of carbon and energy) process would not be lost through evolution otherwise. However, the exact nature (and existence) of those benefits has been the subject of a wide range of research and, despite recent advances, remains to be conclusively determined.

Isoprene has been shown over the last few years to have a number of functions that increasingly appear to be the results of a single mechanism (Vickers et al., 2009). Light and temperature dependence were observed in the first studies of biogenic isoprene emission in the 1950s by Sanadze and co-workers (Sanadze, 2004; Sharkey and Yeh, 2001), and thermotolerance has been discussed as one of its main benefits (Sharkey et al., 2008). Due to the difficulties in accurately measuring leaf temperature, the hypothesis could not be supported until the large fluctuations (up to >10 °C) in the temperature environment of leaves due to heat flecks could be determined several years later (Sharkey et al., 2008, and references therein), indicating a need for leaves to regulate their temperature. More targeted experiments resulting from these findings, including specific enzyme inhibition and genetic modifications, showed that the ability to emit isoprene conveyed thermoprotection to the tested species (Sharkey and Yeh, 2001; Velikova and Loreto, 2005).

A further role of isoprene emission has been identified in the protection of plants from reactive oxygen species (ROS) such as ozone, singlet oxygen, superoxide, hydrogen peroxide and hydroxyl radicals (Vickers et al., 2009; Sharkey et al., 2008; and references therein). These species act as signalling molecules and can initiate defence responses; they are normally closely controlled within cells, but this careful balance can be upset by stresses. The production of ROS species is a common response to various types of stress and can cause direct and indirect damage to cells, going as far as programmed cell death (Vickers et al., 2009, and references therein). When the complex antioxidant defence network of a plant can no longer cope with the level of ROS, it experiences oxidative stress. A variety of

compounds and enzymes form this network, including non-volatile isoprenoids, and Vickers et al. (2009) propose that volatile isoprenoids such as isoprene and monoterpenes are also a part of the non-enzymatic antioxidant defence network, by a number of mechanisms (see Vickers et al. (2009) Figure 5 for details).

Several other suggestions have been made regarding isoprene emissions, most of which have been dismissed more recently due to emerging evidence; for example, it is now regarded as highly unlikely by some authors that isoprene may act as a "safety valve" for excess energy, metabolites or carbon on the basis of stoichiometric and biochemical arguments (Vickers et al., 2009; Sharkey et al., 2008; and references therein). In contrast, Lichtenthaler (2009) still proposes a "safety valve" function through which volatile isoprenoid synthesis could protect the photosynthetic system by maintaining its activity under heat and light stress, in a similar way to the continuous *de novo* synthesis of carotenoids.

Monoterpenes have been found to have a large variety of functions in plants, ranging from thermoprotection or general protection against oxidative stress (like isoprene; Vickers et al., 2009; Velikova et al., 2012) and response to insect or herbivore attack to acting as infochemicals and attracting enemies of attackers (e.g. Kesselmeier and Staudt, 1999; Owen and Peñuelas, 2005; Pichersky et al., 2006). Emissions from plants that store monoterpenes in specialised organs depend on temperature as the volatility of the terpenes determines when they can be emitted. It is believed that replacing isoprene emission with monoterpene emission could be a more efficient response for plants in environments with long-term stresses (Harrison et al., 2013; Dani et al., 2014), as most species emit either only isoprene or monoterpenes at any one time (Harrison et al., 2013).

The fact that not all plants emit isoprene and/or monoterpenes (only ca. 20 % of all plants emit isoprene; Loreto and Fineschi, 2015) suggests that neither are vital to plant survival and reproduction (Owen and Peñuelas, 2005). In combination with the common pathway for essential and volatile isoprenoids, this has led to some debate regarding the function and evolutionary benefits of the emission of "non-essential" isoprenoids (Pichersky et al., 2006; Owen and Peñuelas, 2005; Sharkey et al., 2008; Loreto and Fineschi, 2015) which has not yet reached a conclusion regarding the "opportunist hypothesis" put forward by Owen and Peñuelas (2005). There appears to be general agreement that isoprene production does take advantage of a pathway necessary to the synthesis of many other important compounds (the MEP pathway), but not to what extent the isoprene emission rate is

determined by the need to produce longer-chain isoprenoids, as apparently contrasting experimental evidence and mechanistic arguments exist (Sharkey et al., 2008; Loreto and Fineschi, 2015). Similarly, there is an ongoing discussion concerning the evolution of isoprene emission, with suggestions including a single evolutionary event (single gain) with multiple losses (e.g. Sharkey et al., 2013; Sharkey, 2013) and multiple gains and multiple losses (e.g. Sharkey et al., 2008; Monson et al., 2013; Dani et al., 2014), and separate evolution in mosses and ferns that lack the gene family needed to produce isoprene in higher plants (Loreto and Fineschi, 2015).

1.3 Aerosols from volatile isoprenoids

Aerosols affect the Earth's climate directly by scattering and absorbing incoming radiation or indirectly by modifying the number and properties of cloud condensation nuclei which in turn affects the properties of clouds (IPCC 2013). They can be primary particles such as primary organic aerosols (POA), dust, sea salt and black carbon, or secondary particles (either inorganic or secondary organic aerosol (SOA)). SOA is typically derived from VOCs that may be of biogenic or anthropogenic origin, with a general consensus that the terrestrial biosphere is contributing the largest proportion (e.g. Andreae and Rosenfeld, 2008).

Aerosol from natural sources was first reported in the literature by Went (1960) who attributed the blue haze observed in many densely forested areas to terpenes in the air which formed fine particles that reflected blue light, further accumulating to larger particles that let the haze appear brown/grey later in the day. VOC gas-phase photochemistry and impacts of the aerosols on tropospheric ozone pollution and regional air quality were main drivers of the initial research (Hoffmann and Warnke, 2007; Fehsenfeld et al., 1992, and references therein) and are still important in more recent studies, now alongside the aim to increase our understanding of atmospheric processes in relation to human health and generally in order to be able to model climate and project future developments more accurately (Hoffmann and Warnke, 2007). Monoterpenes form low-volatility products from fast reactions with ozone (O_3) and hydroxyl (OH) and nitrate radicals (NO_3) and are well established as SOA precursors (Hoffmann and Warnke, 2007, and references therein). Isoprene has been more recently recognised as a source of SOA (Claeys et al.,

2004) and important on a global scale due to the large biogenic isoprene source strength, despite much smaller aerosol yields compared to monoterpenes (see Chapter 5 Table 5.2; Henze and Seinfeld, 2006; Andreae and Rosenfeld, 2008; Carlton et al., 2009). Although its first-generation products such as methyl vinyl ketone (MVK) or methacrolein (MACR) are too volatile to form aerosol, further oxidation steps can explain the SOA observed in more recent studies (Carlton et al., 2009, and references therein). Henze and Seinfeld (2006) reported an increase in global SOA burden by a factor of two when isoprene SOA was included in a global model at ca. 3 % yield from photooxidation. There may even be evidence for significantly higher SOA yields from isoprene oxidation under certain conditions (acid-catalysed particle phase reactions accounting for yields up to >28 %; Surratt et al., 2010).

1.3.1 Oxidation mechanisms

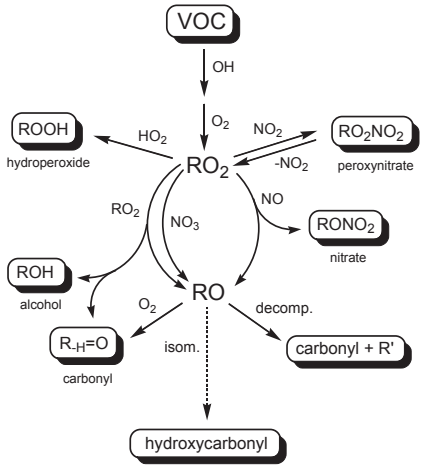

Figure 1.3 – Generic VOC photooxidation scheme (taken from Hallquist et al., 2009). The initial photooxidation step leads to formation of an alkyl radical by H-atom abstraction or radical addition.

High concentrations of VOCs lead to a decrease in the oxidising capacity of the atmosphere by removing OH (illustrated by a generic reaction scheme in Figure 1.3), which is then no longer available to oxidise methane, resulting in an increased lifetime of this greenhouse gas and hence an indirect effect on climate (e.g. Collins et al., 2002). Recent reaction schemes of isoprene photooxidation propose some recycling of OH radicals, but there is significant uncertainty regarding the magnitude of this process (see also section 1.3.2). Furthermore,

VOC oxidation reactions have implications for air quality (photochemical air pollution), as ozone is produced during VOC photooxidation under high-NO_x conditions (Fehsenfeld et al., 1992; Atkinson and Arey, 2003; Zeng et al., 2008). The formation occurs as a result of the reaction of alkyl peroxy or hydroperoxy radicals with NO and subsequent photolysis of NO_2:

$$RO_2^{\cdot} + NO \longrightarrow RO^{\cdot} + NO_2 \tag{1.1}$$

$$HO_2 + NO \longrightarrow OH + NO_2 \tag{1.2}$$

$$NO_2 + h\nu \longrightarrow NO + O(^3P) \tag{1.3}$$

$$O(^3P) + O_2 + M \longrightarrow O_3 + M \tag{1.4}$$

Terpene reactions can also lead to the formation of OH radicals during ozonolysis, which constitutes an additional source of OH including at night when photolytically generated OH radical concentrations are very low (Atkinson and Arey, 2003, and references therein).

More specifically, a simplified reaction scheme of isoprene atmospheric oxidation reactions is shown in Figure 1.4a, illustrating the main products and pathways. In fact, the processes are far more complex: including multi-generation reactions, the complete degradation of isoprene is represented in the most recent update of the Master Chemical Mechanism (MCM) by almost 2000 reactions (Jenkin et al., 2015). There are still a number of global climate models that do not account for isoprene at all in their treatment of organic aerosol (Carlton et al., 2009; Tsigaridis et al., 2014).

Monoterpene reactions (a simplified reaction scheme of myrcene ozonolysis is displayed in Figure 1.4b as an example) are not represented in models to the same level; for example, only α- and β-pinene and limonene are included in the MCM at all (http://mcm.leeds.ac.uk/MCM, accessed Sept 2015) and global models often treat all monoterpenes as one species (either represented by α-pinene or lumped into a single surrogate species; Tsigaridis et al., 2014). This is due to a lack of knowledge of specific multi-generation reactions, products and yields for most of these compounds and, perhaps more importantly, to the complexity of their possible reactions – an attempt to balance accuracy and simplicity in global chemistry climate models (Hallquist et al., 2009; Tsigaridis et al., 2014). However, it has been noted by a number of authors that this may not be adequate in view of large differences in reactivity between monoterpene species. For instance, chamber studies conducted on monoterpene oxidation by NO_3 radicals by Hal-

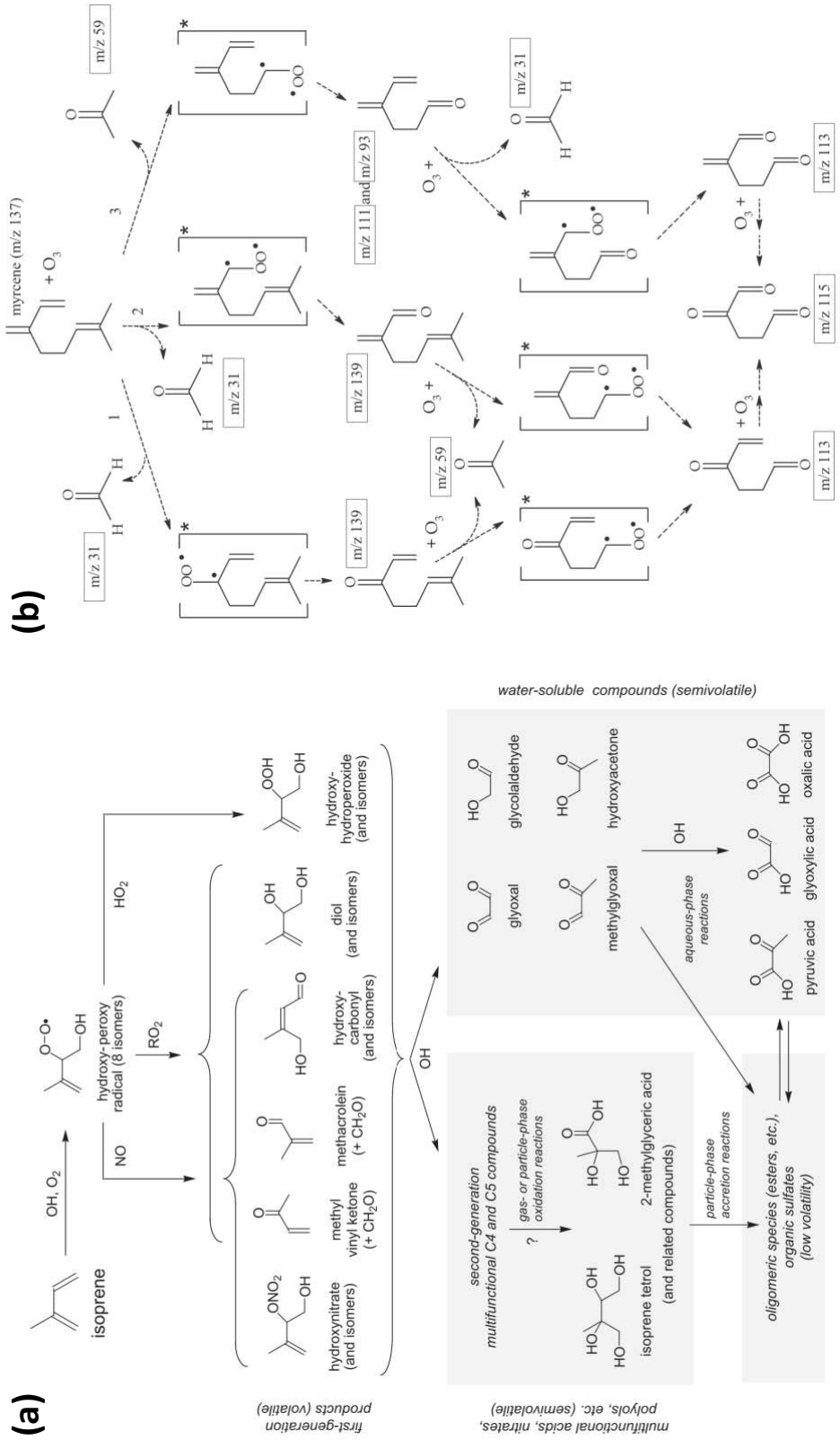

Figure 1.4 – (a) Isoprene reaction scheme illustrating SOA formation pathways from photooxidation (taken from Carlton et al., 2009); (b) example monoterpene reaction scheme: partial mechanisms and proposed structures in myrcene ozonolysis (taken from Lee et al., 2006a).

lquist and co-workers (Hallquist et al., 1999) already highlighted the need for speciation of monoterpenes to accurately represent their widely different characteristics (in terms of both gas-phase partitioning and products); similarly, Jardine et al. (2015) emphasise the importance of speciated measurements and subsequent treatment in Earth system models in order to understand impacts of monoterpenes on aerosols, clouds and BVOC production.

1.3.2 Additional processes

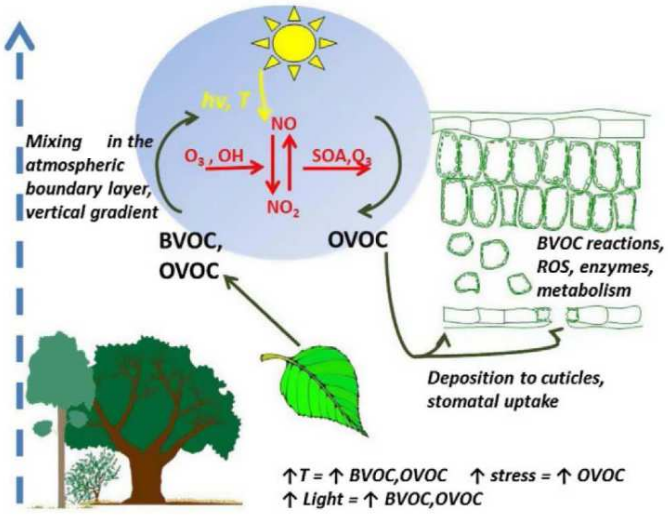

Figure 1.5 – Schematic illustrating bidirectional fluxes and oxidation processes of BVOCs and oxygenated VOCs; details see text (atmosphere-ecosystem exchange dynamics, modified from Niinemets et al., 2014).

Chamber studies cannot replicate all mechanisms of SOA formation that may occur in the natural environment; this is desirable in order to elucidate individual processes that could not be studied in the complex matrix of the atmosphere, but at the same time limits the applicability of the results to nature. For example, the amount and nature of any pre-existing aerosol or competition for atmospheric oxidants with other gas-phase compounds could significantly alter the terpene SOA yield potential. A recent study by Kiendler-Scharr and co-workers (2009) showed that in the presence of isoprene, the SOA from monoterpenes was substantially reduced; the authors deduced that the fast reaction of isoprene with OH in combination with its low SOA yield was partially preventing photooxidation of the terpenes at higher SOA yields, decreasing the overall SOA formation in the system.

Understanding of the processes in aerosol formation and their effects on atmospheric chemistry is further complicated by recent reports of bi-directional fluxes of BVOCs, i.e. plants not only emitting but also taking up organic compounds including oxygenated species (Figure 1.5; Niinemets et al., 2014), and of oxidation reactions taking place *in planta* (within leaves of the emitting plant/ in or on leaves of other plants within the canopy; Jardine et al., 2012, 2013; Niinemets et al., 2014; and references therein). Within-leaf oxidation of volatile isoprenoids prior to emission is also consistent with the antioxidant mechanism for abiotic stress protection proposed by Vickers et al. (2009). Uptake is determined by the relative mixing ratios within the leaves and in ambient air (could also be a combination of emitting and non-emitting plant species), which are in turn dependent on the rate of production of the VOC and a complex combination of various environmental factors (at plant, canopy and even ecosystem scale; Niinemets et al. (2014) and references therein). Bidirectional fluxes are already partially accounted for in some of the latest BVOC emission models (e.g. MEGAN2.1; Guenther et al., 2012) and could have impacts on model SOA and tropospheric ozone and OH concentrations (Karl et al., 2010).

The emission of isoprene oxidation products such as MVK and MACR rather than isoprene could mean that the OH loss over remote forested (isoprene-rich) areas like the Amazon basin is in fact overpredicted because observed oxidation products are attributed to atmospheric oxidation rather than primary emission. As a result, expected OH concentrations ([OH]) from chemistry transport models would appear too low compared to measured concentrations, which has led to the inclusion of OH recycling mechanisms in isoprene oxidation schemes (Jardine et al., 2012; Peeters et al., 2014). While the suggestion put forward by Jardine et al. (2012) may help to close gaps in modelled *versus* measured [OH], it should nevertheless be considered that the argument depends on the magnitude of within-plant compared to atmospheric oxidation, and that evidence from both theoretical and chamber studies supports the OH recycling mechanisms at least in principle (Peeters et al., 2014). However, the authors do highlight the need for further research, and a combination of the two approaches may bring estimated and observed [OH] into closer agreement than previously achieved even including OH recycling (Peeters et al., 2014, and references therein).

1.4 Clouds and climate

Regardless of the exact mechanisms involved in SOA formation or its molecular composition, which will clearly continue to be the subject of active research, aerosols in general are known to affect the properties of clouds by modifying the number of particles that can act as cloud condensation nuclei (CCN), as already mentioned above (e.g. Boucher et al., 2013, and references therein). Whether particles act as CCN depends on their size and chemical composition in a complex fashion, with soluble compounds contributing to the CCN activation properties. Aerosol-cloud interactions are still one of the most uncertain contributions to effective radiative forcing (low confidence level) in the most recent IPCC assessment report (Myhre et al., 2013; Figure 1.6a) due to a combination of a medium amount of evidence with a low level of agreement. One of the reasons for this large error bar is the lack of understanding of aerosol-related processes in an unpolluted (pre-industrial) atmosphere that would be required to model the reference conditions. Several recent publications (e.g. Meskhidze et al., 2011; Andreae, 2007; Andreae and Rosenfeld, 2008; Carslaw et al., 2013; Rosenfeld et al., 2014; Koren et al., 2014) emphasise the need to understand the numbers and composition of aerosols in pristine environments in order to be able to predict the effects of anthropogenic influences and better constrain future developments.

The IPCC report summarises advances made in understanding of aerosol-cloud interactions since the previous report in 2007, which indicate that the system is subject to more complex processes than the simple cloud albedo effect (Boucher et al., 2013; Rosenfeld et al., 2014). Albedo describes the fraction of incoming solar radiation that is reflected back into space by a surface, with bright surfaces reflecting almost all of the light (e.g. snow has an albedo of ca. 0.9; marine stratiform clouds around 0.4; Bender et al., 2011) and dark surfaces absorbing most of the radiation (ocean albedo can be as low as 0.1). The cloud albedo effect (or Twomey effect; Twomey, 1977) is responsible for an increase in the albedo of liquid clouds through an increase in the cloud droplet number concentration (CDNC) and resulting decrease in droplet size, which in turn are the result of an increased aerosol number concentration (Boucher et al., 2013; Figure 1.6b). Despite the uncertainties in combined effects and more detailed processes documented by recent advances, the basis of the albedo effect remains applicable; especially in clean atmospheres

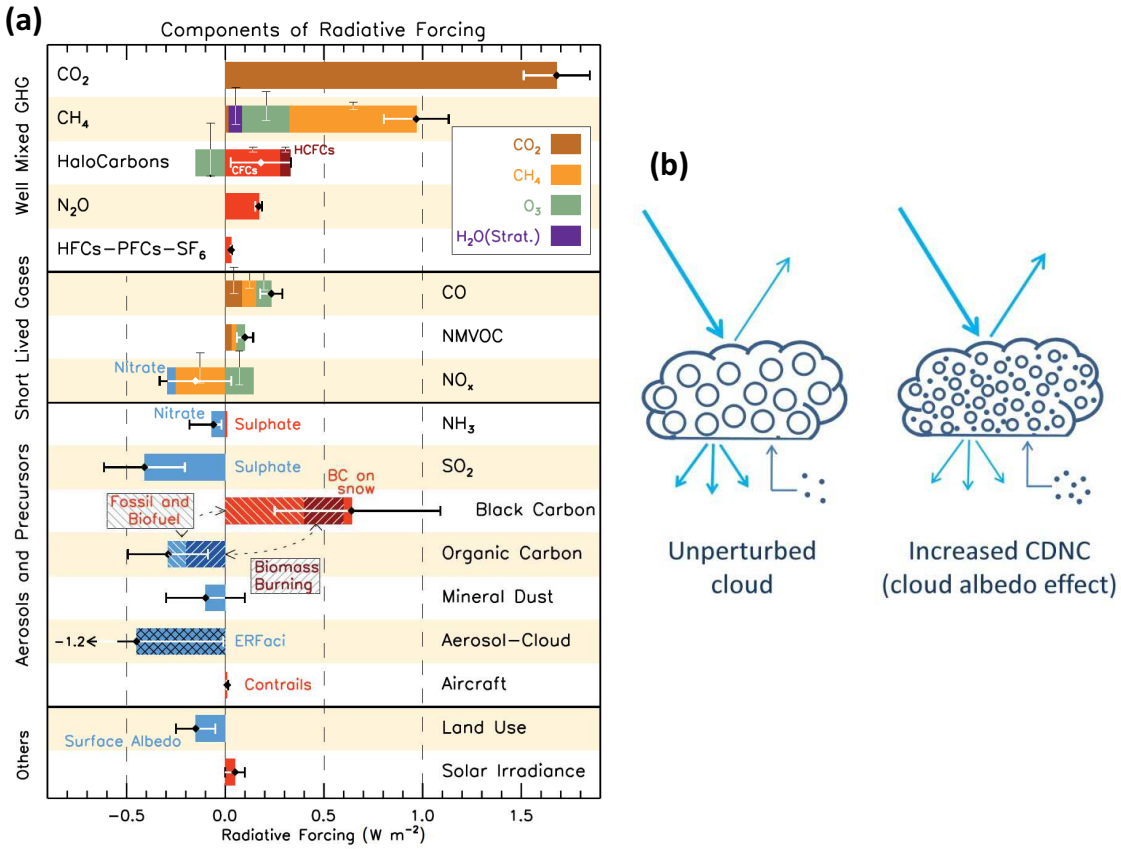

Figure 1.6 – (a) Contributions to radiative forcing (Myhre et al., 2013); (b) schematic of cloud albedo effect, which forms part of the effective radiative forcing from aerosol-cloud interactions (ERFaci) shown in (a); open circles represent cloud droplets, dots represent aerosol particles, CDNC = cloud droplet number concentration (modified from Haywood and Boucher, 2000).

(low aerosol loading), there is a near-linear effect of aerosol on cloud albedo, while higher aerosol concentrations tend to lead to saturation of the CDNC and a suppression of the activation of further aerosol particles (Boucher et al., 2013; Carslaw et al., 2013). Thus, clouds are most sensitive to changes in aerosol loading in a clean background such as the pristine open ocean (Koren et al., 2014), where changes in albedo could also potentially occur over a large surface area and hence impact global climate, leading to a significant role of aerosol-cloud interactions in the remote marine environment.

1.4.1 Feedbacks

One of the main foci of interdisciplinary research into aerosol-cloud interactions in the last two decades has been the feedback effects of ecosystems with clouds and hence climate, sparked by the so-called CLAW hypothesis (Charlson et al., 1987). The authors suggested a negative feedback loop between ocean biological productivity and climate via the emission of dimethyl sulfide (DMS) by phytoplankton that is oxidised in the atmosphere, so that an increased biological production would result in an increase in (sulfate) aerosol and hence CCN and cloud albedo, which in turn would lead to a climate cooling effect and cause a reduction in the biological activity (see Figure 1.7). The hypothesis is arguably responsible for DMS being the most extensively studied oceanic trace gas (Carpenter et al., 2012). It has resulted in considerable scientific debate based on evidence emerging over time which has highlighted many shortcomings of the initial feedback mechanism, discovered additional complexity linked to other ocean/climate feedbacks and greatly improved our understanding of many ocean-atmosphere-climate system interactions (e.g. SOLAS 2015-2025: Science Plan and Organisation, 2015), but so far not come to a generally accepted conclusion regarding the original proposition (e.g. Ayers and Cainey, 2007; von Glasow, 2007; Quinn and Bates, 2011; Krüger and Graßl, 2011).

The more recent debate about isoprene as a potential source of marine SOA and thus CCN is also a result of the CLAW hypothesis, following a similar idea of oxidised plankton emissions affecting climate, similarly not being universally accepted due to limited evidence (Meskhidze and Nenes, 2006; Miller and Yuter, 2008; Meskhidze and Nenes, 2010), and often cited as an additional explanation of observed relationships that cannot be (fully) explained by DMS (Ayers and Cainey, 2007; Leck and Bigg, 2007; Spracklen et al., 2008; Arnold et al., 2009; Gantt et al., 2009; Meskhidze and Nenes, 2010). Meskhidze and Nenes

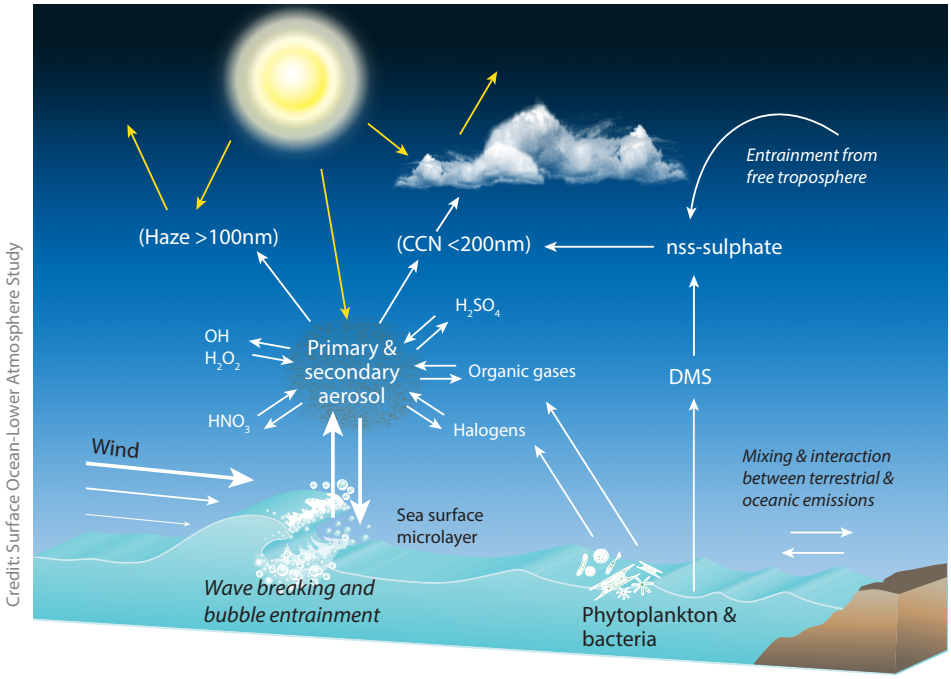

Figure 1.7 – Sources and production mechanisms for CCN in the remote MBL. Reproduced from Law et al. (2013).

(2006) described a correlation between an observed decrease in cloud droplet effective radius above the Southern Ocean and enhanced biological activity in the sea below. They argued that this must be the result of organic compounds emitted by the phytoplankton, specifically isoprene, that were oxidised in the marine boundary layer and contributed to the number of CCN and therefore cloud droplets, leading to a decrease in their effective radius. Their estimates of isoprene emissions were based on previously published isoprene-Chl-*a* relationships (Wingenter et al. 2004) and were corrected significantly downwards in response to a letter by Wingenter (2007); however, in their response, Meskhidze and Nenes (2007) maintained that their conclusions remained valid. Miller and Yuter (2008) performed a similar analysis of satellite data over regions of phytoplankton blooms and proceeded to show that the correlation between Chl-*a* and cloud effective radius found by Meskhidze and Nenes (2006) was a coincidence, since no other region showed a similar relationship. A further publication by Meskhidze and Nenes (2010) supports their initial findings, obtaining positive relationship for Chl-*a* and isoprene when they applied a modified methodology to a number of locations in the Southern Ocean. They argued that there were continental influences in the regions chosen by Miller and Yuter (2008) which made marine controls hard to extract, and that their own improved methodology

was better suited for the analysis (larger grid cell size and exclusion of non-marine biogenic influences). No further investigations into this particular topic have been reported, but research focusing on the relative contribution of isoprene emissions and marine organic carbon to aerosol and CCN (details in section 1.7.1) does not appear to sustain the suggestion that isoprene could be responsible for large numbers of CCN (Spracklen et al., 2008; Arnold et al., 2009).

1.5 Oceans

The oceans cover approximately 70 % of the earth's surface and are intricately linked with other earth systems such as the terrestrial biosphere and the atmosphere *via* feedback mechanisms, as well as being strongly affected by climate change, including ocean acidification and global warming (e.g. Doney, 2010). To be able to better understand and characterise these interactions and effects, research related to the oceans has become increasingly interdisciplinary (e.g. SOLAS 2015-2025: Science Plan and Organisation, 2015).

The world's oceans can be divided into eutrophic and oligotrophic regions (high and low biological productivity, respectively), which are determined mainly by nutrient availability, that is in turn controlled by a combination of ocean currents and atmospheric deposition.

The large-scale ocean current system is dominated by the meridional overturning circulation (MOC) which affects all ocean basins and is driven by differences in temperature and salinity and by wind (Figure 1.8). Dense cold and salty water sinks at high latitudes (deep water formation) in the Northern Hemisphere due to open-ocean deep-water convection, and in the Southern Hemisphere due to brine rejection when sea ice is formed. In the Atlantic, the deep waters travel southward in western boundary currents; in the southern hemisphere, the Antarctic Bottom Water is spread into the three ocean basins where it drives current systems mainly in the Indian and Pacific Oceans. Water rises to the surface over time and eventually returns to the Atlantic Ocean.

Surface water becomes depleted in nutrients due to biological activity, while deep water nutrient concentrations are higher due to bacterial decomposition of sinking organic matter (remineralisation). As a consequence, upwelling regions are highly productive as nutrient-

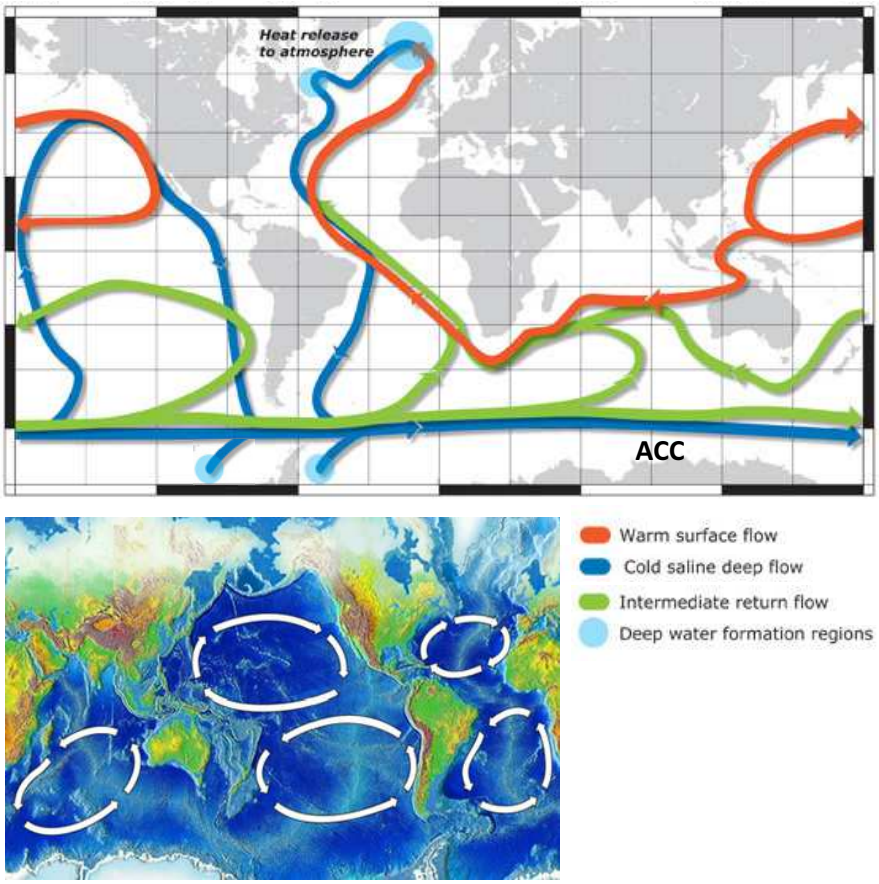

Figure 1.8 – (a) Global ocean circulation (adapted from Oppo and Curry, 2012) and (b) ocean gyres (from oceanservice.noaa.gov/education/kits/currents/05currents3.html); ACC = Antarctic Circumpolar Current.

rich waters are transported to the euphotic zone.

Large-scale wind-driven current systems (gyres) in the northern hemisphere circulate clockwise, while those in the southern hemisphere circulate anti-clockwise. Wind-driven deep water upwelling occurs at the eastern coastal boundaries of each system, with winds along the shore resulting in Ekman transport of water away from the coasts (with the most nutrient-rich upwelling systems found off the west coasts of Africa (Mauritanian Upwelling) and South America (off Peru)). The equatorial upwelling and the Antarctic frontal systems are further productive ocean regions created through the impact of surface winds on vertical mixing. The gyres themselves are depleted in nutrients (to different extents for different nutrients), and all five subtropical gyres (North and South Atlantic, North and South Pacific and Indian Ocean) exhibit low biological production.

It should be borne in mind that oceanographic research must be spatially and temporally extensive in order to understand and represent these large differences between different ocean basins and water masses, and apparently disparate results can often be explained by sampling location or season and their effects on the biological community.

1.6 Marine emissions

1.6.1 Marine (B)VOCs

In recent decades, the ocean has been increasingly recognised as a potentially globally significant source or sink of a number of atmospherically relevant VOCs apart from DMS (see section 1.4.1), including alkanes, alkenes, oxygenated VOCs (oVOCs) and halogenated hydrocarbons (reviewed by Carpenter et al., 2012; Liss et al., 2014; Carpenter and Nightingale, 2015). Even for small source strengths, the large surface area from which these compounds can be emitted and the generally pristine environments into which they are introduced could result in significant effects on aerosols and hence radiative forcing and climate (Andreae and Rosenfeld, 2008; Koren et al., 2014).

The limiting factors in the analysis of many of these compounds were the low levels at which they are present in the marine atmosphere or in the ocean. As a result, the analytes were often below the detection limits of available instrumentation and therefore

not considered important compared to terrestrial concentrations that tend to be orders of magnitude higher. In addition, the logistical challenges of studying the remote marine boundary layer were considerable (and still are to some extent). As our understanding of atmospheric chemistry increases, analytical and logistical capabilities improve and gaps in our ability to explain observations with models become apparent, the interest in oceanic fluxes of various chemical species has been increasing. Several of those species are known to be important in the terrestrial environment, e.g. alkanes and alkenes (e.g. Guenther et al., 2012), others have predominantly oceanic sources, such as iodinated hydrocarbons (e.g. Carpenter et al., 2012).

1.6.2 Marine isoprene and monoterpenes

1.6.2.1 Sources

While the larger isoprenoids such as pigments are commonly found in marine photosynthetic organisms, marine sources of volatile isoprenoids were generally not believed to exist as recently as the 1990s; with Bonsang et al. reporting the first evidence for marine production in 1992. Even in 2001, Sharkey and Yeh stated that the observations of isoprene in seawater and the marine atmosphere were more likely derived from bacteria associated with phytoplankton than from the plankton itself. There was initially some debate about their source, and some authors suggested a photochemical production mechanism from dissolved organic matter as for other alkenes (ethene, propene; Ratte et al., 1993; Broadgate et al., 1997). A number of measurements were able to relate isoprene in the water to chlorophyll-a (Chl-a) concentrations (Bonsang et al., 1992; Milne et al., 1995; Broadgate et al., 1997 (seasonal cycle)), which in conjunction with laboratory experiments on phytoplankton monocultures (Moore et al., 1994; Milne et al., 1995; Shaw, 2001; Shaw et al., 2003) led to the general acceptance of a biogenic source. The shape of the vertical concentration profile in the water column was one of the arguments for biological production, as it typically followed the distribution of Chl-a, albeit with a shallower isoprene than Chl-a maximum (Bonsang et al., 1992; Milne et al., 1995; Figure 1.9a).

Reported concentrations of isoprene in the surface ocean range from <1 to >150 pmol L^{-1}, often averaging around 20-50 pmol L^{-1}, with large variations between study regions and seasons. Differences between air mixing ratios are even larger, with publications varying

from <0.1 to 375 pptv isoprene over the ocean. Table 3.2 in Chapter 3 lists reported observations of marine isoprene in air and water, and relevant literature is discussed in Chapter 3 section 3.1. Published sea-to-air fluxes fall into a similarly large range of ca. $1 \times 10^6 - 2 \times 10^8$ molecules cm^{-2} s^{-1}, with large error bars (see Chapter 3 Figure 3.5 and Shaw et al., 2010); global flux estimates are between 0.1−11.6 Tg C yr^{-1} (Chapter 5 Table 5.1; Shaw et al., 2010).

The main focus of the more recent research has been to reconcile some of the large differences in observations by establishing parameterisations for this source with respect to a proxy (mostly Chl-*a*) (Bonsang et al., 2010; Exton et al., 2013; Meskhidze et al., 2015) and the global extrapolation of fluxes (see also section 1.9), which is described in more detail in Chapters 3 and 5.

Incidentally, some recent findings from studies of the sea surface microlayer (Ciuraru et al., 2015b) indicate an additional, photochemical source of isoprene after all. In laboratory studies using artificial and natural sea surface microlayer (SML; from a Norwegian fjord), the authors observed significant, almost instantaneous and consistent isoprene emission upon irradiation. They showed that isoprene production occurred only when both a photosensitiser (humic acid, mimicking dissolved organic matter (DOM)) and a surfactant (nonanoic acid or fatty acids in natural SML) were present and that factors including pH and choice of fatty acid (due to their effects on the formation of a surfactant monolayer) and humic acid concentration affected the emission. Suitable photosensitisers and fatty acids are commonly found in the marine environment, making this mechanism a likely abiotic source of isoprene at the ocean surface.

Oceanic monoterpenes were first reported in 2008 from air measurements during field studies (Yassaa et al., 2008; Colomb et al., 2009) and laboratory culture experiments (Yassaa et al., 2008). Since then, merely two further sets of observational data (stating only a mean mixing ratio in air for the study period; Lawson et al., 2011, 2015) and a further laboratory investigation (Meskhidze et al., 2015) have been published (details see Chapter 4). Values observed in marine air range from <1 to 225 pptv (total monoterpenes or α-pinene), as detailed in Chapter 4 Table 4.1; while no sea-to-air emission rates have been reported, one study estimated the global flux of α-pinene as 0.013−29.5 Tg C yr^{-1} (Luo and Yu, 2010; see also Chapter 4 section 4.1 and Chapter 5 section 5.2.5).

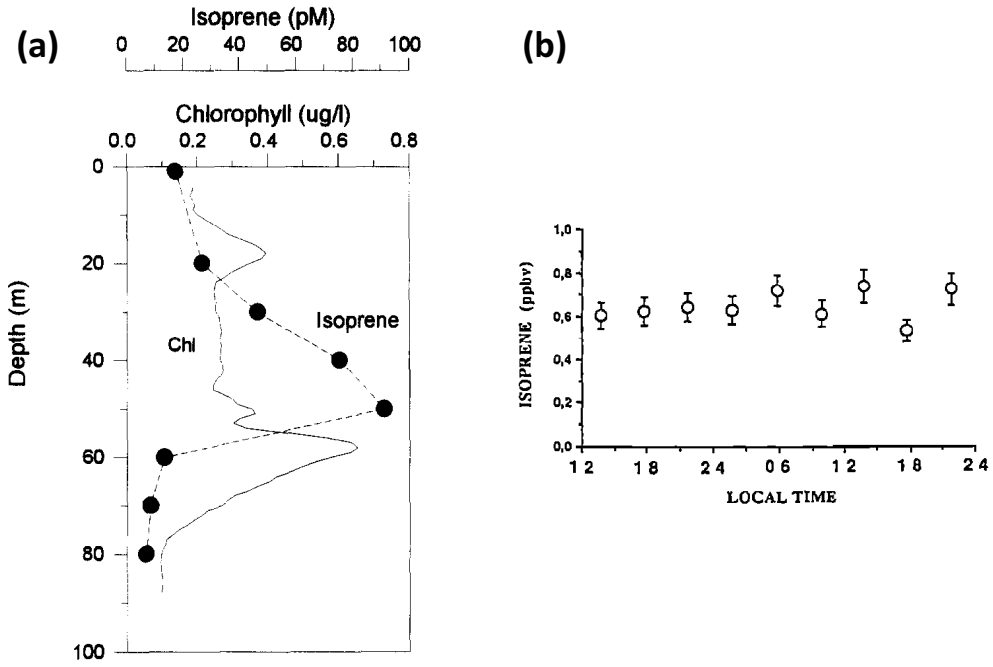

Figure 1.9 – Typical depth profile of isoprene alongside chlorophyll concentrations (reproduced from Milne et al., 1995); (b) Diurnal study of isoprene seawater concentrations at 15 m depth (reproduced from Bonsang et al., 1992).

1.6.2.2 Functions

As with terrestrial isoprenoids, a knowledge of the function of these compounds in phytoplankton could provide a basis for more directed future research into specific proxies for emissions, which would in turn improve global estimates and constrain the magnitude of the impact on marine SOA (see Chapters 3 and 4; also section 1.7.1). There have been no reports of marine heterotrophic bacteria producing (or consuming) volatile isoprenoids, and all observed emissions to date have been from photosynthetic phytoplankton (see Shaw et al., 2010 for a summary). However, the (sometimes tenuous) correlations with Chl-*a*, temperature and light of isoprene concentrations in water have been the only indication towards a comparable function as that of terrestrial isoprene. While this may seem a relatively strong similarity, it has been argued that the necessity for thermotolerance and mitigation of light stress is much lower in the marine environment as the large heat capacity of water effectively avoids temperature fluctuations like those experienced by leaves exposed to sunlight, and the light levels in the water column are generally much lower than on land (Shaw et al., 2003). The proposed mechanism for general oxidative

stress reduction in higher plants by Vickers et al. (2009; see section 1.2.2) has not been discussed with respect to phytoplankton in the literature to date.

Correlations with light or light stress have only been seen in laboratory studies (Shaw et al., 2003; Gantt et al., 2009; Meskhidze et al., 2015; lack of diurnal variation in field observations also illustrated in Figure 1.9b), while a dependence on temperature has also been reported from field data (in water, Ooki et al., 2015; laboratory data: Exton et al., 2013), and most studies (field and laboratory) found some positive relationship of isoprene emissions or water concentrations with Chl-*a* (e.g. Shaw et al., 2010, and references therein; Exton et al., 2013 (laboratory); linear regression equations for field data published by Broadgate et al., 1997; Hashimoto et al., 2009; Kurihara et al., 2010, 2012; Ooki et al., 2015). No strong correlation with any of the above factors has been observed for air measurements, although links of isoprene and/or monoterpenes with water Chl-*a* concentrations (*in situ* or upwind) have been suggested by some investigations (Yassaa et al., 2008; Colomb et al., 2009). More details of these relationships are discussed in Chapters 3 and 4.

1.7 Marine aerosol

As discussed in section 1.4 above, aerosols emitted from the terrestrial biosphere and the surface oceans can impact cloud formation and microphysical properties and therefore regional and global climate (Boucher et al., 2013). Marine aerosol comprises a wide variety of compounds and particles of both continental and marine origin, with extensive interaction resulting in aerosol that is difficult to attribute to either source. It can be primary aerosol such as black carbon from terrestrial biomass burning, Saharan dust, pollen and sea spray (organic and inorganic) or secondary aerosol, including sulfuric acid, from both biogenic and anthropogenic sources. Particles are mostly in the Aitken (<0.1 μm), accumulation (0.1-1 μm) and coarse (>1 μm) modes, with only few observations of nucleation mode aerosol (<0.01 μm) (Heintzenberg et al., 2004). The majority of coarse mode aerosol is sea salt, while non-sea-salt sulfate aerosols and organic carbon make up most of the smaller particles (Saltzman, 2009, and references therein). Its global source strength is highly uncertain, with estimates between 8 and 75 Tg C yr^{-1}, although agreement on the magnitude of sub-micron POA as around 10 Tg C yr^{-1} is emerging (Spracklen et al., 2008;

Roelofs, 2008; Gantt et al., 2009; Vignati et al., 2010; Meskhidze et al., 2011; reviewed by Gantt and Meskhidze, 2013).

1.7.1 Marine organic carbon aerosol

1.7.1.1 Aerosol formation

Marine POA consists of organic matter emitted directly from the sea surface in bubble-bursting processes (at wind speeds above ca. 5 m s^{-1}, increasing with wind speed in a highly non-linear fashion), and has been associated with biological activity since higher primary production leads to higher concentrations of dissolved organic matter in the surface water (e.g. O'Dowd et al., 2004; Spracklen et al., 2008; Quinn et al., 2015). SOA is formed from nucleation and condensation of gas phase molecules or *via* heterogeneous and aqueous phase reactions in pre-existing aerosol.

Aerosol number concentrations in marine air are around an order of magnitude lower than in terrestrial environments, but the marine contribution to global aerosol loading has recently received considerable attention due to its large potential impact on cloud microphysical properties in this clean background (Twomey, 1977; Luo and Yu, 2010; Koren et al., 2014). As well as the total aerosol mass, its size distribution and chemical composition are the subject of ongoing research, since both are key parameters that determine the particles' CCN activation potential (see section 1.4). While a more detailed knowledge of aerosol composition and distribution could help to infer aerosol sources, conversely an improved understanding of aerosol precursors in the marine boundary layer could help to constrain or validate model predictions of CCN sources, properties and abundance in this environment.

Of particular interest with respect to climatic effects is the process of nucleation, as the number of CCN can only increase if the aerosol number concentration increases. Nucleation is not well understood; it has only recently been directly observed in continental air and was found to involve clusters of sulfuric acid and oxidised VOCs (Kulmala et al., 2013; Riccobono et al., 2014), partially confirming a previously suggested model (Metzger et al., 2010). In the marine environment, new particle formation events have been associated with iodine oxides in coastal areas (O'Dowd and de Leeuw, 2007; Allan et al., 2015; and

references therein); sulfuric acid from atmospheric DMS oxidation also has the potential to nucleate new particles if it is not scavenged by existing aerosol before stable clusters can form (but requires additional species to grow into particles; Pirjola et al., 2000). The current view regarding organic compounds such as isoprene oxidation products is that they could be involved in new particle formation by accelerating growth once nucleation has taken place (O'Dowd and de Leeuw, 2007), and it is emerging from research in chamber and terrestrial environments that they could also take part directly in the nucleation step (Metzger et al., 2010; Kulmala et al., 2013; Riccobono et al., 2014). Relatively frequent spatially extensive open-ocean nucleation events observed over several years during the productive season in the North-East Atlantic do suggest a biogenic source of SOA (O'Dowd et al., 2010), but a further analysis of the chemical composition of aerosol during these events suggested mainly SOA from organic amines and other nitrogen-containing compounds in the nucleation, with only a potential contribution from aliphatic vapours (Dall'Osto et al., 2012).

1.7.1.2 Contributions of terpene SOA to global marine aerosol

Impacts of volatile isoprenoids on atmospheric chemistry as described in section 1.3 above are often dependent on the air mixing ratios of the VOCs and not necessarily applicable to the much cleaner marine environment. For instance, a reduction in the atmosphere's oxidative capacity would only occur when OH is not in excess of the isoprene or monoterpenes, and a reduction in terpene SOA yield (as suggested by Kiendler-Scharr et al., 2009) is similarly only likely if sufficient isoprene is present to act as a sink for OH. A recent analysis by Gantt et al. (2015) showed a decrease of OH and changes in O_3 as a result of including marine isoprene and POA in an online-coupled model, but in fact the reported changes amount to only around 1 % or less of typical atmospheric concentrations (despite a relatively large predicted increase in surface isoprene of 5-10 pptv in remote marine areas).

Modelling studies to date generally conclude a minor influence of isoprene (or monoterpene) SOA, with estimated contributions to the global marine organic carbon (OC) of around 1-2 % (Arnold et al., 2009; Myriokefalitakis et al., 2010; Anttila et al., 2010; see also Chapter 5). However, there are suggestions of much higher impacts in regions with high isoprene emissions and if specifically sub-micron aerosol (which affects cloud proper-

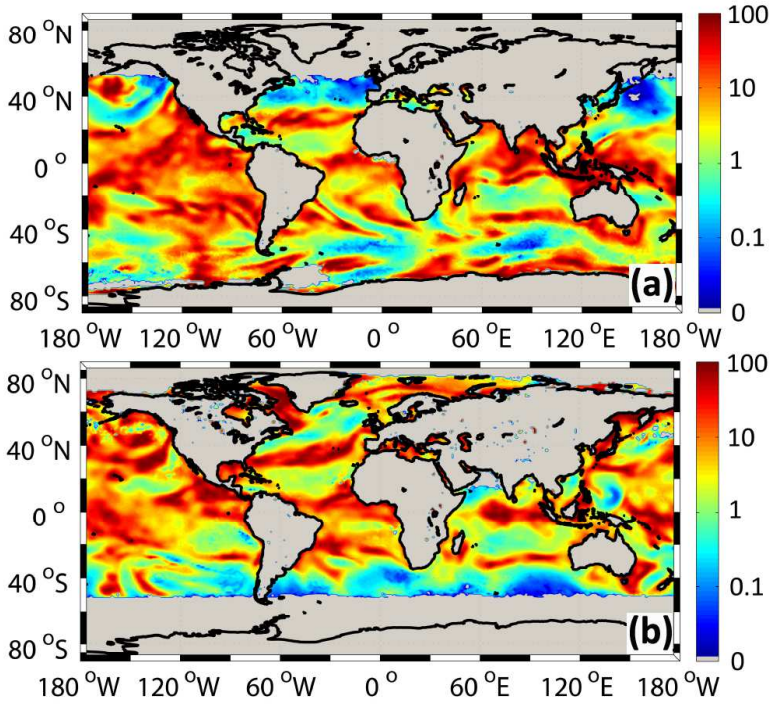

Figure 1.10 – Monthly-average percentage contribution of marine isoprene SOA to total sub-micron OC emissions for (a) January and (b) July 2001; taken from Gantt et al. (2009).

ties) is considered: Gantt et al. (2009) found that isoprene SOA could account for up to 30 % of marine sub-micron OC in the tropics and even up to 50 % at mid-day (Figure 1.10; based on a light-dependent isoprene production algorithm). There appears to be some support for the hypothesis that isoprene- (and likely terpene-) derived aerosol could still be important locally/regionally despite the low global contribution. Hu et al. (2013) reported measurements of isoprene and α-pinene oxidation products (SOA tracers) in aerosol filter samples taken during cruises around the world. They derived isoprene and monoterpene fluxes from clean marine samples of a similar order as previous studies (ca. 1.4-3.8 $\times 10^8$ molecules cm^{-2} s^{-1}), but attributed the majority of the observed tracer concentrations to long-range transport from continental sources, with higher concentrations observed in coastal areas and where samples were affected by continental air masses. However, they also highlighted the example of Prydz Bay (Antarctica), which likely has no significant terrestrial contributions to aerosol precursors: during bloom events in the austral summer, observed isoprene SOA was of comparable magnitude to DMS SOA, indicating isoprene fluxes of up to 30-90 times higher than for typical remote marine samples. Monoterpene SOA was not enhanced during those episodes.

1.8 Effects of climate change

A better understanding of the environmental factors and processes controlling BVOC emissions is frequently highlighted as an area for further research in order to predict future emissions in a changing climate (e.g. Pacifico et al., 2009; Yuan et al., 2009; Sharkey and Monson, 2014). This is certainly true in the terrestrial ecosystems that are responsible for the vast majority of biogenic emissions and have large effects on atmospheric chemistry above the continents, but no less important for the oceanic environment that includes some of the ecosystems most sensitive to climate change such as the Arctic and Antarctic, and where current behaviour is even less well understood.

Rising global temperatures and atmospheric CO_2 concentrations affect the ocean through warming the surface ocean and increasing its acidity, which causes a number of feedback mechanisms that are likely to have impacts on primary productivity and emissions of BVOCs (e.g. SOLAS 2015-2025: Science Plan and Organisation, 2015). Increasing surface winds especially around Antarctica (Korhonen et al., 2010) also increase the magnitude of sea-air exchange (which is dependent on the square of the wind speed, see Chapter 3 section 3.2.3). In the Arctic and Antarctic the decreasing trend in sea ice cover may have a profound influence on the biological activity, as the melting ice releases nutrients into the sea, solar radiation can reach more of the surface ocean and the effective barrier to sea-air gas exchange is removed (Tovar-Sánchez et al., 2010; Carpenter et al., 2012). The microbial loop, i.e. the cycle of production and consumption of matter in the oceans, is a carefully balanced system which will respond to external perturbations in a variety of ways. Marine biota, including different phytoplankton species, will adapt differently to warmer and more acidic oceans (e.g. Hays et al., 2005), resulting in complex changes to the entire system such as shifts in community structure (Constable et al., 2014) that are likely to affect BVOC production patterns.

1.9 Extrapolation: measurements, models and satellites

Models are important tools to explore and predict developments of the changes and feedbacks in the different earth systems. The key to achieving accurate projections is sufficient knowledge of past and current environments and processes, and models are typically

compared to observations to assess how well the parameterisations can reproduce measurements, or even tuned to minimise the bias between predicted and actual values. Earth system models that account for complex feedback mechanisms, the coupling of different ecosystems and processes on various scales are still in the early stages of development (Carslaw et al., 2010), although much progress has been made in recent years (Flato et al., 2013). The balance between the amount of detail needed to correctly model a process and the computational cost (and feasibility) of running a model is difficult, especially when the process in question is only poorly understood and therefore no simple parameterisation can be made (or none at all).

In the case of marine BVOC emissions, models are starting to include marine isoprene and resulting SOA (see section 1.7), but validation against observations is difficult due to the lack of available data from remote marine environments. Global extrapolation from the few *in-situ* measurements is prevented by the large spatial and temporal variability of the data, so that in order to include emissions in a global model, a parameterisation requires a suitable proxy for the species to be estimated. A proxy should show a robust relationship with the target species and exist for as much of the target region as possible, which could be in the form of widely made measurements (*in situ* or remote) and a large available database or climatology. Most models use remotely-sensed Chl-*a* as a proxy for biological activity and therefore isoprene production, but a comparison to the observed spatial distribution of isoprene concentrations has only recently become possible (and not yet been made) following the publication of an extensive dataset of surface ocean isoprene observations (Ooki et al., 2015). The discrepancies between bottom-up and top-down emission estimates and the range of estimates from different studies (see Shaw et al., 2010, for a summary) indicate that the sources of isoprene on a global scale are not yet well enough understood to reach a common parameterisation. Linear isoprene-Chl-*a* relationships exist, but are rather variable and may need further refinement using different parameters such as temperature or phytoplankton speciation (see section 1.6.2 and Chapter 3).

1.10 Project aims

This project aimed to develop and deploy a robust measurement system for *in-situ* high-resolution concurrent air and water measurements (Andrews et al., 2015) of isoprene and monoterpenes, in order to substantially increase the available dataset for these compounds in the marine environment. The system, its characteristics and details of the data processing are described in Chapter 2. Observational data is presented and analysed in Chapters 3 (isoprene) and 4 (monoterpenes). In the case of monoterpenes, these measurements represent the first reported water concentrations. This much-needed data will help to evaluate current model estimates and gain a better understanding of the spatial and temporal variability of oceanic terpenes.

In order to evaluate widely used proxies for isoprene and monoterpenes in the ocean, namely Chl-*a* and proposed refinements (phytoplankton functional types, temperature), and investigate any further controls, observations of a suite of biological, physical and chemical measurements and relationships of these parameters with marine terpene concentrations was investigated (detailed in Chapters 3 and 4 for isoprene and monoterpenes, respectively). If sufficiently robust correlations can be established with suitable parameters, such relationships could form the basis of model algorithms for global marine volatile terpenoid fluxes.

Ultimately, the data presented in this thesis will help to evaluate the relative importance of marine isoprene and monoterpene emissions for global climate, in view of previously published studies regarding the oceanic organic carbon source. An intial exploration of the potential atmospheric impacts of the analytes measured in this study is presented in Chapter 5.

Chapter 2

Experimental methods

All the marine boundary layer and surface ocean observations of isoprene and monoterpenes discussed in this thesis were quantified by P&T-TD-GC-MS (Purge&Trap - Thermal Desorption - Gas Chromatography - Mass Spectrometry), and this chapter describes the different instrumental set-ups and approaches to data collection, processing and validation.

A description of the P&T system in section 2.1.3 in this chapter and its performance characteristics has been published in the article:

Andrews, S. J., Hackenberg, S. C., and Carpenter, L. J.: Technical Note: A fully automated purge and trap GC-MS system for quantifcation of volatile organic compound (VOC) fluxes between the ocean and atmosphere, Ocean Science, 11, 313-321, doi: 10.5194/os-11-313-2015.

2.1 Fundamentals of analytical techniques

2.1.1 Gas chromatography (GC)

Chromatography is a group of widely used, powerful and versatile analytical techniques which can separate components of complex mixtures and, in conjunction with standards, allow their identification and quantification, based on the components' migration rates through a stationary phase when carried by a mobile phase. Among a variety of different types, it includes liquid chromatography (liquid mobile phase, solid stationary phase), e.g. high-performance liquid chromatography (HPLC) that can be used for pigment analysis (Chapter 3), and gas chromatography (GC; gaseous mobile phase, liquid stationary phase). Capillary GC involves the use of capillary columns made of fused silica coated with a viscous liquid that acts as the stationary phase; a range of liquids with different polarities are commercially available to suit different applications and analytes.

The characteristics of a chromatographic system can be described by a number of equations that will be explained below, illustrated by examples from the method development for the present study. The performance of a column is typically expressed by stating its efficiency and the resolution of two critical analytes.

Column efficiency is measured quantitatively by the plate height H, which is related to the number of theoretical plates N by

$$N = \frac{L}{H} \tag{2.1}$$

where L is the length of the column packing in cm. Plate heights and number of plates can vary over several orders of magnitude for different column types, mobile and stationary phases; in capillary GC, H is of the order of a few thousand plates per metre of column (Skoog et al., 2004). Since the breadth of a typical Gaussian-shaped chromatographic peak reflects column efficiency H and is given by the standard deviation σ (in cm) and hence the variance σ^2, the variance per unit column length (in cm) is used as a measure of H (in cm):

$$H = \frac{\sigma^2}{L} \tag{2.2}$$

This theoretical concept can be applied to experimental data by determining the number of plates from the retention time t_R of a peak and the width at its base W (both in units time), derived from the above relationships in combination with properties of a Gaussian peak (see also Figure 2.1)

$$N = 16 \left(\frac{t_R}{W} \right)^2 \tag{2.3}$$

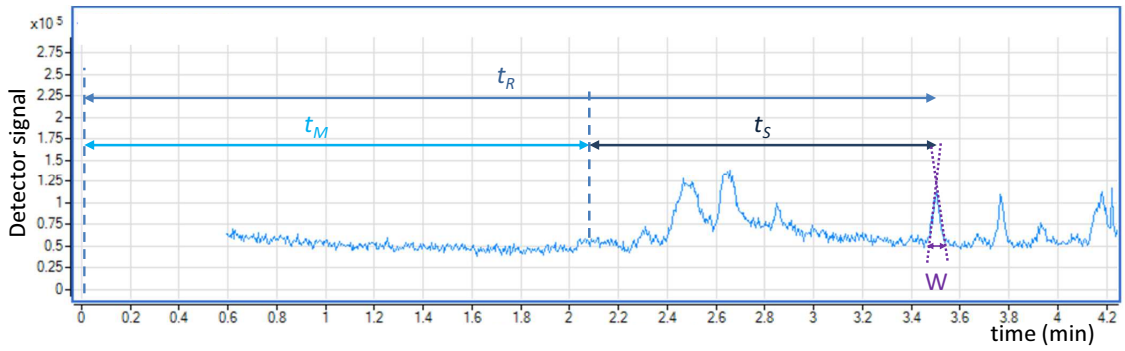

Figure 2.1 – Chromatogram section (gas standard) illustrating retention time, holdup time and time spent in the stationary phase (t_R, t_M and t_S, respectively) as well as peak width W.

The retention time is the sum of the time that an analyte spends in the mobile phase (t_M; identical for all species) and in the stationary phase (t_S). In practice, t_M was never directly observed in this study due to the solvent delay at the start of each sample that was written into the method in order to extend detector lifetime. However, it can be derived from known column dimensions and method parameters if needed for calculations as in this section (Table 2.1). t_R is determined by the column length and the average linear rate of solute migration, $\bar{\nu}$ (in cm s^{-1})

$$\bar{\nu} = \frac{L}{t_R} \tag{2.4}$$

and the average linear velocity u of the mobile-phase molecules is

$$u = \frac{L}{t_M} \tag{2.5}$$

In order to compare the migration rate of analytes on columns, the retention factor k is used; e.g. k_A for analyte A is defined as

$$k_A = \frac{K_A V_S}{V_M} \tag{2.6}$$

Table 2.1 – Calculated values of holdup time t_M for the different columns used in method development for the present study; relevant column and method parameters also listed (calculations by Agilent Technologies Pressure Flow Calculator).

Column number	Column (manufacturer)	Length / m	internal diameter / mm	Film thickness / µm	He flow / mL min^{-1}	t_M / min
1	BPX5 (SGE)	50	0.32	1.0	2.0	2.10
2	HP-5MS (Agilent)	30	0.25	0.25	2.0	0.97
3	Rtx502.2 (Restek)	20	0.18	1.0	2.0	0.53
4	Rtx-5 (Restek)	10	0.18	0.4	3.0	0.15

where V_S and V_M are the volumes of the stationary and mobile phases, respectively, and K_A is the distribution constant for analyte A, which describes the equilibrium of A between the mobile and stationary phases (with concentrations c_M and c_S, respectively):

$$K_A = \frac{c_S}{c_M} \tag{2.7}$$

The migration rate $\bar{\nu}$ can be related to the velocity of the mobile phase u by substituting equation 2.7 into

$$\bar{\nu} = u \times \frac{c_M V_M}{c_M V_M + c_S V_S} \tag{2.8}$$

to give

$$\bar{\nu} = u \times \frac{1}{1 + K_A V_S / V_M} \tag{2.9}$$

and further substitution of equation 2.6 into 2.9 yields

$$\bar{\nu} = u \times \frac{1}{1 + k_A} \tag{2.10}$$

Applying this to a chromatogram is possible by substituting equations 2.4 and 2.5, so that

$$\frac{L}{t_R} = \frac{L}{t_M} \times \frac{1}{1 + k_A} \tag{2.11}$$

which can be rearranged to

$$k_A = \frac{t_R - t_M}{t_M} = \frac{t_S}{t_M} \tag{2.12}$$

showing that the retention factor equates to the ratio of the amount of time spent in the stationary phase compared to that spent in the mobile phase (Figure 2.1). Changes in stationary phase and in temperature result in changes in k, as illustrated in Figure 2.2 and discussed in more detail below. Retention factors of 1 to 5 for all components in a mixture are considered ideal; values up to 10 are acceptable and sometimes needed in order to achieve the desired resolution (see below).

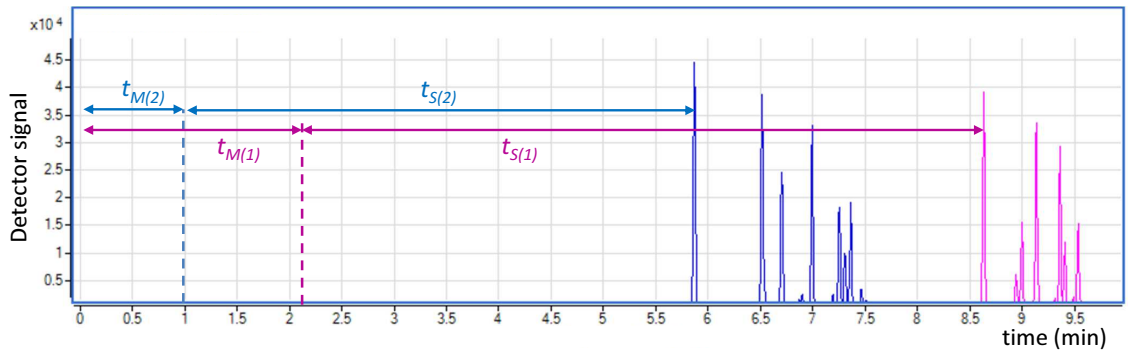

Figure 2.2 – Chromatogram sections (gas standard; extracted ion for monoterpenes, see section 2.1.2) from two columns with different stationary phases (column numbers and calculated t_M see Table 2.1). Using equation 2.12, retention factors for α-pinene are k_1 = (6.5 min/2.1 min) = 3.1; k_2 = (4.9 min/1.0 min) = 5.1.

As the retention factor alone cannot provide information on how well a column is able to separate two analytes (its resolution), an additional measure is needed - the selectivity factor α, defined as the ratio of the distribution constant of the more strongly retained analyte A to that of the less strongly retained analyte B. It can also be expressed in terms of the retention factors of the two species (by substituting equation 2.6), and hence can be obtained from a chromatogram using the relationship in equation 2.12:

$$\alpha = \frac{K_B}{K_A} = \frac{k_B}{k_A} = \frac{(t_R)_B - t_M}{(t_R)_A - t_M} \tag{2.13}$$

The resolution R_S of a column in terms of experimental parameters as shown in Figure 2.3 is defined as

$$R_S = \frac{\Delta Z}{W_A/2 + W_B/2} = \frac{2\Delta Z}{W_A + W_B} = \frac{2[(t_R)_B - (t_R)_A]}{W_A + W_B} \tag{2.14}$$

and can be re-written in a form that relates it to N and to α and k for a pair of analytes A and B as above (with B as the more retained species):

$$R_S = \frac{\sqrt{N}}{4}\left(\frac{\alpha - 1}{\alpha}\right)\left(\frac{k_B}{1 + k_B}\right) \tag{2.15}$$

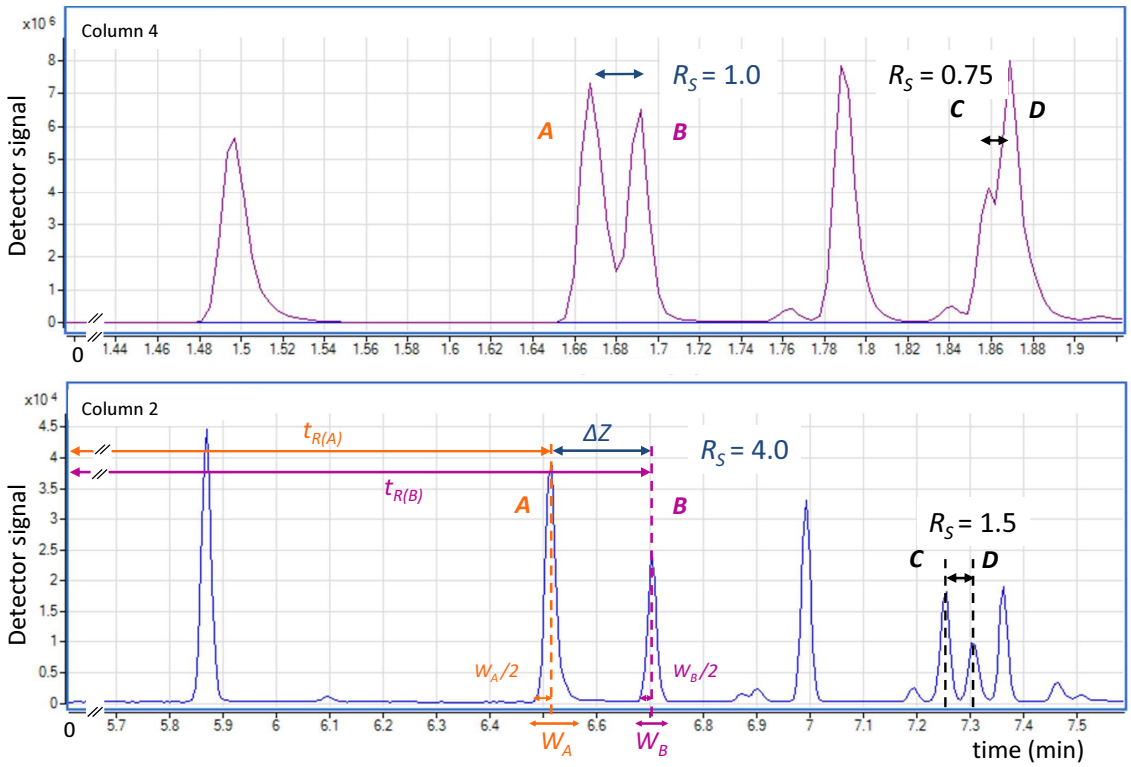

Figure 2.3 – Chromatogram sections (gas standard; extracted ion for monoterpenes) from two different columns (2 and 4, see Table 2.1) displaying experimental parameters needed to calculate resolution R_S as in equation 2.14, along with R_S shown for two pairs of peaks (A/B = myrcene/β-pinene; C/D = limonene/eucalyptol). Note that the second pair consists in fact of three peaks that column 4 cannot resolve, as seen in the bottom panel (column 2 does have the necessary resolving power).

Rearranging this allows the determination of the number of plates required to obtain a given resolution

$$N = 16R_S^2 \left(\frac{\alpha - 1}{\alpha}\right)^2 \left(\frac{k_B}{1 + k_B}\right)^2 \tag{2.16}$$

Employing a number of the equations given above, the time needed to elute components A and B with a resolution R_S can be described by

$$(t_R)_S = \frac{16R_S^2 H}{u} \left(\frac{\alpha - 1}{\alpha}\right)^2 \frac{(1 + k_B)^3}{(k_B)^2} \tag{2.17}$$

A resolution of at least 1.5 is generally accepted to describe a pair of peaks with baseline resolution. From equations 2.15 and 2.1, it is clear that an increase in column length leads to a larger number of plates and hence improved resolution; however it is often impractical to achieve the desired separation by a measure that lengthens analysis time. An alternative is to reduce the plate height, which for capillary GC can be accomplished by reducing the stationary phase film thickness or the column diameter. Additionally, the carrier gas (mobile phase) flow can be optimised. These approaches are based on the principles described by the commonly used van Deemter equation, which expresses column efficiency (or plate height) H in terms of the linear flow rate of the mobile phase and coefficients of multiple-path effects, longitudinal diffusion and mass transfer (A, B and C, respectively):

$$H = A + \frac{B}{u} + Cu \tag{2.18}$$

Multiple-path effects (A) are also referred to as eddy diffusion and this term is flow rate-independent at high mobile phase linear velocities. It is caused by the different pathways that molecules can take through packed columns, leading to a difference in overall distance travelled and hence time taken to pass through the column. For capillary columns, it is related to the column diameter, and it can also be reduced considerably by decreasing the diffusion coefficient by lowering the temperature.

The longitudinal diffusion term B/u describes the diffusion of an analyte in a band towards the edges of that band (where its concentration is lower than in the centre of the band), resulting in band broadening. It is directly proportional to the diffusion coefficient of a

species and inversely proportional to the linear flow velocity, as a faster flow results in a shorter amount of time in which diffusion can occur.

The mass transfer term Cu is directly proportional to the square of the film thickness of the stationary phase, as a thicker film leads to a longer distance for the analyte to travel to the interface of the stationary and mobile phases, where transfer occurs. It is also inversely proportional to the diffusion coefficient of the analyte in the stationary phase, since a slower migration to the interface also reduces the rate of mass transfer and increases the plate height.

A schematic van Deemter plot as in Figure 2.4 shows that the minimum plate height as determined by all contributions to the equation can be achieved at a certain flow rate, but the actual values depend also on column diameter and film thickness, as discussed above. In the method developed for the current study, the need for high column efficiency was offset by aiming to separate a range of analytes that required certain column characteristics as described below.

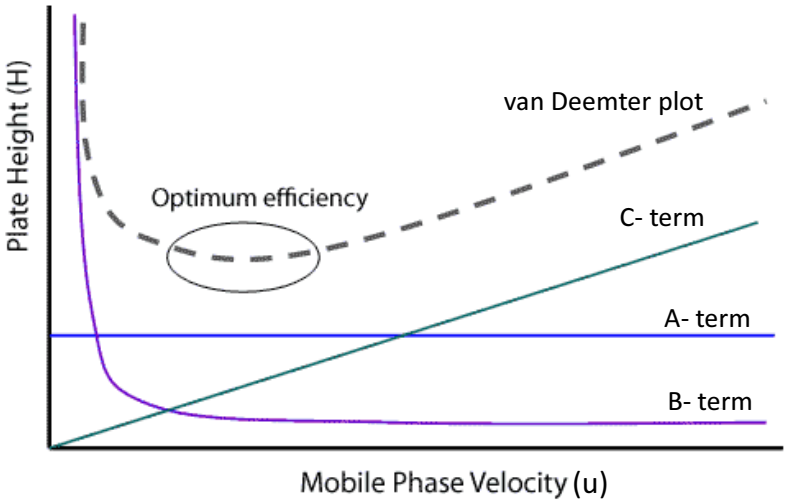

Figure 2.4 – Schematic van Deemter plot, also showing the separate contributions of the three terms of equation 2.18 to the overall curve (adapted from restek.com).

The second and third terms of equation 2.15 may also be addressed in order to improve resolution; while the stationary phase film thickness also has an effect, optimisation of k by varying the temperature is often considered the easiest way (increasing the temperature leads to an increase in k). An increase in the selectivity factor must be balanced with changes in k, which should be between 1 and 10, and for GC can be achieved by changing

the temperature or the stationary phase.

In this project, a combination of measures was taken to optimise performance: the final column was much longer than used initially (50 m as opposed to 10 m), chosen for its improved resolving power and because a longer analysis time was acceptable for this application. It also contained a thick-film stationary phase in order to adequately retain the highly volatile analytes (1 µm; 0.25 and 0.4 µm were also tried), along with a relatively wide bore (0.32 mm rather than 0.25 or 0.18 mm) that allowed the higher flow rate of 2 mL min^{-1} necessary for improved peak shape (as it permits faster desorption from the cold trap of the thermal desorption unit). Both of those parameters did impact on the resolution of the less volatile species, but a compromise was necessary to maintain a method suited to the range of target analytes. A further consideration was column bleed, which becomes stronger for thicker films and at high temperatures; however the analytes studied here eluted early enough to avoid the increased background signal (baseline) associated with column bleed.

The so-called general elution problem is effectively the challenge of obtaining the best possible separation of a possibly large number of analytes with different properties in the shortest possible time. It is one of the main issues encountered with the analysis in the present study, as the target analytes comprised very volatile to much less volatile (and some very similar) species, which needed to be separated in a single method. To solve the problem, elution conditions (most commonly temperature in GC, as mentioned above) are varied to change the value of k. The method employed for the majority of the study included a temperature programme, with a low-temperature hold at the start in order to resolve isoprene from other highly volatile gases that may interfere with the peak, followed by a relatively slow temperature ramp (20 °C min^{-1}) that gradually changed k for the more retained analytes so they elute in a reasonable timeframe while still being as highly resolved as possible.

2.1.2 Mass spectrometry (MS)

GC can be coupled to one of a variety of detectors including a Flame Ionisation Detector (FID) or different types of mass spectrometer (MS). The advantage of mass spectrometry is its ability to increase sensitivity and specificity of the overall method by adding an extra

dimension to the analysis (in addition to GC retention time).

The MS used here was a single quadrupole with an electron ionisation (EI) source (also referred to as mass selective detector, MSD), which is depicted schematically in Figure 2.5. In an EI source, which is held at a vacuum of ca. 10^{-6} Torr, a tungsten filament is heated in order to emit electrons that are accelerated across a potential difference (typically 70 V between the filament and the source block, resulting in 70 eV electron energy) and enter the source block through a hole as an electron beam. In the source block, the molecular species entering the source from the end of the column are ionised by the electrons to form a radical cation; this process is no longer referred to as electron impact ionisation since it has been recognised that it is not the electron impacting the molecule but a transfer of energy that causes ionisation. As the amount of energy transferred is in excess of that required to ionise a molecule (typically, 10-20 eV are transferred while ionisation energies are between 6-15 eV for most molecules), this excess energy must be lost from the newly-formed ion, commonly leading to fragmentation of the molecular ion into fragments that can provide structural information from the fragmentation patterns. A positive voltage on the repeller pushes the ions into the lens stack, which consists of several lenses that form the ion beam (drawout plate) and focus it to reduce ion beam diameter and to optimise sensitivity for the application, which in the current case was in the low mass range (ion focus lens and entrance lens).

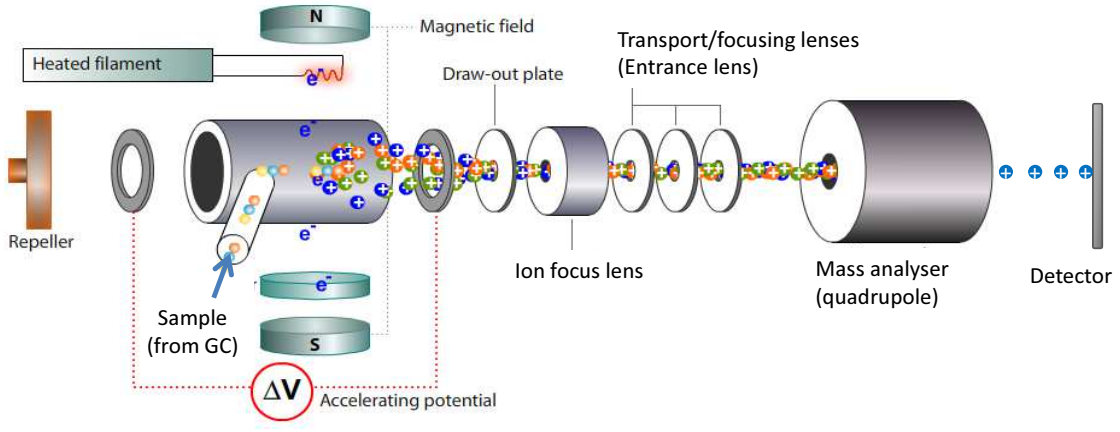

Figure 2.5 – Schematic drawing of the MS components (adapted from chromacademy.com).

The quadrupole acts as a mass filter which separates the ions by their mass to charge ratio (m/z), allowing only ions of a specific m/z to pass through at any given time to reach the detector. This selection is achieved by varying a combination of DC (direct current)

and RF (radio frequency) signals to the two pairs of rods (opposing rods form a pair) within the quadrupole. The DC-to-RF ratio determines the resolution (width of the mass peaks), while the RF voltage is varied to select the desired m/z to pass through to the detector. The detector itself is formed by a high energy conversion dynode and an electron multiplier and generates an electronic signal proportional to the number of ions arriving at it. All components of the MS chamber are heated to minimise condensation of sample and general organic vapours present in the source chamber onto the metal surfaces and keep them as clean as possible for as long as possible, to maintain sensitivity.

The default setting of the mass analyser is the scan mode, in which the quadrupole RF voltage is increased stepwise for a specified mass range to measure the signal at each m/z in turn (the quadrupole mass resolution is 1), with a very short dwell time each (0.2 ms; the time that the RF voltage remains on each setting) in order to achieve an acceptable number of measurement cycles within a short amount of time. Fewer cycles may result in missing sharp chromatographic peaks or at least poorly representing their shape (the effect is even visible for a relatively broad peak; see Figure 2.6). Due to this short analysis time for each m/z, small peaks become undetectable if the background signal is noisy, and the larger the analysed mass range, the longer each measurement cycle and hence the fewer points per unit time are available for a specific m/z, so that even extracting analyte-specific ions (more detail below) from the total ion chromatogram in scan mode can often yield only poor peak shape and poor sensitivity. Peak shape is therefore a result of both chromatography and the detector performance, and it is important for later quantitative analysis in chromatographic analysis software such as GCWerks (details in section 2.1.1) which is based on peak area (so that missing the top of a peak results in underestimation) or on peak height, for which the software uses a Gaussian peak shape fit which may become distorted if the measurement represents that shape poorly.

The ability to selectively monitor only certain m/z can be exploited in order to gain sensitivity in an analysis: the fragmentation patterns mentioned previously are often molecule-specific and spectra can be compared to standards or extensive libraries to aid peak identification. Known patterns can be used to choose a few diagnostic m/z to be monitored by the quadrupole at a given time in the analysis when a compound is expected to elute from the GC column. This mode is referred to as Selected Ion Monitoring (SIM) mode and can greatly improve sensitivity towards analytes as it only cycles through those selected

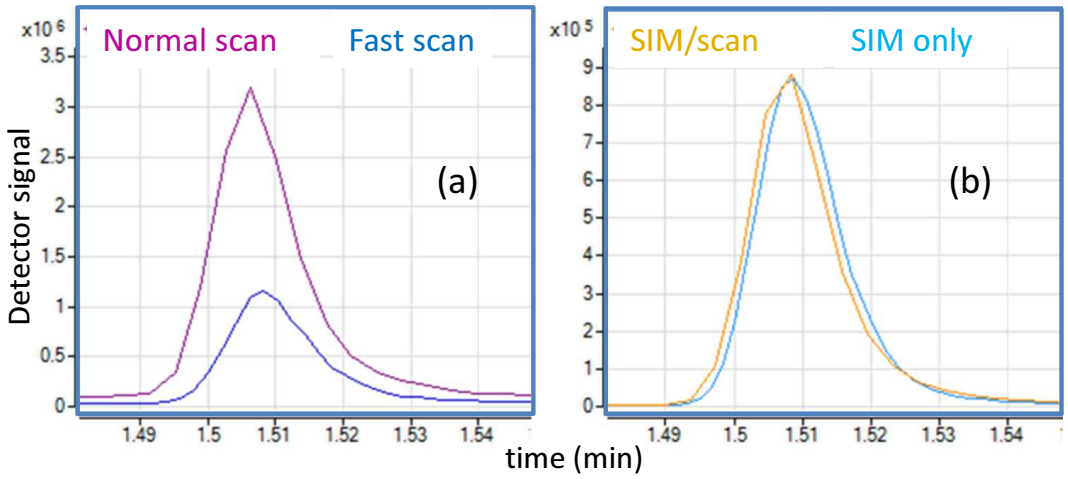

Figure 2.6 – Comparison of α-pinene peak shape (number of points per unit time) for (a) scan TIC (total ion chromatogram) with normal and fast scan rates and (b) SIM mode extracted ion chromatograms (SIM EIC) of m/z 93 from a method with SIM/scan versus SIM only acquisition. Fast scan results in a smoother peak in scan mode but also loses sensitivity; acquiring data in SIM only mode (faster overall cycle time) results in a smoother SIM peak (identical sensitivity to the SIM peak from a SIM/scan method), but loss of information for the whole chromatogram (see text).

ions to let them pass through the mass filter while background ions are not monitored. However, a mass filter can only monitor one m/z at a time and requires time to adjust the RF voltage for each SIM ion. As a result, the number of ions specified at any one time must be balanced with the need for an adequate number of points per chromatographic peak that is needed to correctly represent that peak (see Figure 2.6). One step that can be taken to minimise the number of SIM ions at a given time is to divide an analysis into separate SIM windows, time windows during an analysis in which specified SIM ions are measured. With adequate chromatographic resolution, relevant ions can be monitored for each analyte peak, giving a greater number of points (measurement cycles) per peak as well as good sensitivity from longer dwell times per m/z (longer dwell times allow more ions to strike the detector, increasing the signal). The more ions are in a SIM window, the shorter the dwell times must be for each ion so that the measurement cycle does not become too long. In SIM/scan mode, the instrument performs a scan cycle followed by the specified SIM ions for the relevant time window before starting the next scan cycle. This combined mode results in a longer overall cycle time than either scan or SIM only modes (effect on peak shape as for SIM/scan compared to SIM only in Figure 2.6; SIM/scan overall cycle time is longer).

Typically, the most abundant fragment ion that is also sufficiently specific to the target species is chosen as a quantifier ion, i.e. to be used for quantitative analysis of the resulting chromatogram. It is good practice to include at least one qualifier ion as well as the quantifier ion for each analyte so that the relative abundance of the two (determined by the molecule-specific fragmentation pattern) can be used to confirm the peak identity. For less specific fragment ions such as common hydrocarbon fragments, more than one qualifier may be required to confirm the peak identity, and the most abundant fragment is often not specific enough (e.g. for linear alkanes that fragment extensively, small fragments are the most abundant, but can also be too ubiquitous in the relevant SIM window to allow their use as quantifiers).

The operator can choose to run the instrument in scan only, SIM only or SIM/scan mode. In the current study, the nature of the samples and analytes resulted in SIM/scan being the best choice (section 2.1.2). While adding a scan to the method does increase the cycle time, it was deemed necessary to maintain confidence in the peaks identified in SIM mode and exclude the possibility of contamination.

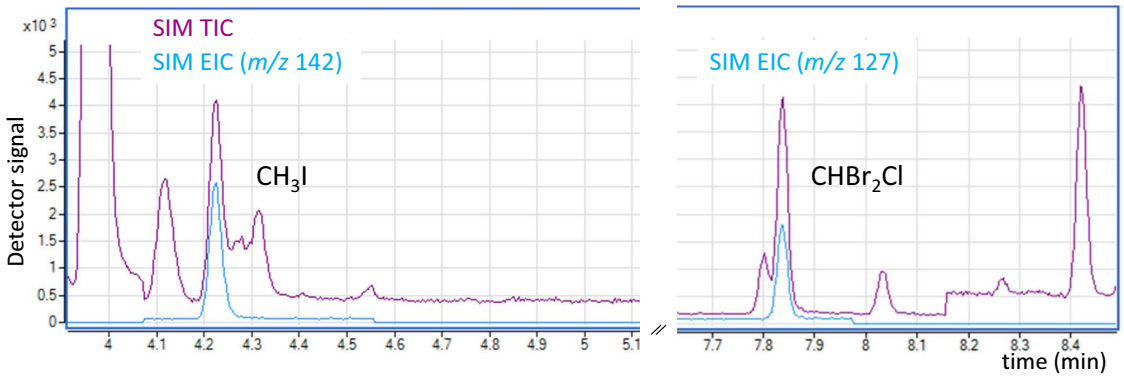

Figure 2.7 – Chromatogram sections (gas standard) illustrating additional resolution gained by MS: SIM TIC (total ion chromatogram) and extracted ion chromatograms (EIC) for m/z 142 and 127, the quantifier ions for CH_3I and $CHBr_2Cl$, respectively.

For peaks that cannot be resolved chromatographically, MS can provide additional information that may allow separation of the analytes in question by using different species-specific quantifier ions, as seen in Figure 2.7. However, this approach relies on the analytes having sufficiently different fragmentation patterns with distinct ions. The poor chromatographic resolution of especially the carene/ocimene pair shown in Figure 2.8 could not be overcome by MS in the current method, as the closely-eluting peaks contain the same

fragment ions due to the similarities in chemical structures, even if the ion ratios are slightly different (Figure 2.8, bottom panel). In practice, these slight differences are only visible in standard analyses where they were employed to assign peak identities. Some fragment ions appear to show better resolution than others (e.g. m/z 121 ct. 93); however to use those as quantifiers would be detrimental to sensitivity since the resolution is only achieved due to the much smaller peak size compared to the chosen quantifier ion (m/z 93 for most monoterpenes). In fact, this effectively enhanced resolution for smaller peaks did simplify the method development for this project, as initial tests that struggled to resolve monoterpene peaks were carried out at much higher sample loadings (large volumes of high-concentration standard), and a marked improvement was observed upon changing to sample loadings more representative of ambient levels. Some peaks in unusually high-concentration ambient samples (especially contaminated air) therefore still cannot be fully resolved.

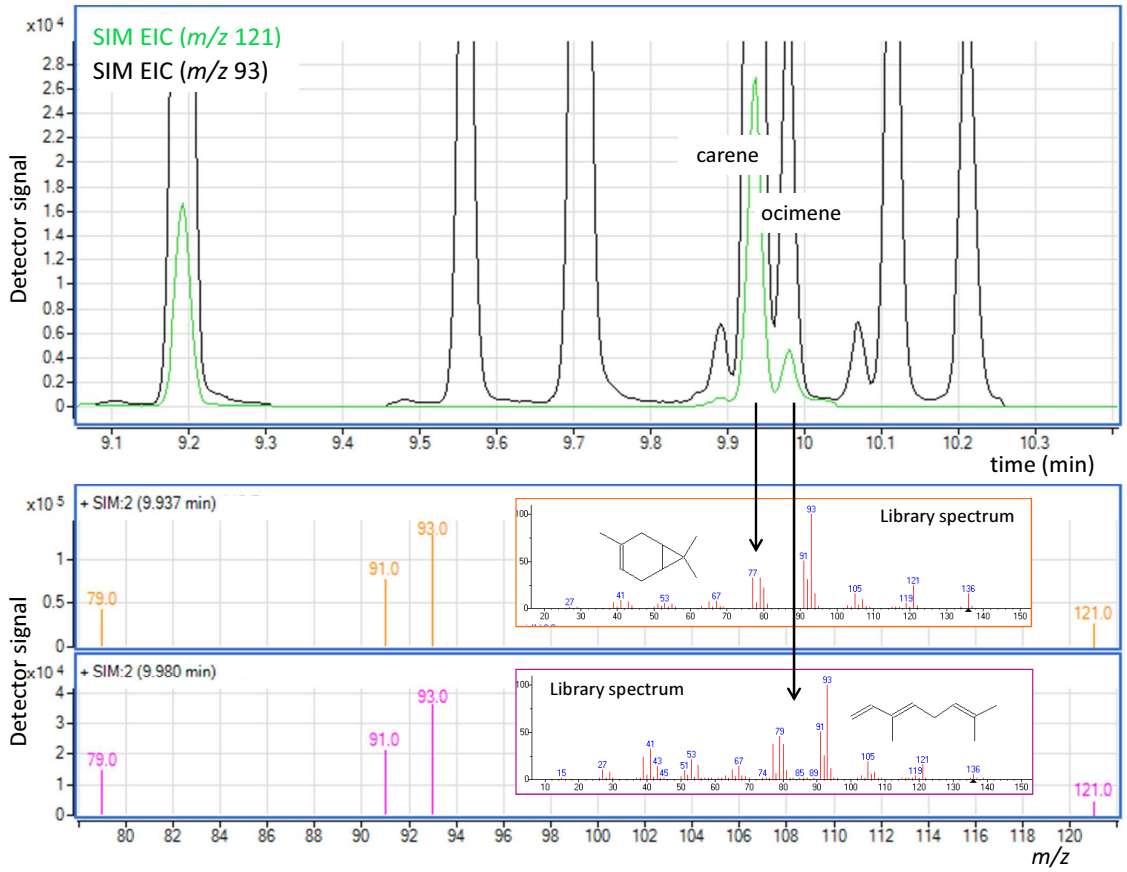

Figure 2.8 – Carene/ocimene resolution for different extracted ions (upper panel) and the corresponding SIM and library spectra (NIST) for those compounds, illustrating the difficulty in further separating the peaks based on MS.

Despite this inability to obtain better resolution for the monoterpenes themselves, MS still provides additional specificity in ambient samples where interferents with monoterpene peaks are common and fragment ions are often the same as those of the monoterpenes (Figure 2.9).

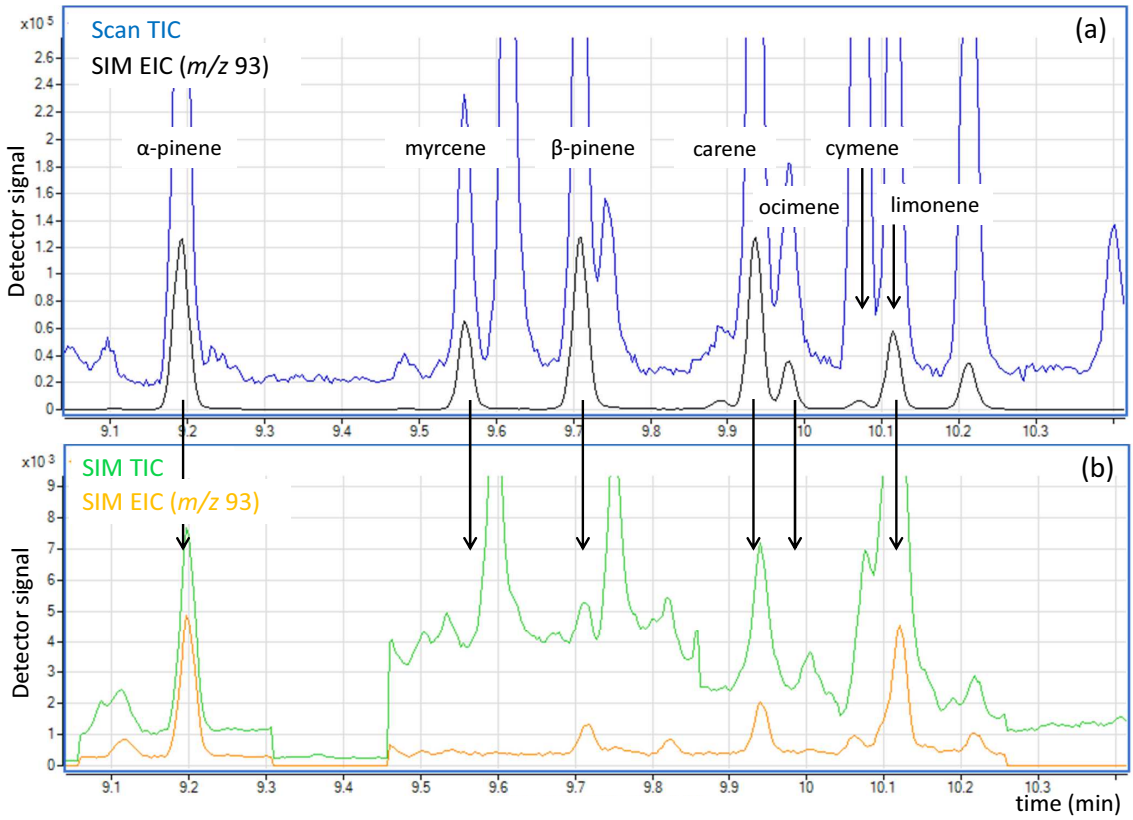

Figure 2.9 – (a) Chromatogram (section) of a gas standard comparing the total ion chromatogram (TIC) in scan mode to the extracted ion chromatogram in SIM mode (SIM EIC) for m/z 93 (monoterpenes). It is obvious that SIM provides higher specificity than only retention time to identify the monoterpenes, e.g. limonene which elutes closely to another standard component with different fragment ions (cymene), and are in a region with generally noisy background; (b) Chromatogram of ambient air (same time window as (a)) comparing SIM TIC to SIM EIC: despite the already reduced number of monitored ions compared to a scan, some fragment ions are still in common with interferents, highlighting the need for SIM EIC for quantitative analysis.

2.1.3 Purge & Trap (P&T)

Analysis of VOCs in seawater is typically performed by either P&T (e.g. Bonsang et al., 1988; Baker et al., 2000; Kettle et al., 2001; Chuck et al., 2005) or by online equilibrator techniques such as Weiss-type, membrane-type equilibrators or equilibrator inlet (An-

drews et al., 2015; Johnson, 1999; Groszko and Moore, 1998; Ooki and Yokouchi, 2008; Kameyama et al., 2010). Weiss-type equilibrators have been widely used for volatile trace gases such as CO, CO_2, N_2O, CH_4 and DMS (Johnson, 1999), and an equilibrator inlet setup has been employed for a number of studies in recent years (e.g. Kameyama et al., 2014, 2010; Beale et al., 2011; Omori et al., 2013).

Equilibrator techniques minimise the amount of water vapour in the gas phase compared to a P&T setup and may not require sample preparation (filtration); however, they are also limited to relatively high-volatility analytes, while samples in a P&T can be heated and purged extensively in order to efficiently extract analytes with lower volatilities.

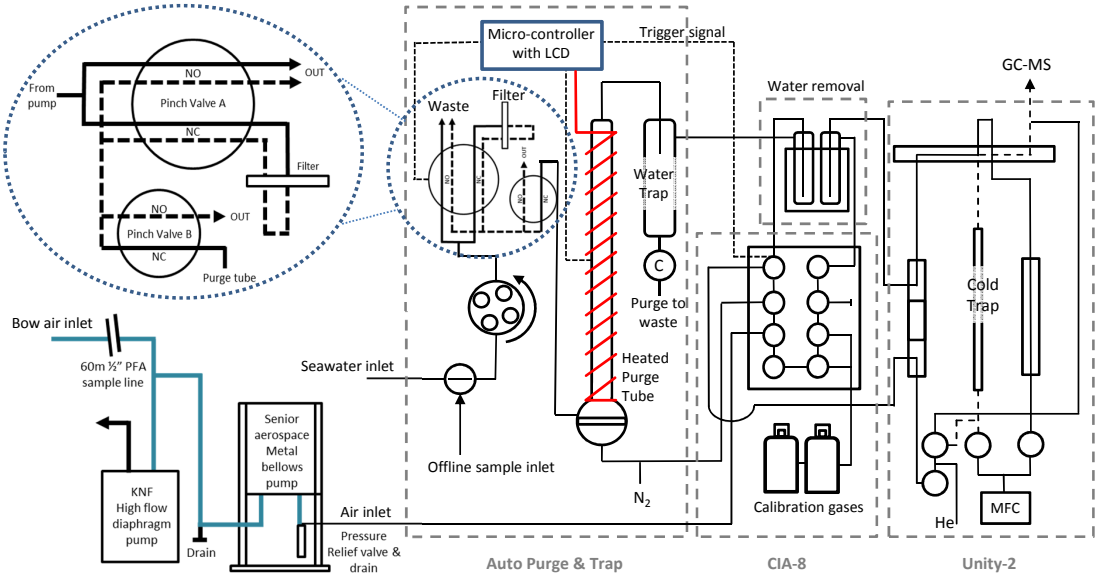

Figure 2.10 – Schematic setup of the P&T system (reproduced from Andrews et al., 2015). NO = normally open, NC = normally closed, MFC = mass flow controller; water trap = drip catcher, water removal = coldfingers in Stirling cooler.

A description of the automated P&T setup used during this study can be found in Andrews et al. (2015). Figure 2.10 shows a schematic drawing of the system, which comprised a peristaltic pump (Watson-Marlow, 1208/DV) transferring the water sample from a high-flow tap to a heated glass purge tube (glass frit porosity 3; large tube: diameter 2.5 cm, height ca. 44 cm; small tube: 2 cm, height ca. 33 cm) *via* a set of valves that were programmed to allow automated filling and emptying of the tube. A dry, clean purge gas (zero grade nitrogen (N4.8), BOC) was bubbled through the water, through a frit in the bottom of the purge tube, and the resultant gas stream containing the analytes

was transferred to the thermal desorption stage. It passed through two water removal setups, one small glass tube designed to condense out some water just after the purge tube ("drip catcher"), the other a water trap held at -30 to -35 °C to significantly reduce the remaining humidity in the sample ("coldfinger"; see also section 2.3.2.4). The whole setup was controlled by code written on Arduino Uno (see modified code for this project in Appendix A).

The system went through several iterations (changes between field campaigns are listed in Table 2.4), one of the most important ones being a change from three-way PTFE diaphragm valves (BioChem 150L3MP24-156) to pinch valves (one dual-channel (valve A), BioChem 100PD3MP24-02S; one single-channel (valve B), BioChem 100P3MP24-02S). The diaphragm valves were found to wear with prolonged exposure to salt water containing biological matter and to start leaking when under pressure, especially during ACCACIA 2. Pinch valves avoid this issue as they have no wetted parts, i.e. no contact with the sample which is transferred via 1/8" clear silicone tubing connected by polypropylene connectors; the flow is stopped by pinching the tubing from the outside. Build-up of biological matter, another disadvantage of the diaphragm valves as they could not be cleaned easily, can be seen in the tubing and addressed by soaking in an acid bath or simply by replacing the tubing.

A further change was the automation of the drip catcher by replacing a manual tap with a 2-way PEEK solenoid valve (valve C, Figure 2.10, BioChem 100T2NC24-62-5P) which was added to the Arduino code in order to empty the drip catcher after each sample. This reduced the risk of breakage from frequent handling of a fragile glassware setup, the need for the presence of the operator to monitor water levels and empty the tube, and also the potential for analytes to re-dissolve when the gas sample stream passed over the liquid water (the latter being of more concern for the more soluble halocarbons than for the terpenes).

The Arduino code was also changed over time to include additional emptying and nitrogen flushing steps to minimise carryover between water samples. Changes to the filtering setup are described in section 2.2.2. A check valve (Swagelok, SS-2C-1) in the gas flow path between the regulator and the purge tube was introduced to avoid water being pushed back into the regulator by the pressure in the purge tube especially during purge efficiency tests, but also to stop the general migration of moisture in the gas lines that would cause

the regulator to break.

2.2 Laboratory method development and validation

2.2.1 Standards

A 16-component NPL (National Physical Laboratory, UK) monoterpenes standard with analytes at 4-5 ppbv was used as the basis for all terpenes calibrations and standard development work during this project ("NPL-MT"; Table 2.2).

Prior to and during AMT 22, the NPL-MT standard was either used directly or diluted to near-ambient concentrations with a clean dilution gas using a set of Mass Flow Controllers (MFCs). A homemade low-concentration standard (NPL-MT standard diluted to around 300 ppt for terpenes, "dmsterps"; Table 2.2) was used for all hydrocarbon calibrations after AMT 22 (laboratory and fieldwork).

Typically, a multi-component ambient concentration halocarbon standard ("NOAA"; National Oceanic and Atmospheric Administration, USA; SX cylinder filled in 2011; various very short-lived halocarbons (VSLHs) in air) was analysed in each calibration block alternating with the terpenes standard. As the NOAA standard also contained isoprene (ca. 220 pptv), this made it possible to confirm isoprene calibrations using an independent measurement on the same analytical system.

For the NPL-MT standard, the MFC dilution system comprised a low-flow MFC for the high-concentration standard gas (MKS Type 179A, 10 sccm; used at 2-10 mL min^{-1}) and a high-flow MFC for the dilution gas (MKS Type 179A, 1000 sccm; typically set to *ca.* 500 mL min^{-1}). Dilution gas blanks were measured on a regular basis with dilute calibrations. A number of dilution gases were tested during method development and scrubbed ambient air was determined to be the best option. Achieving stable concentrations when diluting the NPL-MT standard was found to depend strongly on the humidity of the dilution gas. Dry cylinder gases (BTCA air or zero grade nitrogen (N4.8); BOC, UK) resulted in poor reproducibility and recovery at low concentrations (*ca.* 50 ppt), while scrubbed ambient air (lab or outside air diverted through a VOC scrubber containing Pt-coated alumina beads in a 1/2" stainless steel tube held at 400 °C) maintained its humidity and

produced stable results. Humidified cylinder gases achieved similar reproducibility. The use of scrubbed ambient air rather than humidified nitrogen during AMT 22 additionally ensured that humidity levels in standards, while variable throughout the cruise, were practically identical to those in air samples and minimised changes in the sample introduction system.

The low-concentration working standard (dmsterps) was prepared by diluting the NPL standard with humidified BTCA air into an Experis cylinder, to approximately 300 pptv terpenes. As part of further standard development work, DMS (dimethyl sulfide) was also added at a similar concentration to the other analytes. Stability of this standard was monitored against the NPL-MT and NOAA standards over time. Standard validation and calibrations are discussed in more detail in section 2.4.3.

Table 2.2 – Components and concentrations (in pptv) of gas standards used during this project.

Standard	**NPL-MT**	**dmsterps** [b]	**NOAA (SX-3750)**
Analyte			
Isoprene	4970 ± 100	360.0 ± 38.8	221 ± 1.56
α-pinene	5040 ± 150	356.9 ± 44.0	-
Myrcene	5560 ± 280	289.8 ± 101.9	-
β-pinene	4750 ± 240	350.7 ± 54.3	-
δ3-carene	5230 ± 260	355.9 ± 56.5	-
Ocimene [a]	5070 ± n.d.	197.3 ± 64.5	-
Limonene	5020 ± 250	323.8 ± 55.6	-
Benzene	5020 ± 100	444.4 ± 59.7	81.7 ± 1.53
Toluene	4960 ± 100	384.4 ± 41.7	49.9 ± 0.88
Ethylbenzene	5240 ± 100	397.8 ± 41.6	-
m-xylene [c]	5330 ± 110	*(m/p)* 396.0 ± 42.7	-
p-xylene [c]	5390 ± 110	*(m/p)* 396.0 ± 42.7	-
o-xylene	5320 ± 110	398.9 ± 42.4	-

[a] Error not stated on certificate, n.d. = not determined.

[b] Also see section 2.4.3 for details.

[c] Unresolved in current method.

2.2.2 Water analyses

The automated Purge & Trap setup (described in section 2.1.3) was tested for monoterpenes sampling in the laboratory prior to deployment on AMT 22. A sample volume of 84 mL was chosen to maximise sensitivity while limiting the sampling time to 10 % of the total 20 min purge time, based on a maximum peristaltic pump flow rate of *ca.* 42 mL min^{-1}. Purge efficiencies were initially established by repeat purges of spiked MilliQ water (pmol L^{-1} -level monoterpenes from Sigma-Aldrich) and found to be approximately 100 % for all target monoterpenes and isoprene at 40 °C and 50 mL min^{-1} purge gas flow (zero grade N_2 or scrubbed ambient air) for 20 min. Limiting the sample volume, the purge time and the purge tube temperature as much as possible helps to maintain the instrument performance as less water vapour is transferred across into the GC-MS. With an increase in the number of target analytes to include VSLHs, which have much lower purge efficiencies, the purge tube temperature was adjusted to 50 °C during AMT 22.

As the target analytes are known to be biogenic (e.g. Shaw et al., 2010; Tokarczyk and Moore, 1994), it was necessary to minimise biological activity in the samples during storage and in the purge tube to maintain dissolved gas concentrations as close to those at the point of sampling as possible. Typically, seawater samples are filtered or poisoned to achieve this (e.g. Bryant et al., 2013). Filtration was chosen as the preferred method since to our knowledge, the effects of the widely used $HgCl_2$ on cells with respect to isoprene or monoterpene production have not been investigated, and adding substances introduces a potential source of contamination. As some authors even avoid filtration altogether based on its potential to introduce contamination or create sampling artifacts (Beale et al., 2010; Tran et al., 2013), careful testing was carried out to establish the suitability of this approach for the present study. Whatman GF/F filters (glassfibre, 0.7 µm nominal pore size) are commonly used to collect samples for e.g. HPLC pigment analysis and were chosen for the current analyses in preference to smaller pore sizes as they remove the majority of the active biological matter present in the water without restricting the water flow rate. Many of the pores in GF/F filters are smaller than the nominal pore size, and the larger pores quickly become blocked by particulate matter from the samples, so that virtually all of the picoplankton present in samples was removed, despite some cells being <0.7 µm, as determined by flow cytometry (P. Lange, pers. comm. 2015). Tests with finer filters strained the peristaltic pump and increased the P&T system pressure and

hence the risk of leaks. Different filter materials were found to introduce contamination, including terpenes, and were therefore unsuitable for this application. A large-diameter (90 mm) GF/F filter was used during AMT 22, but smaller (22 mm) filters during the ACCACIA cruises and AMT 23. Due to filter holders leaking increasingly during the ACCACIA cruises, pre-fabricated syringe filters (26 mm Minisart GF, Sartorius) were used for AMT 23 underway sampling. Sampling protocols for DMS prescribe a filter change after each sample to avoid build-up of biological matter on the filter that may influence results as well as a slow filtration speed to minimise mechanical stress on cells (Bell et al., 2011). A laboratory test using spiked MilliQ water with the large GF/F filter in line however suggested the system needed several samples to condition and as a result, that filter was changed very infrequently during AMT 22. For the later cruises, filters were changed between each sample in order to follow typical DMS protocols, and further laboratory testing showed no terpene losses for those filters. The initial test may have been erroneous, but the waters sampled during AMT 22 were generally oligotrophic and results indicated no adverse effects of the infrequent filter changes.

Post-cruise method qualification work was carried out to determine characteristics of the P&T system including typical seawater purge efficiencies and reproducibility for both the 80-mL and the 20-mL purge tube used on the cruises, with results published in Andrews et al. (2015) (reproduced in Table 2.3). The experiments used Arctic deep water that was collected during ACCACIA 2 and subsequently aged, filtered *via* a 0.2 µm filter and sparged with zero gas (scrubbed outside air) for several hours before using it as a matrix into which near-ambient level terpenes and halocarbons were spiked (pmol L^{-1} range, based on oceanic measurements). Using real seawater ensured a clean background with any potential matrix effects comparable to real samples, which was not possible to achieve with MilliQ or commercially available water such as LC-MS water (these were especially not clean with respect to halocarbons; see Andrews et al., 2015). A variety of tests showed good reproducibility of the system for samples introduced from both bottles and syringes and for different sampling parameters, as used on fieldwork. Additional performance testing was carried out during campaigns with each specific setup (see section 2.3), as some system characteristics changed with even slight differences in conditions.

Table 2.3 – Purge efficiencies for terpenes. RSD = relative standard deviation.

	%purge eff.	**%RSD**	**%purge eff.**	**%RSD**
compound	84 mL	84 mL	20 mL	20 mL
Isoprene	96	1.7	97	0.7
α-pinene	100	1.4	99	1.6
Myrcene	100	9.0	100	20.1
β-pinene	100	0.6	96	3.2
Carene	100	1.3	94	0.1
Ocimene	97	1.8	100	5.2
Limonene	100	2.1	98	3.3

2.2.3 Sample analysis

Water removal by counter-flow MD^{TM}-series Nafion® gas drier (Permapure^{TM}) was found to remove or degrade monoterpenes and therefore a glass water trap ("coldfinger") was used, held at -25 to -30 °C by an ethylene glycol chiller (Grant R3) or by a free piston Stirling cooler (Twinbird, SC-UD08 FPSC) fitted with a coldfinger holder and controlled by Arduino Uno code (Andrews et al., 2015). The coldfinger also caused monoterpene losses for temperatures below -40 °C.

The GC-MS method used for laboratory method development was identical to that used during fieldwork (described in section 2.2.3), after initial optimisation of the method described in section 2.1.

2.3 Cruise measurements

2.3.1 Details of the field campaigns

Data for this study was collected during four research cruises and also at the Cape Verde Atmospheric Observatory (CVAO). Two of the research cruises (AMT 22 and AMT 23) were part of the Atlantic Meridional Transect (AMT), a multidisciplinary programme coordinated by Plymouth Marine Laboratory (PML) and the National Oceanography Centre in Southampton (NOCS). The programme is now funded by NERC's National Capability, after a period of funding through NERC's Oceans 2025 programme, and cruises are

undertaken on the research ships' annual return passages between the UK and the South Atlantic (e.g. Montevideo, Chile, Falkland Islands, South Africa; http://amt-uk.org/; Robinson et al. (2006)). AMT 22 (JCO79; Southampton (UK) - Punta Arenas (Chile), 10/10-24/11/2012) took place on the RRS James Cook; AMT 23 (JR300; Immingham (UK) - Port Stanley (Falkland Islands), 05/10-06/11/2013) on the RRS James Clark Ross (JCR).

The other two cruises formed part of the ACCACIA (Aerosol-Cloud Coupling and Climate Interactions in the Arctic) project by a consortium of the Universities of Leeds, York, Manchester and East Anglia as well as the British Antarctic Survey (BAS) funded under the NERC Arctic Research Programme (http://arp.arctic.ac.uk/projects/aerosol-cloud-coupling-and-climate-interactions-ar/). The first of the two (ACCACIA 1; 15/03-31/03/2013) went out of Tromsø (Norway) into Arctic waters on the Norwegian research ship R.V. Lance (Norwegian Polar Institute, NPI); for ACCACIA 2 the JCR travelled to similar regions of the Greenland/ Iceland/ Norwegian (GIN) Seas from the UK (JR288; Immingham - Dundee, 14/07-12/08/2013). Cruise tracks are shown in Chapter 3 (section 3.2.2).

Measurements of a number of VOCs and VSLHs in ambient air and surface seawater as well as at depth were made during the AMT 22, AMT 23 and ACCACIA 2 cruises using the (AutoP&T)-TD-GC-MS system described above. Measurements during the ACCACIA 1 cruise were obtained in an identical fashion to ACCACIA2, using the NOAA standard for calibration of isoprene data (no monoterpenes calibration available). On all cruises except AMT 22, two instruments were deployed, with one dedicated to water and one to air analysis (only one instrument for both air and water on AMT 22). A typical measurement cycle on the water instrument ("Wendy", AutoP&T-TD-GC-MS) consisted of an air and a water sample followed by a nitrogen blank to reduce carryover and water levels in the system, with a cycle time of between 60-90 minutes. The air instrument ("Anna", TD-GC-MS only) sampled between 2-3 air samples per hour. Details of the setup changes and parameters used on the different field campaigns are listed in Table 2.4.

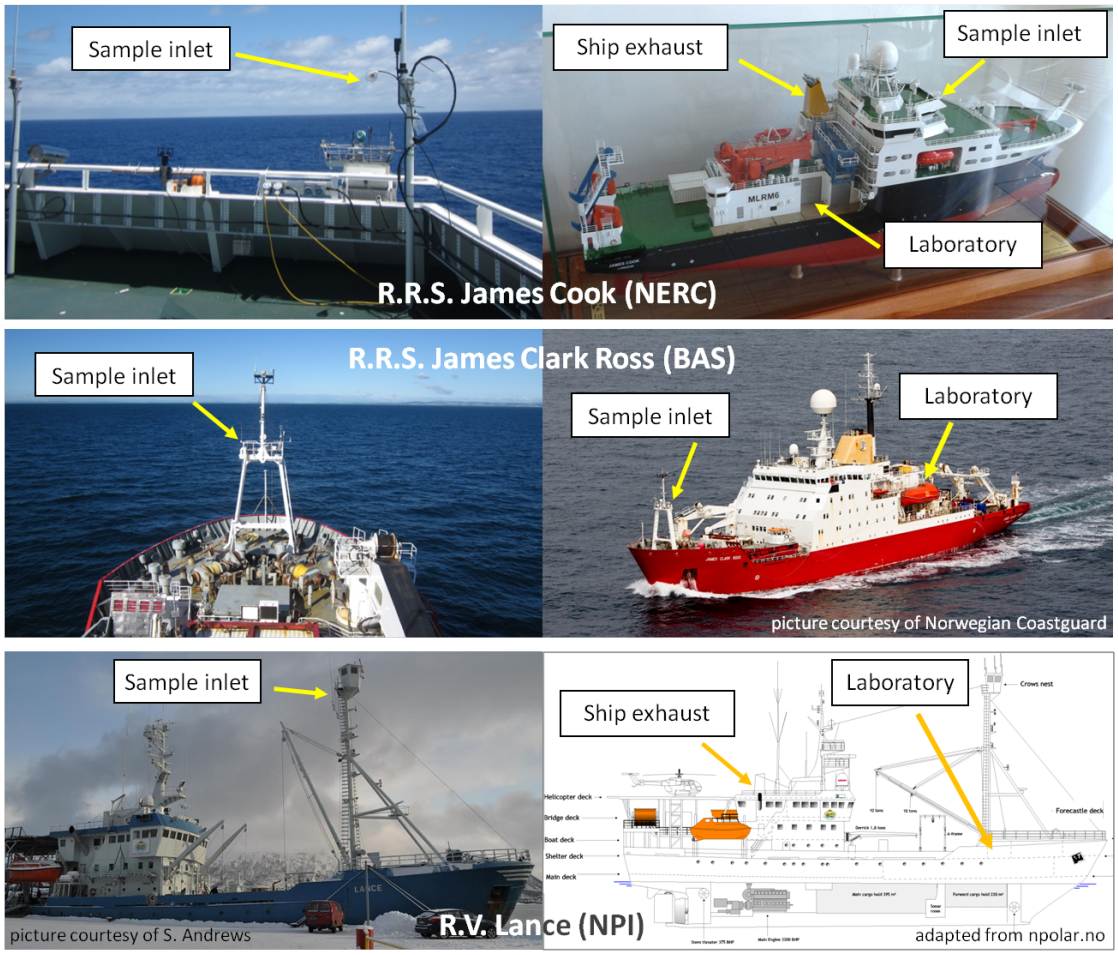

Figure 2.11 – Locations of the sample inlet and laboratories on the R.R.S. James Cook (Natural Environment Research Council, NERC), R.R.S. James Clark Ross (British Antarctic Survey, BAS) and R.V. Lance (Norwegian Polar Institute, NPI).

Table 2.4 – Sampling parameters for the autoP&T system throughout the different cruises.

	AMT 22	**ACCACIA 1 and 2**	**AMT 23**
Tubing and valves	Tygon tubing (1/8" ID), diaphragm valves	Tygon tubing (1/8" ID), diaphragm valves	Tygon tubing (1/8" ID); silicone tubing (1/8" OD) in pinch valves
Transfer line to TD	1/8" instrument grade steel tubing	1/8" instrument grade steel tubing	1/16" stainless steel tubing
Peristaltic pump speed	42 mL min^{-1}	12.5 mL min^{-1}	12.5 mL min^{-1}
Filter	90 mm GF/F in stainless steel holder	22 mm GF/F in polycarbonate holders	26 mm GF/F Minisart syringe filters
Water volume	84 mL	20 mL	80 mL
Purging	20 min at 50 mL min^{-1} Prepurge 5 min	20 min at 50 mL min^{-1} Prepurge 5 min	30 min at 50 mL min^{-1} Prepurge 5-7 min
Trapping	(Wendy) -20 °C	Anna -30 °C Wendy -27 °C	Anna -26 to -30 °C Wendy -27 to -25 °C
Water removal	One coldfinger between CIA8 and Unity	One coldfinger between CIA8 and Unity *plus* one each on the air and water sampling lines (pre-CIA8)	One coldfinger each on the air and water sampling lines (pre-CIA8); some periods with additional coldfinger between CIA8 and Unity
CTD sampling	Screwtop amber glass bottles; stored unfiltered until analysis	Stoppered amber glass bottles; filtered via syringe into bottle	Stoppered amber glass bottles and glass syringes (different filtration methods, see text)
Calibration standards	NPL-MT (pure/via MFC dilution box), calibration *ca.* every 1.5 days; NOAA (in SilcoCan®), calibrated after each instrument tune	*ACCACIA 1&2:* NOAA, daily calibration; *ACCACIA 2 only:* dmsterps, daily calibration	dmsterps and NOAA, daily calibration

2.3.2 Sample introduction

2.3.2.1 Air and standards

Air was drawn down a sample line (shrouded 1/2" PFA (Swagelok), *ca.* 80 m long) by a diaphragm pump (KNF, model N035.1.2AN.18; flow rate *ca.* 4.5 L min^{-1} (AMT 22)/*ca.* 34 $Lmin^{-1}$ (AMT 23, ACCACIA)) and sub-sampled through a metal bellows pump (Senior Aerospace, MB-158; via heated 1/4" and 1/8" stainless steel lines). During AMT 22, the sample stream was also diverted via a heated gas ballast (glass, volume *ca.* 0.7 L) in order to minimise flow and pressure fluctuations caused by the pumps that affected MFC stability. All lines were maintained at a temperature of around 40-60 °C (constant for each setup, but variable between cruises) with heating tapes (RS Components) and insulation (Armaflex). The sample line inlet was situated forward of the bridge on the monkey island or on the meteorological platform at the bow of the ship (see Figure 2.11), in order to minimise the influence of ship exhaust on samples. It was also protected from rain by the top of a plastic bottle attached to the end of the sampling line, and from sampling insects or large particles by a Swagelok stainless steel in-line filter (SS-8F-x; x = 7 or 60 (µm pore size)).

The setup during AMT 22 included the MFC system detailed in section 2.2.1 in order to dilute the high-concentration NPL-MT standard to near-ambient levels (*ca.* 20 - 250 pptv). A 3-way tap on the air sampling line downstream of the gas ballast allowed switching between sampling air directly and diverting the flow through the VOC scrubber, to use as a dilution gas for calibrations.

Separate sampling ports were used for undiluted standards, N_2, P&T and air samples, while dilute standard was introduced from the MFC system via the same setup as air (AMT 22; see Figures 2.10 and 2.12; all lines heated 1/4", 1/8" or 1/16" stainless steel). A pressure relief valve just before the sampling port allowed continuous air flow through the setup to minimise the volume of stagnant air between sampling periods and ensure consistent mixing of the two gas streams in the case of dilute calibrations. During ACCACIA 2 and AMT 23, the pressure relief valve was situated before the air sample passed through the in-line water trap ("coldfinger") on the air line and a longer sample pre-purge was used to ensure good flushing of the system before each air sample.

Ambient air and dilute standard were typically sampled at 100 mL min^{-1} for 10 min (increased to 20 min for air samples at different points during the different cruises), NOAA standard generally at 100 mL min^{-1} for 5 min, pure NPL-MT standard at 50 mL min^{-1} for 0.5-3 min and dmsterps standard at 50 mL min^{-1} for 2-6 min. Calibrations during AMT 22 were performed as close to once every 1.5 days as sampling allowed, occasionally using undiluted standard. NOAA standard (in a 3 L SilcoCan® canister (Restek) filled from the original NOAA SX-3750 standard) was sampled once after each instrument tune where possible. On ACCACIA 2 and AMT 23, instruments were calibrated daily, alternating the dmsterps and NOAA standards; during ACCACIA 1, daily calibrations were performed using only the NOAA standard (no calibration available for monoterpenes on that cruise). Most calibrations were one-point calibrations (2-3 replicates), with several linear calibrations throughout each cruise which were achieved by different dilution settings for the MFC setup and by sampling different volumes for undiluted standards.

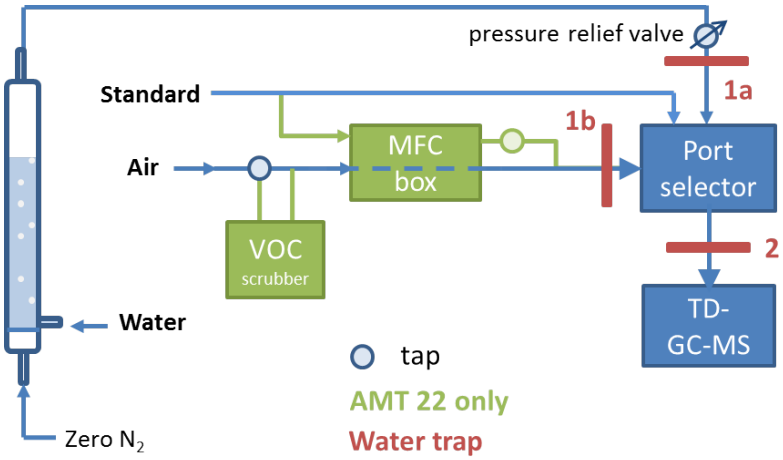

Figure 2.12 – Schematic setup of the sample introduction system (purge tube on the left); items only used on AMT 22 are shown in green. Water removal is shown as for ACCACIA 1 & 2; for AMT 22 only water trap 2 was in place, for AMT 23 only 1a & b. Also see Figure 2.10 and Table 2.4 for more detail.

2.3.2.2 Water samples

Dissolved trace gases in seawater were analysed by autoP&T (Andrews et al., 2015; details in section 2.1.3). Water was taken from the ship's non-toxic seawater supply (*ca.* 5 m depth) by subsampling from a fast flow (*ca.* 3-4.5 L min^{-1}; 1/2" ID Tygon tubing connected to the tap) using a peristaltic pump (Watson-Marlow; at *ca.* 12.5 mL min^{-1}

(42 mL min^{-1} for AMT 22)). A 3-way tap allowed manual switching to discrete samples from CTD casts (semi-automated), introduced from bottles or syringes.

CTD samples were collected directly from the Niskin bottles on the CTD rosette into amber glass bottles or glass syringes (screwtop for AMT 22, glass stoppers for all other cruises; syringes or bottles for AMT 23), using a piece of Tygon tubing and overflowing the bottle for several seconds (2-5 bottle volumes) or rinsing the glassware 2-3 times for slower sampling techniques with direct filtration, taking care to avoid bubbles and headspace. For all cruises except AMT 22, water was filtered through a GF/F filter immediately upon sampling; samples were then stored in a fridge until analysis (dark; *ca.* 2-8 °C). More specifically, both ACCACIA cruises employed a combination of syringes, taps and a filter to transfer water directly from the Niskin bottles into the glass sample bottles (slightly overflowing the bottles). During AMT 23, CTD water was generally sampled into bottles (due to time constraints) and subsequently filtered into glass syringes before storage. Later in the cruise, when timings allowed the sample to be analysed within approximately 30 minutes, some unfiltered samples were also directly introduced from the glass bottles via the peristaltic pump and in-line filter in an identical fashion to underway samples and all of AMT 22.

During P&T sampling, water (*ca.* 80 mL (AMT) / 20 mL (ACCACIA)) was introduced into the purge tube (held at 50 °C) through a series of valves and flexible tubing as well as a 400 µm steel mesh and a GF/F filter (Whatman; none for pre-filtered discrete samples) to avoid valve blockages and remove the majority of biologically active sample content, respectively. Using zero-grade nitrogen as the purge gas, samples were purged for 30 min (20 min for AMT 22) at 50 mL min^{-1} and the gas stream was transferred to the sampling port via heated stainless steel tubing. Table 2.4 gives sampling setup and parameter details for each cruise.

Storage tests indicated that the typical time elapsed between CTD sampling and analysis (performed as soon as possible after collection and generally <10 h for full profiles with 6-9 samples) did not adversely affect concentrations within analytical uncertainty for most compounds (see Figure 2.13). For AMT 22, myrcene, carene and ocimene fell to below detection limit (DL) at the 24h-point. For AMT 23, it was not possible to evaluate tests for myrcene, carene and ocimene as these analytes were below the DL for part of the tests; this was also the case for β-pinene on ACCACIA 2. Storage stability of β-pinene on

AMT 23 could not be assessed as no usable data was available for the compound at the time of the tests.

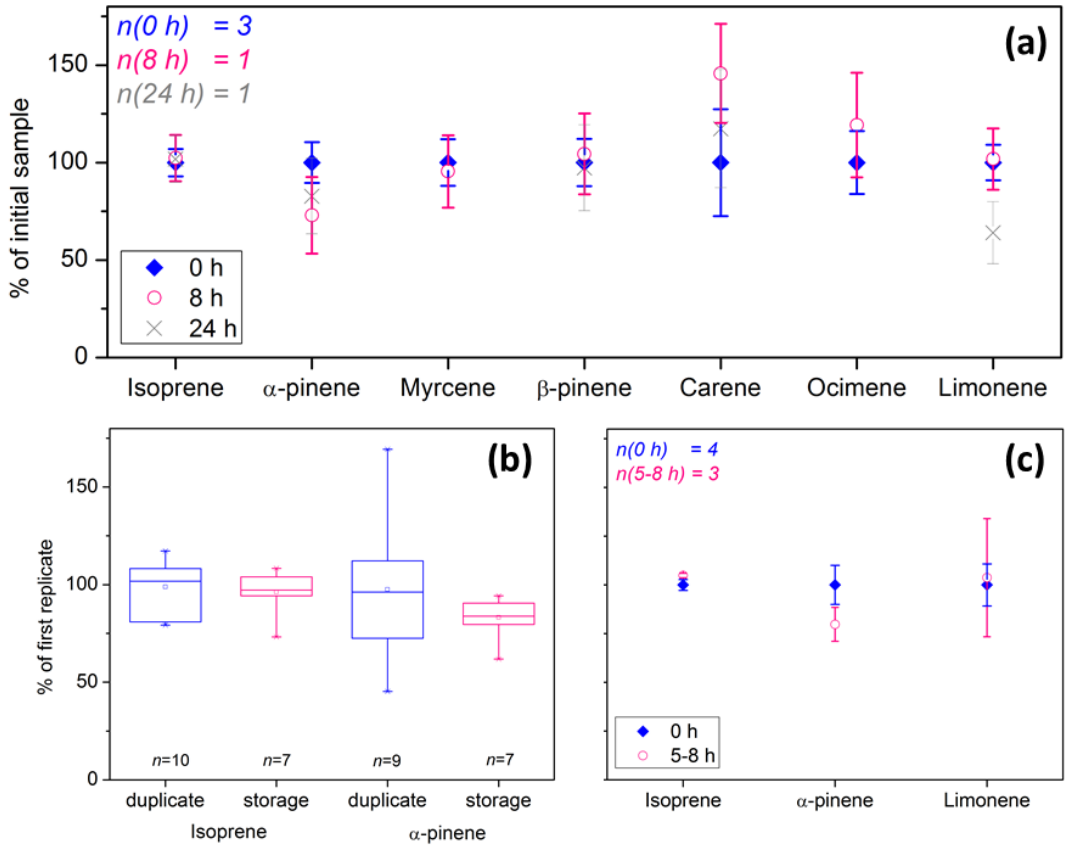

Figure 2.13 – Effect of storage on duplicate CTD samples during (a) AMT 22, (b) ACCACIA 2 and (c) AMT 23; no usable data available for compounds that are not shown (calibration issues or values below detection limit). (a) error bars showing propagated analytical errors; (b) mean (symbol), median (line), 25^{th} to 75^{th} percentile (box), 5-95 % (whiskers); (c) error bars showing standard deviation of the test results.

2.3.2.3 Ozone removal

Ozone trapped alongside the analytes has been reported to cause degradation of the samples on the cold trap (e.g. Helmig, 1997; Dettmer and Engewald, 2002) and therefore should be removed from the sample stream. To achieve this, the 1/8" stainless steel lines after the metal bellows pump were heated to *ca.* 60-70 °C along a length of *ca.* 80 cm (similarly to Hopkins et al. (2011)) in addition to the pump itself being at comparably high temperatures when in operation.

This setup removed *ca.* 30 % of the ozone present in the air, as measured by a UV photometric ozone analyser (Thermo Electron Corporation, Model 49i) from the same air inlet as the GC-MS air samples, which was considered acceptable since ambient ozone levels were typically only between 20-50 ppbv. Terpene losses observed by various authors are generally from relatively humid air (mostly 50 % humidity or higher) sampled onto sorbent tubes (Tenax TA or other materials) rather than on a thermal desorption cold trap with prior water removal.

2.3.2.4 Water removal

Marine air samples and especially P&T samples introduce large amounts of water into the system that must be removed prior to trapping and analysis to ensure continued instrument functionality. A "drip catcher" (small glass water trap) removed water from the P&T sample gas stream immediately after the purge tube, condensing typically 1-2 mL per sample that could then be discarded via an opening at the bottom of the glass tube. The design improved from a manual tap that was opened every few samples (with increased risk of breaking glassware in the fragile setup) to a code-controlled solenoid valve emptying the water after every sample (see also section 2.1.3).

Further water removal from all sample types was achieved by one to two in-line glass water traps ("coldfinger") held at *ca.* -30 °C by a free piston Stirling cooler as in the laboratory (more suited to shipboard use than an ethylene glycol chiller). Details of this setup varied between cruises (listed in Table 2.4) as the system and our understanding of it improved over time. AMT 22 used a single coldfinger between the CIA8 and the Unity. This was found to need frequent changing, causing downtime approximately once every 1-2 days, and had strong memory effects for some analytes (especially ocimene and myrcene). Since the design was still in an early development stage, the temperature control was also likely not always accurate, which may have led to some losses if temperatures became too low (monoterpenes were partially removed if the coldfinger was below -40 °C; Andrews et al., 2015). Instrument sensitivity decreased significantly throughout the cruise.

Both ACCACIA cruises used a coldfinger at that same point (on both instruments), but additionally one coldfinger each on the air and water sample lines in order to remove more moisture prior to entering the sampling ports. The air and water line coldfingers

could be changed with a minimum of sampling downtime and both pre-Unity coldfingers collected very little water during the whole cruise. For AMT 23, the pre-Unity coldfingers were therefore largely not used, in order to reduce memory effects in the lines and allow a shorter pre-sample flushing time. However, they were put in line several times due to issues with calibrations that had not been observed previously, but were not used permanently on both instruments due to the overall setup making it highly impractical/impossible. Figure 2.14 displays the sensitivity changes for the water instrument for the four cruises.

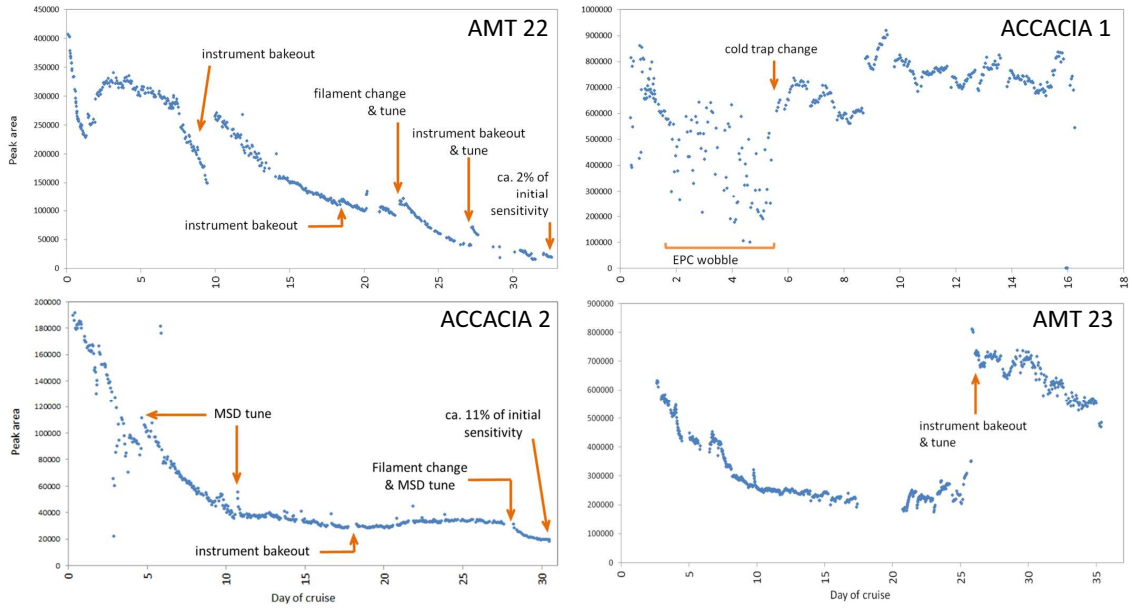

Figure 2.14 – Instrument sensitivity changes tracked by CCl_4 in air: for ACCACIA 1 & 2 and AMT 23, optimised MS parameters (temperatures, drawout plate) were used, resulting in more stable instrument performance overall compared to AMT 22. The change from using one (AMT 22) to two (ACCACIA) and back to one (AMT 23) coldfinger did not appear to affect the air data.

2.3.2.5 Sample enrichment

Analytes were trapped on a cold trap (packed with Tenax TA (20/35 mesh) and quartz or glass wool; materials from Markes Int. and Supelco) held at -20 to -30 °C (see Table 2.4) and desorbed without split at 240 °C for 3 min. Breakthrough tests confirmed quantitative retention of low-concentration standards using up to 2.5 L sample volume at these temperatures.

2.3.3 GC-MS methodology

A new GC-MS method capable of resolving most target analytes was developed in preparation for AMT 22 (also see section 2.1). Analysis was performed on an Agilent 6850 GC with a 5975C MS, coupled to a Markes International flow selection and thermal desorption unit (CIA8-UNITY2) as the sample introduction system. A description of the theoretical background for this instrument can be found in section 2.1.

The final method used a BPX5 capillary column (5 % Phenyl Polysilphenylene-siloxane stationary phase; 50 m, 0.32 mm ID, 1 µm film thickness, SGE) with a helium (CP grade, BOC) flow rate of 2 mL min^{-1} and the following temperature programme: 2 min hold at 40 °C, increase to 240 °C at 20 °C min^{-1} and 2-5 min hold at 240 °C. The final hold time was adjusted for different sample types in order to maintain the sampling time as the limiting step in the analysis while maximising the column bakeout time. After AMT 22, the MS temperatures were increased compared to standard settings to maintain the instrument cleaner and more sensitive for longer, to 200 °C for the MS source and 250 °C for the quadrupole. The usual 3 mm drawout plate was also replaced with a 6 mm drawout plate, aiming to stabilise MS sensitivity despite high sample water content. These measures contributed significantly to an improved instrument performance throughout the latter cruises (Figure 2.14).

Table 2.5 – Quantifier and qualifier SIM ions for each analyte (terpenes) in the final GC-MS method.

Analyte	**Quantifier ion**	**Qualifier ion(s)**
Isoprene	67	68
α-pinene	93	77, 121
Myrcene	93	69, 41
β-pinene	93	69, 41
3-carene	93	79, 91, 121
Ocimene	93	79, 91, 121
Limonene[a]	93 (68)	68 (93)

[a] Limonene was usually quantified using m/z 93, but some instances exist where m/z 68 was more suitable (see section 2.4.1).

The MSD acquired both scan and SIM data, with one quantifier ion and one to three qualifier ions for each analyte as detailed in Table 2.5. Including too many ions increases the duration of each measurement cycle time and reduces the number of points per chromatographic peak (also see section 2.1.2). A scan cycle, even if it is kept to as small a range as the analyte and sample characteristics allow (in this case, *m/z* 58-160), has the same overall effect. However, availability of scan data can in some cases help to identify an interference, but more importantly can help to confirm the presence (or absence) of contamination if a sample appears suspect, where SIM (selected ion monitoring) data does not provide sufficient information. Ideally, SIM ions should be selected to include potential interferent ions and eliminate the need for scan data, but as the monoterpenes elution window was often noisy due to a variety of contamination, it was decided to keep the scan to detect major contaminants or their fragments rather than add numerous ions to monitor contamination and potentially still miss some. Scan data was also useful for adding SIM ion windows for further analytes in some cases.

Baseline resolution was achieved for most components in standard runs at low concentrations (equivalent to *ca.* <100 pptv in 1 L sample, depending on instrument sensitivity; carene/ocimene pair never resolved) in SIM mode. Sampling larger amounts of standard resulted in peaks merging; however, expected/typical atmospheric mixing ratios were at or below levels for which peaks were resolved. The much more complex matrix of environmental samples contained a variety of interfering species that were often poorly resolved from analyte peaks in air and water samples and caused a generally high and variable baseline for the main monoterpene quantifier ion (*m/z* 93).

As indicated above, the instrument dedicated to water analysis (Wendy) typically followed each water sample with a cleaning sample and an air sample. The cleaning sample was a zero N_2 sample with the cold trap held at +50 °C and run with a GC-MS bakeout method (oven held high for most of the run), designed to flush all TD lines and the cold trap with dry, clean gas and to keep moisture in the overall system as low as possible. The air sample was usually a smaller air volume than that sampled on the air instrument (Anna) at the time, e.g. 500 mL rather than 1-2 L, resulting in higher limits of detection for those samples. However, its predominant purpose was to supply bracketing CCl_4 measurements for the water samples, which did not require a low LOD due to high atmospheric CCl_4 concentrations. Where air measurements from a second instrument are available, air data

from the water instrument are ignored.

During AMT 23, the cycle consisted of only water and air samples, as an increased air pre-purge volume was sufficient to flush the TD lines. This was largely due to a reduced dead volume compared to the other cruises, achieved by removing the pre-Unity coldfinger (as discussed above). During this cruise, water sampling was also periodically switched to Anna due to instrument issues, so that the separation of air and water analyses was lost, similarly to AMT 22 when only Wendy was deployed.

2.3.3.1 In-situ method development/performance tests

Purge tube temperature and purge time were varied (40/50/70 °C and 10-50 min) in a number of in-campaign experiments and purge efficiency evaluated for the different settings. For the terpenes, the most commonly used parameters (see Table 2.4) all gave results similar to the laboratory tests (Table 2.3, around 100 % purge efficiency within analytical error), which were therefore considered to be representative of all campaign data.

System reproducibility was tested by analysing replicates of underway water stored in a Tedlar bag, and sample reproducibility and stability by analysing several bottle samples filled from the underway supply at the same time and stored unfiltered in the fridge or at lab temperature for up to 24 hours (AMT 22), or by taking replicate samples from Niskin bottles and analysing them immediately and up to 10 hours after sampling (stored at 2-8 °C in bottles for ACCACIA 2/ syringes for AMT 23).

2.4 Data analysis

2.4.1 Peak integration

In the past, research groups have often relied on manual integration of environmental samples as integration software has not been able to process data with poorly resolved, badly shaped or small peaks (Plass-Dülmer et al., 2002). This is extremely time-consuming for large numbers of samples and analytes and introduces an error associated with the an-

alyst performing the integration. A software designed mainly for long-term atmospheric observations at e.g. Global Atmospheric Watch stations, GCWerks (P. Salameh, USA, 2011; gcwerks.com), was used for all results in this study. Initial checks, especially during deployment, and qualitative investigations into contamination using the MS scan chromatograms were performed in the Agilent Chemstation software.

Analyte peaks were integrated from extracted quantifier ion chromatograms of the SIM trace for each sample (Table 2.5), using automated integration in the GCWerks software where possible, with optimised integration parameters for each peak. Where automatic integration failed to adequately integrate or identify the peak, further adjustments were made to the integration parameters as necessary. This intervention is referred to as "manual integration" here, even if it is dissimilar to "traditional" manual integration (drawing a baseline by hand), as it is manually adjusted within a software which has limited provisions for manual integration otherwise. This integration method is of course not free from error and different analysts will still optimise parameters differently, but it provides a more robust approach. Sources of error, including integration error, and their contributions to the final uncertainty of the measurement, are described in section 2.4.4.

GCWerks smoothes the first derivative (slope) of the chromatogram trace according to a parameter termed peak width (PW) and uses a threshold for the slope (peak threshold, PT) to determine the peak start and end. It is recommended to use the typical analyte peak width at half height as PW so that narrower noise peaks are smoothed out and not integrated, and PT depends strongly on the baseline noise and the shape of the analyte peak. A high PT can be set for large, narrow peaks, avoiding integration of noise, while shallower peaks require a lower PT.

In addition to these initial parameters, a number of further options including specific baseline treatment are available to better characterise analyte peaks, which are often far from the ideal peak shape. Separate sets of parameters are applied to each extracted ion from the SIM data, and a peak ID window is set for each analyte with one quantifier and up to two qualifier ions (only two qualifiers can be set in the software).

Despite the automated approach, the need remains to thoroughly check all integrations and adjust parameters for either individual peaks or periodically shift the relevant parameters as retention times vary between and even within each cruise. This is possible, albeit not

designed to be used that way initially, since long-term observations tend to require fewer changes in parameters as methods and conditions remain constant for much longer periods than in this study.

Integration errors were estimated for each analyte by adjusting integration parameters within reason and exploring the effect on peak area or height for very large to very small peaks. The result was typically a percentage error for very large peaks and a fixed area or height unit error for smaller peaks, with between one and three size thresholds in order to keep the error appropriate.

To set data into context, a detection limit (DL) is useful to show the limitations of an analysis and to give an upper constraint for data below that limit. Additionally, quantification limits may be quoted with a dataset. In this study, the term "DL" is used to describe an effective working detection and quantification limit determined for each individual analyte that also reflects changing conditions between and within each dataset. To determine it, the integration (height or area, depending on the analyte) of a peak that was clearly visible above the noise (*ca.* 3x noise level) in a sample with typical background was processed in the same way as the sample integrations. A "typical background" could be in an air or water sample and not necessarily in a blank sample that might indicate unrealistically low noise, and the smallest quantifiable peak size was assessed repeatedly within each cruise dataset, and instrument response changes were also taken into account (see sections 2.4.3.1 and 2.4.3.2), giving a dynamic working DL throughout.

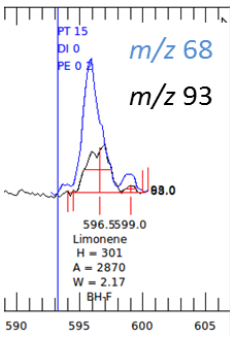

Figure 2.15 – Limonene peak during ACCACIA 2, quantified by height on m/z 93 since peak area and m/z 67 were not suitable (left-hand peak is interference).

A specific case of quality control specifically related to DLs was that of limonene: it was discovered that marine air samples consistently (but not at consistent levels) contained an

interference eluting only very slightly before limonene and hence never baseline resolved, with a large *m/z* 68 peak and some contribution to *m/z* 93 if present at high levels. This led to the decision to use *m/z* 93 as a quantifier for all datasets - except AMT 22 where this problem was not observed and *m/z* 68 was a slightly cleaner ion overall - and to also use peak height rather than area for AMT 23 and ACCACIA 2 (Anna datasets only; example see Figure 2.15). Most of both datasets was usable that way, but in some time periods low limonene coincided with high interference levels, strongly affecting the *m/z* 93 peak and effectively making the minimum detectable peak height for limonene the height of the interferent peak.

2.4.2 Data processing

2.4.2.1 Carbon tetrachloride as internal standard

Carbon tetrachloride (CCl_4) is an anthropogenic compound with a long tropospheric lifetime (*ca.* 26 years; Carpenter and Reimann, 2014). It is classified as an ozone depleting substance and has been banned since 1987 (UNEP, 1987), resulting in a uniform global atmospheric mixing ratio that decreases slowly, at a known rate (*ca.* 1 pptv per year, http://www.esrl.noaa.gov/gmd/hats/). Recent research has shown that the actual measured decrease is slower than that expected from its loss rate, and that concentrations are not in fact globally completely uniform (Liang et al., 2014; Carpenter and Reimann, 2014), but for the purposes of this study, the differences are negligible over the relevant timescales.

The essentially constant atmospheric mixing ratio makes it possible to use CCl_4 to monitor instrument performance, and alternating air and water measurements allowed the use of CCl_4 in air as an internal standard not only for air but also for water samples by interpolation. Similarly, terpene standard measurements were corrected using interpolated CCl_4 levels from bracketing air samples or NOAA standard as the terpene standard itself contained no CCl_4 (see section 2.4.3 for details of the calculations).

Wherever possible, the nearest previous and next air samples acquired within 1-2 hours of the relevant water sample were used for bracketing. If only one usable air sample fell within that time period, generally only that single CCl_4 value was used; if no air sample

was available, the time window could be extended manually provided the interpolated CCl_4 ("pseudo-CCl_4") followed a smooth trend overall.

For terpene standards, the same approach was followed, but where a NOAA standard was closer in time than an air sample, the NOAA CCl_4 value was used preferentially.

2.4.2.2 Quality control

One of the most important components of data processing is good quality control. The datasets acquired during this study have presented a variety of data quality concerns that had to be addressed in order to produce reliable results. Initial checks were carried out on the integrations and the DLs as detailed above (section 2.4.1). For flagging the resulting data, a modified standard system (WOCE) was applied as described in Table 2.6 and the section below.

Various instances of instrument or setup issues resulted in periods with missing data during all cruises; these are not further discussed here, but are apparent in the datasets themselves.

As a first step for air data, samples were discarded if the associated Unity report showed low sampling flow or sample volume (flag 5). Sudden changes in CCl_4 levels were also considered to indicate poor air sample quality (flag 3) and those samples were not used to determine pseudo-CCl_4 (see section 2.4.3.3).

Data for analytes at the start of the chromatogram was flagged (flag 3) if EPC (electronic pressure control) wobble was present – an oscillating baseline in chromatograms sometimes observed when the EPC in the GC cannot control the carrier gas pressure sufficiently to keep the vacuum and background noise at the detector consistent. The problem can be caused by trapped water that expands rapidly as the cold trap is heated and therefore occurs during trap desorption, affecting the first few minutes of a chromatogram (Figure 2.17a).

One challenge for air data was to exclude any samples with influence from the ship, mainly from the exhaust plume. It was obvious from the hydrocarbon data that some samples were strongly contaminated and could not be used, as e.g. Figure 2.17b, but some situations

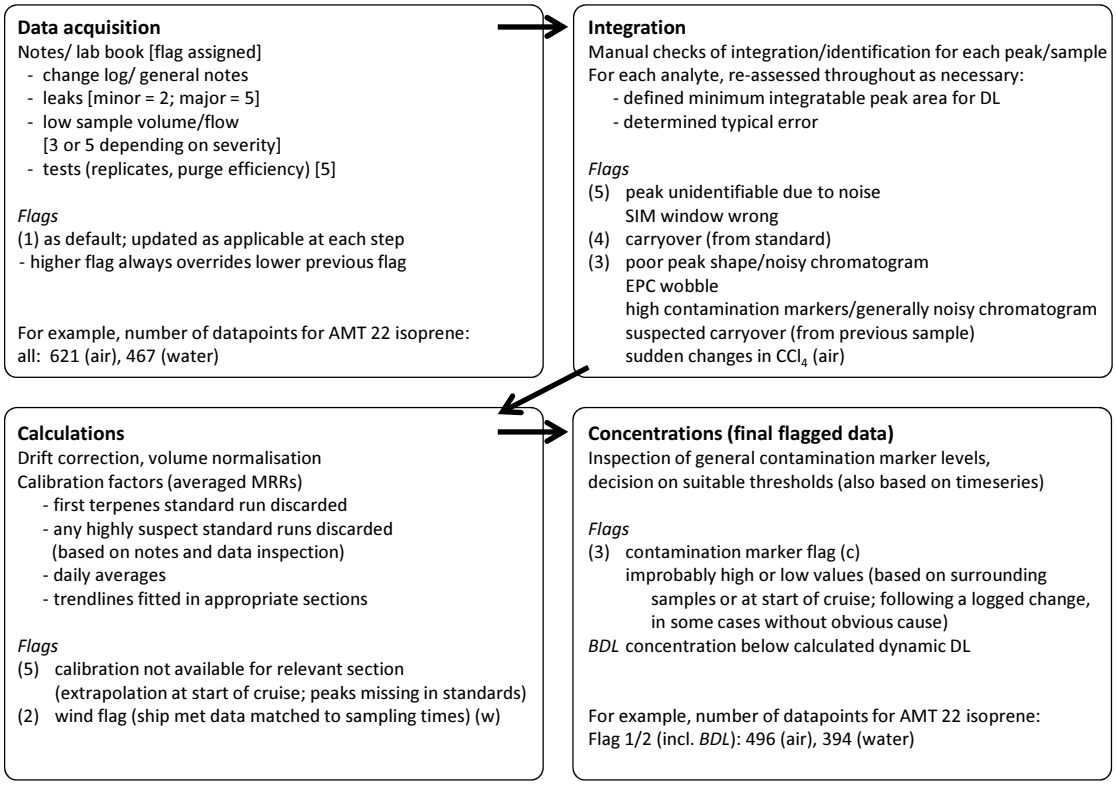

Figure 2.16 – Data processing steps, showing flags added at the separate stages. Hydrocarbon contamination thresholds mostly based on inspection of timeseries as shown in Figure 2.18

Table 2.6 – Adapted WOCE flagging system used in this study, hierarchy applied in the order listed here. Flags in bold are always included; additional flags were used for specific datasets as needed, with a maximum of one flag from each group.

Flag group	Flag	Description
A	**0** or **Q**	no QC performed,
		e.g. different analytical method
A	**5**	missing/ removed data,
		e.g. no data available, various *in-situ* tests, no calibration available
A	**4**	bad data,
		e.g. carryover from a previous sample, major leak
A	**3**	"probably" bad data,
		e.g. contamination noted in log, EPC wobble
A	**2**	"probably good" data,
		e.g. minor leaks, wind flag
A	**1**	good data
B	BDL	Below Detection Limit (<DL)
C	c	contamination indicated by hydrocarbon marker flag
C	w	wind flag (direction or speed); air data only

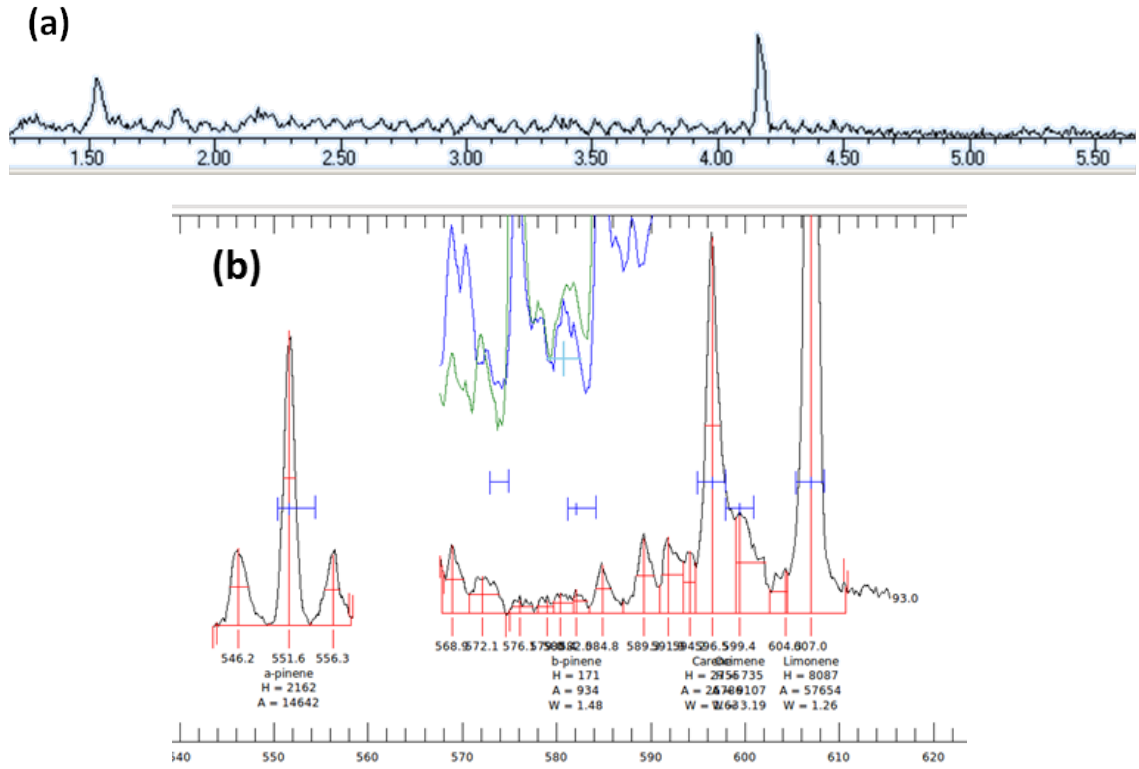

Figure 2.17 – (a) Chromatogram strongly affected by EPC wobble, making integration of peaks up to 4.5 min impossible. (b) Monoterpene region of chromatogram with hydrocarbon contamination (qualifier ions off-scale).

were less clear-cut. The approach adopted for all cruises was a combination of visual inspection, a hydrocarbon threshold and a wind filter:

- A high background and noisy chromatogram trace in the monoterpenes region often made bad contamination immediately visible.

- In addition, benzene and *m*-/*p*-xylene were used as marker compounds for hydrocarbon contamination, and a typical "clean air" value determined based on the overall cruise dataset (varied between cruises). The absolute threshold values were estimated from a visual inspection of the hydrocarbon time series and confirmed by plotting the data before and after filtering, which showed that the filter generally removed noisy/elevated samples for all hydrocarbons including terpenes (without strongly affecting the median of the data; example of α-pinene shown in Figure 2.18). If either benzene or *m*-/*p*-xylene concentrations were above the relevant threshold value or if either peak exhibited a concentration spike compared to the surrounding samples, the sample was flagged. The removal of spikes is common in atmospheric datasets (e.g. Vickers and Mahrt, 1997) as a true high reading is generally considered unlikely in a well-mixed air mass such as for example the marine atmosphere. One approach is to flag data that is more than two or three standard deviations different from a running average; this is unsuitable for this dataset as irregular gaps in the time series can cause apparent step changes and make a running average inappropriate. Another issue are ironically the contamination events themselves: they can increase the standard deviation to such levels across several samples that slightly lower contamination is not flagged. The alternative approach employed here uses the absolute threshold explained above as well as highlighting samples that are >20 % higher than the value of both the bracketing samples, as long as the absolute value is above a set minimum to avoid flagging low-level noise.

- Thirdly, a wind filter was defined for each ship (different set-ups) which flagged air samples that had wind coming from the "dirty" sector or relative wind speeds below 2 m s^{-1} during the sampling time. The cut-off angles for the dirty and clean sectors were based on the relative locations of the sample inlet and the ship stack. The wind flag was often not coincident with obviously "dirty" samples and therefore applied as a less strict flag (flag 2, "probably good data", or simply a specific "w" flag for use in this data analysis).

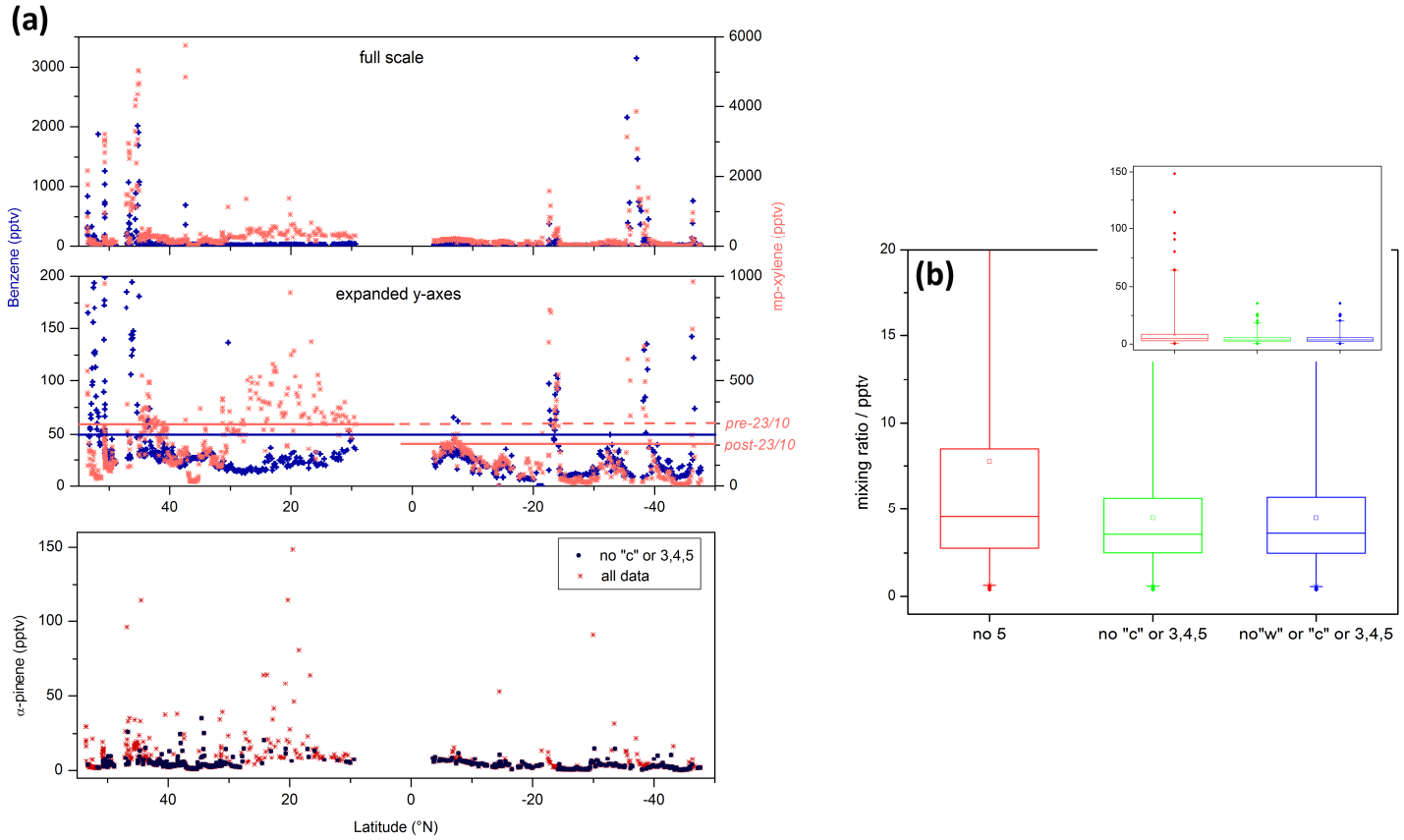

Figure 2.18 – (a) Example for determining threshold values for hydrocarbon contamination (AMT 23, Anna); thresholds indicated by lines on the expanded benzene/ *m/p*-xylene plot; α-pinene air data shown alongside to illustrate effect of filtering. (b) Box and whisker diagram of α-pinene data with different filters applied; insert showing full range, illustrating that the median remains almost constant and only high-concentration outliers (contaminated samples) are discarded; wind flag (w) has very little effect on whole dataset. For definitions of flags used for filtering see Table 2.6.

The hydrocarbon marker approach worked particularly well for ACCACIA 2, when atmospheric concentrations of these compounds were generally very low. For AMT 23 especially, the threshold had to be increased significantly, as background levels appeared to be much higher. Air data from that entire cruise appeared to be substantially higher than during the other cruises, indicating a contamination issue throughout, and was therefore disregarded when investgating relationships with biological parameters. It was however reported (Chapter 4 section 4.2) and partially analysed further (Chapter 4 section 4.3.3) in order to highlight consequences of the suspected contamination and to avoid completely discarding data based on strong suspicion alone.

Additionally, individual analyte data points were flagged if concerns had been noted while checking the integration; this would typically be integration of an interferent peak or very poor peak shape.

Water samples were discarded if major leaks (approximately >25 % of the target sample volume) were recorded; those samples may have had contact with air during the filling step, compromising their integrity. Water data for β-pinene during AMT 23 was excluded from further analysis since the surface CTD samples were below the detection limit which was typically a factor of four less than the measured underway concentrations and it could not be determined which of the two methods was more reliable.

Data acquired on Wendy during AMT 23 was also entirely discarded due to noisy data and highly improbable sample values for water as determined by comparison to AMT 23 (Anna) and AMT 22 datasets (Figure 2.19).

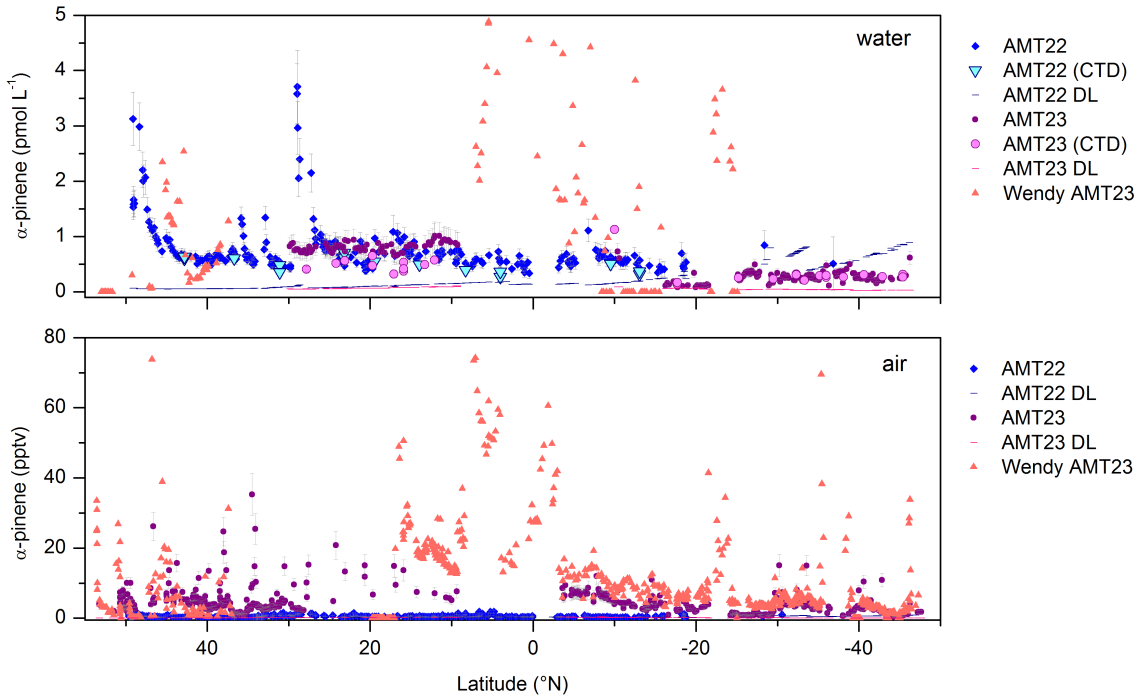

Figure 2.19 – α-pinene water (pmol L^{-1}) and air (pptv) data from Anna and Wendy (red dots, no QC performed) during AMT 23, illustrating the need to discard Wendy data for that cruise.

2.4.3 Calibrations

2.4.3.1 Standard stability

As described in section 2.2.1, a number of standards were used during the course of this study. The stability of the dmsterps standard was monitored against the NPL and NOAA standards (assumed to be stable) over time, with good results for isoprene, benzene and toluene. Analyte concentrations in the dmsterps standard for all subsequent calculations were taken from an analysis on Wendy between ACCACIA 2 and AMT 23 (September 2013), considered stable based on a number of observations including the results of continual validation against the NOAA standard (Figure 2.20). A discarded analysis in February 2014 also provided useful information, as the consistent decrease of *ca.* 30 % for all analytes including those known to be stable compared to the previous check implied an analytical problem rather than standard degradation.

Ocimene was only detected at very low levels in the September 2013 analysis, but was present at higher levels in the February one, which was attributed to instrument issues (known issues with the transfer line for some analytes around this time). As a result, the

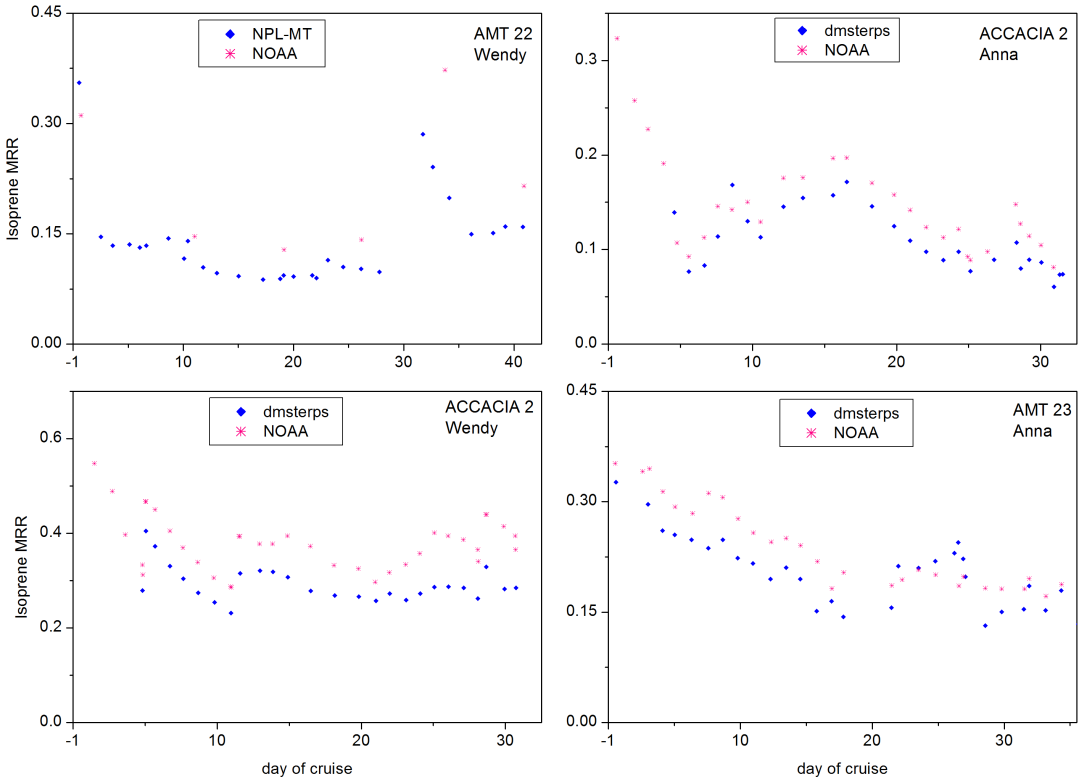

Figure 2.20 – Standard stability validation for terpenes standards based on consistent response for isoprene compared to NOAA standard during field campaigns (plotted here as timeseries of molar response ratios (MRRs, explained in section 2.4.3.2)).

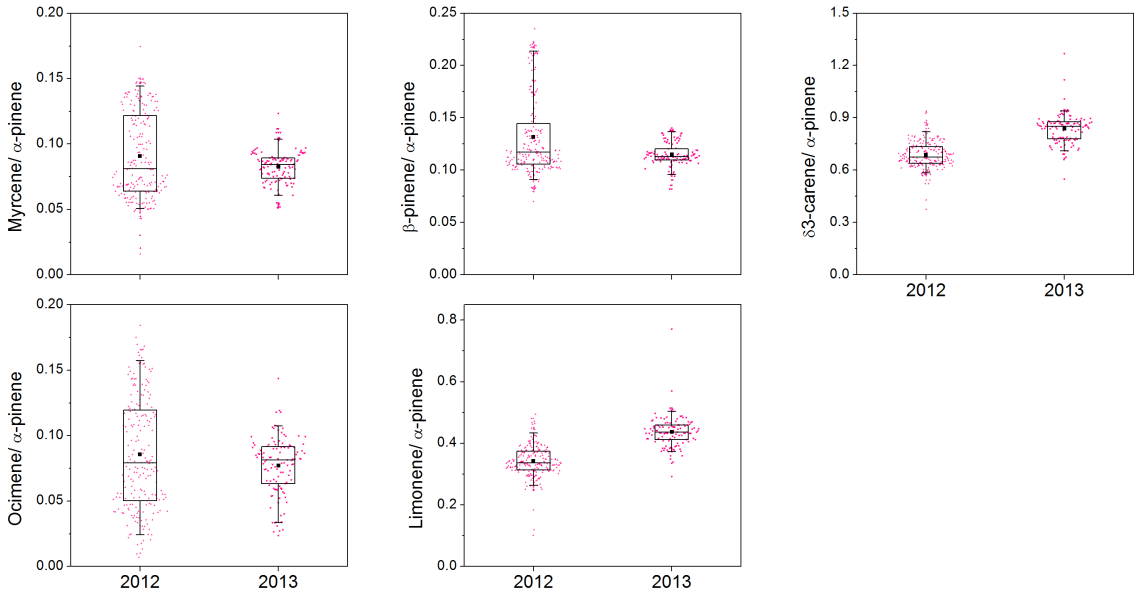

Figure 2.21 – Monoterpene ratios to α-pinene in the NPL-MT standard between 2012 and 2013; mean (filled square), median (line), 25^{th} to 75^{th} percentile (box), 5-95 % (whiskers), data points (dots; potential patterns have no significance).

ocimene standard concentration was extrapolated by dividing the February 2014 value by the average ratio for Feb/Sept of the other terpenes.

It was assumed that the NPL-MT standard was not degrading and concentrations could be used as given on the certificate, which was supported by the observation that ratios of peak areas of each monoterpene against α-pinene in the standard between delivery in 2012 and September 2013 (for both pure and dilute NPL-MT, shown in Figure 2.21) did not change substantially, given the overall scatter in the data and the absence of any consistent trends over time (timeseries not shown). The comparison was possible due to the use of the same quantifier ion for all terpenes so that tuning or other instrument condition changes should not affect their ratios. The scatter in the data indicates that the ratio must also be affected by other factors (e.g. losses in the sample introduction system) that are unrelated to standard stability; however these factors would be accounted for by calibrations and hence not affect the calculated analyte concentrations. Additionally, any changes may be a contribution of either of the two species in the ratio since no more is known about the stability of α-pinene than that of the other monoterpenes, so that changes in the standard concentrations could not be derived based on the available information, leading to the assumption of acceptable standard stability as the best estimate.

Comparison against isoprene in the NOAA standard (Figure 2.20) showed that there was minimal to no degradation of isoprene in the dmsterps standard over the course of the project and provided a confirmation of isoprene calibration factors, validating the parameters chosen for the dmsterps calibration (namely flow rate and sampling volume, which deviated from the methods for air and water samples). The difference in isoprene concentration in the dmsterps standard (September 2013) based on the NPL compared to that derived from the NOAA standard was less than 8 % (only just outside the range of the analytical error). Ambient water and air isoprene concentrations from the two independent calibrations displayed a bias of 20 % or less; dmsterps calibration gave higher values compared to NOAA, which is consistent with a slightly overestimated concentration in the dmsterps standard if degradation is present but neglected.

2.4.3.2 Molar response ratios

In order to correct for fluctuations in instrument response on timescales shorter than the calibration intervals when calculating analyte concentrations, an internal standard (IS) can be used as a reference, such as CCl_4 (described in section 2.4.2.1). The ratio of the analyte to IS response in the calibration is established (accounting for differences in concentration), referred to as Molar Response Ratio (MRR), and used in subsequent calculations as detailed below, employing the IS response and its known concentration in the sample to obtain the analyte sample concentration based on its response and MRR.

MRRs were determined with respect to CCl_4 as follows, e.g. for isoprene with the help of bracketing air samples as described in section 2.4.2.1:

$$MRR_{isp} = \frac{isp_{std}}{\mathrm{CCl}_{4air}} \times \frac{[\mathrm{CCl}_4]_{air}}{[isp]_{std}} \tag{2.19}$$

where CCl_{4air} and isp_{std} are peak areas of CCl_4 and isoprene (normalised to 1 L sample volume) in bracketing air samples and the terpenes standard, respectively, and $[\mathrm{CCl}_4]$ and $[isp]$ their mixing ratios in pptv. $[\mathrm{CCl}_4]_{air}$ was taken from literature (e.g. 84.3 pptv for Oct 2013, http://www.esrl.noaa.gov/gmd/hats/) and $[isp]_{std}$ is the known concentration of isoprene in the standard. If a NOAA run was closer than an air sample (usually the case for second and subsequent standard runs), CCl_{4NOAA} and $[\mathrm{CCl}_4]_{NOAA}$ were used instead of air values.

By normalising all runs to 1 L based on the sample volume in mL from the Unity report, all calculations effectively deal with directly comparable amounts, as a mixing ratio of n pptv in 1 L at 1 atm and 0 °C (MFC reference conditions) is equivalent to $0.04461n$ pmol.

Typically, the first terpenes standard run in each calibration was discarded and an average MRR for each calibration block calculated from the second and any subsequent runs. These averages were then fitted with one or more polynomials, depending on the shape of the curve and breaks due to known changes such as MS tunes (example shown in Figure 2.22). Interpolation could also be done by linear trendlines and in some cases average MRRs for certain time periods. The resulting analyte concentrations were checked for any obvious trends or step changes introduced by the MRR and adjustments made as necessary. The error associated with each MRR was the standard deviation of the points

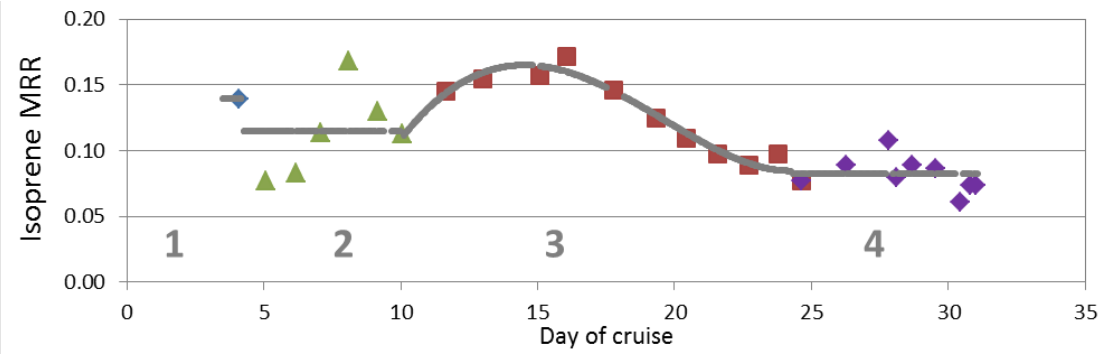

Figure 2.22 – Example of MRR treatment (dmsterps isoprene, ACCACIA 2, Anna) showing the separate sections of MRR trendline fitting (section 2 and 4: simple averages; 3: polynomial fit; solid symbols with grey combined trendline).

used for averaging (for averaged MRRs) or the y-error of the regression (calculated by Excel).

2.4.3.3 Determination of sample concentrations

Analyte atmospheric mixing ratios were established by normalising peak areas to CCl_4 within each sample (hence no volume normalisation necessary) and applying the relevant interpolated MRR at the time the sample was taken, e.g. for isoprene in an air sample:

$$[isp]_{sample} = \left(\frac{isp_{sample}}{\mathrm{CCl}_{4sample}} \times [\mathrm{CCl}_4]_{air} \right) / MRR_{isp} \tag{2.20}$$

For analyte concentrations in water samples in units of pmol L^{-1}, the equation was modified to

$$[isp]_{sample} = \left(\left(\frac{isp_{sample}}{\mathrm{CCl}_{4pseudo}} \times [\mathrm{CCl}_4]_{air} \right) / MRR_{isp} \right) \times \frac{1000mL/L}{water\ vol} \tag{2.21}$$

- using *"pseudo-CCl_4"*, the average of the peak areas of CCl_4 in the two bracketing air samples, normalised to 1 L sample volume (also see section 2.4.2.1);
- using $[CCl_4]_{air}$ converted into pmol L^{-1} , e.g. 3.76 pmol L^{-1} in Oct 2013, equivalent to 84.3 pptv in 1 L air by MFC, i.e. 84.3 pmol/ 22.45 L at 0 °C and 1 atm;
- introducing a correction for the actual water volume sampled (*water vol*, in mL), but not for the gas volume sampled as it is irrelevant to the concentration in water.

2.4.3.4 Linear calibrations

Multi-point calibrations showed good linearity throughout the project, with the exception of AMT 23 (Figure 2.23). There was always a slightly negative intercept if the line was not forced through zero, which could be attributed to analyte losses in the system. For the purposes of determining response factors as detailed above (section 2.4.3.2), individual runs in multi-point calibrations were averaged in the same way as one-point calibrations. Reproducibility of repeated analysis of a mid-range standard for both linear and one-point calibrations was typically within 10 % for the monoterpenes and 5 % or less for isoprene.

During AMT 23, neither NOAA nor dmsterps calibrations were fully linear, potentially caused by humidity changes in the system. Checks carried out on air samples at different volumes showed good linearity of the CCl_4, suggesting that only standard runs at higher volumes were affected. Those runs were excluded from data processing where they clearly followed a non-linear trend, otherwise they were incorporated into averages used for response factors.

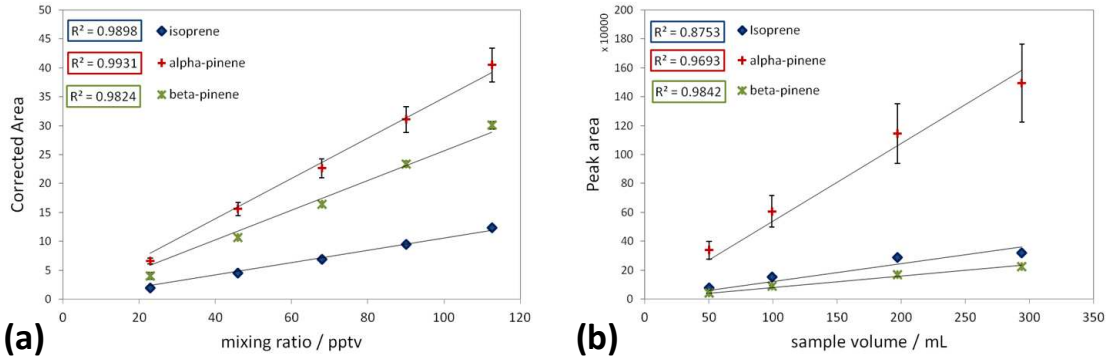

Figure 2.23 – Linear calibrations during AMT 22 (a; dilute NPL-MT) and AMT 23 (b; dmsterps), showing isoprene, α- and β-pinene as examples; error bars (standard deviation) based on relative standard deviation of several replicates measured at 67 pptv and 50 mL sample volume, respectively (often smaller than symbols).

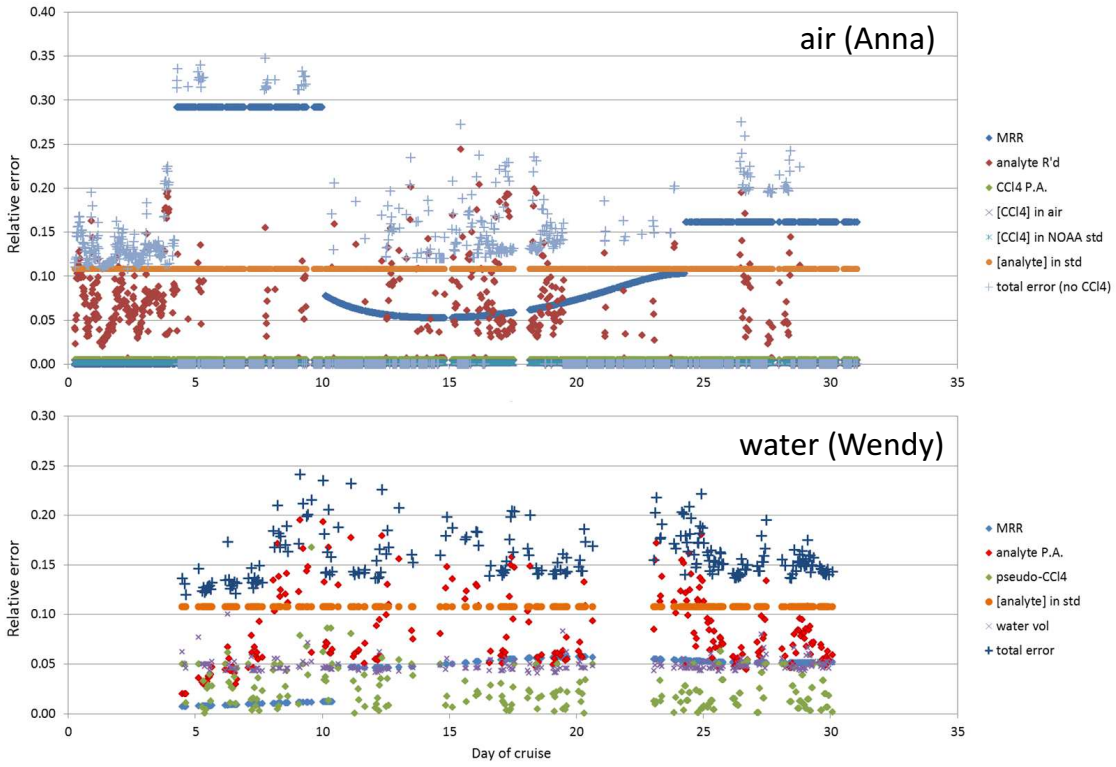

Figure 2.24 – Relative contributions to errors for ACCACIA 2 isoprene data as an example of the error analysis performed in this study. The legend refers to the errors associated with the listed components; "analyte R'd" = sensitivity-corrected analyte peak area, pseudo-CCl4 = average of bracketing CCl_4 peak areas, water vol = water volume. Large integration errors tend to be associated with concentrations near the DL.

2.4.4 Error analysis

An important aspect of data analysis and quality control is error analysis, which was done in this study by a simple propagation of errors through all calculations. This section lists all main contributions to the final errors and describes the error analysis performed using isoprene (ACCACIA 2) as an example. Figure 2.24 shows the relative error for each of the contributing components as well as the final propagated error for a typical error analysis.

Some sources of error have been discussed in the sections above, e.g. integration and calibration (sections 2.4.1 and 2.4.3, respectively). Each sample (air and water) has an individual error associated with it, calculated from all the contributing errors from the following:

Air

- integration (peak area)
- calibration (polynomial fit to MRR trends, analyte standard concentration)

Water

- integration (peak area)
- calibration (polynomial fit to MRR trends, analyte standard concentration)
- sensitivity correction (from *"pseudo-CCl_4"*)
- water volume

Errors for concentrations of atmospheric CCl_4 (both in the sample and in the standard, using published NOAA HATS values, http://www.esrl.noaa.gov/gmd/hats/combined/CCl4.html) were disregarded for the final total error as they were found to be negligible (typically $\ll$1% contribution to total error, as can be seen in Figure 2.24). The main contributor to air concentration errors was the integration error (small peaks), while relative contributions to water concentration errors varied with cruise and analyte (often also with major contribution from the integration). The *"pseudo-CCl_4"* error was taken to be the difference of the bracketing values, or set 5 % error if only one value was used.

Additionally, it should be taken into consideration that the analytical system appeared to display slightly different characteristics with respect to analyte losses for every setup change (with the most significant changes aimed at improving water removal), and that

calibration tests at the Cape Verde Atmospheric Observatory even highlighted the possibility of a single piece of stainless steel tubing compromising the analysis. As a result, the calculated errors may not reflect the total error associated with the measurements.

Chapter 3

Isoprene – controls in the surface ocean

Atmospheric isoprene has been the subject of decades of research due to its impact on atmospheric chemistry processes, particularly in terrestrial environments, as outlined in Chapter 1. Only recently, the marine environment has also received increasing attention as a potentially significant source of isoprene to the atmosphere. This chapter will present results from four research cruises, describing isoprene concentrations in the surface ocean and the lower marine boundary layer and derived sea-to-air fluxes, and compare them to current literature values. It will aim to establish relationships with potential controls of isoprene in surface waters, which could then be used to estimate global fluxes more accurately than previously possible.

3.1 Introduction

3.1.1 Marine isoprene measurements

Since Bonsang et al. (1992) first reported evidence for the marine production of isoprene, there has been growing interest in the subject, and results from a number of studies on isoprene and monoterpene emissions have been published (seefor example Shaw et al., 2010, and references therein - e.g. Yokouchi et al., 1999; Shaw et al., 2003; Colomb et al., 2009; Gantt et al., 2009; Bonsang et al., 2010; Palmer and Shaw, 2005; Luo and Yu, 2010; Exton et al., 2013; Kameyama et al., 2014; Ooki et al., 2015). Both field measurements and modelling approaches have been used to determine production rates and emissions of these compounds, with published data broadly falling into three categories:

- Measured atmospheric and seawater concentrations (field studies)
- Laboratory-based emission measurements
- Remotely-based observations (using Chl-a as a proxy, in conjunction with emission rates from laboratory studies)

All three employ calculations and models in order to estimate fluxes, and several papers attempt to calculate global averages (e.g. Arnold et al., 2009; Palmer and Shaw, 2005). The results vary widely; the discrepancy between estimates from bottom-up and top-down approaches in particular is up to an order of magnitude. A review by Shaw et al. (2010) summarises all previously published data on emissions, seawater and air concentrations and should be referred to for a comprehensive overview of literature on the subject prior to 2010. In addition, several papers on isoprene field- and lab-based measurements have been published in the last five years and are summarised in Table 3.2 along with the previously available data. Data represent values from the North Sea to the Southern Ocean, with little coverage of the Atlantic Ocean. This chapter will focus on marine isoprene; monoterpenes are discussed in Chapter 4.

Despite the recent increase in interest, there is still only sparse data available for marine isoprene, and most studies are single or few measurements with no indication of seasonal or diurnal variations in emissions. However, several publications exist that include more observations over a period of time: Lewis et al. (1997b, 2001) report diurnal cycles for

atmospheric isoprene at Mace Head, Ireland, and Cape Grim, Tasmania, with a clear maximum around solar noon and values below detection limit at night. For both water and air observations, seasonal studies were performed in the field (Broadgate et al., 1997; Exton et al., 2012) and controlled variation of conditions such as temperature and light intensity for phytoplankton monocultures in the laboratory (Moore et al., 1994; Milne et al., 1995; Shaw et al., 2003; Gantt et al., 2009; Bonsang et al., 2010; Exton et al., 2013). Ooki et al. (2015) very recently published a large dataset of marine isoprene observations made over a wide latitudinal range and in different seasons. These studies report evidence of a dependence of the production on a number of factors:

- Temperature (water temperature)
- Solar radiation intensity (PAR)
- Chl-a abundance (phytoplankton abundance)
- Phytoplankton Functional Type (PFT)

Dependence on all factors causes seasonal trends, while diurnal variability also follows logically from the first two. Clearly, all factors additionally result in large spatial variability.

Most laboratory studies have concluded that there is a linear relationship with Chl-a (e.g. Milne et al., 1995; Exton et al., 2013), or in a more refined approach, with Chl-a associated with specific PFTs (e.g. Shaw et al., 2003; Bonsang et al., 2010), however there are substantial variations between and even within studies, for different phytoplankton classes and also within species.

3.1.2 Global extrapolation

Due to the lack of data and limited understanding of the variation in the data available, any calculations of annual and global averages must be subject to large uncertainties; however several attempts at estimating them have been made (Palmer and Shaw, 2005; Gantt et al., 2009; Arnold et al., 2009; Luo and Yu, 2010; Exton et al., 2013; Ito and Kawamiya, 2010).

All of those estimates take laboratory-based production rates and scale them globally using an appropriate satellite product – for simple Chl-a-normalised rates, this is typically Chl-a from SeaWiFS, while for PFT-dependent rates, an ocean colour-based algorithm such as

PHYSAT (see 3.2.4.2) is employed first to determine the relevant production rate to be used with the Chl-*a* data. Meskhidze and Nenes (2006) derived isoprene concentrations as well as emissions in a similar manner.

While an increasing number of field measurements can provide some groundtruthing for the satellite-based approaches, there is still a considerable need for validation of the results by further observational data, especially at a large scale and in previously undersampled regions.

The aim of the present study was to sample surface water and air *in situ* in the Atlantic and Arctic Oceans, in order to provide a valuable addition to the isoprene database over a large latitudinal range, and to investigate potential controls of the observed distributions. This will help to improve our understanding of the ocean as a source of isoprene, and contribute to the development of more accurate algorithms for predicting isoprene at different temporal and spatial scales.

3.2 Results and discussion

3.2.1 Synoptic conditions and cruise background

This section will present a summary of general conditions encountered and measurements made for each of the four cruises (AMT 22 and 23, ACCACIA 1 and 2) introduced in Chapter 2.

3.2.1.1 AMT 22 and 23

AMT 22 (JC079) departed from Southampton, UK, on 10/10/2012 onboard the R.R.S. James Cook and arrived in Punta Arenas, Chile, on 24/11/2012 after having crossed almost 100 latitudinal degrees and a wide variety of ocean regions, from productive upwelling systems and shelf areas and the spring blooms in the Southern Ocean to the oligotrophic gyres of the North and South Atlantic (cruise track shown in Figure 3.1).

The R.R.S. James Clark Ross (JCR) departed the UK from Immingham on 05/10/2013 for AMT 23 (JR300) and travelled south along a similar route to AMT 22, reaching Port

Stanley (Falkland Islands) on 06/11/2015. Due to constraints on ship time, the cruise track was a more direct line between the start and end points, passing closer to Cape Verde and the Mauritanian Upwelling zone as well as the Brazilian coast, traversing less of both the North and South Atlantic Gyres than preceding AMT cruises including AMT 22 (see Robinson et al., 2006; Figure 3.1). The overall scientific objectives and core measurements were identical to those for AMT 22, resulting in a similar suite of supporting data to this study for both years (see below and AMT 23 cruise report).

Typically, the AMT cruises start in the Northern Hemisphere in boreal autumn (September/October) and travel south to the South Atlantic for austral spring (October/November). This pattern has been maintained for a number of years under the more recent funding (see amt.org.uk for details), aiming for a similar cruise track every year in order to provide a platform for consistent measurements to build a long-term database of ocean observations (e.g. Robinson et al., 2006). The resulting time series of basin-scale studies now spanning 20 years of core measurements is unique, as most other programmes either cover much smaller regions, vary their cruise tracks or change their range of observations (or a combination of several of these points). The opportunity to repeat a study in a very similar region at almost the same time of year was extremely useful in this case in order to validate the first dataset, despite limiting the conclusions that can be drawn about any seasonality of the observed species.

During the cruise, a number of different biological, chemical and physical measurements were made in air, surface water and at depth (AMT 22 and 23 cruise reports, available from http://www.bodc.ac.uk/projects/uk/amt/cruise_programme/), including

- continuous underway data and vertical profiles (CTD, Conductivity-Temperature-Depth) for Chl-*a*, water temperature, salinity;
- various continuous meteorological observations including air temperature, solar irradiance (total and PAR), relative humidity and atmospheric pressure;
- optical characteristics of the water column (including scattering coefficients and down-/upwelling irradiance);
- biogeochemical measurements on water samples including nutrients, pigments, dissolved gases (including dissolved oxygen) and particulate carbon and nitrogen;
- primary, new production and respiration measurements as well as microbial plankton characterisation (abundance and composition).

A number of these measurements have been made available to aid interpretation of the isoprene data (listed below); results of those explorations are discussed in section 3.2.4.

- Chl-*a* (by underway fluorescence, discrete measurements or HPLC analysis)
- Pigments by HPLC
- Pico- and nanoplankton by flow cytometry
- Nutrients by autoanalyser
- Primary Production (PP) by ^{14}C-method
- Dissolved oxygen including incubations for determination of gross and net PP and community respiration
- General surface and meteorological data

Both AMT 22 and 23 followed typical trends compared to other years in terms of biological productivity, nutrients, temperatures and wind conditions encountered (Figures 3.19, 3.2 and 3.8; Aiken et al., 2000; Robinson et al., 2006).

The conditions in the North and South Atlantic gyres (NAG and SAG, respectively) were representative of the respective regions, although care should be taken with extrapolations to other oligotrophic ocean gyres. Several years of observations have now established that not all gyres exhibit the same characteristics as initially assumed two decades ago, and that for example the nutrient profiles are very distinctly different for NAG and SAG; especially phosphate which is depleted in the NAG but not SAG (e.g. Mather et al., 2008; Wu et al., 2000). The surface waters of both gyres are nutrient limited and Chl-*a* levels are very low (generally $<$0.1 mg m^{-3}), and the deep chlorophyll maximum (DCM) occurs much deeper than in more productive waters (generally below 100 m compared to a few tens of metres or shallower; SAG often even up to 150 m or more).

Despite the more inherently variable conditions both in equatorial waters and towards the Southern Ocean, the AMT 22 and 23 cruises encountered conditions overall typical of those ocean regions. The equatorial upwelling provides nutrients from deeper waters, leading to higher biological activity and more turbid waters. The increased availability of light in the Southern Ocean compared to the winter months, along with the generally high-nutrient regime due to deep mixing caused by high wind speeds and small temperature gradients, enables the occurrence of the typical spring blooms in that region (Sigman and Hain, 2012). Because recent AMTs arrive there at the beginning of the season, different years

can see very different patterns in those high southern latitudes. However, the general trends are still similar if the region is compared as a whole, with increased but highly variable biological productivity, as can be seen from the Chl-*a* traces in Figure 3.8.

3.2.1.2 ACCACIA 1 and 2

ACCACIA 1, the first of two research cruises associated with the ACCACIA project (Aerosol-Cloud Coupling and Climate Interactions in the Arctic, http://arp.arctic.ac.uk/projects/aerosol-cloud-coupling-and-climate-interactions-ar/) took place onboard the R.V. Lance out of Tromsø(Norway) between 15-31/03/2013, sampling Arctic waters in the Greenland, Iceland and Norwegian Seas (GIN seas).

The ACCACIA 2 cruise (JR288; 14/07-12/08/2013, Immingham (UK) to Dundee (UK), onboard the JCR) provided the opportunity to sample a similar ocean region to that of ACCACIA 1 during a different season, as envisaged by the project objectives. Unfortunately, the supporting information available for both Arctic cruises is much less extensive than that of AMT, making seasonal comparisons of controls difficult. Some analysis of potential biological controls was possible for ACCACIA 2, but no analogous analysis could be carried out for ACCACIA 1 due to the lack of suitable biological measurements.

ACCACIA 1 saw mostly very low biological activity, with no definite Chl-*a* maximum in the water column, while during ACCACIA 2, some stations saw higher Chl-*a* levels, with some exhibiting a subsurface Chl-*a* maximum (SCM, as opposed to DCM), but the sampling period was too late in the year to observe any of the spring blooms at the retreating ice edge. The mixed layer was generally ten to several tens of metres deep. During both cruises, Polar and Atlantic water masses were sampled which had distinct physicochemical and biological features such as salinity, temperature and levels of plankton biomass (Figures 3.2 and 3.8).

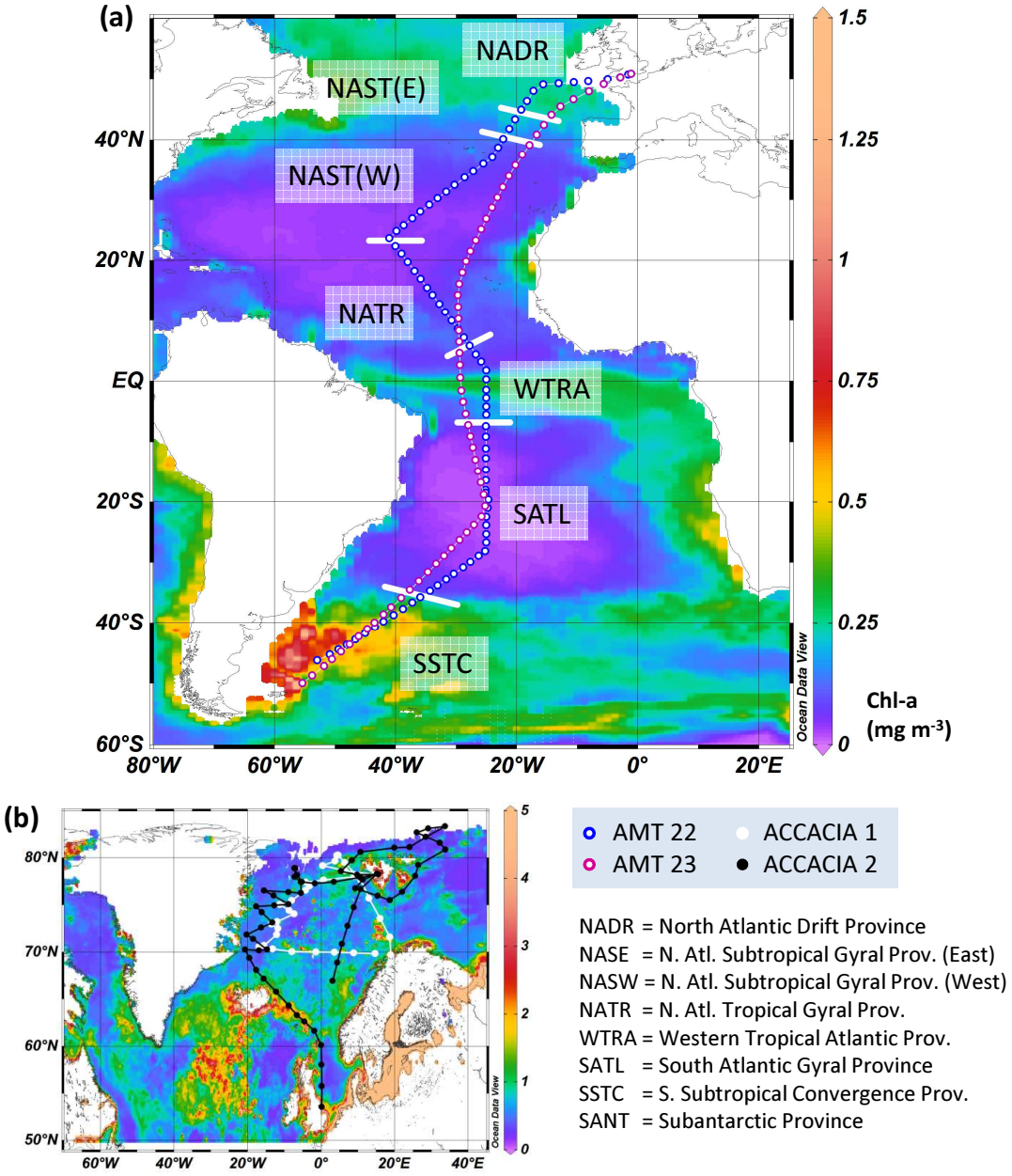

Figure 3.1 – (a) AMT cruise tracks plotted on a background of composite remotely-sensed (MODIS Aqua) Chl-*a* concentrations (Oct-Nov 2012), showing Longhurst province boundaries (Longhurst, 2007; section 3.2.2.2); (b) ACCACIA cruise tracks with Chl-*a* for July/Aug 2013. Satellite data from NASA Giovanni for MODIS Aqua, plotted in OceanDataView; white background over land/where no satellite data was available.

3.2.2 Air and water concentrations

3.2.2.1 Summary of results

Results for isoprene for all four cruises are shown in Figure 3.2a-c alongside sea surface temperature (SST) and salinity (transect or timeseries plots) as well as in Figure 3.3 (surface plot). Water concentrations ranged from *ca.* 2 to almost 70 pmol L^{-1}, comparing very well for the two AMTs despite longitudinal differences in the cruise tracks. Concentrations observed in the Arctic summer were similar to those in the Atlantic, while lower levels in the winter/spring are consistent with much lower biological activity during that cruise. With the exception of ACCACIA 1, measurements were easily above the detection limit (DL) for water, whereas atmospheric mixing ratios were often at or below the DL. Maximum, minimum, mean and median concentrations as well as DL ranges are listed for each cruise for water and air in Table 3.1. The range of encountered air mixing ratios (flag 1 or 2) was <DL (sub-pptv) to over 18 pptv; however, as discussed in Chapter 2 (section 2.4.2.2), air during AMT 23 and ACCACIA 1 may have been contaminated throughout the cruises, apparent from elevated levels of hydrocarbons in particular. Even if the effect on isoprene was not as strong as on the monoterpenes, and careful flagging excluded much higher values of up to 150 pptv, the results should be treated cautiously. Periods with missing data are explained in Chapter 2 (typically instrument issues or flagged data, see section 2.4.2.2).

Published values of isoprene in air and surface waters are listed in Table 3.2 and the surface ocean concentrations from the present study plotted alongside recently published values by Ooki et al. (2015) in Figure 3.3. Overall ranges are comparable between the literature and this study, especially for water concentrations; however there are still large temporal and spatial differences. Air concentrations are much more variable, with results from this project falling within the low range of published values, which could be due to the sampling regions being generally unproductive in comparison to those where very high isoprene mixing ratios were observed (Yokouchi et al., 1999).

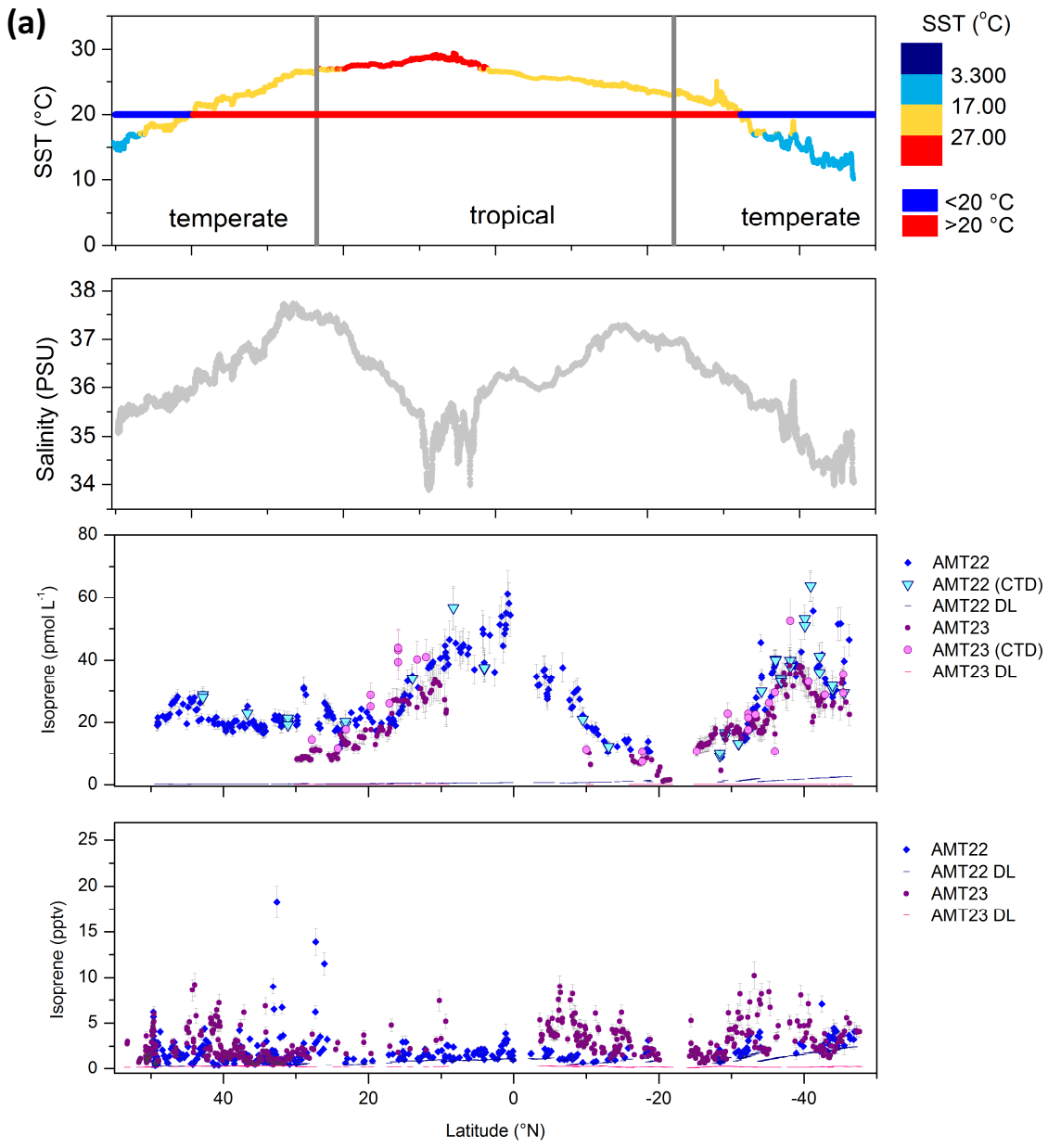

Figure 3.2 – **(a)** Surface water and air concentrations (including surface CTD samples) and dynamic detection limits of isoprene along the AMT transects, corresponding SST and Sal for AMT 22 only as they were representative of both cruises. Lines on the SST plots mark different temperature range boundaries; biome latitudinal ranges (after Exton et al., 2013) are also labelled. Error bars shown are the propagated measurement error described in Chapter 2 section 2.4.4. *Continued over...*

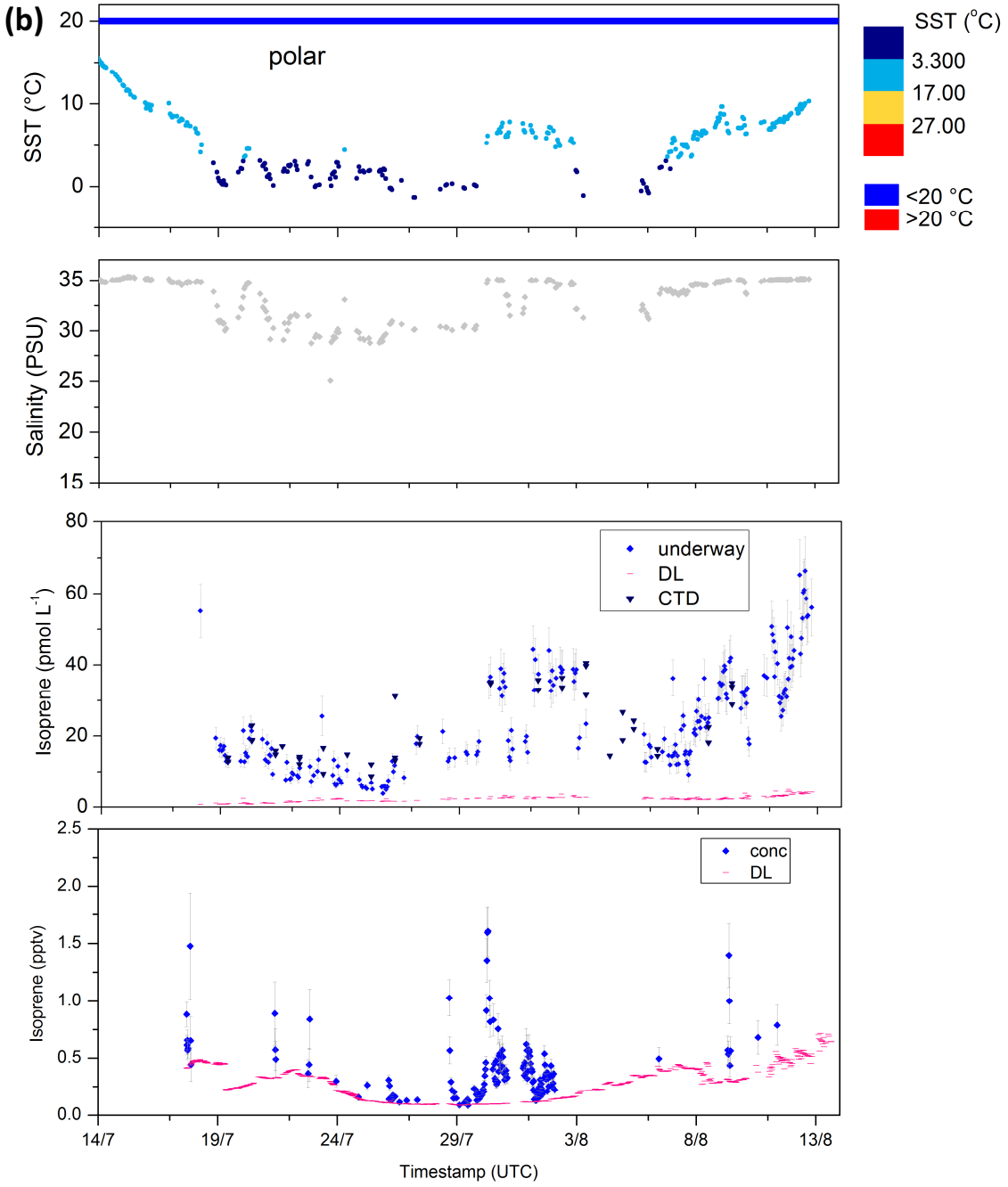

Figure 3.2 – **(b)** Surface water and air concentrations (including surface CTD samples) and dynamic detection limits of isoprene during ACCACIA 2, corresponding SST and Sal. Lines on the SST plots and error bars as for (a). *Continued over...*

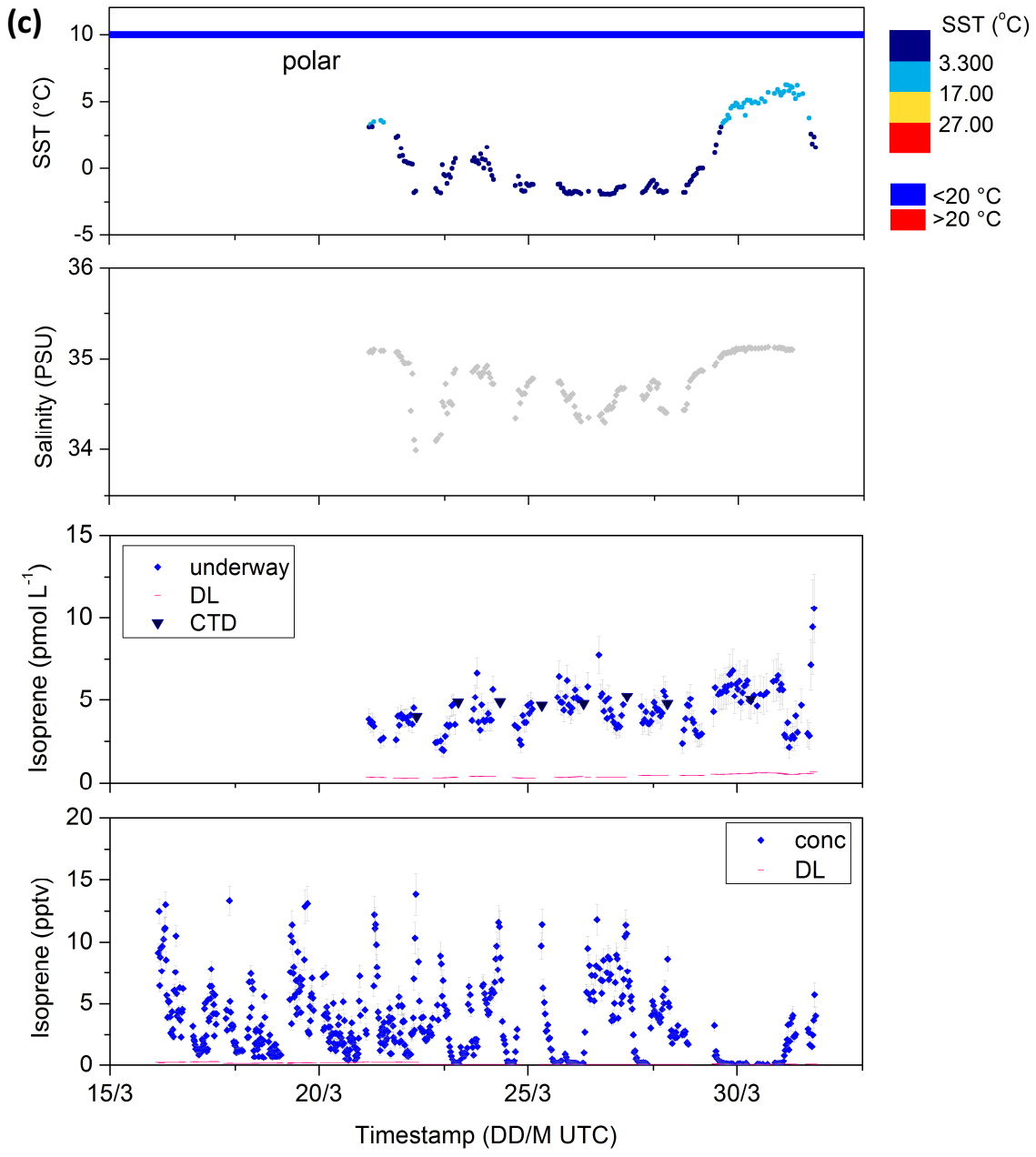

Figure 3.2 – **(c)** Surface water and air concentrations (including surface CTD samples) and dynamic detection limits of isoprene during ACCACIA 1, corresponding SST and Sal. Lines on the SST plots and error bars as for (a).

Table 3.1 – Results for each cruise for isoprene in water and air.*

	Cruise	Mean (range)	Mean (0.5xDL)[b]	Median (n)	Median (n) (0.5xDL)[b]	DL range[c]	surf. CTD mean (n)
Isoprene							
water	AMT 22	26.76 (8.75-63.36)	()	23.18 (290)	()	0.12-2.57	29.59 (37)
(pmol L^{-1})	AMT 23	18.74 (1.12-38.20)	()	17.20 (196)	()	0.07-0.12	25.85 (28)
	ACCACIA 1	4.40 (1.96-10.57)	()	4.25 (166)	()	0.28-0.68	6.29 (9)
	ACCACIA 2	24.12 (3.86-66.38)	()	19.91 (221)	()	0.80-4.88	22.01 (43)
air	AMT 22	1.88 (<DL-18.28)	1.47	1.51 (341)	1.07 (496)	0.09-2.42	
(pptv)	AMT 23[a]	2.76 (<DL-10.24)	2.72	2.27 (502)	2.24 (509)	0.05-0.47	
	ACCACIA 1[a]	3.37 (<DL-13.82)	3.17	2.61 (610)	2.41 (648)	0.03-0.27	
	ACCACIA 2	0.41 (<DL-1.61)	0.19	0.35 (150)	0.16 (891)	0.08-0.71	
	ORC3[d]	1.69 (<DL-13.60)	1.40	1.34 (860)	1.09 (1049)	0.03-0.48	

* Number of data points n applies to both mean and median (only shown with median); empty brackets indicate that no data was <DL (n is the same for both datasets).

[a] May be compromised due to hydrocarbon contamination.

[b] Using a value of half the DL for points that fall below the DL but are otherwise not flagged as bad (or probably bad) data.

[c] Dynamic detection limit (DL), described in Chapter 2 section 2.4.1; the minimum measured value may have been only <DL where the DL was high.

[d] Also shown are results from intensive operating periods at Cape Verde Atmospheric Observatory as part of the ORC3 project (details see Chapter 5 section 5.2.1).

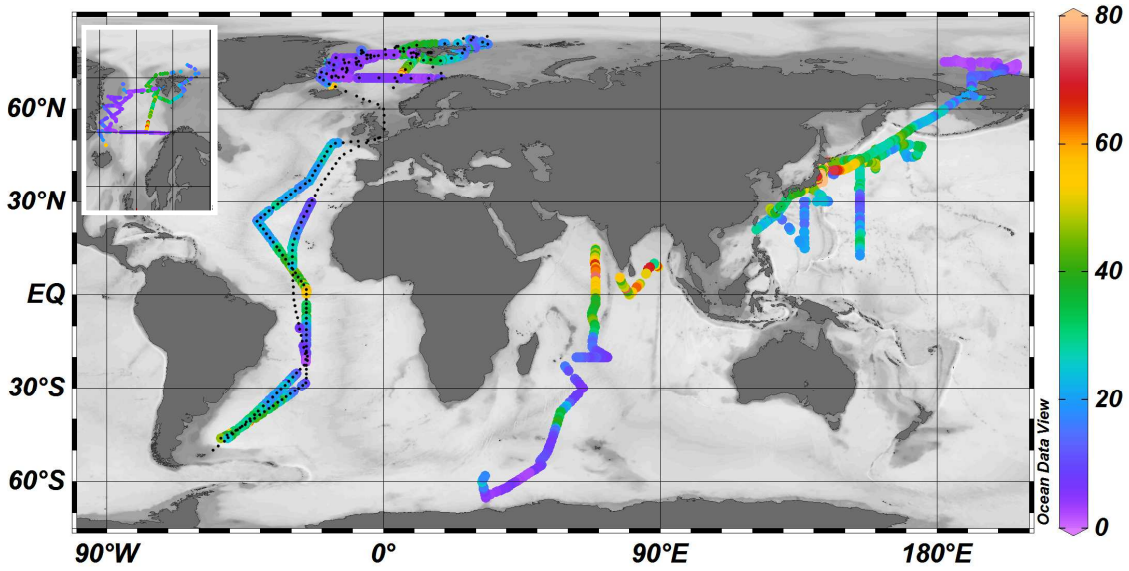

Figure 3.3 – Isoprene concentration in the surface ocean (pmol L^{-1}) along the cruise tracks for AMT 22 & 23 and ACCACIA 1 & 2 (Atlantic; cruise tracks marked; inset showing enlarged ACCACIA sampling region), alongside published values for the Pacific, Indian and Southern Oceans taken from the supplementary information in Ooki et al. (2015).

Table 3.2 – Published air and water concentrations of isoprene.

Mean ± error (range)	Technique	Location[a] (month)	Reference
air			
< 2-36 pptv (S Pac);	GC-FID (not in situ)	Mediterranean (Oct/May),	Bonsang et al. (1992)
<10-20 pptv (S Indian Ocean)		Pacific (April/May/June)	
<5-11 pptv	GC-FID (via canister)	Florida Gulf (Sept)	Milne et al. (1995)
6.2 (SW), 3.9 pptv (NW winds) (<5-24)	PTV-GC-FID[c]	Mace Head observatory (Aug)	Lewis et al. (1997a)
<0.1 pptv - 250 pptv	GC-MS (not in situ)	SE Asian Sea, Indian Ocean,	Yokouchi et al. (1999)
		SO (2 cruises, Nov-Mar)	
<1.6 (night), 5.7 pptv (day)	TD-GC-FID	Cape Grim observatory	Lewis et al. (2001)
45 pptv (7.2-110)	Cryo-GC-MS	Western N Pacific (May)	Matsunaga et al. (2002)
1.9 (oceanic), 0.9 pptv (arctic air)	PTV-GC-FID[c]	Arctic (summer)	Hopkins et al. (2002)
<3 pptv		Southern Ocean (Jan)	Wingenter et al. (2004)
180 pptv (<60-2380)	PTR-MS	mesocosm (Norway; June)	Sinha et al. (2007)
66 ± 44 pptv (remote);	GC-MS (not in situ)	Southern Ocean (January)	Williams et al. (2010)
274 ± 40 pptv (bloom)			(leg 1)
2.1 ± 2.1 pptv (remote)	GC-MS (not in situ & in situ)	Southern Ocean (Jan/March)	Williams et al. (2010)
			(av. of both legs)
26 pptv (<(1-5) - 48) (remote);	GC-MS (not in situ)	Southern Ocean (January)	Yassaa et al. (2008) (leg 1;
99 pptv (60-138) (distant bloom);			same cruise (and samples?)
187 pptv (32-375) (bloom)			as Williams et al., 2010)
40 (20-340)	PTR-MS	Southern Indian Ocean	Colomb et al. (2009)
20 ± 20 (background)		(south of 35 °S; Dec)	
14 pptv (2006)	PTR-MS	Cape Grim observatory	Lawson et al. (2011)
21 pptv (2007)		(hourly mean, marine air)	and Galbally et al. (2007)
14 pptv	PTR-MS	SW Pacific Ocean (Mar)	Lawson et al. (2015)
water			
up to 23.3 pmol L^{-1} (Med);	GC-FID (not in situ)	Mediterranean (Oct/May),	Bonsang et al. (1992)
up to 91 pmol L^{-1} (Pac)		Pacific (April/May/June)	
30.8 ± 16.3 pmol L^{-1} (9.8-50.8)	GC-FID ("spray extraction")	Florida Gulf (Sept)	Milne et al. (1995)
0.7-54 pmol L^{-1}	P&T-GC-FID	North Sea (Feb-Sep)	Broadgate et al. (1997)
14-61 pmol pmol L^{-1}	P&T-GC-FID	eastern Atlantic (May)	Baker et al. (2000)
30 pmol L^{-1} (<12-94)	Cryo-GC-MS	Western N Pacific (May)	Matsunaga et al. (2002)
1.8 pmol L^{-1} (out of patch);	Equilibrator (not in situ) -	Southern Ocean (Jan)	Wingenter et al. (2004)
7.3 pmol L^{-1} (in patch)	GC-FID/ECD/MS		
19.7 pmol L^{-1} (3.8-68.2)	P&T-TD-GC-MS	W N Pacific (April)	Kurihara et al. (2010)
70.6 ± 17.3 pmol L^{-1}	EI-PTR-MS	NW Pacific (July-Aug)	Kameyama et al. (2010)
7.3 pmol L^{-1} (4.4-10.0)	P&T-TD-GC-MS	Sagami Bay	Kurihara et al. (2012)
		(Japan/Pac; April-Dec)	
26 ± 31 pmol L^{-1} (1-541)	Equilibrator - GC-PID	Arctic and Atlantic Oceans	Tran et al. (2013)
		(June/July)	
78.7 pmol L^{-1} (0.2-348)	EI-PTR-MS	Southern Ocean (Dec-Jan)	Kameyama et al. (2014)
25.7 ± 14.7 pmol L^{-1} (ca. 5-60)	Equilibrator- Mini-CIMS	East Atlantic (Nov)	Zindler et al. (2014)
27 pmol L^{-1} (1.3-121) (basin)[b]	Equilibrator- or	Arctic, Pacific, Indian	Ooki et al. (2015)
44 pmol L^{-1} (1.5-165) (slope)	P&T-GC-MS	and Southern Ocean	
30 pmol L^{-1} (2.7-136) (shelf)			

[a] Ship unless specified.

[b] Basin (Bottom Depth >2000 m), Slope (200-2000 m), and Shelf (<200 m) Areas

[c] Programmable temperature vaporisation-GC-FID

3.2.2.2 Binning

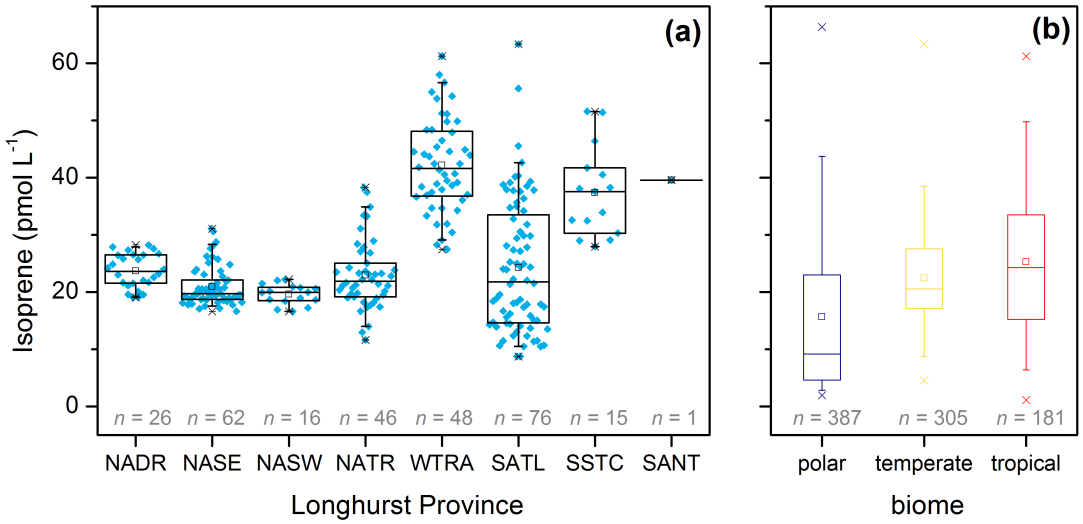

Figure 3.4 – Isoprene in surface water; (a) during AMT 22 binned by Longhurst Province (NADR = North Atlantic Drift Province, NASE = N. Atl. Subtropical Gyral Province (East), NASW = N. Atl. Subtropical Gyral Province (West), NATR = N. Atl. Tropical Gyral Province, WTRA = Western Tropical Atlantic Province, SATL = South Atlantic Gyral Province, SSTC = S. Subtropical Convergence Province, SANT = Subantarctic Province); (b) data from all four cruises binned by biome after Exton et al. (2013); mean (open square), median (line), 25-75th percentile (box); 5-95th percentile (whiskers), min./max. (cross).

For the water concentrations, several different approaches were taken to group results (Figure 3.4): Longhurst ocean biogeochemical provinces (Longhurst, 2007) are widely used in the oceanographic community (Reygondeau et al., 2013). They are defined by four primary biomes or domains (polar, westerlies, trades and coastal) and further divided into provinces by regional differences in a number of physical properties including mixed layer depth, chlorophyll concentrations from satellite and light characteristics, and in biological properties taken from the available literature such as photosynthesis-irradiance curves (Vichi et al., 2011; Reygondeau et al., 2013; Ducklow, 2003). While it has been recognised more recently that these provinces are not static (Reygondeau et al., 2013), they still provide a good initial framework for comparing data. AMT crossed 7 provinces (see also Figure 3.1) and ACCACIA covered another 3, with between 7 and 250 datapoints for each province when using the whole dataset (Figure 3.4). The NASE, NASW and NATR provinces all form part of the North Atlantic Gyre; the South Atlantic Gyre is covered by the SATL province (see caption of Figure 3.4 for abrreviations). Isoprene concentrations

were highest in the WTRA Province, while those in the North Atlantic Gyre were low and without much variation. These patterns are already visible in the transect plots, due to the provinces being crossed sequentially along the cruise track.

Following research by Exton et al. (2013) who reported that isoprene production rates differed significantly between plankton species adapted to different temperature environments, the results were inspected with regards to whether they were in polar, temperate and tropical regions (marked in Figure 3.2; defined by latitude; 90-60 °N and S, 60-23.5 °N and S, 23.5 °N-23.5 °S, respectively). Temperate regions exhibited the lowest variability, with a similar mean and median concentration to tropical waters. In polar regions, concentrations varied strongly and were generally lower than at lower latitudes.

Further explorations of the data will mainly focus on direct correlations with different parameters, with only limited reference to the bins explained here. Binning could be considered useful if those overall comparisons did not yield linear relationships and further subdivision could achieve better agreement for some of the data, or for examining results from different cruises if they passed through different parts of a province; however the relatively straight nature of the AMT cruise tracks allows comparison by latitude between cruises.

3.2.3 Sea-to-air transfer

In order to assess the atmospheric impact of a dissolved gas, it is necessary to calculate its sea-to-air flux; determining whether the ocean is a source or sink, and the magnitude of the transfer. Measuring surface water concentrations alone cannot answer the question of how much of the gas is emitted to the atmosphere, and air concentrations alone do not give an indication of the direction or the magnitude of the flux. Global extrapolations are needed as a basis to assess the significance for global atmospheric chemistry, which localised emissions cannot provide. This section presents a bottom-up approach to estimating sea-to-air fluxes. This extrapolates measured emissions to a global scale, while the top-down approach described in Chapter 5 5.2.2 constrains the source strength to force a match of modelled concentrations with atmospheric observations. Ideally, results from the two methods are in good agreement, implying that they are likely to be accurate.

3.2.3.1 Bottom-up fluxes

Parameterisations of flux calculations have evolved over the past decades and there is still ongoing debate about the validity of generally accepted existing parameterisations at e.g. high wind speeds or for different gases, resulting in ongoing research on the subject (e.g. Johnson, 2010; Carpenter et al., 2012; Blomquist et al., 2006; Yang et al., 2013). However, several existing analyses are widely used and accepted as valid at least for non-extreme conditions.

Johnson (2010; hereafter referred to as J10) published a comprehensive review of the calculation of marine fluxes based on the two-phase model of gas exchange as applied to the sea-air interface by Liss and Slater (1974), including an approach to determining the salinity dependence of the Henry's Law constant H and taking into account resistance on both sides of the sea-air interface. The relevant calculations from J10 are explained briefly in the following section and subsequently applied to the present data.

Liss and Slater stated that the mass flux of a trace gas across the air-water interface, F (mol m^{-2} s^{-1}), can be expressed as

$$F = k_t \left(C_w - \frac{C_a}{H^{cc}} \right) \tag{3.1}$$

where C_w and C_a are the bulk water and gaseous concentrations, respectively, H^{cc} is the dimensionless gas-over-liquid form of the Henry's Law constant and the total mass transfer velocity k_t (m s^{-1}) is described by

$$k_t = \left(\frac{1}{k_w} - \frac{1}{H k_a} \right)^{-1} \tag{3.2}$$

with k_w and k_a being the respective water and air mass transfer velocities (m s^{-1}).

k_w (conventionally expressed in cm h^{-1}) is based on the Nightingale et al. (2000) empirical parameterisation with wind speed at 10 m, u_{10} (m s^{-1})

$$k_w = \left(0.222 u_{10}^2 + 0.333 u_{10} \right) \times (Sc_w/600)^{-1/2} \tag{3.3}$$

where Sc_w is the Schmidt number of the relevant trace gas in water, scaled to the Schmidt number of CO_2 in freshwater at 20 °C , $Sc_{w(CO_2)} = 600$. It is calculated from

$$Sc_w = \upsilon_w / D_w = \eta_w / \rho_w D_w \tag{3.4}$$

where D_w is the diffusivity of the trace gas in water and υ, η and ρ are the kinematic viscosity, dynamic viscosity and density of water, respectively.

The air-side transfer velocity is calculated from

$$k_a = 1 \times 10^{-3} + \frac{u_*}{13.3Sc_a^{1/2} + C_D^{-1/2} - 5 + \frac{ln(Sc_a)}{2\kappa}} \tag{3.5}$$

where κ is the von Karman constant (commonly taken to be 0.4 in seawater), Sc_a the Schmidt number in air, 1x10^{-3} is the still air diffusive flux, and the drag coefficient C_D and the friction velocity u_* are related to the wind speed by

$$u_* = u_{10}\sqrt{6.1 \times 10^{-4} + 6.3 \times 10^{-5}u_{10}} \tag{3.6}$$

and

$$C_D = \left(\frac{u_*}{u_{10}}\right)^2 \tag{3.7}$$

As isoprene is a sparingly soluble gas in water, the rate of mass transfer can be reduced to $k_t \approx k_w$ as it is largely controlled by the water-side resistance (Carpenter et al., 2012). When an air concentration of zero is assumed (a valid approximation for the observed air concentrations and species such as isoprene that are supersaturated in the water, see section 3.2.3.2), it is therefore possible to estimate the flux F without a known Henry's Law constant or its temperature dependence, modifying equation 3.1 to

$$F = k_t\left(C_w - \frac{C_a}{H}\right) \approx k_w C_w \tag{3.8}$$

This can be considered an advantage as published values of H for isoprene vary by up to a factor of 2 (Sander, 2015; one or two values even more), and there are only two reported temperature dependence measurements (Ooki and Yokouchi, 2011; Leng et al., 2013) and one estimated value (Kameyama et al., 2010). Here, sea-to-air fluxes of isoprene were calculated using only water-side limitation in the parameterisation (equation 3.8), with a simple sensitivity analysis presented below comparing them to fluxes obtained using both water- and air-side resistance (equation 3.1).

Figure 3.5c shows the calculated results for seawater-derived (bottom-up) isoprene sea-to-air fluxes for all four cruises alongside published values taken from a range of studies (Atlantic only; Baker et al., 2000; Broadgate et al., 1997; Meskhidze and Nenes, 2006;

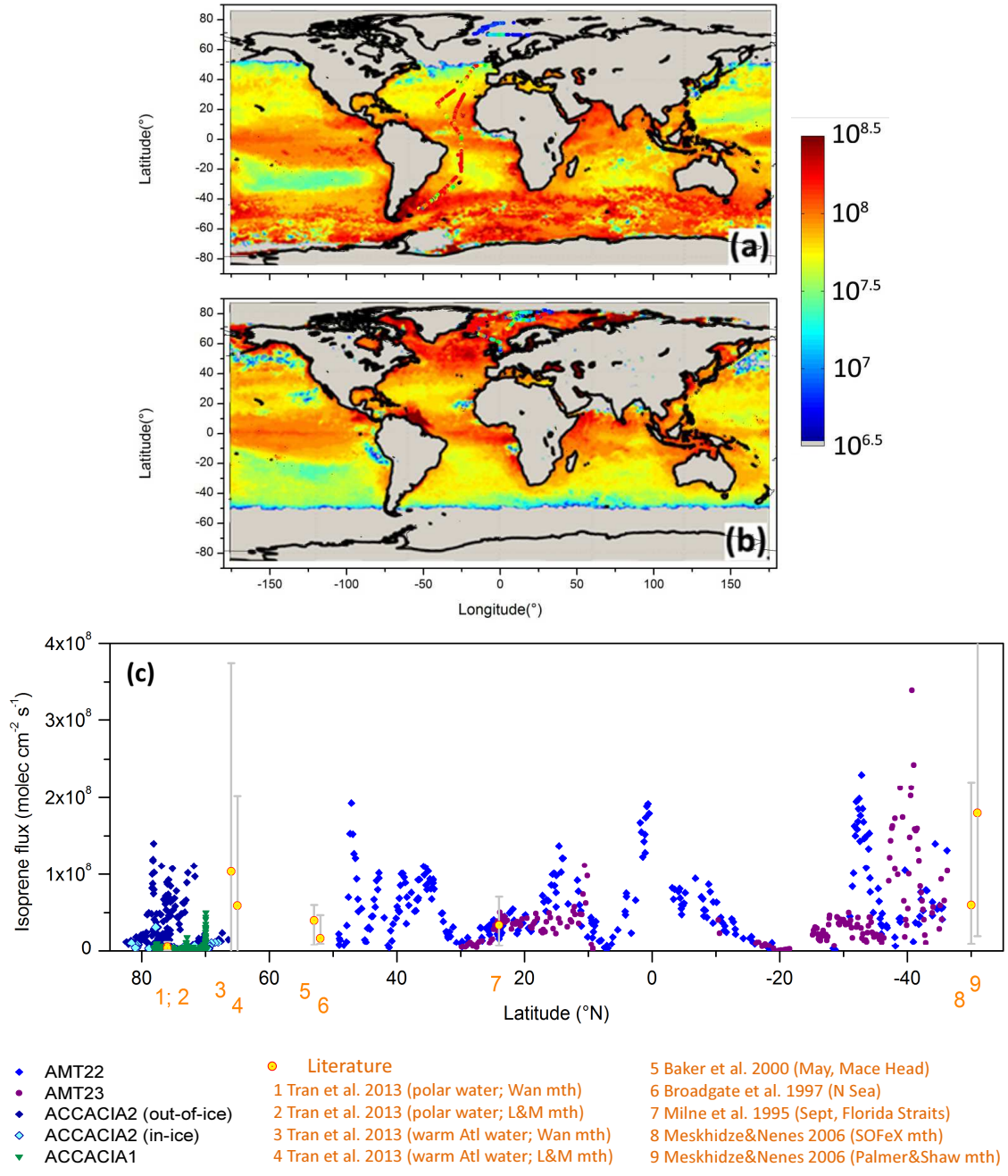

Figure 3.5 – (a) January and (b) July 2001 global fluxes reproduced from Gantt et al. (2009) showing monthly-averaged marine isoprene emission rate (molecules cm^{-2} s^{-1}) with results from this study overlaid on the same scale for comparison ((a) AMTs and ACCACIA 1; (b) ACCACIA 2); (c) Latitudinal transect of seawater-derived sea-to-air fluxes for all four cruises and showing literature values for Atlantic waters, Wan mth = flux parameterisation from Wanninkhof (1992), L&M mth = flux parameterisation from Liss and Merlivat (1986), literature values shown at approximate latitudes; with ACCACIA 2 separated into in-ice and out-of-ice sampling regions. Errors on literature values represent ranges given in the references.

Milne et al., 1995) which were often calculated for a different season compared to the datasets from this project. The same results are overlaid on maps of globally extrapolated seasonal fluxes taken from Gantt et al. (2009) in Figure 3.5a-b. Generally, the agreement with literature values is good, considering the large variability within published data, and data falls mainly within the same order of magnitude. An obvious feature is the large spatial and seasonal variability which often makes comparisons of different studies difficult.

Figure 3.6 uses the example of AMT 22 to highlight the effect of wind speed (vector magnitude) on isoprene flux (colourmap): higher wind speeds typically caused high fluxes (Figure 3.6a; due to the squared relationship in the flux equation), although sufficiently high water concentrations (Figure 3.6b) are also needed for a large flux. Results from the Arctic winter/early spring (ACCACIA 1) were very low, owing to very low isoprene concentrations in the water. Emissions from the same area in the summer (ACCACIA 2) were similarly low between sea ice, in this case due to a combination of relatively low isoprene and very calm conditions. Open water stations showed much higher (up to *ca.* 20×) fluxes comparable to those calculated for the Atlantic, where both wind speeds and water concentrations were generally higher. Despite the very similar concentrations of isoprene in water for both AMT cruises, fluxes were up to a factor of 6 different in sections where wind speeds differed markedly between cruises.

Parameters such as salinity and air or water temperature had very little effect on the flux estimates, as did air concentrations. Fluxes calculated using measured values for isoprene in air (equation 3.1, substituting k_t by k_w) were only marginally different from those using an assumed concentration of zero (equation 3.8; 0-1 % higher when assuming $[isp]_{air} = 0$) and even the elevated air levels observed during AMT 23 did not significantly affect emission estimates (0-2 % higher for $[isp]_{air} = 0$ compared to air data including all except the most strongly contaminated samples). While the approach using equation 3.1 (with k_t) should be more accurate as it accounts for limitation by both sides of the interface, it did in fact not differ significantly from estimates based on water-side control only, due to the low observed air concentrations and therefore low air-side resistance (0-1.5 % higher for only water-side limitation compared to limitation by both sides using measured air concentrations for AMT 22; still only 0-3 % for AMT23).

Estimates of flux estimates using a top-down approach (assuming steady-state conditions

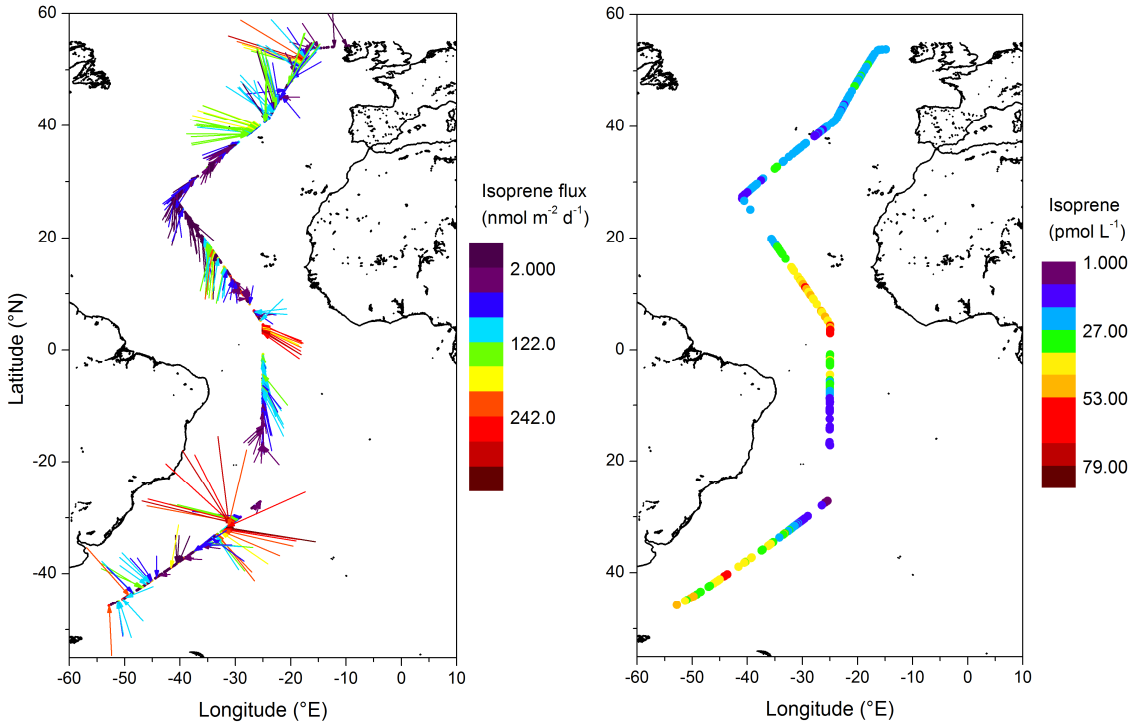

Figure 3.6 – AMT 22 cruise track with (a) wind vectors arriving at the track for every water sample, coloured by isoprene flux and with a magnitude proportional to wind speed; (b) colourmap indicating isoprene concentration in surface water. Wind data provided by BODC/NERC.

where the flux F from the water equals the losses in the atmosphere) are described in Chapter 5 5.2.2; factors affecting the two approaches and differences between them are discussed in Chapter 5 sections 5.2.3 and 5.2.5.

3.2.3.2 Saturation anomaly

It can also be useful to examine the saturation anomaly (SA) of isoprene in the water as it eliminates the wind speed dependence, one of the main drivers of flux, and can therefore indicate where conditions generally favour an ocean source or sink. SA compares the equilibrium analyte concentration in water based on its Henry's Law solubility ($H = C_w/C_a$) and the observed air concentration C_a to the observed water value C_w. A SA of zero indicates equilibrium (Equation 3.9).

$$\text{Saturation Anomaly} = 100\% \times \frac{C_w - C_a/H}{C_a/H} \tag{3.9}$$

Isoprene is typically supersaturated in the water by up to several orders of magnitude, which is in agreement with the literature (e.g. Broadgate et al., 1997; Milne et al., 1995; Wingenter et al., 2004), implying that the flux will always be from water to air. Figure 3.7 shows a comparison of saturation anomalies and fluxes for the two AMTs, which could be expected to have similar SAs given the close agreement of the water concentrations (section 3.2.2). In fact, the apparent large difference in SA between AMT 22 and 23 especially towards the southern high latitudes, but also around the equator, can largely be attributed to air concentrations being below the detection limit (DL) for AMT 22. For those datapoints, $[isp]_{air}$ was set to 0.5×DL, leading to a factor of 2 increase in the SA compared to a datapoint just above the DL. For the Arctic, the picture is dominated by the air concentrations even more: ACCACIA 2 shows SA values of up to 15× higher than AMT in some cases (typically 10×) due to atmospheric mixing ratios <DL, while ACCACIA 1 SAs are generally lower, but vary by several orders of magnitude within the cruise due to highly variable isoprene in air (200-150 000 %) (data not shown). It becomes apparent that the very low air concentrations influence the SA results strongly, so that a comparison is not necessarily useful beyond observing that they are of the same order of magnitude for both AMTs, extremely variable in the Arctic and much smaller for the winter; however, the ocean is a strong source in all cases.

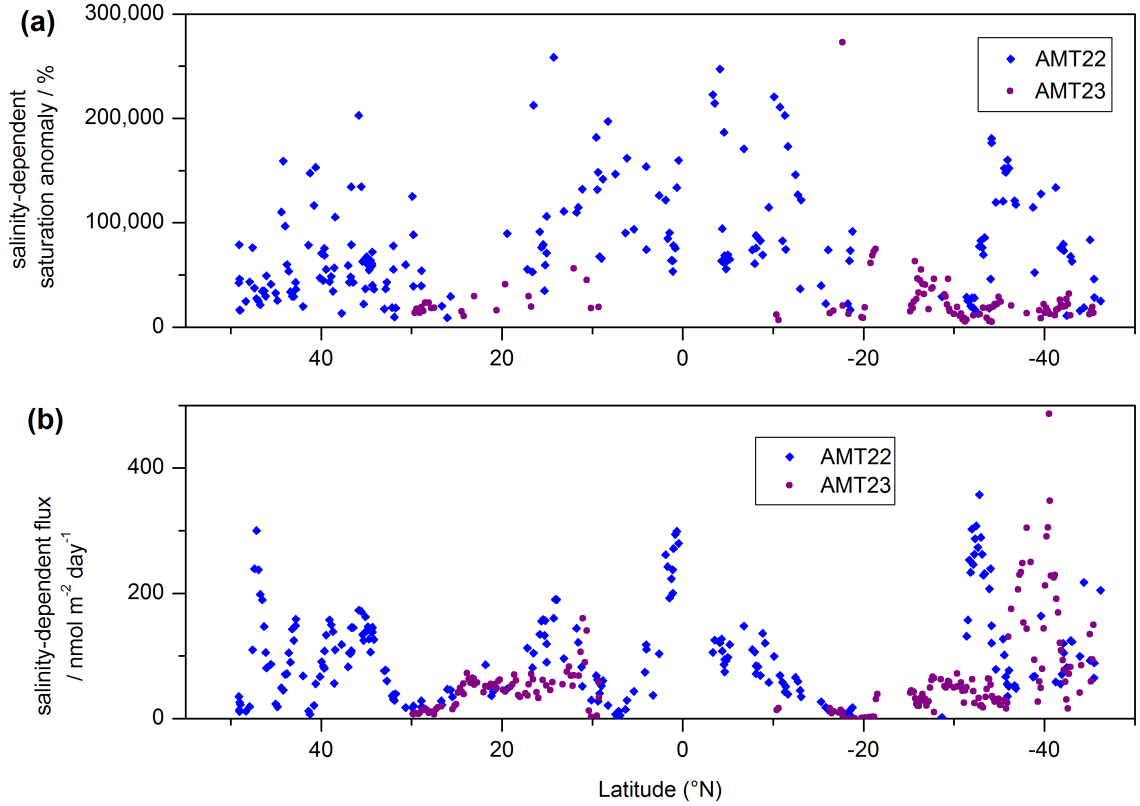

Figure 3.7 – Comparison of (a) saturation anomalies (SA) and (b) fluxes for AMT 22 and 23. SAs are dominated by air concentrations, fluxes by wind speed. SA calculated setting $[isp]_{air}$ data below DL to 0.5×DL

As discussed above, the main controls of the calculated fluxes are the wind speed and the isoprene concentration in water. The former can be obtained on a global scale from a number of sources including climatologies, comprehensive databases and satellite products (e.g. from http://giovanni.gsfc.nasa.gov/giovanni/). Clearly, a better understanding of the factors affecting the latter would be a large step towards a more accurate global extrapolation of isoprene fluxes, and the remainder of this chapter will therefore focus on potential controls of isoprene in the water.

3.2.4 Correlations with isoprene in surface waters – potential controls on emissions

In order to investigate controls on concentrations of isoprene in seawater, this section necessarily assumes that concentrations are directly correlated with production, i.e. that oceanic losses do not vary significantly across the different water bodies sampled. Chemical and physical loss rates due to reactions in the water column and downward mixing are believed to be slow (Palmer and Shaw, 2005), thus to a first approximation they can be assumed to be constant. Biological losses as a result of bacterial consumption were similarly assumed to be very small by these authors, based on evidence from laboratory experiments by Shaw et al. (2003). The main loss from the surface ocean is in fact due to sea-air gas exchange, which is strongly dependent on wind speed as shown above (section 3.2.3). This means that our assumption breaks down at high wind speeds especially, as the concentrations are controlled by losses to a larger extent and therefore no longer proportional to production.

In the following analyses, data from ACCACIA 1 will not be considered due to the lack of supporting biological measurements on that cruise.

3.2.4.1 Chlorophyll-a

It is now generally accepted that a biological source of marine isoprene exists (e.g. Shaw et al., 2010; Bonsang et al., 2010; Kameyama et al., 2014; Ooki et al., 2015; Zindler et al., 2014). However, no consensus has been found on what this source and its magnitude are exactly and hence what proxy may be suitable in order to extrapolate emissions globally,

or what – if any – function isoprene has in the marine environment (e.g. Shaw et al., 2003; Gantt et al., 2009; Bonsang et al., 2010; Kameyama et al., 2014; Ooki et al., 2015; Zindler et al., 2014). Data gathered during this study, especially during the AMT cruises, provide an excellent basis to explore these questions as they span a huge latitudinal range comprising different ocean basins, provinces and climate regions and were made alongside a large range of biological and physical measurements.

Since the early research into marine isoprene reported a correlation of isoprene concentrations in water with Chl-*a* concentrations (or fluorescence where no Chl-*a* calibration was available) (Bonsang et al., 1992; Milne et al., 1995; Broadgate et al., 1997), every published study has attempted to find a relationship with this parameter, with varying success. Some observe excellent correlation (Wingenter et al., 2004), others moderate to weak (but still significant) correlations (e.g. Kameyama et al., 2014; Baker et al., 2000), and in some cases the agreement improves when the data is grouped by various parameters. However, a few researchers do not find any significant correlation for their results (Zindler et al., 2014; Bravo-Linares et al., 2007). There does not appear to be any association of the observed Chl-*a* - isoprene correlations with the study region, implying that it is not a simple geographic difference in conditions which is responsible for the discrepancies. Authors have attempted to fit a linear regression to their data in order to give a quantitative relationship with Chl-*a* where the dataset allowed it; some published equations are given in Table 3.4.

Recent culture studies by Exton et al. (2013; hereafter referred to as E13) proposed a modified approach which is based on the observation that phytoplankton species produced different amounts of isoprene, depending on whether they were typically found in polar, temperate or tropical regions or biomes, with polar species showing the lowest rates. The paper concludes that a different factor should be applied for the relationship with chlorophyll for each of those climates (roughly defined by latitude, as described in section 3.2.2.2). Ooki and co-workers (2015; hereafter referred to as O15) have published an extensive dataset for isoprene from several field campaigns in the Pacific, Indian and Southern Oceans which appears to support the conclusion of Exton et al., as they also found that binning data by temperature yielded the best results. They do not refer to E13, but formulate empirical equations based on both sea surface temperature (SST) and Chl-*a* to predict surface ocean isoprene for four temperature ranges (SST <3.3, 3.3-17,

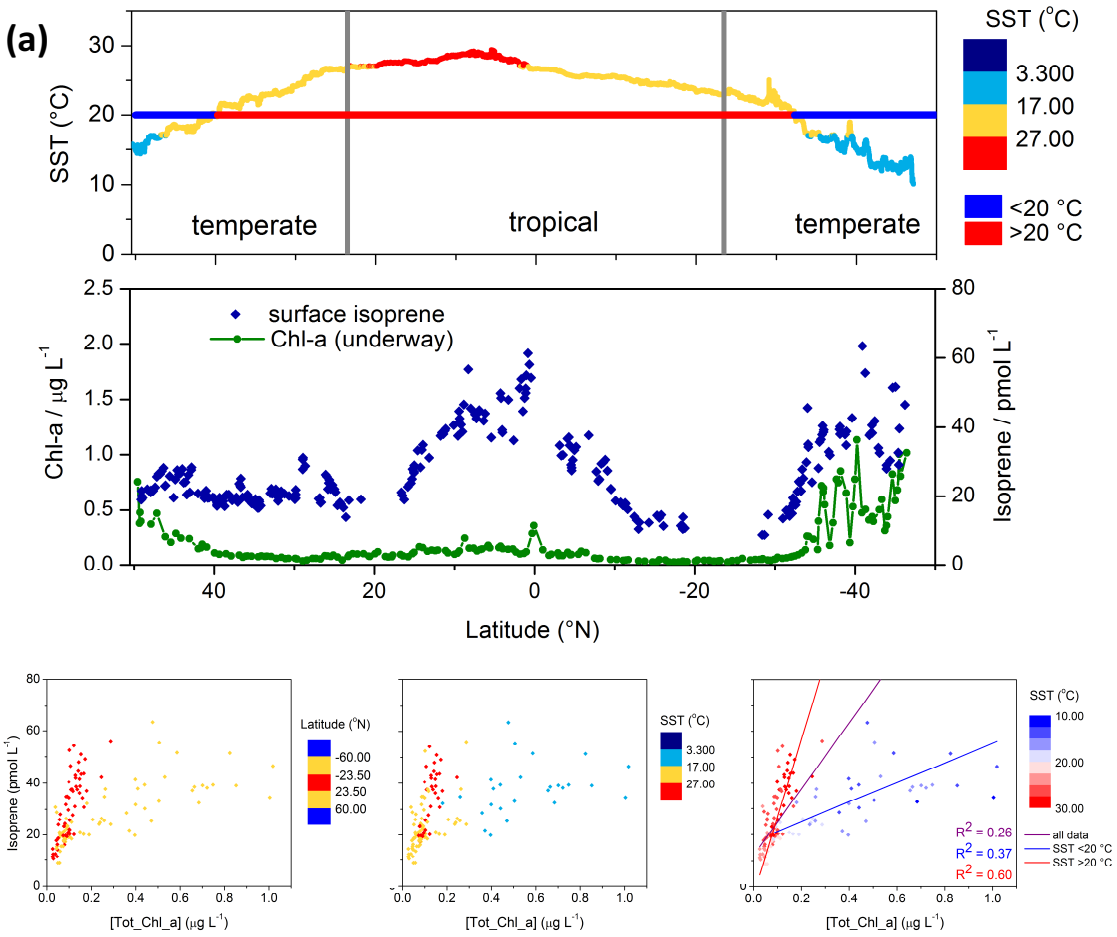

Figure 3.8 – **(a)** Sea surface temperature along with temperature and latitude bins following O15 and E13 (see text), surface Chl-*a* and isoprene during AMT 22; correlation plots below the transect/timeseries graphs show the same data coloured by latitude or temperature ranges (averaged higher- to lower-resolution data as needed, details see text). Biological and temperature data provided by BODC/K. Reifel (Oregon State University). *Continued over...*

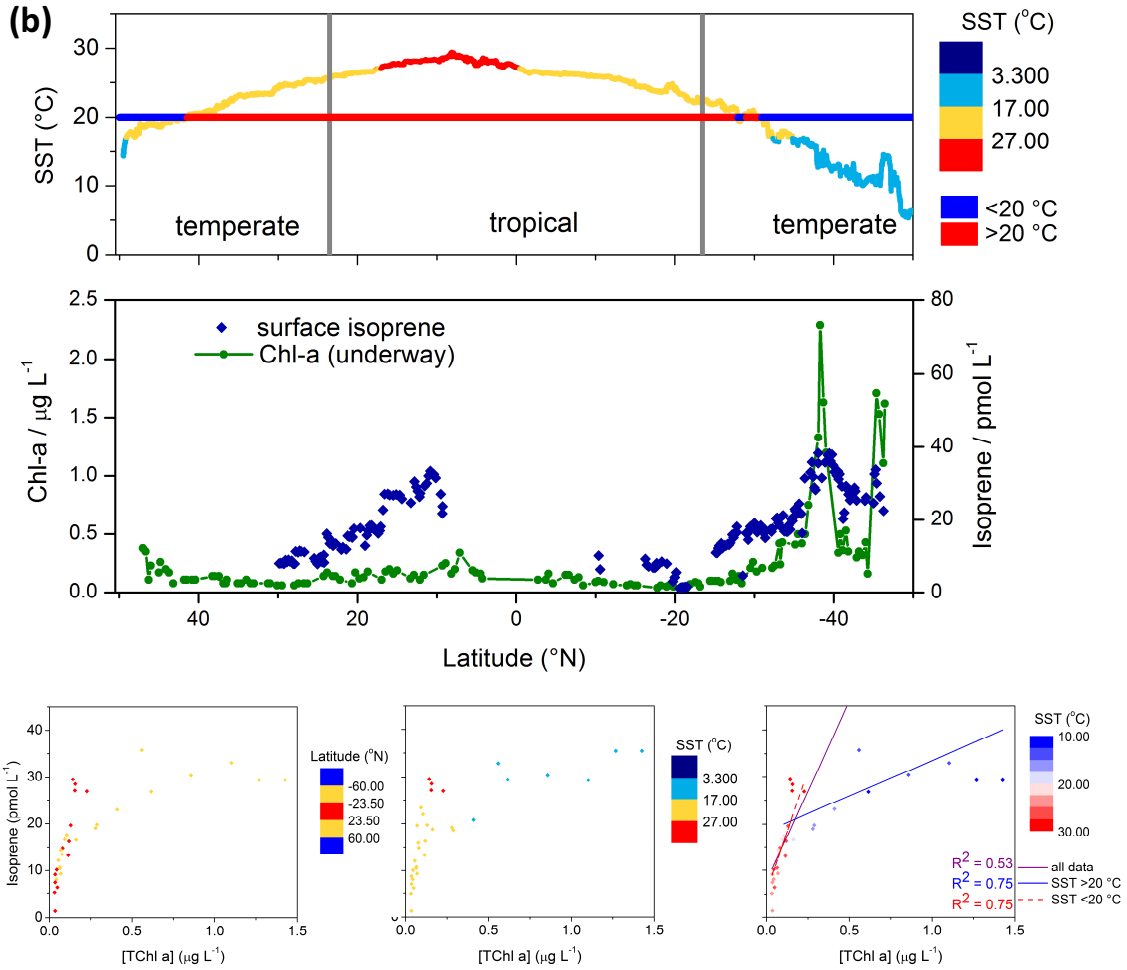

Figure 3.8 – **(b)** As (a) but for AMT 23. Biological data provided by BODC/R. Airs (PML).

Continued over...

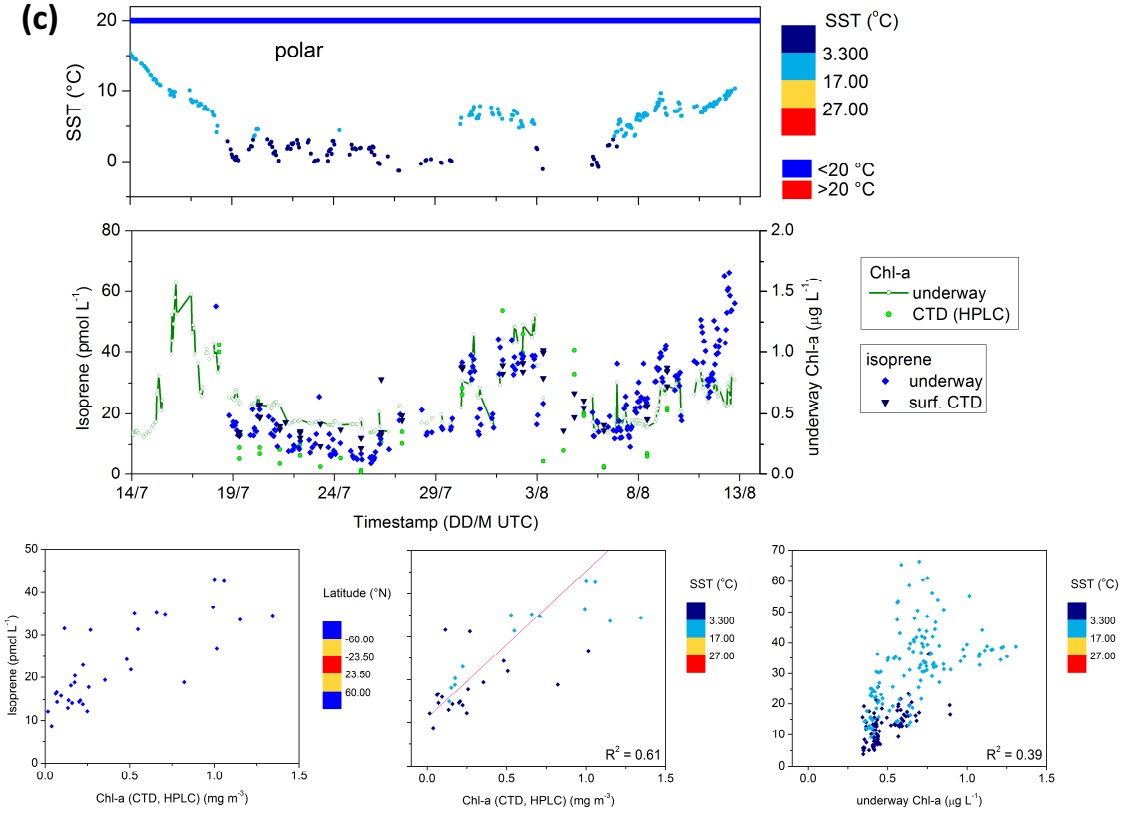

Figure 3.8 – **(c)** As (a) but for ACCACIA 2. Biological data provided by H. Bouman/A. Small (University of Oxford), C. Hughes/J. Stephenson (University of York).

17-27, and >27 °C).

Figure 3.8 shows AMT and ACCACIA 2 data as transect or timeseries plots alongside Chl-*a* and SST. Also shown are Chl-*a* - isoprene correlation plots for the same datasets after averaging the higher- to the lower-resolution data, with points coloured by the latitude or temperature bins suggested by E13 (latitude) or by O15 (SST), respectively, and by the actual SST value for each sample. Where two different measurements of Chl-*a* were available, a further plot (coloured by SST) was included. Isoprene data was at higher resolution than Chl-*a* from underway fluorescence data for AMT 22 and 23 where HPLC pigment data was used (AMT 22: underway; AMT 23: surface CTD) and lower than Chl-*a* for AMT 22 (interpolated discrete measurements) and ACCACIA 2 (continuous underway sensor) . ACCACIA 2 CTD pigment data was at the same frequency as CTD isoprene. All further analysis was performed using HPLC pigment data only.

It was decided to group the dataset from this study into two temperature bins, with a threshold value of SST = 20 °C, based on the apparent change in the isoprene-chlorophyll relationship at that temperature for both AMT cruises (Figure 3.8a,b). This threshold coincided more closely with the change in the relationship than the value of 17 °C used by O15. Correlation coefficients for each complete dataset and when separated into different temperature or latitude bins are shown in Table 3.3; most correlations are significant at the 95 %-level or higher.

The separation at 20 °C SST coincides with the transition into more productive waters in the southern latitudes, at the boundary of the South Atlantic Gyre to the Southern Subtropical Convergence (Longhurst provinces SATL and SSTC, see Figure 3.1). It also separates the more productive waters in the North Atlantic from the rest of the dataset, in effect producing a binning by chlorophyll concentrations as well as SST, at least for the Atlantic. For ACCACIA, there seemed to be no clear distinction in the correlation based on SST (all <20 °C) or [Chl-*a*], which resulted in only two temperature ranges for the isoprene-chlorophyll regression analysis. Regression equations for data from this study were determined by the method described by Khalil and Adamowski (2012), the Robust Line of Organic Correlation (RLOC). It takes into account the fact that the x-values have an error associated with them in the same way as the original LOC (line of organic correlation) approach, but uses median and percentile values instead of average and standard deviation, making it more robust to outliers and censored data (Khalil and

Table 3.3 – Correlation coefficients for isoprene versus Chl-*a*, for the different SST or latitude ranges described in the text; $p < 0.05$ for all correlations except those in grey font ($p < 0.12$).

Correlation coefficient R^2 for ...	*bin*	*criteria*	**AMT 22**	**AMT 23**	**ACCACIA 2**
Whole dataset		-	0.26	0.49	0.61
Binned dataset	*1*	*<20*	0.35	0.55	(0.61)[a]
(SST / °C)	*2*	*≥20*	0.60	0.82	-
Ooki et al. (2015)	*1*	*<3.3*	-	-	0.21
temperature bins	*2*	*3.3-17*	0.10	0.06	0.72
(SST / °C)	*3*	*17-27*	0.24	0.61	-
	4	*>27*	0.37	0.50	-
Exton et al. (2013)	*1*	*polar*	-	-	(0.61)[a]
biome bins		*(60-90 °N & S)*			
(degrees latitude)	*2*	*temperate*	0.58	0.71	-
		(23.5-60 °N & S)			
	3	*tropical*	0.61	0.82	-
		(23.5 °N- 23.5 °S)			

[a] Whole dataset in one bin.

Adamowski, 2012). The calculations for the slope (b_R) and intercept (a_R) are

$$b_R = \text{sign}(r)\ \frac{y_{(75)} - y_{(25)}}{x_{(75)} - x_{(25)}} \tag{3.10}$$

$$a_R = \text{median}(y) - b_R\,\text{median}(x) \tag{3.11}$$

where sign(r) is the algebraic sign of the Pearson correlation coefficient, and $y_{(75)}$, $y_{(25)}$, $x_{(75)}$ and $x_{(25)}$ are the 75^{th} and 25^{th} percentiles of the estimates (measurements) of y and x. Equations for RLOC performed on isoprene in conjunction with Chl-*a* are given in Table 3.4, with additional equations from the literature for comparison. Overall, the slope values span two orders of magnitude (6.4 to 330 pmol isp (µg L^{-1} Chl-*a*)$^{-1}$) and are consistently much higher for tropical regions than colder areas. The spread of slopes for the latter is within one order of magnitude for all values, and within a factor of three for the data from this study. E13 values are production rates rather than concentrations and are not directly comparable with the other data; however it can be seen that the difference between the slope for the temperate and tropical bin is not as pronounced as for all other datasets that distinguish between these in some way (less than a factor of two, compared to a factor of *ca.* 7-15 for other studies).

The relationship by Ooki et al. (2015) takes into account different SST ranges, making it the most refined published approach available to contrast with the current dataset (which also appears to require differentiation by SST). A predicted isoprene concentration was calculated and compared to the measured values in this study, with results shown in Figure 3.9.

Despite being a different type of measurement, an attempt at a comparison with the E13 production rates can be made by simply looking at the correlation of the predicted rates versus measured concentrations while disregarding the absolute values. This assumes that concentrations are dominated by production processes by biomass containing Chl-*a*, and that any other production and losses are negligible in comparison (both biotic and abiotic, including sea-air exchange). Conclusions can only be qualitative and comparisons are only useful if the data spans at least two latitude bins; where it falls within a single bin, the correlation will be identical to that with Chl-*a*. It is a very similar approach to that adopted in the sections below that investigate correlations with parameters potentially controlling isoprene production.

Table 3.4 – Regression equations for isoprene *vs.* Chl-*a* for the different SST or latitude ranges as in Table 3.3, with additional studies for comparison. Published relationships and R^2-values taken from the relevant papers; [Chl-*a*] in mg m^{-3}.

Study *(location)*	***Binning criteria/ Study location***	**Regression equation**	**R^2**
This study	*<20 °C*		
SST-binned dataset	AMT 22	37.9*[Chl-*a*] + 17.5	0.37
(Atlantic Ocean)	AMT 23	15.1*[Chl-*a*] + 18.4	0.55
	ACCACIA 2	34.1*[Chl-*a*] + 11.1	0.61
	≥20 °C		
	AMT 22	300*[Chl-*a*] - 3.35	0.60
	AMT 23	103*[Chl-*a*] + 5.58	0.82
	ACCACIA 2	-	
Ooki et al. (2015)	*<3.3 °C*	9.8*[Chl-*a*] + 1.49*SST + 0.649	0.71
SST bins	*3.3-17 °C*	14.3*[Chl-*a*] + 2.27*SST + 2.83	0.64
(Pacific/Indian/Arctic/	*17-27 °C*	20.9*[Chl-*a*] - 1.92*SST + 63.1	0.77
Southern Ocean)	*>27 °C*	319*[Chl-*a*] + 8.55*SST - 244	0.75
Broadgate et al. (1997)	*Southern Ocean & North Sea*	6.4*[Chl-*a*] + 1.2	0.62
Kurihara et al. (2010)	*North Pacific*	18.8*[Chl-*a*] + 6.1	0.79
Kurihara et al. (2012)	*Temperate Pac. (Sagami Bay)*	10.7*[Chl-*a*] + 5.9	0.49
Hashimoto et al. (2009)[b]	*Subarctic Pacific*	8.2*[Chl-*a*] + 16	0.67
Exton et al. (2013)[a]	*polar*	$0.03(\pm0.006)$*[Chl-*a*] + $6.20(\pm8.39)\times10^{-7}$	0.76
biome (latitude) bins	*(60-90 °N & S)*		
(Laboratory;	*temperate*[c]	$0.24(\pm0.056)$*[Chl-*a*] + $2.50(\pm4.18)\times10^{-6}$	0.43
production rates)	*(23.5-60 °N & S)*	{$0.04(\pm0.025)$*[Chl-*a*] +$1.50(\pm0.32)\times10^{-5}$}	{0.08}
	tropical	$0.39(\pm0.221)$*[Chl-*a*] + $1.30(\pm1.44)\times10^{-5}$	0.15
	(23.5 °N - 23.5 °S)		

[a] (± standard error)

[b] Values given by Kurihara et al. (2012); not in original paper.

[c] Without outlying value; equation in curly brackets includes the outlying value.

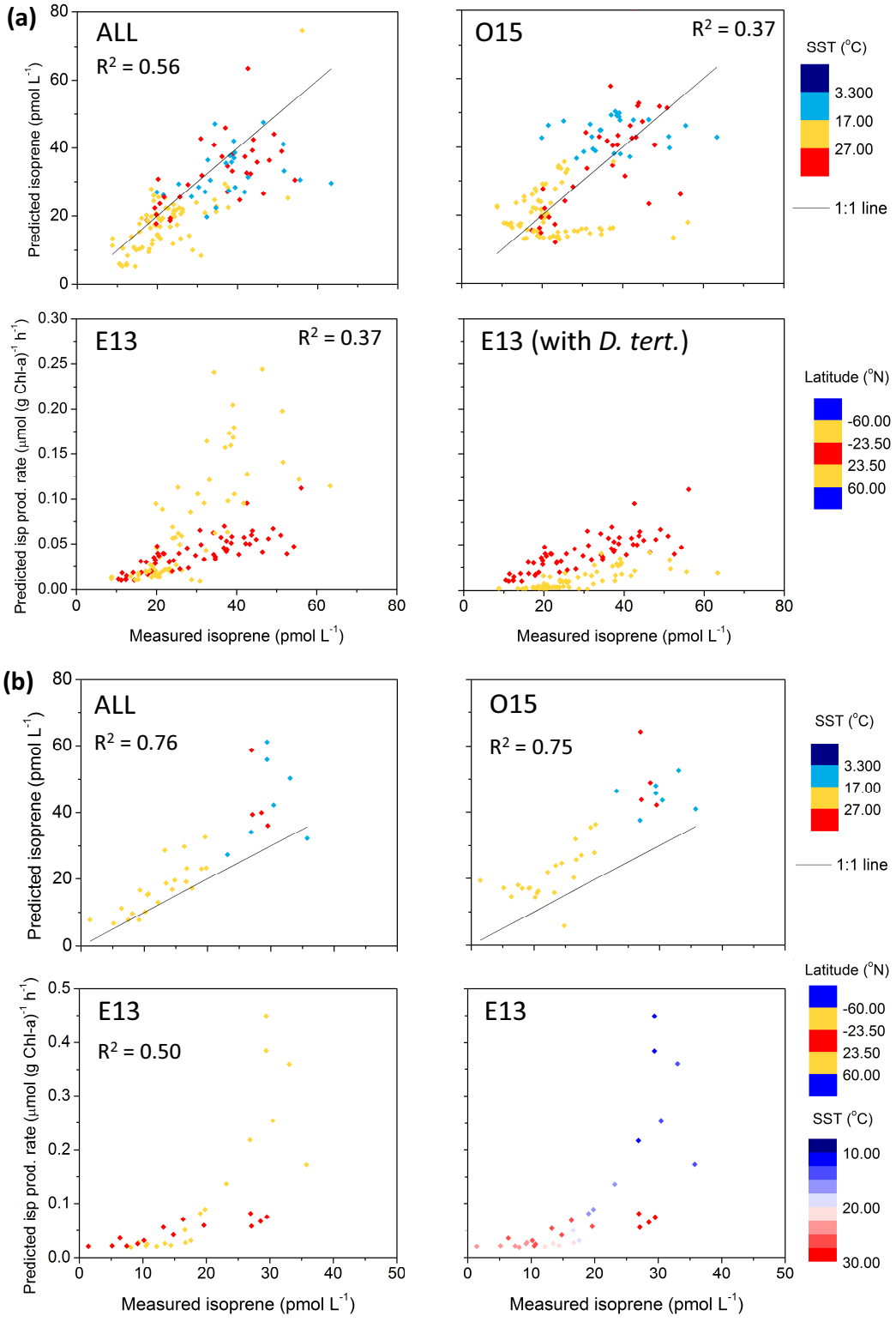

Figure 3.9 – Correlations of predicted compared to measured isoprene concentrations for different predictive approaches for **(a)** AMT 22 and **(b)** AMT 23; coloured by SST or latitude bins, with 1:1 line. Isoprene predicted using equations from O15, E13 and derived from the combined datasets from the current study (*ALL*). E13: predicted isoprene production rates rather than concentrations; E13 temperate biome parameterisation including outlying *D. tert.* also shown for AMT 22; AMT 23 coloured by both latitude bin and SST to highlight change in relationship at 20 *degree*C SST; further details see text. R^2 values only shown for significant relationships ($p < 0.05$).

Continued over...

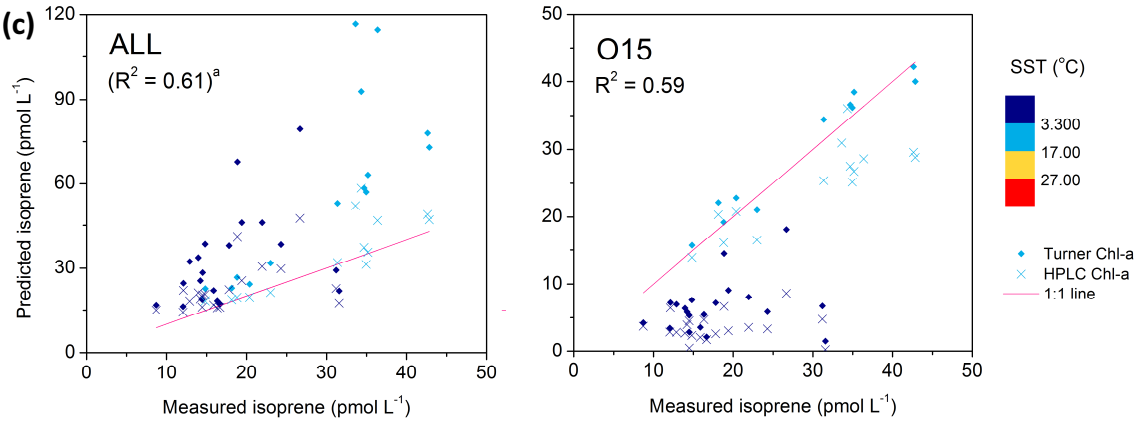

Figure 3.9 – **(c)** Correlations of predicted compared to measured isoprene for different predictive approaches for ACCACIA 2, using different Chl-*a* datasets; coloured by SST bins, with 1:1 line. Isoprene predicted using equations from O15 and derived from the combined datasets from the current study (*ALL*); further details see text. R^2 shown is for HPLC Chl-*a* dataset. [a] whole dataset in one bin, hence correlation same as for whole dataset in Table 3.3.

Figure 3.9 shows that despite overall acceptable correlation coefficients, the different predictive equations do not perform equally well for all of the data and agreement is not always close throughout. O15 achieves reasonably close values for the warmer waters in ACCACIA 2, but underpredicts for polar waters <3.3 °C. Both *ALL* an O15 result in a positive bias of several pmol L^{-1} and considerable scatter with respect to the measured values. The differences could perhaps be attributed to different plankton community structures with different emitting species present.

Production rates based on the E13 parameterisation are fairly proportional to the isoprene distribution in the tropics and for part of the temperate biome (where SST >20 °C), however it suggests that production at higher latitudes/lower SST is much higher than the corresponding observed concentrations would indicate (Figure 3.9a/b). The discrepancy is caused by high Chl-*a* resulting in high predicted isoprene production rates that are not matched by an equal increase in measured concentrations. Wind speeds at the relevant times were no higher than generally at lower latitudes and hence are highly unlikely to be responsible for decreased surface water concentrations due to enhanced sea-air emissions. This implies that either production in laboratory monocultures is higher than that by mixed plankton communities in the field, or that unknown loss processes in the environment lead to a lower net production. If the equation for the temperate bin includes the outlying results for the chlorophyte species *Dunaliella tertiolecta* (*D.tert.*, much smaller

slope; lower R^2 value for the regression; discussed in the original paper), the production is much lower for that latitude range compared to the tropics. As the pattern of a linear distribution at lower rates and a steeper, more scattered spread at higher rates remains (Figure 3.9a), this equation seems even less likely to accurately reflect the environmental processes responsible for the observed isoprene concentrations at all latitudes within the "temperate" bin.

Figure 3.9c highlights the importance of comparable Chl-*a* values in order for any of the predictive equations to yield useful results. Using Chl-*a* measured by HPLC as opposed to Turner fluorescence for predicting ACCACIA 2 isoprene does affect the numbers based on O15 to some extent without changing the overall trends, but makes a large difference to those based on A22. Both methods are widely used to determine Chl-*a* concentrations; and underway fluorescence sensors are typically calibrated by discrete samples analysed with a Turner fluorometer (standard procedure for AMT cruises). HPLC pigment analyses are generally accepted as more reliable, but not a feasible method for high-resolution underway measurements such as those obtained by underway fluorescence. Comparison to a satellite composite product shows that extrapolation using remotely-sensed Chl-*a* could also be affected by a discrepancy between isoprene/Chl-*a* relationships derived from in-situ data, as the satellite Chl-*a* shown as background in Figure 3.1 does not always agree well with the Chl-*a* from HPLC analysis plotted in Figure 3.8a (AMT 22). As previously seen in Figure 3.8c, the frequency and type of the additional data (in this case Chl-*a*) may also affect the fit and coefficients of linear regressions, especially for data near the detection limit of underway sensors (e.g. AMT 22; the ACCACIA 2 underway sensor data can be used for trends only as it has not yet been calibrated).

This section has shown that while linear relationships with Chl-*a* can be used to predict isoprene concentrations in surface water, the results are scattered and often deviate substantially from observed values. Binning by SST or latitude both greatly improve the predictive capability of linear regression analyses across different environmental conditions; however the measured data still cannot be reproduced accurately (temperature-binned predictions only capture between 57 and 79 % of the variability). This appears to be particularly the case at higher Chl-*a* concentrations, where shallower slopes indicate that phytoplankton biomass alone cannot account for the observed isoprene, as found by Broadgate et al. (1997), Kameyama et al. (2014) and this study. Empirical equations

based on field studies (O15 and A22) have yielded closer agreement with observations than laboratory-based relationships (E13), implying that there are additional processes in the environment that were not captured by the monoculture experiments. Overall, a different set of parameters more closely related to isoprene measurements would be useful in constraining the global isoprene budget better than with the available Chl-*a*-based relationships.

3.2.4.2 Phytoplankton functional types (PFTs)

As an increased number of laboratory studies has been published and more refined production rates are becoming available, it has become obvious that not all phytoplankton species emit isoprene at the same rates, even if normalised to Chl-*a* (e.g. Colomb et al., 2008; Gantt et al., 2009; Bonsang et al., 2010; Exton et al., 2013). Most experiments investigated commonly found species (e.g. Shaw et al., 2003) and grouped plankton cultures by functional type or class in order to obtain average emission rates that could be used for extrapolating to a larger scale (e.g. Arnold et al., 2009; Gantt et al., 2009; Colomb et al., 2009), but also reported some large inter-species variations within those classes (e.g. Bonsang et al., 2010, for diatoms). Field observations were initially also contributing qualitative associations seen in the ocean (Moore and Wang, 2006) and it has more recently been attempted to link field data to the laboratory results (Kameyama et al., 2014; Tran et al., 2013; Colomb et al., 2009). More accurate global emission estimates than from Chl-*a*-normalised production rates have been generated (Gantt et al., 2009; Arnold et al., 2009; Colomb et al., 2009) by combining the more specific emission rates with algorithms such as PHYSAT (Alvain et al., 2005, 2008), which uses ocean colour satellite output to detect the major dominant phytoplankton group (phytoplankton functional type, PFT). PHYSAT can distinguish between nanoeukaryotes, *Prochlorococcus*, *Synechococcus*-like cyanobacteria (SLC), diatoms and more recently also a phaeocystis-like group. The published calculations using PHYSAT for global emission estimates assume that all satellite-derived Chl-*a* in a certain grid box is solely due to the dominant PFT as determined by PHYSAT, and apply the relevant emission rate for the entire grid box, which is a simplification and may lead to erroneous results in any situation where that dominant PFT is closer to 50 than 100 % contribution to the total biomass.

Unsurprisingly, *in-situ* determinations of plankton classes are a more accurate represen-

tation of the actual community structure, and – if available – more appropriate to use in order to investigate potential controls of isoprene in the water. Flow cytometry data can provide information on the smaller cells in a sample, i.e. pico- and nanoplankton, and is one of the core measurements on the AMT programme. The available dataset contains *Synechococcus* (*Syn*) and *Prochlorococcus* (*Pro*) cell counts alongside those for picoeukaryotes (Peuk), nanoeukaryotes (Nano), coccolithophores (Cocco) and cryptophytes (Cryp) (G. Tarran, in AMT 22/23 cruise reports). Larger cells such as diatoms cannot be analysed by flow cytometry. Significant positive (mostly weak) correlations were seen between isoprene and most classes (Figures 3.11 and 3.12; RLOC analysis performed as detailed in section 3.2.4.1), but it is also apparent from the graphs that for all but *Pro*, there is a distinct difference between high and low SST (threshold 20 °C, as for Chl-*a*) and that any analysis for the complete dataset is likely not meaningful. The few points at lower SST (n = 19 (12) for AMT 22 (23)) are scattered; values at higher SST are generally considered to be in the noise for all classes except *Pro* where conversely this is the case for low-SST observations. This analysis will focus on *Syn* and *Pro* data (transect plots shown in Figure 3.10), as several reports of isoprene production and rates are available for these classes (*Syn* and *Pro* in Shaw et al., 2003; *Syn* in Bonsang et al., 2010; Gantt et al., 2009, merely quote *Syn* and *Pro* values from Shaw et al., 2003) and no obvious strong relationship exists for any of the other observed groups that would invite further exploration.

In Figures 3.10 to 3.12, the *Syn* cell counts have been scaled by a factor of 3.5 to reflect the higher isoprene emission per cell compared to *Pro* (Shaw et al., 2003). The association of *Syn* and isoprene at low SST was strong for AMT 22 (R^2 = 0.64), but neither strong nor significant for AMT 23. For both cruises, *Pro* exhibited a relatively strong linear interdependence with the trace gas at high SST, with R^2 = 0.46 (0.45) during AMT 22 (23). For AMT23, the analysis for the sum of (*Pro* + scaled *Syn* (referred to as *Pro*+*Syn* in the following for simplicity) returned a significant correlation with R^2 = 0.65 for SST >20 °C and for the full dataset (R^2 = 0.12), but an insignificant relationship for the low-SST bin; meanwhile all three combinations gave good agreement for the AMT 22 data (R^2 = 0.49-0.56).

The increase in R^2 from *Pro* to *Pro*+*Syn* in AMT 22 implies that for this campaign, *Pro* cell counts alone cannot account for the isoprene distribution as well as a combination of

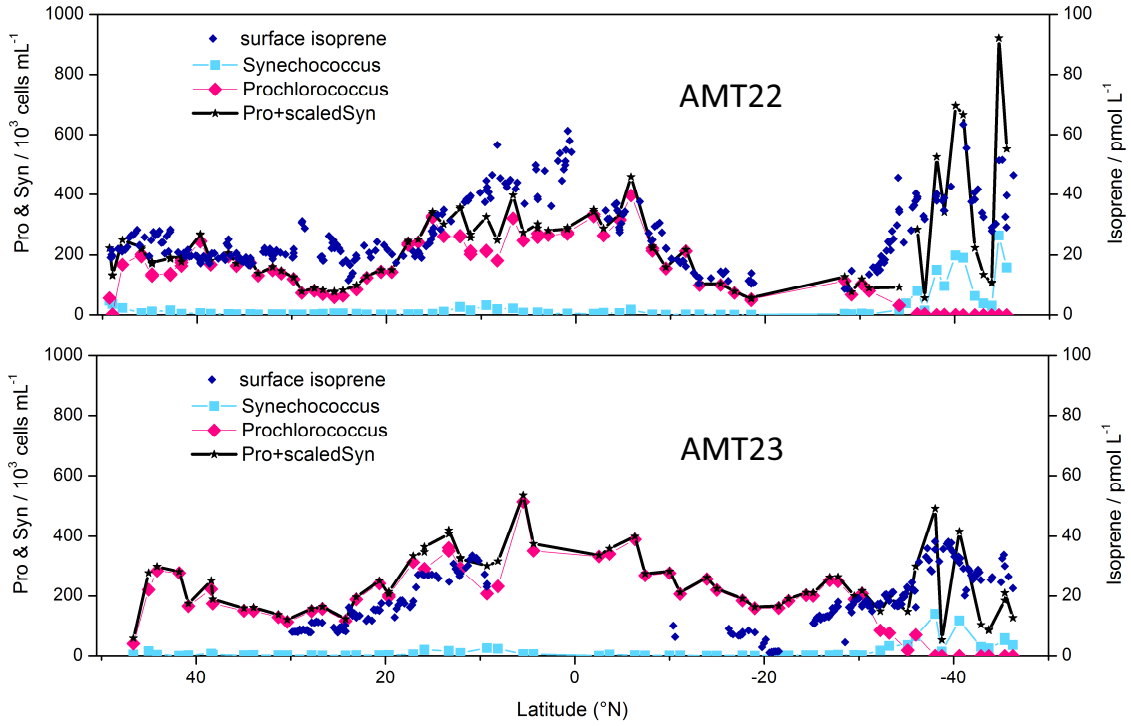

Figure 3.10 – Surface cell counts of *Synechococcus* and *Prochlorococcus*, the sum of *Pro* + scaled *Syn*, and surface isoprene during AMT 22 and 23. Flow cytometric data provided by G. Tarran (PML).

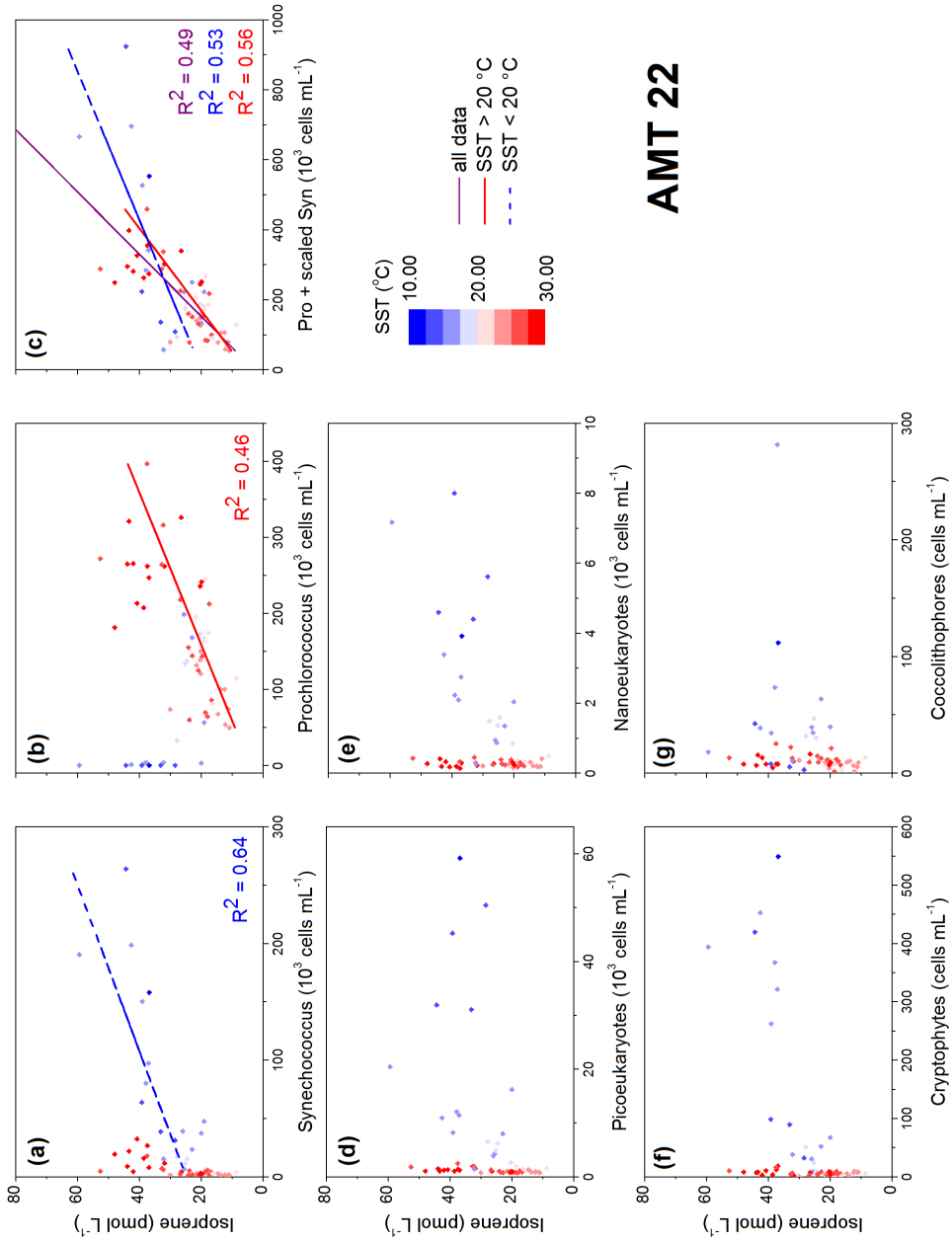

Figure 3.11 – Correlation plots for AMT 22 for isoprene with flow cytometric data (provided by G. Tarran, PML), coloured by SST. Regression lines (RLOC, see text) only drawn where a significant ($p < 0.05$) correlation with $R^2 > 0.4$ existed for *Syn* and *Pro* data (with the exception of *Pro* <20 °C, not shown).

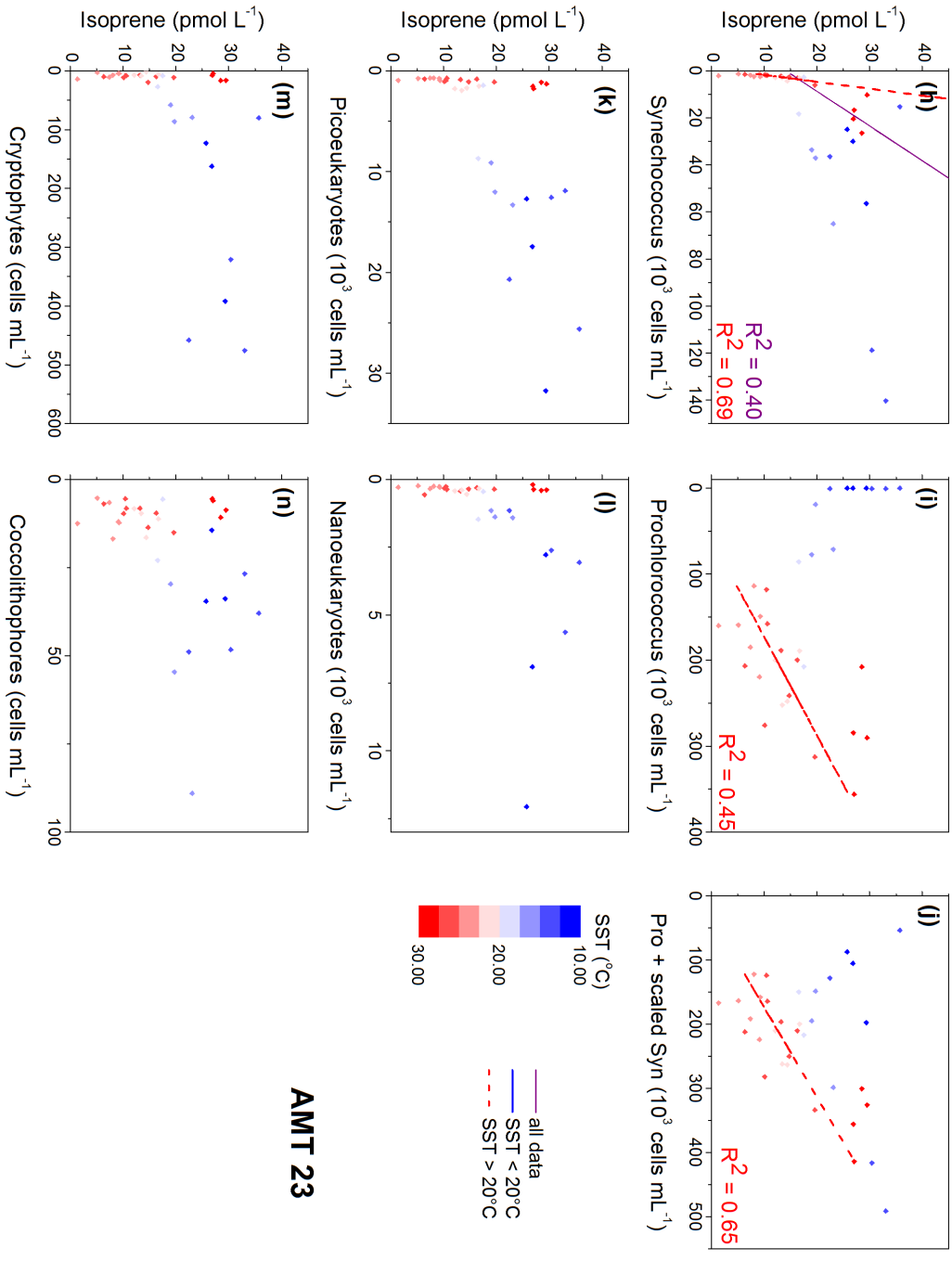

Figure 3.12 – As Figure 3.11 but for AMT 23.

the two species, which is consistent with both being known as relatively strong emitters (Shaw et al., 2003; Bonsang et al., 2010). The same is true for the high-SST data from AMT 23, while unfortunately the picture is much less clear for lower-SST regions on that cruise, as *Syn* counts were not sufficiently high to explain the constant isoprene concentrations. These are however only a few points, which may be exceptions to the generally observed trends and could potentially be explained by another isoprene emitter being present at those sites, or if a change in the community structure and plankton abundance occurred more rapidly than isoprene concentrations changed to reflect this. The latter proposal could be supported by the apparent slight offset between biological and isoprene data seen in the southern latitudes for AMT 22.

The discrepancies between the cruises currently prevent the extrapolation of either relationship to other datasets since cell counts of *Pro* and *Syn* alone do not appear to fully explain the observed isoprene distribution; the two datasets do however follow the same trends, and predicted values agree within a factor of two.

The linear associations found with *Pro*+*Syn* in this study overall agree well with the concept, based on published production rates (Shaw et al., 2003; Bonsang et al., 2010), that *Syn* and *Pro* could be deemed responsible for most of the observed isoprene where these species are the dominant component of the planktonic community, as is the case for *Pro* in the tropical Atlantic; they can also still account for at least a proportion of the isoprene distribution in a more mixed community structure such as in the southern latitudes. In order to evaluate results quantitatively compared to published values, a production rate would need to be estimated, either normalised to cell count, or for more widely comparable values, the cell counts would need to be converted to equivalent Chl-*a* concentrations to obtain Chl-*a*-normalised emission rates. Despite the limitations of the PHYSAT-based approach discussed above, it is more accurate than applying a single emission rate across all grid boxes as previously done for Chl-*a*-based relationships. It could therefore provide an improved estimate, especially if the field-derived production rates from this study are found to agree with literature values from monoculture experiments.

3.2.4.3 Other pigments

Pigments, or chemotaxonomic data, can be used to infer the composition of the observed phytoplankton community and determine more than only the dominant PFT derivable from satellite ocean colour products (see 3.2.4.2). The CHEMTAX software (Mackey et al., 1996) is one of the tools that can calculate the contributions of different phytoplankton classes to the total Chl-*a*. It is based on a matrix of typical pigment:Chl-*a* ratios for algal taxa expected in the sample, which are derived from the literature or from experience in a sampling region, and the algorithm goes through an iterative process modifying the pigment:Chl-*a* ratios to obtain the closest possible match between calculated and observed Chl-*a* (Higgins et al., 2011).

Several pigments in addition to Chl-*a* were measured on AMT 22, 23 and ACCACIA 2. Briefly, a quantity of seawater (1-4 L, volume dependent on biomass content of the water) was filtered through a GF/F filter that was shock frozen in liquid nitrogen and stored at -80 °C until analysis by HPLC ashore, following procedures by Welschmeyer (see AMT 22/23 cruise reports). Relationships with isoprene were investigated for a variety of accessory pigments (e.g. Zeaxanthin, Figure 3.13), with a selection of the most relevant results presented in this section.

For ACCACIA 2, both pigment data and the corresponding CHEMTAX output are available for CTDs, and pigment data from the upper 5 m of the water column were matched to isoprene from the same CTD stations and depths for comparison. As CTD and surface samples agree well for isoprene (see Figure 3.8c), this can be considered a valid alternative to the approach used for AMT data, namely averaging surface isoprene data around the time of the CTD.

Figures 3.14 and 3.15 show correlation plots for the discussed pigments for all three cruises, with regression lines and R^2 shown for the whole dataset where a significant relationship existed ($p < 0.05$) and for temperature-binned data where relevant/calculated; similarly Figure 3.16 for CHEMTAX data from ACCACIA 2. Slopes from the RLOC analysis (details of the calculations given in section 3.2.4.1) are shown in Table 3.5.

Both AMTs followed similar patterns, although this discussion will mainly focus on AMT 22 for which more datapoints are available, giving a clearer picture of the isoprene-pigment

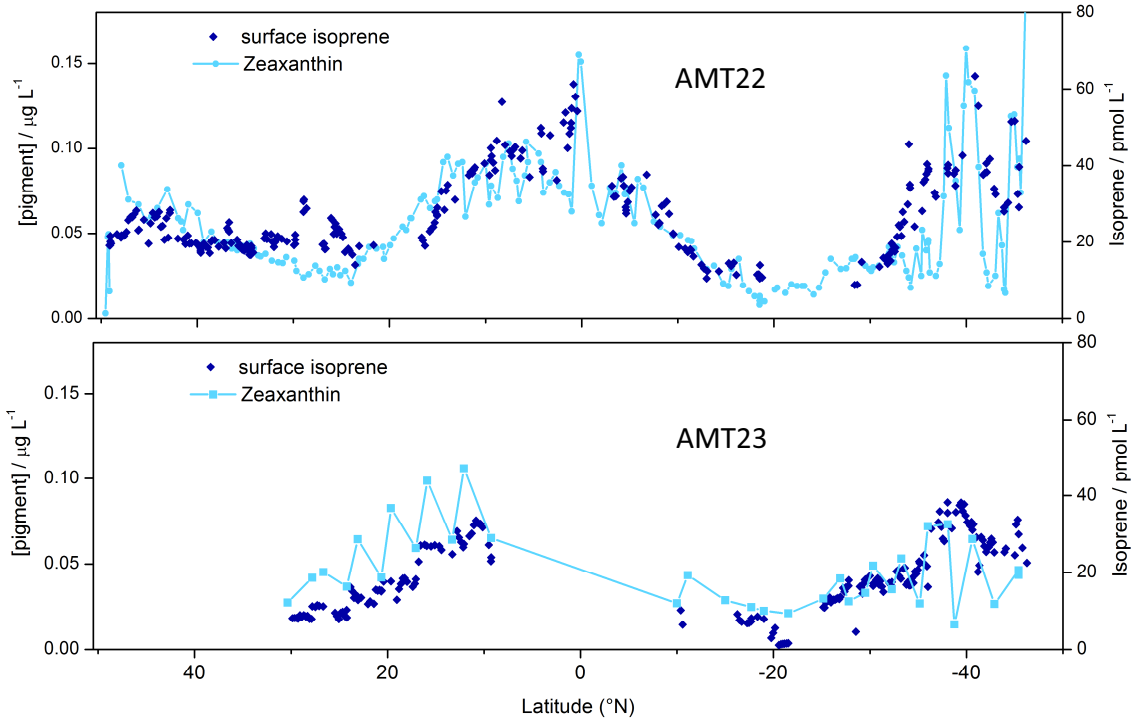

Figure 3.13 – Surface zeaxanthin and isoprene during AMT22 and 23. Pigment data provided by PML/NERC/ BODC and by K. Reifel (Oregon State University).

relationships. Pigments that exhibited an reasonably strong association with isoprene data ($R^2 > 0.4$) for the whole AMT 22 transect were Zeaxanthin (Zea, transect plots see Figure 3.13), carotenes (Caro) and the sum of photoprotective carotenoids (PPC = Zea + Allo + Diadino + Diato + Caro; Alloxanthin, Diadinoxanthin, Diatoxanthin). When grouped by SST (20 °C threshold as for Chl-*a*, section 3.2.4.1), the R^2 for Zea and divinyl-Chl-*a* (DV-Chl-*a*) in the ≥20 °C bin increase to 0.65 and 0.63, respectively.

Fucoxanthin (Fuco) is often used as a marker for diatoms and showed relatively strong significant correlations for higher latitudes during AMT and in the Arctic (R^2= 0.30-0.42; see Figures 3.14 and 3.15, Table 3.5). A link between observed enhanced Fuco (or diatoms) and isoprene levels was also suggested by Moore and Wang (2006) during a fertilisation experiment in the Southern Ocean and several other studies (Baker et al., 2000; Sinha et al., 2007; Kameyama et al., 2014). However, it could be allocated to a variety of taxa that may be present at similar levels (e.g. dinoflagellates and haptophytes; Jeffrey et al., 2011; Higgins et al., 2011).

For ACCACIA 2 (Figure 3.15), a number of pigments in addition to Chl-*a* (Figure 3.8c) and Fuco, including Allo and Caro, showed significant but not very strong positive correlations

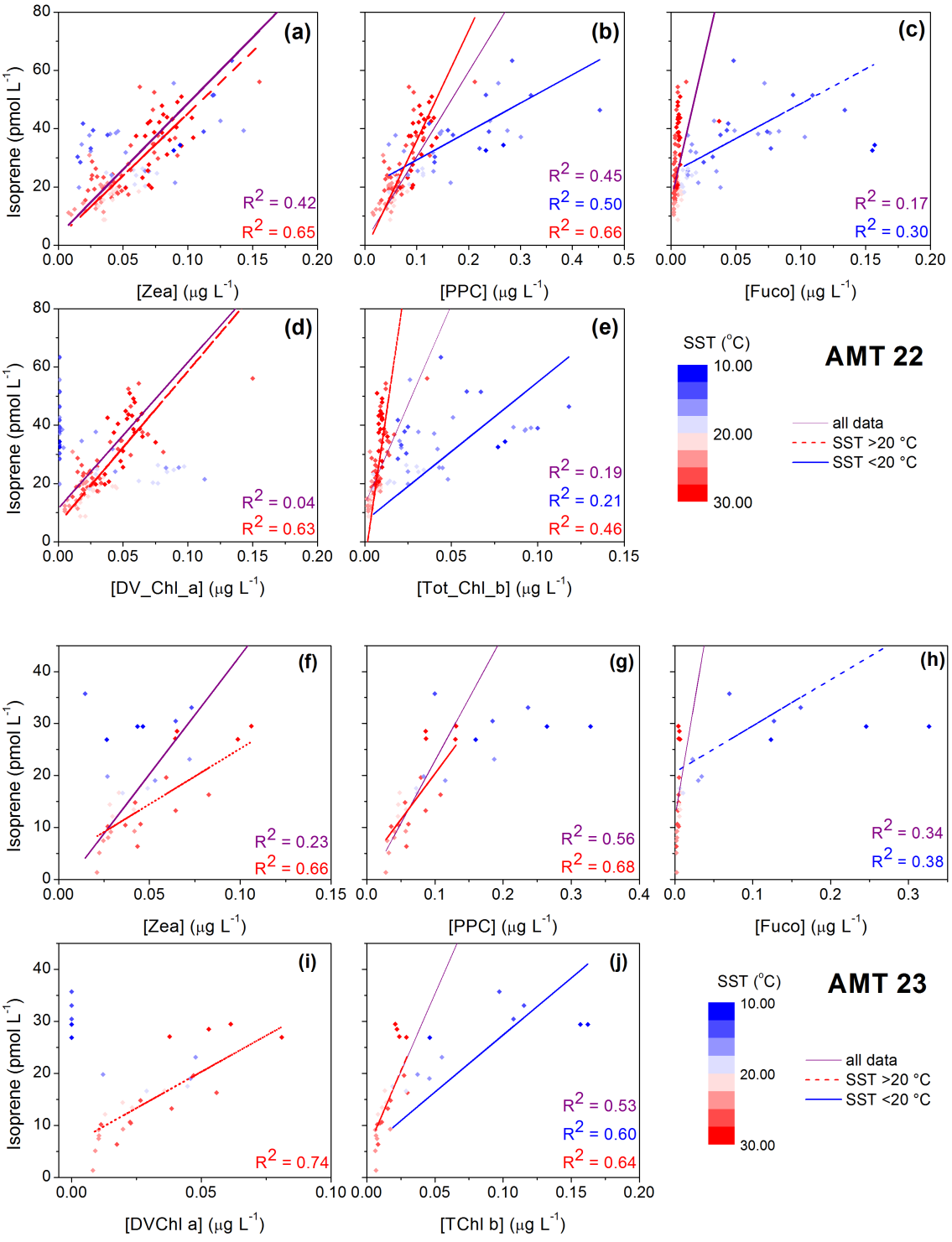

Figure 3.14 – Correlation plots of isoprene with various pigments for AMT 22 (a-e) and AMT 23 (f-j); regression lines and R^2 shown for the whole dataset where a significant relationship existed ($p < 0.05$) and for temperature-binned data where calculated. Pigment data provided by PML/NERC/BODC and by K. Reifel (Oregon State University).

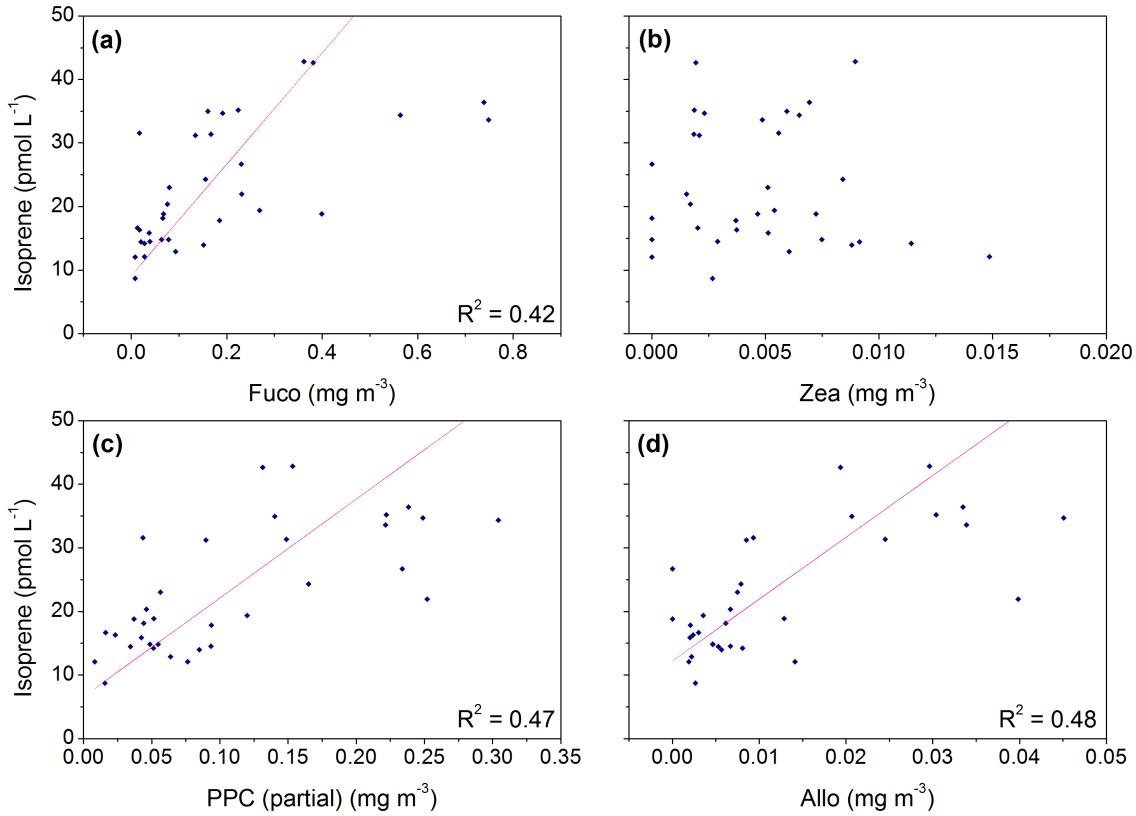

Figure 3.15 – (a-d) Correlation plots of isoprene with various pigments for ACCACIA 2; regression lines and R^2 shown for the whole dataset where a significant relationship existed (p <0.05) and for temperature-binned data where calculated. Pigment data provided by A. Small (University of Oxford).

with isoprene data ($p < 0.05$, R^2 = 0.22-0.48), while several other pigments including Zea had no significant correlation. PPC (calculated from a reduced number of terms compared to the AMT datasets, as no Diato data was available) also had a relatively high R^2-value of 0.47, but unlike AMT where Zea was a major contributor, in Arctic waters the sum was largely dominated by Diadino, a shared marker pigment for various phytoplankton classes. For the CHEMTAX data (absolute Chl-*a* concentration from each phytoplankton plankton class), significant positive, albeit weak, correlations ($p < 0.05$) exist for prasinophytes1&2, dinoflagellates, haptophytes3, diatoms and chrysophytes, which implies all of these classes produce, or are associated with classes which produce, isoprene. Diatoms display the strongest correlation (R^2= 0.49), which is consistent with other studies that found diatoms to be one of the strongest emitters (Milne et al., 1995; Shaw et al., 2003; Bonsang et al., 2010; Kameyama et al., 2014). Chlorophytes, cryptophytes and haptophytes4 show no significant correlation with isoprene at the 95 % confidence level, which could be due in part to their low abundance, as previous investigations have found that all species studied in monocultures to date emitted isoprene (e.g. Shaw et al., 2010). Kameyama et al. (2014) also reported a significant but weak association with haptophytes (R^2 = 0.21; haptophyte type unspecified).

The limitations of pigment analysis can be seen from the example of alloxanthin (a marker for cryptophytes, Jeffrey et al., 2011; Higgins et al., 2011) and cryptophytes: while the former exhibits a reasonably strong relationship with isoprene, the latter does not even have a significant correlation with the trace gas (Figures 3.15 and 3.16). This highlights the fact that, in order to draw conclusions about phytoplankton classes present at the sampling site (and hence potentially responsible for observed isoprene emissions), a more detailed analysis than a simple check for marker pigments is required, such as CHEMTAX; especially for pigments that are not unambiguous markers of one class. However, in the absence of CHEMTAX data, pigments do give some indication of the dominant species present. In addition, they can vary within a class depending on e.g. light adaptation, which can give an indication of the function of the correlated parameter (isoprene) rather than an association with a specific emitting phytplankton class (Rodríguez et al., 2006).

Most of the pigments that were relatively closely related to the isoprene distribution (as discussed above) appear to have remarkably similar relationships with the trace gas between campaigns, especially the carotenes for all three datasets (slopes of 1700, 1600

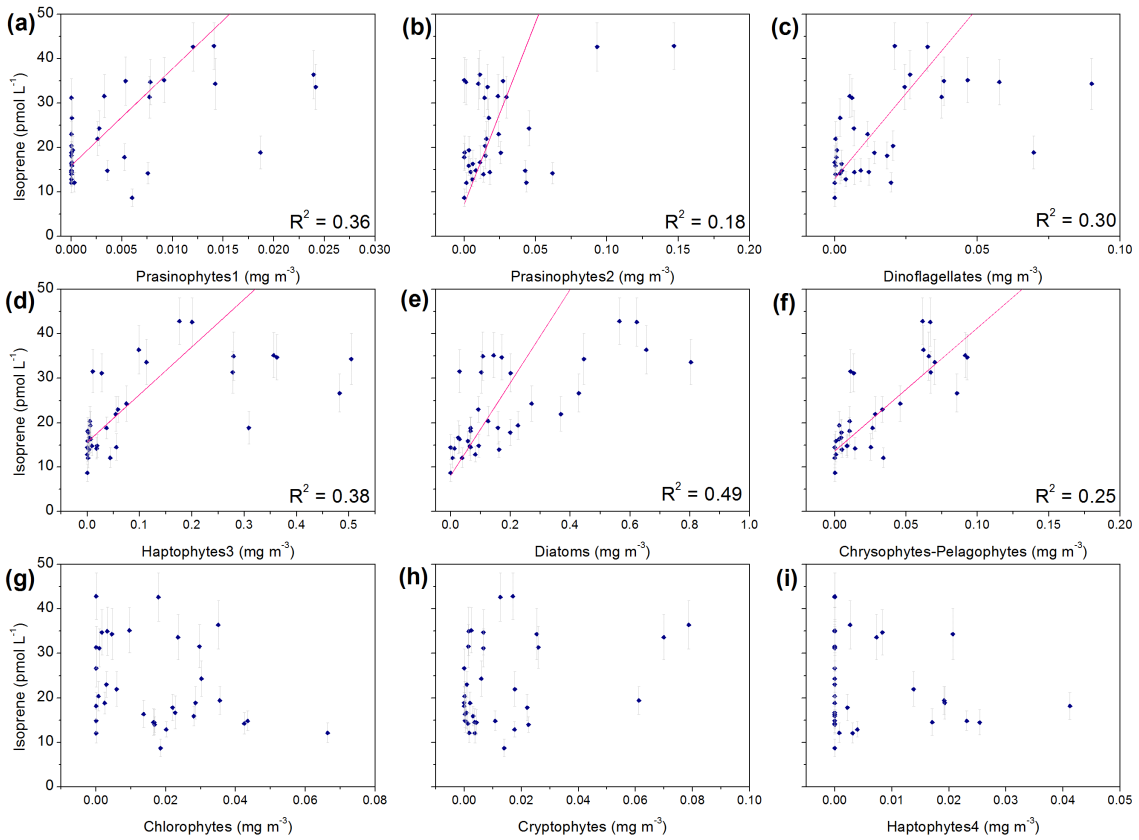

Figure 3.16 – (a)-(i) Correlation plots of isoprene against CHEMTAX data (ACCACIA 2 only; Chl-*a* concentration from each phytoplankton class); R^2 values and regression line shown where a significant ($p < 0.05$) correlation existed; isoprene error bars as in Figure 3.2. CHEMTAX data provided by A. Small (University of Oxford).

Table 3.5 – Slopes from RLOC analysis for various pigments, with binned data shown where investigated.*

Slope (n, R^2) for ..	*bin*	**AMT 22**	**AMT 23**	**ACCACIA 2**
Zeaxanthin (Zea)	*all data*	450 (*132*, 0.42)	460 (*33*, 0.23)	-
	≥20 °C SST	430 (*93*, 0.65)	210 (*22*, 0.66)	
Fucoxanthin (Fuco)	*all data*	1900 (*132*, 0.17)	890 (*33*, 0.34)	(all <20 °C)
	<20 °C SST	240 (*39*, 0.30)	90 (11, 0.38)	90 (*34*, 0.42)
Divinyl-Chl-*a* (DV-Chl-*a*)	*all data*	500 (*132*, 0.04)	-	*n.d.*
	≥20 °C SST	520 (*93*, 0.63)	280(*22*, 0.74)	
Carotenes (Caro)	*all data*	1700 (*132*, 0.45)	1600 (*33*, 0.67)	1400 (*34*, 0.40)
Photoprotective	*all data*	290 (*132*, 0.45)	240 (*33*, 0.56)	(all <20 °C)
Carotenoids (PPC)[a]	*<20 °C SST*	100 (*39*, 0.50)	90 (*11*, 0.33)[b]	155 (*34*, 0.47)
	≥20 °C SST	380 (*93*, 0.66)	180 (*22*, 0.68)	
Chl-b	*all data*	1400 (*132*, 0.19)	600 (*33*, 0.53)	-
	≥20 °C SST	4100 (*93*, 0.46)	610 (*22*, 0.64)	

* Dashes represent no significant correlation at the 95 % level for the pigment in question; *n.d.* means not determined/detected (A. Small, pers. comm.).

[a] PPC = Zea + Allo + Diadin + Caro + Diato (Diato not available for ACCACIA 2).

[b] $p = 0.06$

and 1400 for AMT 22, AMT 23 and ACCACIA 2, respectively), and still only <20 % differences between slopes for Zea and PPC *(all data)* for both AMTs. Some variation in those results could be due to the more sporadic nature of the data from AMT 23 and the longitudinal differences in cruise track compared to AMT 22. Given that Fuco is not in fact a marker for a single phytoplankton and that PPC is a sum of several pigments (with one term missing for ACCACIA 2), and community structure may have varied considerably between the sampling sites, an agreement of the correlation slopes within a factor of two to three for all three campaigns is still rather close.

DV-Chl-*a* is a marker for prochlorophytes (*Prochlorococcus*, Jeffrey et al., 2011; Higgins et al., 2011). Its comparatively strong correlation with isoprene at lower latitudes (>20 °C SST), and the distribution along the meridional transects (not shown) of that taxon seen in the flow cytometric data (section 3.2.4.2), are consistent with *Prochlorococcus* being the dominant producer of isoprene in those regions (Shaw et al., 2003).

Zeaxanthin is a photoprotective pigment as well as a marker for cyanobacteria and is found at increased concentrations at higher irradiance levels (Bidigare et al., 1987; Rodríguez et al., 2006; Jeffrey et al., 2011; Higgins et al., 2011). The strong correlation found here indicates that isoprene emission may be a response to light stress in addition to (or even instead of?) simply being a by-product of photosynthesis as suggested previously (Ooki et al., 2015; Shaw et al., 2003). This would be a similar function to isoprene emissions in terrestrial plants where releases of the gas as a response to oxidative, temperature or light stress are some of its main functions (Sharkey and Yeh, 2001; see section 3.1). Higgins et al. (2011) state that in polar waters where there are practically no cyanobacteria, bacteria may be the main source of the pigment.

Further work on this group of potential controlling parameters will include CHEMTAX analysis on the AMT data in order to provide a more complete picture of the phytoplankton community.

In contrast to the promising results for understanding isoprene emissions from studying pigment analyses described in this section, Zindler et al. (2014) reported that no correlation was found with phytoplankton pigments during their cruise in the Atlantic Ocean (near the African coast). As for Chl-*a*, this could be due to the fact that net emissions may be affected by more than the production rates related to only phytoplankton and that not all

investigations necessarily yield clear results. Zindler et al. (2014) suggest that pigments do not provide information on all biological processes in a sampling location, but that an approach including nutrient availability may be more suitable (section 3.2.4.7).

3.2.4.4 Primary production (PP)

Moore and Wang (2006) stated that isoprene production was directly linked to the rate of primary production (PP; see below for different definitions and method details), and almost all studies to date have similarly concluded that biological production is related to isoprene, as determined by various proxies also discussed in this chapter, such as Chl-*a*, pigments, PFTs or dissolved gases. It should therefore be possible to link the observed isoprene distribution to PP data directly, and it is presumably mainly a lack of availability of such measurements made concurrently with isoprene observations that has prevented other authors from attempting it. The advantage of this approach would be that if a robust relationship could be found, it would avoid the issues encountered with pigment or PFT data of potentially only capturing a subset of the species responsible for isoprene emissions, since it (technically) determines total community production.

Plankton production can be measured in several different ways that all differ slightly in the processes they capture (Robinson et al., 2009). One of the most widely used methods is the ^{14}C-PP method, in which incubation experiments with radio-labelled media determine the amount of carbon incorporated into particulate carbon over a set incubation time (e.g. Robinson et al., 2009; Quay et al., 2010; Tilstone, AMT 22/23 cruise reports). Data from such experiments is available for both AMT cruises, including separate values for the three size fractions pico- (0.2-2 µm), nano- (2-10 µm) and microplankton (>10 µm). This section focuses on relationships with PP integrated over the whole water column (intPP); results of that exploration are displayed in Figure 3.18 and Table 3.6.

Figure 3.17 shows that the total intPP fits the surface isoprene distribution better throughout AMT 22 compared to the following year, and overall levels of PP are lower for AMT 23. The general trends are however still similar, with an increase in both intPP and isoprene at higher southern latitudes and north of the equator. In the correlation plots (Figure 3.18), all points at higher PP values not matched by isoprene are in colder waters at higher southern latitudes, as observed for Chl-*a* (section 3.2.4.1).

Table 3.6 – Slopes from RLOC analysis for integrated primary production (intPP) including size fractionated data; dash or grey font used where the regression was not significant at the 95 % level; where different from the heading, n is given as italics after the R^2 value.

Regression equation (R^2) for ...	AMT 22 (n = 31)	AMT 23 (n = 17)
intPP (total)	0.038*(intPP) + 14 (0.44)	0.051*(intPP) + 1.4 (0.32)
≥20 °C SST	0.017*(intPP) + 19 (0.64; *10*)	– [a]
<20 °C SST	0.059*(intPP) + 8.2 (0.73; *21*)	0.091*(intPP) - 7.2 (0.57; *11*)
intPP (0.2-2 µm, pico)	0.069*(intPP) + 16 (0.61)	0.12*(intPP) - 2.5 (0.36)
intPP (2-10 µm, nano)	0.21*(intPP) + 9.8 (0.26)	0.13*(intPP) + 6.1 (0.39)
intPP (>10 µm, micro)	0.32*(intPP) + 10 (0.22)	0.26*(intPP) - 0.32 (0.19)[b]

[a] $p > 0.5$

[b] $p = 0.08$

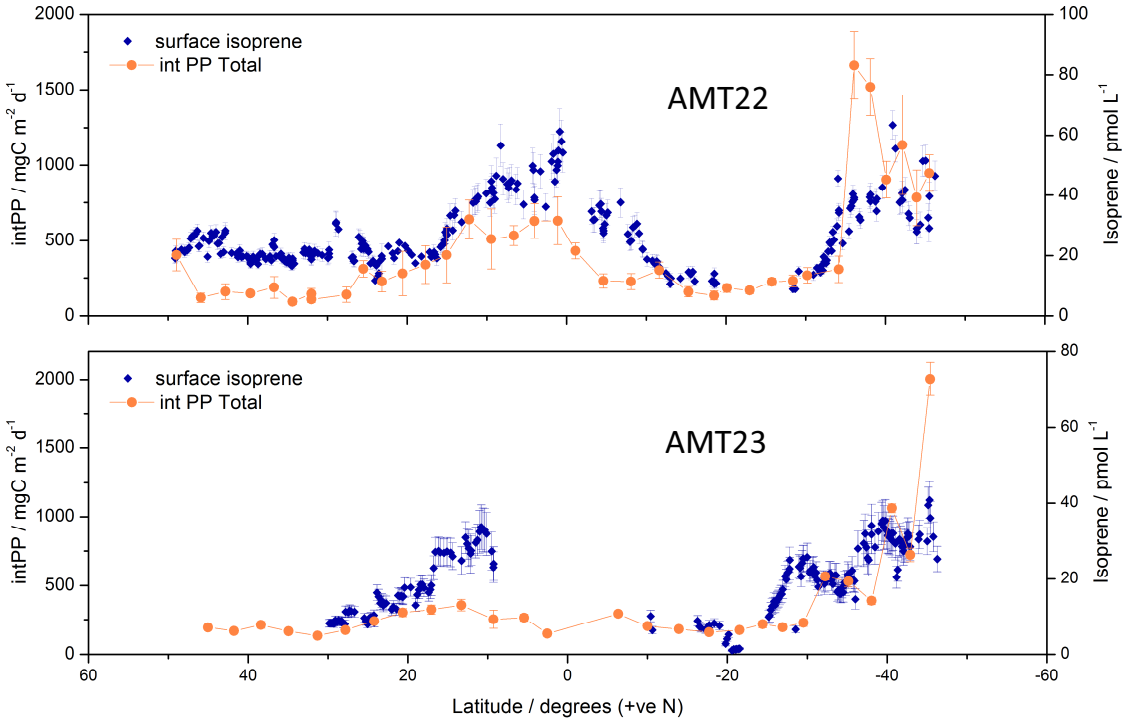

Figure 3.17 – Water-column integrated primary production (picoplankton) and surface isoprene during AMT 22 and 23; Error bars indicate one standard deviation for biological data; for isoprene as in Figure 3.2. Biological data provided by G. Tilstone (PML).

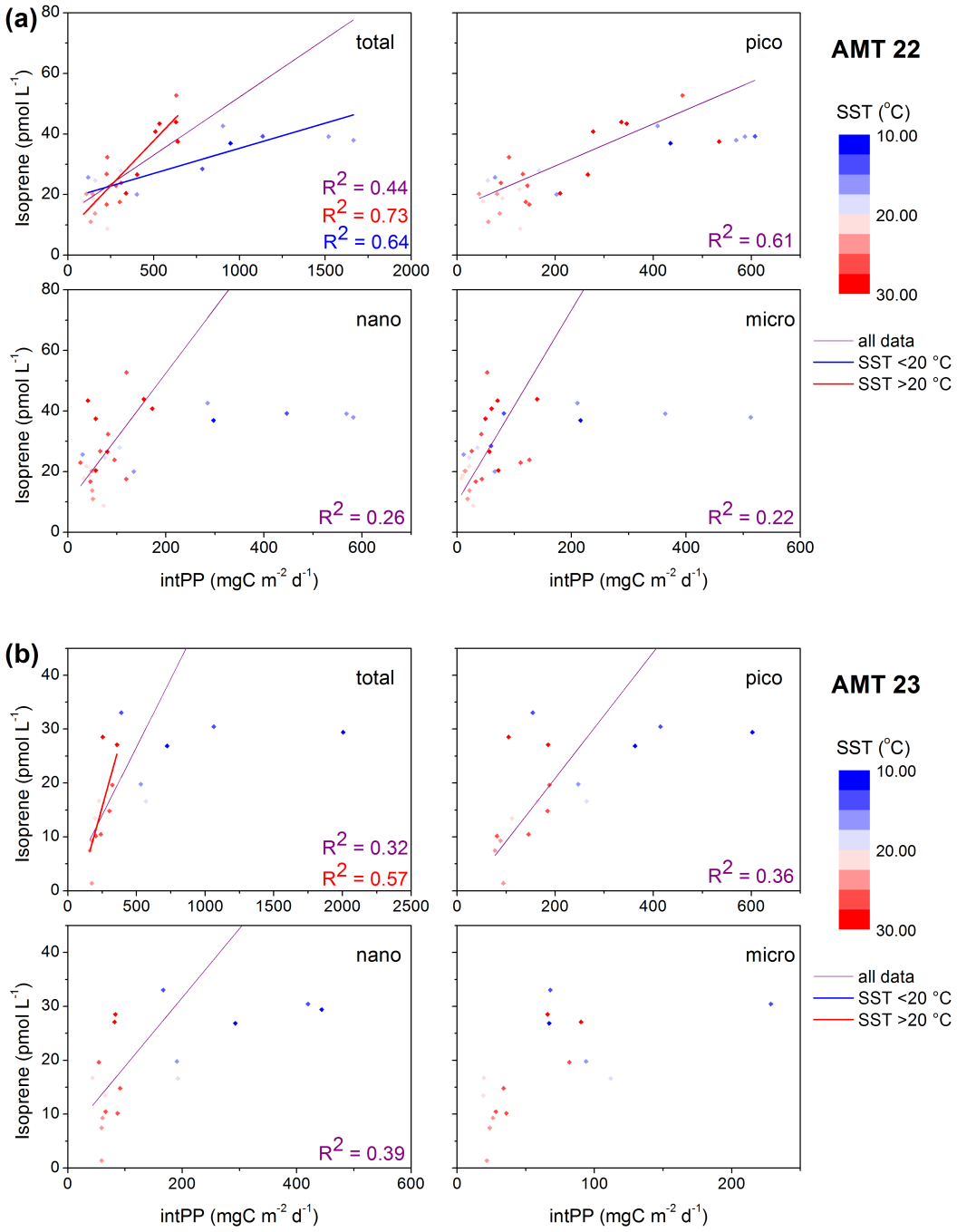

Figure 3.18 – Correlation plots of water-column integrated primary production (total and size-fractionated intPP) and surface isoprene for (a) AMT 22 and (b) AMT 23; R^2 values and regression line shown where a significant ($p < 0.05$) correlation existed. Biological data provided by G. Tilstone (PML).

The calculated slopes (by the RLOC approach, as detailed in section 3.2.4.1) for each size fraction agree within a factor of two or better between the two years (15-50 % difference), which can be regarded as a reasonable result considering the smaller number of samples for AMT 23, slight differences in sampling month and cruise track, and biological variability generally, as mentioned previously. Linear regression analyses were also carried out for SST-binned data (total intPP only), generally yielding improved correlations as observed for PFTs and pigments discussed above; results are shown in Table 3.6.

3.2.4.5 CO_2 and O_2 - dissolved gases as proxies for plankton production

Kameyama et al. (2014) observed an inverse relationship of isoprene with temperature-corrected pCO_2 in the Southern Ocean, which can be a proxy for net community production (NCP) under certain circumstances. NCP is defined as the difference of gross primary production (GPP) and Community Respiration (CR), i.e. NCP = GPP - CR. Any part of the biological community including both autotrophic and heterotrophic organisms contributes to the process of CR, while GPP measures the net amount of organic carbon produced. The latter is equivalent to the net biological consumption of inorganic carbon, so that pCO_2 can be used to estimate integrated biological activity in the euphotic layer over time (Kameyama et al., 2014). The prerequisites are however very stable oceanic conditions in terms of community structure, temperature and mixing, as potential influences on pCO_2 other than biological activity need to be excluded.

The rationale for using pCO_2 as a proxy for biological production is the consumption of CO_2 during photosynthesis by autotrophic phytoplankton, with concurrent emission of oxygen. Therefore, Wingenter et al. (2004), who saw a strong negative correlation with dissolved CO_2 and a strong positive correlation of isoprene with dissolved oxygen during a fertilisation experiment in the Southern Ocean, attributed these relationships to the biological activity in the fertilised patch. Again, the spatial extent of the study was relatively small, allowing the conclusion that the plankton bloom in the patch was solely responsible for differences of CO_2 and O_2 concentrations in the water between the middle and the edges of the patch.

It was not attempted to replicate either approach in this study as only the North or South Atlantic mid-ocean gyres would satisfy the requirements and the number of measurements

in those regions is insufficient to draw any conclusions. In addition, a more direct measurement of NCP was available for both AMT cruises (see section 3.2.4.6 below).

3.2.4.6 Net community production (NCP)

In a similar way to using dissolved *in-situ* CO_2 and O_2 as proxies for an estimate of NCP, it can be calculated from measurements of dissolved oxygen in incubation experiments, based on the assumption that any O_2 production in the incubations exposed to light is due to photosynthetic activity and hence primary production (referred to as Gross Primary Production, GPP), while any O_2 consumption in dark incubations of the same water is a result of CR (e.g. Serret, AMT22/23 cruise reports; Serret et al., 2015; Robinson et al., 2009). No correlation was observed with isoprene for integrated NCP or GPP for AMT 23. While it is not directly comparable to ^{14}C-PP, GPP can be regarded as a similar quantity under the given circumstances (Robinson et al., 2006), although some debate exists about what ^{14}C-PP actually measures (Quay et al., 2010). This ambiguity and the discrepancies between different measures of plankton production need to be considered when exploring links with isoprene distribution.

3.2.4.7 Nutrients

As mentioned briefly at the end of section 3.2.4.3, Zindler et al. (2014) reported that no linear relationship was present for their whole isoprene dataset with any pigment data. They suggested that nutrient concentrations (nitrate + nitrite + ammonia = nitrogen (N), phosphate (P)) could be used as a proxy for all biological production including by bacteria, not only phytoplankton PP, that had occurred in the water column and could hence have influenced biogenic trace gas concentrations. Binning all data by nitrogen to phosphate ratios (N:P), they did find correlations between isoprene and 19'-hexanoyloxyfucoxanthin (a marker for haptophytes and dinoflagellates, some of which are known to produce isoprene (Shaw et al., 2010)) for all bins with N:P < 8; additional processes dominated by other phytoplankton groups or bacteria were proposed as reasons for the breakdown of the relationship for N:P > 8.

Supporting nutrient measurements for the present datasets only comprise nitrate, nitrite, phosphate and silica for AMTs (Figure 3.19), but in the absence of ammonia data, it is

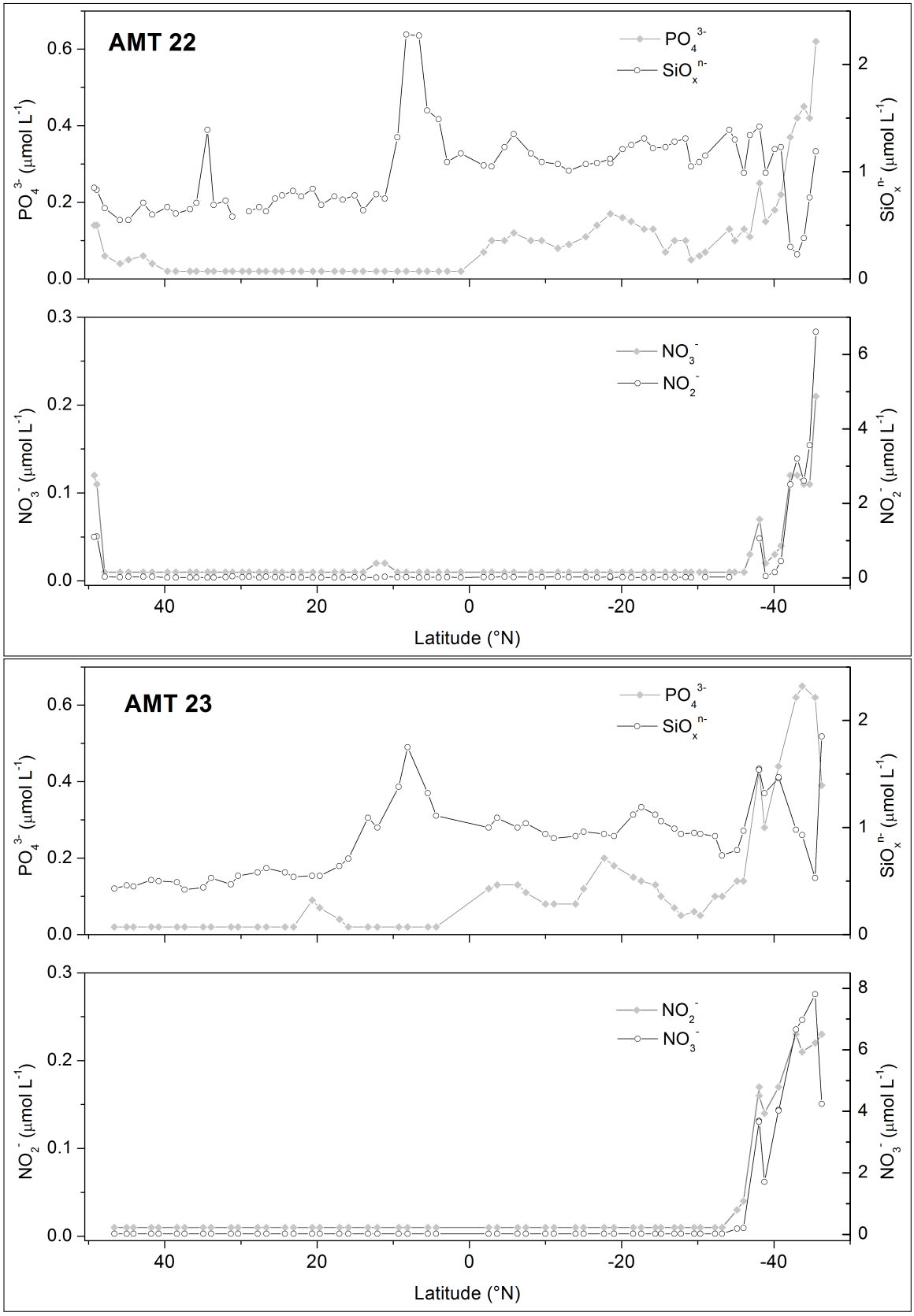

Figure 3.19 – Nutrients in surface CTD samples during both AMT cruises. Data provided by BODC.

possible to use N = nitrate + nitrite, as done by the same authors for a similar investigation (Zindler et al., 2012).

When applied to the AMT data, it becomes apparent that the approach is not suitable for this dataset, due to a strong imbalance in distribution between N:P bins (>80-90 % of all datapoints fall within an N:P range of 0 to 2), and no further exploration was carried out.

3.2.4.8 Salinity

An apparent inverse correlation between sea surface salinity (SSS) and isoprene for the Atlantic transect (shown for AMT 22 in Figure 3.20) is not an indicator of a causal relationship between the two, but rather a reflection of the currents and changes in water mass that also cause variations in the planktonic community which in turn affect the isoprene distribution. Low SSS coincides with high isoprene around the equator and at higher southern latitudes. Salinity is strongly regulated by the balance of precipitation and evaporation, with equatorial waters being less saline due to high precipiation rates and net evaporative loss of water in mid latitudes leading to high salinity (Libes, 1992). These processes could be expected to affect isoprene production in the same direction, with higher irradiation which increases evaporation rates also resulting in higher isoprene production, and dilution from rainwater decreasing the surface concentrations; however the biological controls appeared to exert a much stronger influence on isoprene distribution than the physical processes regulating salinity (which in turn do affect the biological processes, and hence isoprene, but more indirectly).

During ACCACIA 2, a different trend was observed, but this can be attributed to two very distinct water masses with different SSS and other characteristics including biological community (Atlantic and Polar water).

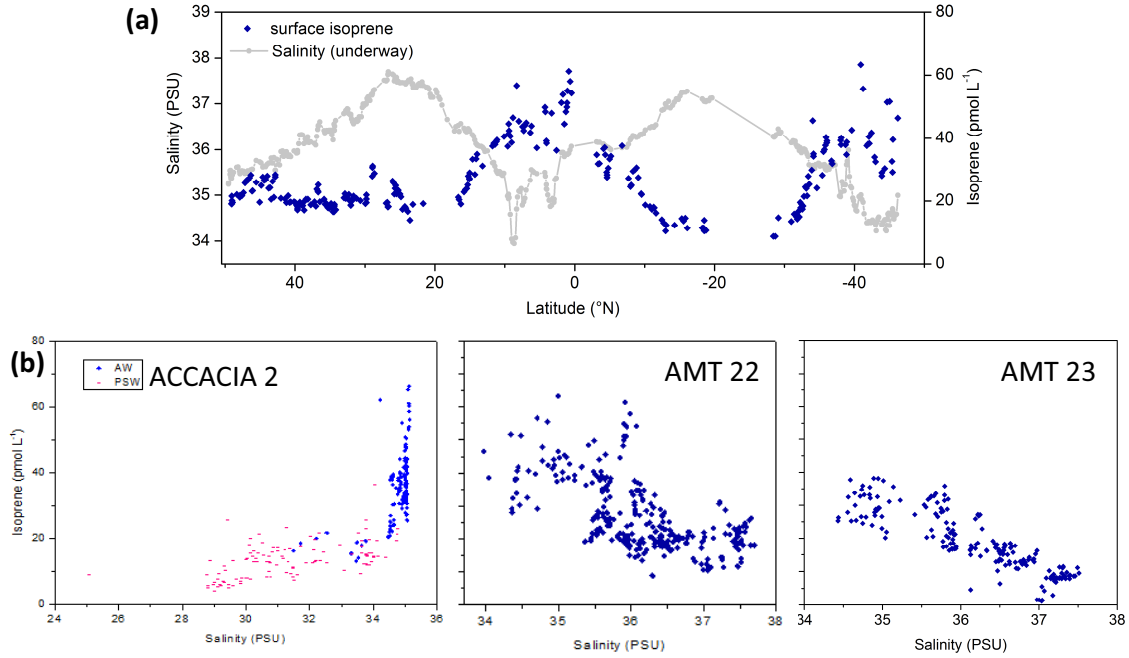

Figure 3.20 – (a) Meridional transect plot of salinity and isoprene (AMT 22); (b) Correlation plots for all three cruises, with AW = Atlantic Water, PSW= Polar Seawater.

3.2.5 Isoprene emission algorithm

One of the published global emission estimates is computed using a physically-based method that takes into account known influences of several parameters on isoprene production based on laboratory studies (Gantt et al., 2009). It takes global PFT distributions and Chl-*a* concentrations from satellite data (PHYSAT and SeaWiFS) and applies PFT-specific monoculture production rates (converted to an emission factor, EF) per grid cell to derive production over the water column based on ambient light levels (photosynthetically active radiation, PAR). A scaling factor accounts for the fraction of isoprene emitted to the atmosphere, giving the total column isoprene emission E_{isp}:

$$E_{isp} = S.A. \times H_{max} \times [Chl - a] \times F_{isp} \times \int_0^{H_{max}} P \, \mathrm{d}h \tag{3.12}$$

with

$S.A.$ = surface area of grid cell;

H_{max} = maximum possible extent of planktonic euphotic zone, dependent on incom-

ing solar radiation and attenuation;

F_{isp} = emission fraction of water column produced isoprene emitted to atmosphere;

$P = EF \times (ln(I))^2$, light (I = ambient PAR) dependent production using an emission factor EF from culture studies. EFs (in units of µmol isoprene (g Chl-a)$^{-1}$ h^{-1}) are quoted for various PFTs, with very similar values for *Prochlorococcus*, *Synechococcus* and "other phytoplankton" (0.032, 0.029 and 0.028, respectively), higher for diatoms (0.042) and lower for coccolithophores (0.019).

This algorithm holds true if isoprene emitters in the field behave in the same way as monocultures in the laboratory, with the same light dependence, and no other processes affect the sea-to-air flux apart from the production in the water column. In their paper, the authors already report that there are discrepancies especially at night between their model emissions and measurement-based values used for comparison (from Matsunaga et al., 2002). Considering all EFs as being of the same magnitude and disregarding the emission fraction term F_{isp}, total emission in the equation depends solely on the production and [Chl-a] terms, which is *de facto* on isoprene concentrations in the water column since they are the product of those two terms. Consequently, in order to obtain a similar algorithm to Gantt and co-workers based on field data from the current study, a diurnal variation would be necessary in the observations. There was however no significant difference between average daytime and night-time concentrations of isoprene in water during any of the cruises (day defined using a threshold of modelled $j_{NO_2} > 5 \times 10^{-5}$ s^{-1} during the sampling period, as the photolysis rate of NO_2 is zero at night (threshold allowing for noise in the data); Figure 3.21). There was no meaningful difference between ACCACIA 2 day- and night-time values (few night-time values due to light summer nights). Therefore, a replication of the algorithm with *in-situ* values for the different parameters was not attempted, as it could only be of limited diagnostic value. Further research will aim to develop a refined model more representative of the relevant processes in order to improve estimates of the global source strength of oceanic isoprene and adequately reflect diurnal and seasonal trends in the surface ocean and MBL.

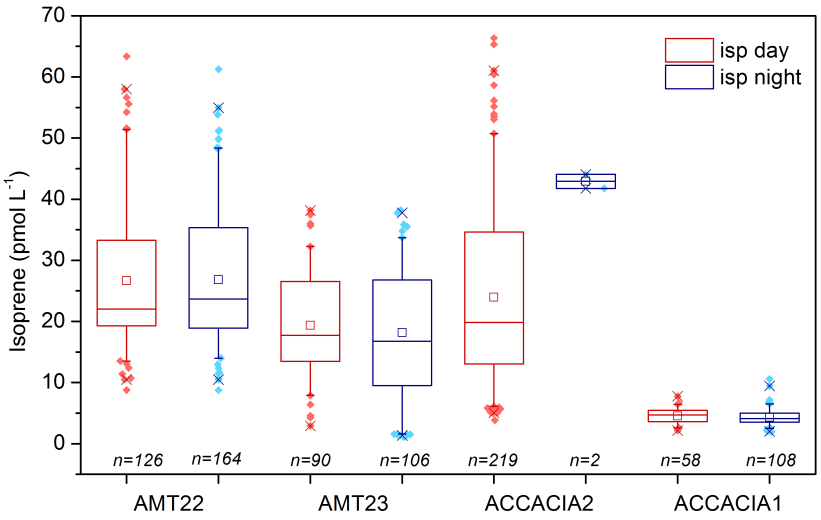

Figure 3.21 – Night (blue) and day (red) isoprene water concentrations for all four cruise; day defined as (modelled $j_{NO_2} > 5 \times 10^{-5}$ s^{-1}) during the sampling period.

3.2.6 Extrapolation of emissions and implications

Most of the parameters investigated in this chapter have shown a linear relationship with isoprene, which is perhaps unsurprising given previously reported associations with biological activity. The main focus here has been to find suitable proxies for predicting isoprene concentrations in water in order to help constrain global emission estimates for use in atmospheric chemical transport models, rather than aiming to elucidate specific processes that lead to net isoprene emission and understanding their function.

It has been shown that a simple relationship with Chl-*a* alone is not able to reproduce observed isoprene distributions, and that a laboratory-derived approach that differentiates between polar, temperate and tropical biomes (E13) does not perform very well against the measurements. However, equations based on studies in the Pacific and Indian Ocean (O15) that predict isoprene as a function of both SST and Chl-*a*, with different coefficients for different SST ranges, do appear to largely match the observed values. Trends in the current dataset suggest that a distinct change in almost all the examined relationships occurred at 20 °C SST (also seen in the correlation plots coloured by SST) rather than the 17 °C proposed by O15, which may point to a difference between the ocean regions sampled; it does indicate that the empirical relationships from that paper are not directly applicable to all parts of the world's oceans and would need some refinement in order to obtain a more accurate global extrapolation.

Other potential controls such as specific PFTs or pigments did not necessarily return better agreement than only Chl-*a*, even though they account for differences in isoprene production by different species and in different environments. Arguably, individual regression analyses have limited diagnostic potential in that each assumes by definition that the investigated parameter is solely responsible for the total isoprene, so that the resulting equation is only useful for predicting isoprene if that assumption is true. Following the same argument, a steeper slope by no means automatically implies that the entity in question (e.g. microplankton) is a strong emitter: the phenomenon can also be caused by the presence of other organisms or processes responsible for isoprene emission in regions where the examined parameter has low concentrations.

Considering the arguments above, and comparing the PP data with PFT and pigment data and quantitative analyses of those variables with respect to isoprene (summarised in Table 3.7), it is likely that a large proportion of the observed isoprene at lower latitudes is due to the phytoplankton biomass and more specifically the picoplankton, i.e. the dominant *Prochlorococcus* in those regions. Therefore, linear regression equations may be meaningful and hence useful for extrapolation purposes over areas where similar conditions are met. Nonetheless, correlations from two separate analyses that were expected to monitor the same species did not always agree, such as *Pro* cell counts and DV-Chl-*a*, a marker for that phytoplankton class, giving R^2-values of 0.46 for *Pro*, but 0.63 for DV-Chl-*a* at SST >20 °C (AMT 22).

Despite this caveat, more specific controls could be useful in developing a single parameterisation for all oceanic regions, if a sufficient number of the major controls could be identified and included. For AMT 22, the sum of *Pro* and *Syn* (scaled to account for different isoprene production) could account for about half of the variation in the whole dataset, but the same approach gave only a weak correlation for AMT 23. Zeaxanthin and the sum of photoprotective carotenoids (PPC) also showed promising results for AMT 22 (accounting for around 40-50 % of the variability) and returned much less regular values for AMT 23 (20-60 %). However, PPC did prove to be the most consistent parameter across all three cruises, with R^2 - values of 0.33 to 0.68 when binned by SST. Picoplankton intPP also appeared to correlate well for both AMTs (R^2 = 0.61 and 0.36 for AMT 22 and 23, respectively), but this relationship could not be verified for the Arctic as no PP data was available for those cruises. Given the difference in plankton community structure in

Table 3.7 – Summary of linear relationships with isoprene for the parameters with the most relevant correlations across AMT 22 and 23 and ACCACIA 2, applied in Figure 3.22. Grey font indicates no significant relationship at the 95 % confidence level for that dataset. Regressions calculated using [isoprene] in pmol L^{-1}, [Chl-*a*] and [PPC] in mg m^{-3}, [*Pro+Syn*] in cells mL^{-1}, (intPP) in mgC m^{-2} d^{-1}.

Parameter	*SST* / °*C*	**Cruise (*n*)**	**Regression equation**	$\mathbf{R^2}$
Chl-*a* (by HPLC)	*<20*	AMT 22 (*39*)	37.9*[Chl-*a*] + 17.5	0.37
		AMT 23 (*11*)	15.1*[Chl-*a*] + 18.4	0.55
		ACCACIA 2 (*34*)	34.1*[Chl-*a*] + 11.1	0.61
		ALL (*84*)	33.2*[Chl-*a*] + 13.7	0.33
	≥20	AMT 22 (*93*)	300*[Chl-*a*] − 3.35	0.60
		AMT 23 (*22*)	103*[Chl-*a*] + 5.58	0.82
		ALL (*115*)	266*[Chl-*a*] − 1.68	0.54
Photoprotective	*<20*	AMT 22 (*39*)	97.6*[PPC] + 19.5	0.50
Carotenoids (PPC)[a]		AMT 23 (*11*)	87.3*[PPC] + 12.9	0.33 ($p = 0.06$)
		ACCACIA 2 (*34*)	155*[PPC] + 6.59	0.47
		ALL (*84*)	102*[PPC] + 14.4	0.48
	≥20	AMT 22 (*93*)	377*[PPC] − 1.88	0.66
		AMT 23 (*22*)	176*[PPC] + 2.75	0.68
		ALL (*115*)	345*[PPC] − 0.81	0.61
Pro+Syn (scaled *Syn*)	*<20*	AMT 22 (*19*)	4.70×10^{-5}*[*Pro+Syn*] + 20.0	0.53
(AMT only)		ALL (*32*)	7.07×10^{-5}*[*Pro+Syn*] + 13.5	0.45
	≥20	AMT 22 (*44*)	8.49×10^{-5}*[*Pro+Syn*] + 5.75	0.56
		ALL (*66*)	8.97×10^{-5}*[*Pro+Syn*] + 9.23	0.34
	all data[b]	AMT 23 (*34*)	1.36×10^{-4}*[*Pro+Syn*] − 11.2	0.12
intPP (total)	*<20*	AMT 22 (*10*)	0.017*(intPP) + 19	0.64
(AMT only)		ALL (*16*)	0.017*(intPP) + 16	0.30
	≥20	AMT 22 (*21*)	0.059*(intPP) + 8.2	0.73
		ALL (*32*)	0.086*(intPP) + 0.084	0.67
	all data[b]	AMT 23 (*17*)	0.051*(intPP) + 1.4	0.32

[a] PPC = Zea + Allo + Diadin + Caro + Diato (Diato not available for ACCACIA 2).

[b] Relationship insignificant for lower SST ($p > 0.4$), so only non-binned results shown.

the respective sampling regions, total intPP across all size classes would be a more widely suitable proxy; the R^2 for this parameter was also relatively consistent between the two AMTs and greatly improved for AMT 22 when a temperature dependence was included (see Tables 3.7 and 3.6); it would however still need to be compared to higher-latitude data to confirm its suitability. Generally lower agreement for AMT 23 could be partly attributed to the smaller number of samples, but the difficulty in comparing even these measurements from cruises that sampled very similar water masses emphasises how uncertain any further extrapolation must always be unless our understanding of isoprene production by plankton improves substantially so that the source of the discrepancies can be accounted for.

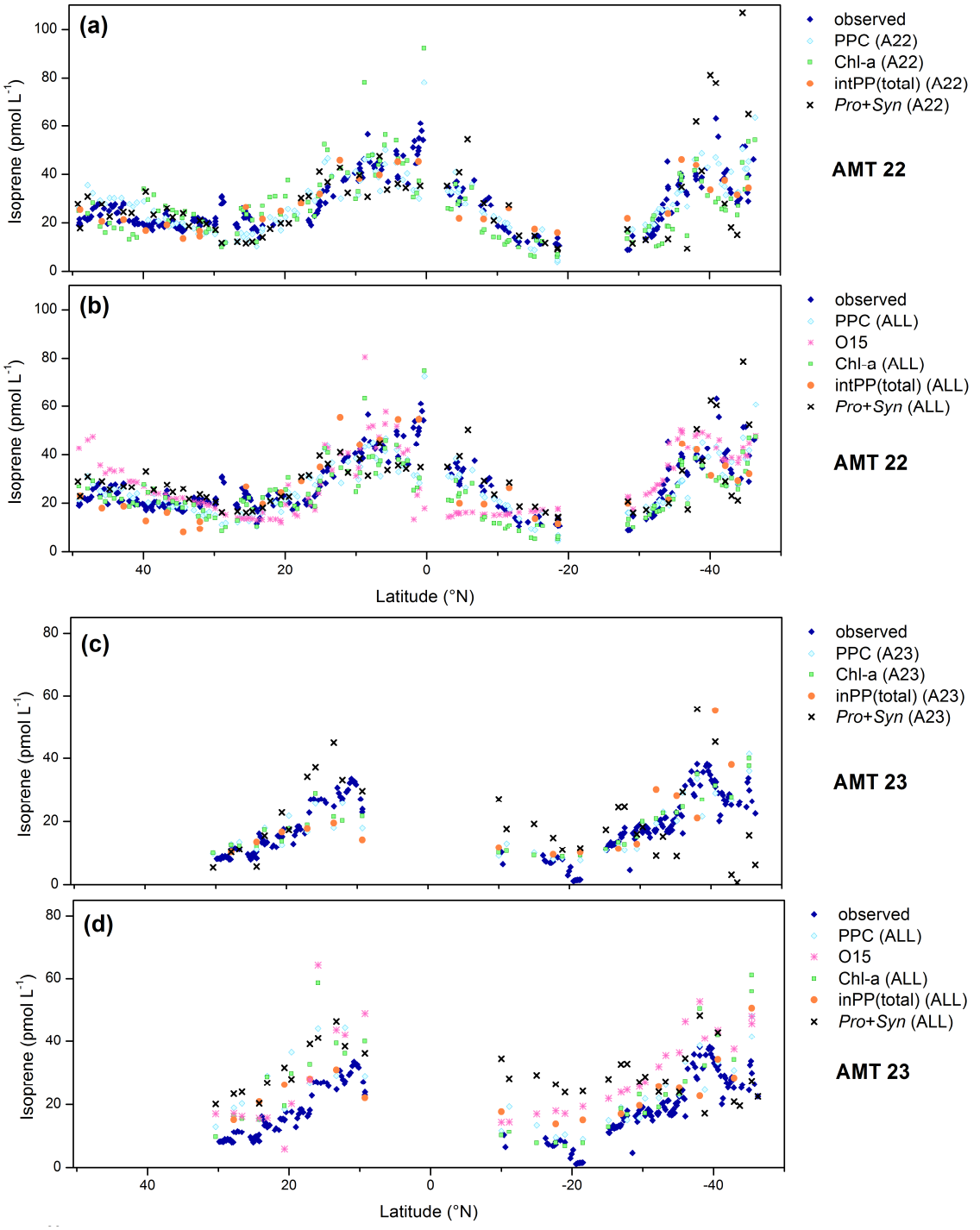

Figure 3.22 – Observed isoprene concentrations alongside predicted values using parameterisations as shown in the legends: relationships based on the respective dataset itself ($A22$ and $A23$) and also O15 and ALL relationships for each cruise: (a) $A22$ and (b) O15/ALL applied to AMT 22; (c) $A23$ and (d) O15/ALL applied to AMT 23. Different parameterisations are also explained in the text and in Table 3.7.*Continued over...*

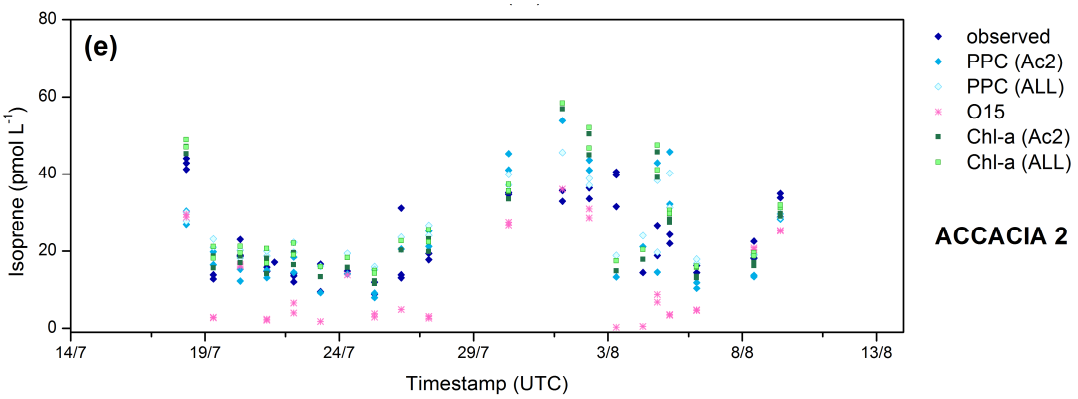

Figure 3.22 – Observed isoprene concentrations alongside predicted values: (e) relationships based on the dataset itself (*Ac*2) and also O15 and *ALL* relationships applied to ACCACIA 2. Different parameterisations are also explained in the text and in Table 3.7.

Figure 3.22 shows measured alongside predicted isoprene concentrations from the most promising linear relationships discussed in this chapter (summarised in Table 3.7) and those based on the Ooki et al. (2015) parameterisation, with correlation coefficients given in Table 3.8. Isoprene concentrations for all cruises were estimated using the *ALL* relationship (derived from combined cruise data) as well as using the relationships derived from the respective cruise itself (*A*22, *A*23 and *Ac*2, respectively; Figure 3.22). While the agreement with predictions based on each dataset internally was naturally the closest, the *ALL* parameterisation also performed rather well; better than O15, which still compared well considering it was determined from data that did not cover any of the Atlantic Ocean, the study region of this project. The main discrepancies between the current study and O15 were in the Arctic and in waters with 27 °C > SST > 20 °C (both underpredicted by O15), indicating a difference between the ocean regions or perhaps seasons studied that require further investigation to consolidate the parameterisations for a globally applicable set of relationships.

Another factor to be considered when choosing a useful approach for global extrapolation is the availability of global data for the selected proxy. Satellite data is available for Chl-*a*, dominant PFTs and even PP, while pigments would have to be extracted from experimental databases or from modelled data, making them a more difficult proxy to use with potentially larger gaps in the data. However, there are different concerns for satellite data, e.g. regarding coverage of high latitudes and uncertainties in the output (even potentially for Chl-*a*, see section 3.2.4.1).

Table 3.8 – Summary of correlation coefficients for predicted *vs.* observed isoprene concentrations for different predictive relationships.

Parameter	**Predictive relationship**	**Cruise**	$\mathbf{R^2}$
Chl-*a* (by HPLC)	*ALL*	AMT 22	0.56
		AMT 23	0.76
		ACCACIA 2	0.61
	O15	AMT 22	0.37
		AMT 23	0.75
		ACCACIA 2	0.59
	same dataset [a]	AMT 22	0.57
		AMT 23	0.79
		ACCACIA 2	0.61
Photoprotective Carotenoids (PPC)[c]	*ALL*	AMT 22	0.64
		AMT 23	0.66
		ACCACIA 2	0.47
	same dataset [a]	AMT 22	0.65
		AMT 23	0.69
		ACCACIA 2	0.47
Pro+Syn (AMT only)	*ALL*	AMT 22	0.53
		AMT 23	0.16
	same dataset [a]	AMT 22	0.57
		AMT 23	0.12[b]
intPP (total) (AMT only)	*ALL*	AMT 22	0.70
		AMT 23	0.48
	same dataset [a]	AMT 22	0.72
		AMT 23	0.32[b]

[a] applying relationship from the dataset itself (see Table 3.7).

[b] using the non-binned relationship to predict concentrations due to the insignificant correlation at lower SST.

[c] PPC = Zea + Allo + Diadin + Caro + Diato (Diato not available for ACCACIA 2).

3.2.7 Conclusions

This study has contributed a large number of observations to the existing dataset of marine isoprene, covering areas of the Arctic and the Atlantic Ocean at basin-scale and providing representative values of isoprene in surface water for a huge range of latitudes (80 °N - 50 °S). Using a variety of supporting data, relationships with different biological parameters have been confirmed and extended. When applied to the different cruises, parameterisations derived from the combined datasets were able to predict isoprene concentrations close to the measured values. However, no single parameter has been identified as a more suitable proxy for predicting isoprene concentrations in water than Chl-*a*, which is currently the most widely used, except perhaps integrated PP and photoprotective pigments (PPC). It was nevertheless shown that a separation of ocean regions by temperature ranges is crucial for most proxies in order to obtain representative predictions with empirical relationships. The uncertainty in setting global threshold values for that separation, as seen when contrasting Atlantic and Pacific/Indian Ocean datasets, highlights the need for further field measurements spanning different oceans and seasons and comparison of empirical relationships between studies. Ideally, trace gas measurements should be accompanied by as wide a range of biological measurements as possible in order to validate the correlations found in this project and examine the suitability of the suggested additional proxies for predicting isoprene concentrations on a global scale.

Further work will include global extrapolations based on the current relationships where possible and comparisons between the different proxies and their suitability, helping to constrain the input for isoprene emissions in modelling studies. Additionally, an ocean mixed layer model will be used to investigate the biological controls in the water column with the aim of better understanding the processes responsible for isoprene emission from the oceans.

Chapter 4

Monoterpenes

This chapter focuses on monoterpene measurements (α- and β-pinene, myrcene, δ3-carene, ocimene and limonene) made in surface waters and marine air during the cruises described in the previous chapter, contrasting them with the available literature and using them as a basis to estimate sea-to-air fluxes. Potential relationships with biological parameters and possible similarities to isoprene will be explored in order to better understand the sources of the monoterpenes in the marine environment in view of their proposed biogenic origin.

4.1 Introduction

Monoterpenes are molecules made up of two isoprene units, molecular formula $C_{10}H_{16}$, and come in a variety of forms (see Chapter 1 section 1.1 and Figure 1.1). They are known to be important secondary organic aerosol precursors (e.g. Hallquist et al., 2009; also see Chapter 1) and contribute a substantial proportion to terrestrial biogenic non-methane hydrocarbons (NMHCs), with global emissions around 26-156 Tg C yr^{-1} (Arneth et al., 2008; Acosta Navarro et al., 2014). Marine emissions have only been estimated by a single study so far (Luo and Yu, 2010), based on one measurements paper (Yassaa et al., 2008, see below) and yielding very different results for a top-down compared to a bottom-up approach (29.5 *versus* 0.013 Tg C yr^{-1}, respectively; see Chapter 5 for further details).

Due in part to the difficulties in measuring monoterpenes at low concentrations and the assumption that they were only of minor relevance to aerosol chemistry in the marine environment, observations of monoterpenes in the marine atmosphere were not reported until 2008, when Yassaa et al. (2008) published evidence for the marine production of these compounds, based on laboratory monoculture studies and field measurements. This was followed by a paper reporting field measurements in the Southern Indian Ocean during which significant levels of monoterpenes had been observed in air (Colomb et al., 2009), and a recent study of glyoxal and methylglyoxal in the Southern Hemisphere that also measured monoterpenes as supporting data (Lawson et al., 2015; air only), but to our knowledge no other fieldwork data has been published to date. Laboratory-based monoculture experiments were performed by Yassaa et al. (2008) and Meskhidze et al. (2015); both articles report emission of several monoterpenes to varying extents by the species studied, with Meskhidze et al. (2015) additionally exploring the effects of temperature and light stress.

Table 4.1 gives results from field and laboratory studies to date (only light-acclimated data for culture studies), clearly showing the large variability within and between the datasets, which in combination with the overall paucity of observational data prevents a good constraint of the global emission estimates. These observational differences are discussed in more detail in section 4.3.1. Different growing conditions and different diatom species were used in the laboratory experiments, which could explain some of the differences; the conditions were chosen to be representative of the species' natural growing conditions by

Yassaa et al. (2008), while the study by Meskhidze et al. (2015) aimed to characterise the effects of stress rather than specifically replicate natural emissions.

No water concentrations have been published at all, making bottom-up emission estimates solely reliant on parameterisations with Chl-*a* derived from the laboratory studies, without validation against empirical relationships based on field measurements.

A further complication in calculating accurate sea-to-air fluxes is the scarcity of reliable Henry's Law constants of these compounds. There are only a few published experimentally determined values, and these can vary by up to an order of magnitude if more than one is available for an analyte. Most theoretical values are being derived from other physico-chemical characteristics (vapour pressure and water solubility) which are in turn not necessarily accurately known, as is evident from the variability of the literature data (compiled in Sander, 2015).

The aim of this aspect of the project was, as for isoprene, to expand the database of speciated monoterpene observations in the marine atmosphere and make concurrent measurements in the surface ocean to facilitate the calculation of sea-to-air fluxes, enabling a better constraint on future modelling studies and thus helping to evaluate the importance of these compounds in marine atmospheric chemistry. This chapter presents the results for the six monoterpenes (α- and β-pinene, myrcene, δ3-carene, ocimene and limonene) that were monitored in water and air during AMT 22 and 23, and for α- and β-pinene during ACCACIA 2 (other monoterpene data discarded due to instrument issues, details see Chapter 2); cruise details can be found in Chapter 2 section 2.3.1 and Chapter 3 section 3.2.1.

Table 4.1 – Previously published monoterpene measurements in air and from laboratory monoculture studies; sum of monoterpenes unless specified; DL = detection limit.

Mean ± error (range)	**Notes**	**Technique**	**Location**[a] **(month)**	**Reference**
air (pptv)				
(sum of (+)/(-)-α-pinene)		GC-MS	Southern Ocean (Jan)	Yassaa et al. (2008)
5 (<DL-14)	far from bloom	(not *in situ*)		
79 (25-130)	distant bloom	(DL = 1-5 pptv)		
125 (56-225)	in bloom			
20-80	range of means	PTR-MS	Southern Indian Ocean	Colomb et al. (2009)
10 ± 10	background		(Dec)	
<DL	2006, DL = 6 pptv	PTR-MS	Cape Grim observatory	Lawson et al. (2011)
21	2007		(hourly mean, marine air)	
32		PTR-MS	Temperate South Pacific	Lawson et al. (2015)
			(Mar)	
monoculture emissions (nmol monoterpene (g Chl-a)$^{-1}$ d^{-1})				
0.3-68.1	Diatoms[c]	GC-MS	(laboratory)	Yassaa et al. (2008)
0.3	Coccolithoporid			
225.9	Chlorophyceae			
0.8-1.1	Cyanobacteria			
27.0-28.5	Diatoms[c]	GC-MS	(laboratory)	Sabolis (2010); also in
21.7	Prymnesiophytes			Meskhidze et al. (2015)[b]
40.3-45.1	Dinoflagellates			
36.5	Cryptophytes			

[a] Ship unless specified.

[b] Rates given are for mean production over first light cycle (12 h) under initial growing conditions (90 µmol m^{-2} s^{-1}, 22 °C); rates in Meskhidze et al. (2015) are the same data, but different units and no total monoterpenes given; speciated measurements for α- and β-pinene, camphene and limonene available.

[c] Different diatom species and growing conditions.

4.2 Results and discussion

4.2.1 Air and water concentrations

4.2.1.1 Data quality and potential contamination issues

Air mixing ratios and water concentrations along the two AMT transects are shown in Figure 4.1 and those for ACCACIA 2 in Figure 4.2. Gaps exist where instrument issues were encountered on AMT 23, and only α- and β-pinene are available for water measurements during ACCACIA 2, as the other monoterpenes could not reliably be detected or calibrated. Air data was not affected by these issues on ACCACIA 2 (measured on a different instrument, see Chapter 2).

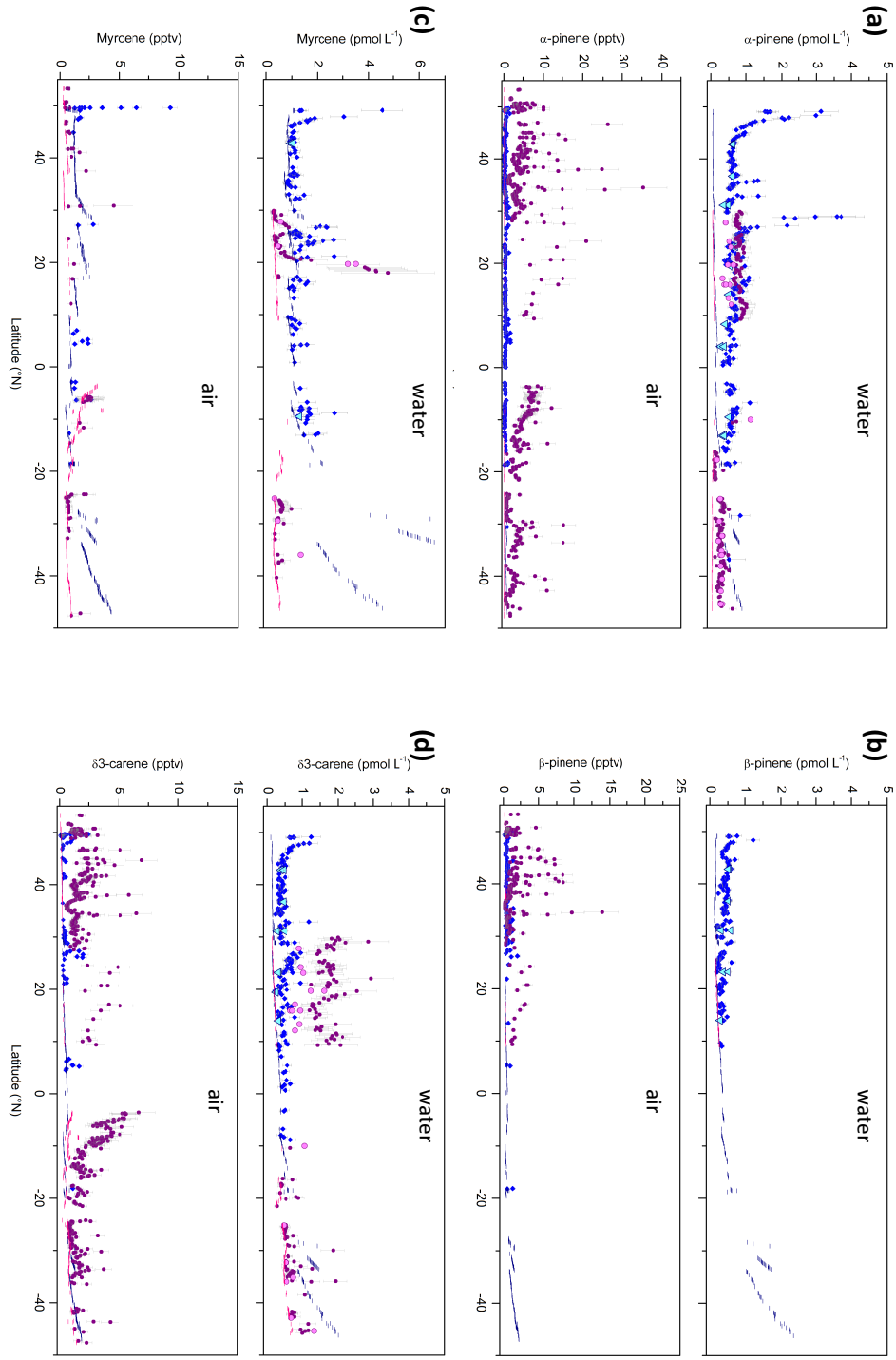

Figure 4.1 – *Continued over...*

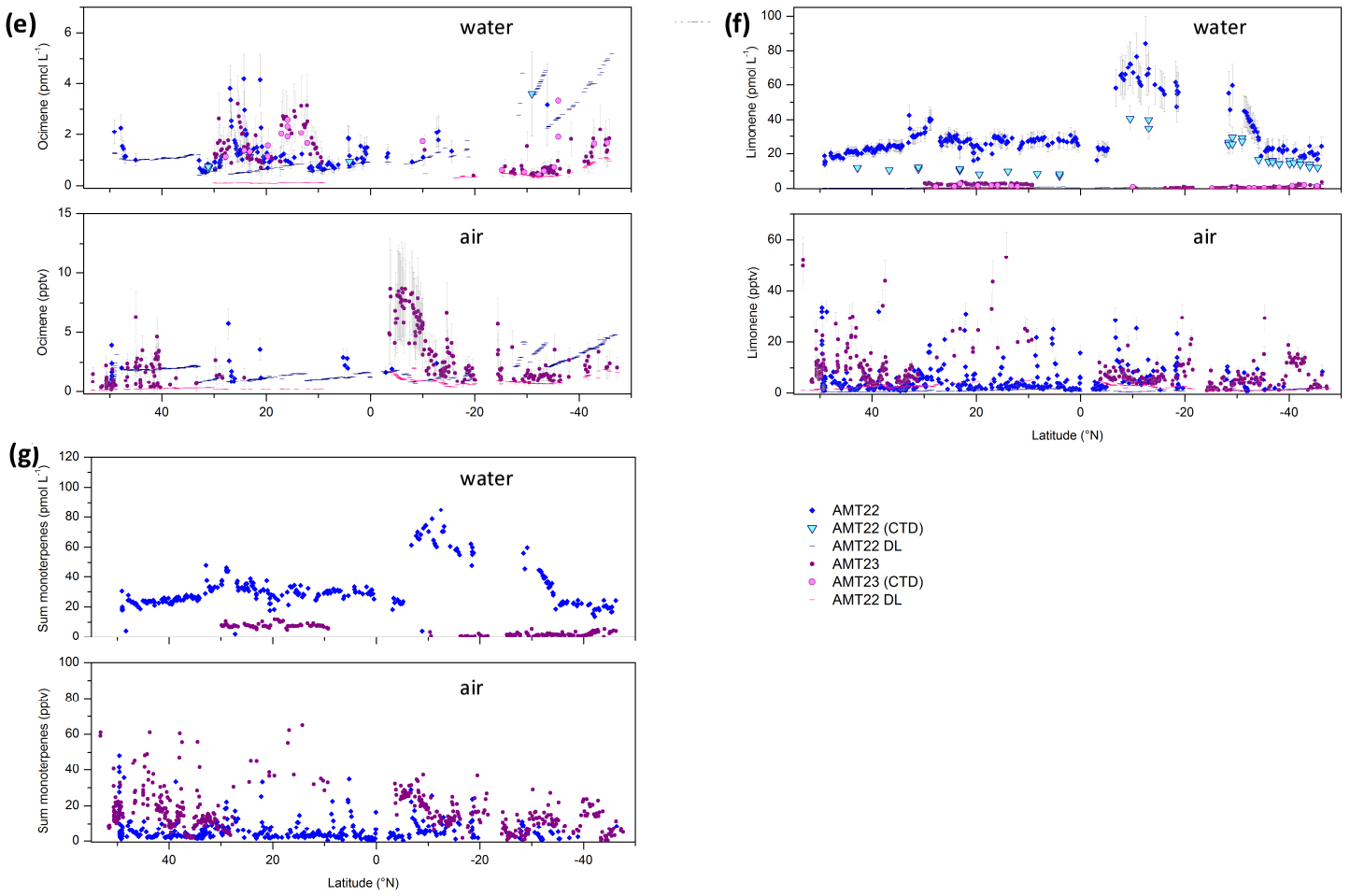

Figure 4.1 – Water and air concentrations of (a-f) α- and β-pinene, myrcene, δ3-carene, ocimene and limonene during both AMT cruises, including surface CTD samples; (g) sum of monoterpenes including limonene; DL = detection limit. Points with zero concentration for sum of monoterpenes are the result of all concentrations being <DL but not flagged as bad (DL displayed in individual concentration plots).

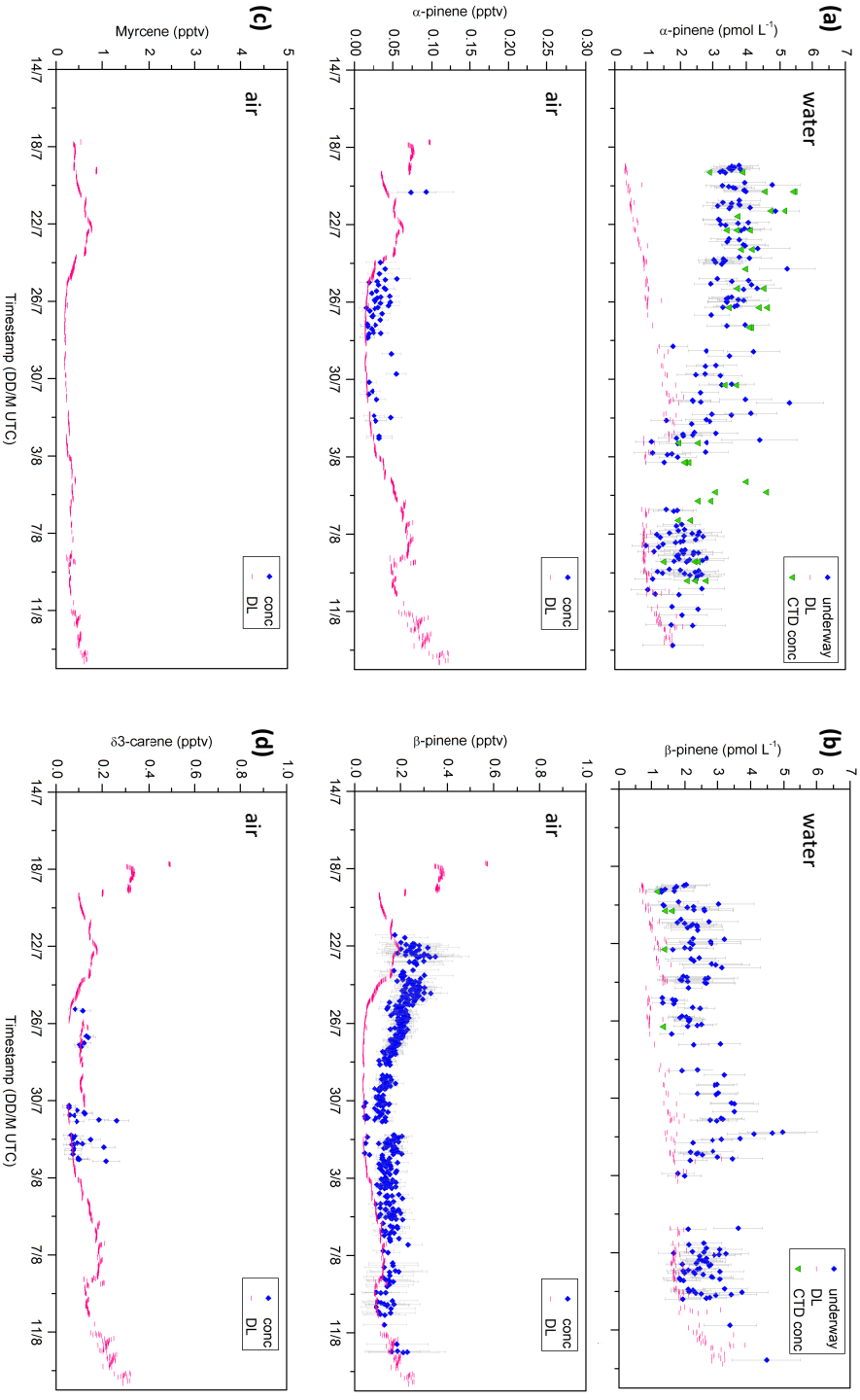

Figure 4.2 – *Continued over...*

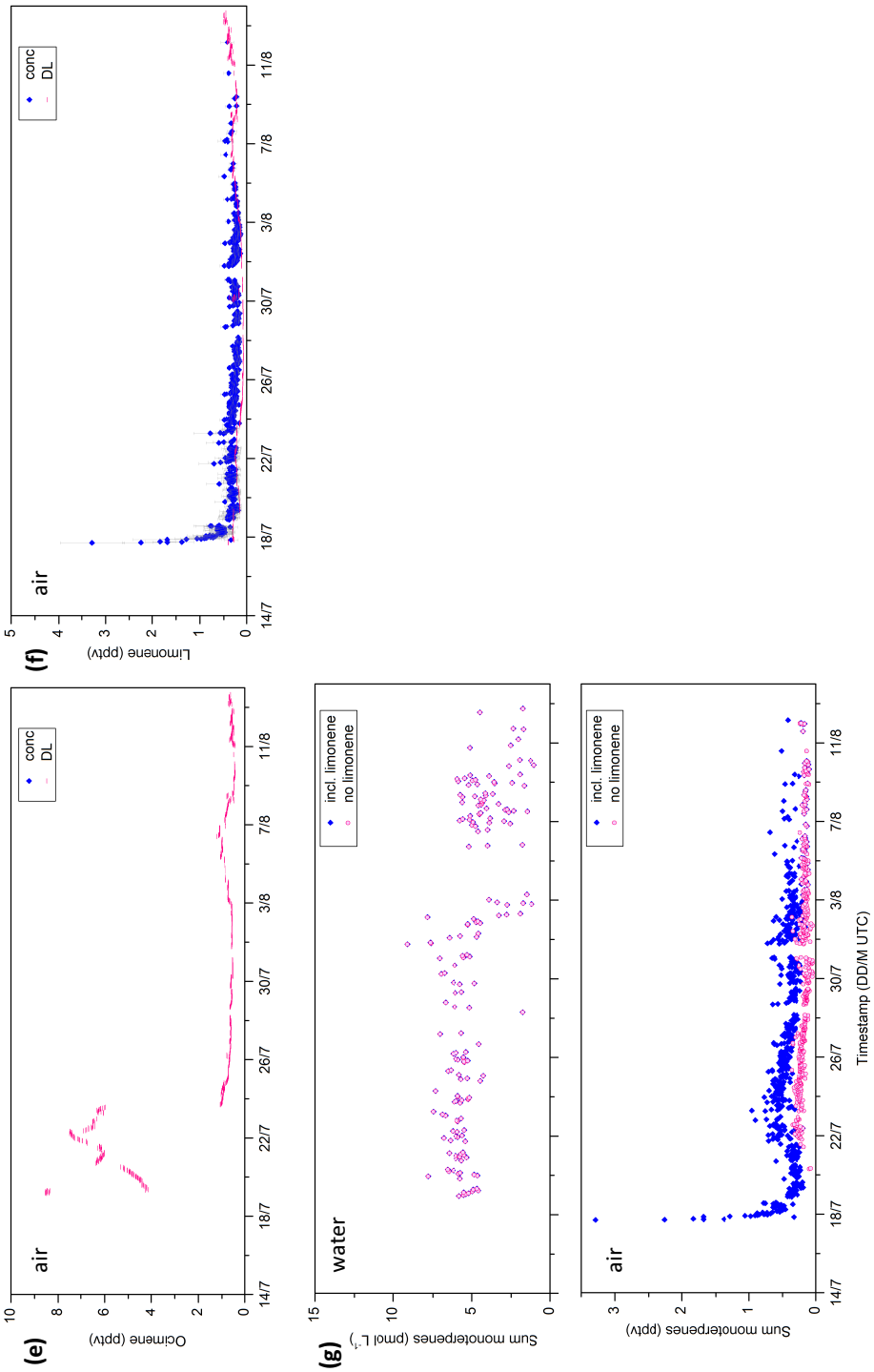

Figure 4.2 – (a-b) Water and air concentrations of α- and β-pinene, including surface CTD samples, and (c-f) air mixing ratios of myrcene, δ3-carene, ocimene and limonene during ACCACIA 2; (g) sum of monoterpenes for water (α- and β-pinene only) and air (with and without limonene); DL = detection limit. Points with zero concentration for sum of monoterpenes are the result of all concentrations being <DL but not flagged as bad (DL displayed in individual concentration plots).

4.2.1.2 Air data

In order to identify any continental influence on the atmospheric data, air mass back-trajectories (approximately 72 h) were calculated by the NOAA ARL HYSPLIT model (http://www.arl.noaa.gov/HYSPLIT.php) for 12-hourly intervals for each cruise track, displayed in Figure 4.3. There was no continental influence within the 72 h prior to reaching the ship during either AMT cruise. Air masses did pass over land frequently during ACCACIA 2, both coastal Greenland and Svalbard. Due to the very short atmospheric lifetimes of the monoterpenes, three-day back-trajectories go far beyond the point at which terrestrial influence could be observed, as the following calculations show. They were performed for daytime for α-pinene, the longest-lived with respect to OH of the monoterpenes quantified in this project (lifetime = 4.4 h at [OH] = 1.2×10^6 molec cm^{-3} (24-h average; based on Vaughan et al., 2012); see also Chapter 5 section 5.2 and Table 5.2). This gives essentially a worst-case scenario for all monoterpenes assuming similar terrestrial air mixing ratios to α-pinene, as other monoterpenes would react faster and hence their levels would decrease faster. Typical measurements of α-pinene in the terrestrial environment are around a maximum of several hundred pptv (e.g. Lee et al., 2005; Hakola et al., 2012; Jones et al., 2011), so a conservative estimate was made for an initial mixing ratio [α-pin]$_0$ = 500 pptv which would decrease to an observed mixing ratio at the ship [α-pin]$_t$ according to

$$[\alpha - pin]_t = [\alpha - pin]_0 / e^n \tag{4.1}$$

where n is the multiple of lifetimes within the time period, e.g. (24 h/4.4 h) = 5.5 for t = 24 h, giving [a-pin]$_{24}$ = 2 pptv and [a-pin]$_{48}$ = 0.01 pptv for t = 48 h, but only 0.00004 pptv for t = 72 h. Up to 48 h, the levels are higher or of a similar magnitude to those observed from onboard the ship, so that periods where the air mass passed over land within 2 days of being sampled appear to have the potential for terrestrial influence. However, the total atmospheric lifetime is reduced substantially by additional oxidation by ozone and the NO_3 radical, so that only negligible levels of terrestrial influence would reach the ship even within less than 24 h. The total atmospheric lifetime is *ca.* 1.6 h during daytime, based on 12-h daytime average [OH] = 2.2×10^6 molec cm^{-3} and 24-h average [O_3] = 6.25×10^{11} molec cm^{-3}, and 1.3 h at night, based on a typical marine 12-h night-time average [NO_3] = 2.5×10^7 molec cm^{-3} and [O_3] as during the day (Carpenter

et al., 2010; Vaughan et al., 2012; Allan et al., 2000). The resulting $[\alpha\text{-pin}]_{24} = 0.0002$ pptv (daytime; much lower for night-time) is far below the detection limit, so that terrestrial emissions are highly unlikely to affect shipboard measurements if the sampled air mass encountered land more than 24 h previously (and still unlikely for over only 12 h).

For ACCACIA 2, the air masses passing over Greenland and Svalbard could have resulted in approximately 0.04 pptv α-pinene (around detection limit, DL) after 24 h based on the total atmospheric lifetime, if an initial mixing ratio of 50 pptv is assumed (neither of those land masses are home to extensive vegetation and therefore much lower emissions compared to forested areas are likely). The total atmospheric lifetime was estimated at 3.3 h, taking into account 24-h average [OH] = 5.3 $\times 10^5$ molec cm^{-3} and [O_3] = 6.1$\times 10^{11}$ molec cm^{-3} from model output for this cruise (details see Chapter 5 section 5.2.3.3), and disregarding NO_3 due to long daylight hours in the Arctic summer. Allowing for actual diurnal variations would in fact result in a shorter lifetime owing to higher daytime OH and night-time NO_3 concentration means. A comparison of mean and median mixing ratios during periods with and without potential land influence did not yield substantial differences for any of the terpenes except β-pinene (data not shown), which however appeared to be consistently higher at the start of the cruise (potential Greenland influence) even on days when back-trajectories had not passed over land in the previous 48 h (cf. Figure 4.2/ 4.3). Since most monoterpenes were not detected in air during the majority of ACCACIA 2 and were generally lower than during AMT 22 (see Figures 4.1, 4.2, 4.5, Table 4.2), any terrestrial influence could only have been minimal, even if it was responsible for all of the observed mixing ratios.

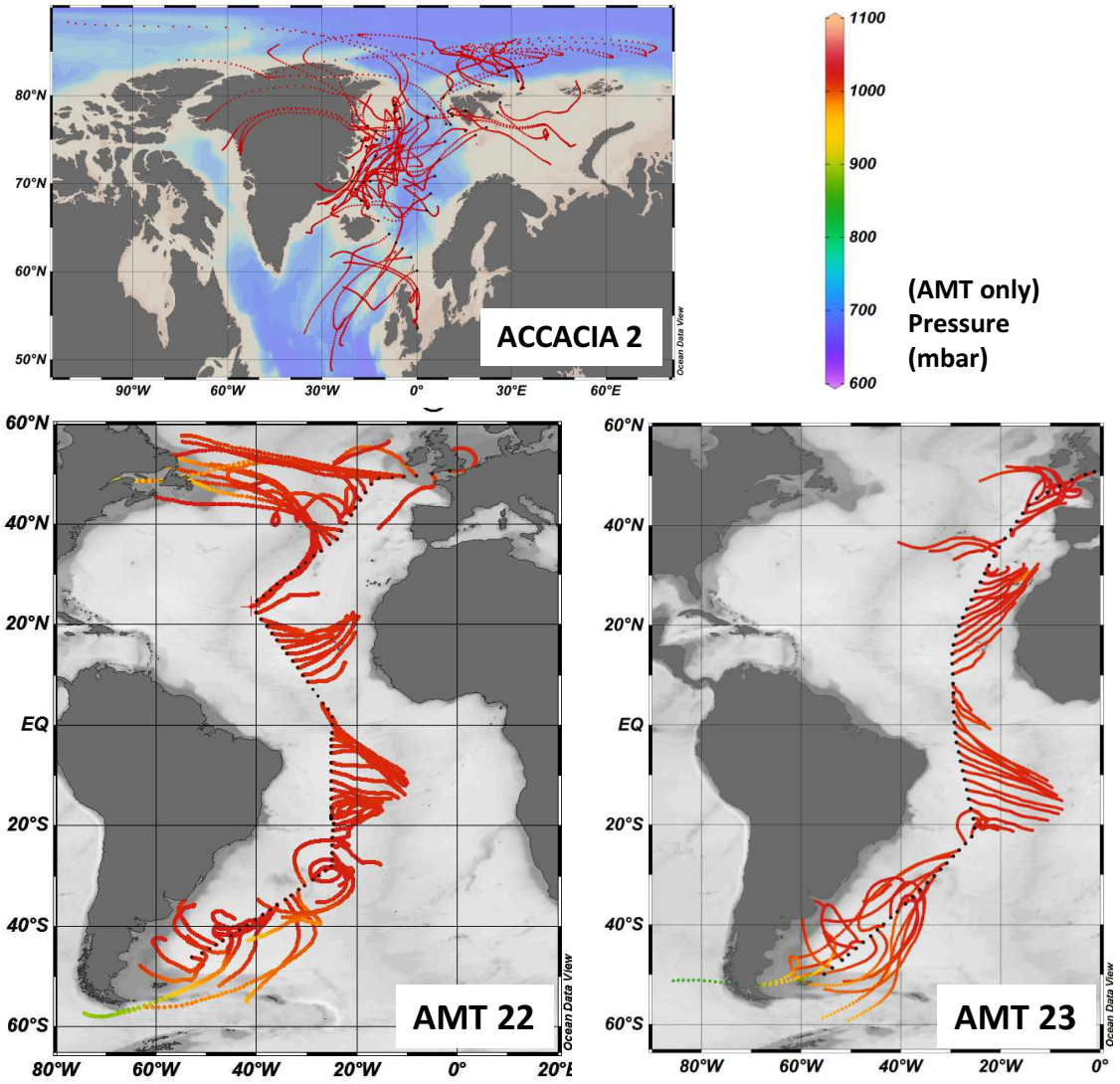

Figure 4.3 – Air mass back-trajectories along the cruise tracks, coloured by pressure (72 h; dots indicating the start of each new trajectory every 12 h). Back trajectories calculated in HySPLIT (http://www.arl.noaa.gov/HYSPLIT.php); plots created in Ocean Data View (Schlitzer, 2015). *NB*: ACCACIA 2 back-trajectories only position dots in order to display trajectories over land.

4.2.1.3 Seawater data

Comparing surface seawater samples taken from the CTD rosette to those from the non-toxic seawater supply can highlight effects of sample collection treatment, including the ship's underway pumping system in contrast with the clean Niskin bottles and any differences in sampling methodology for the two sample types. Ideally, both measurements agree well (within uncertainty), giving greater confidence in the results. Surface CTD samples, which are displayed in Figures 4.1 and 4.2 alongside the underway measurements, were mostly pre-treated and/or introduced in a different manner to the underway samples, as described in Chapter 2. Briefly, CTD samples on AMT 23 and ACCACIA were filtered by hand before storing them in the fridge in bottles or syringes and using semi-automated introduction into the P&T system; on AMT 22, the CTD samples were introduced in the same manner as underway samples, but had previously been stored unfiltered in the bottles. Various tests were conducted to ensure comparability of the methods used for underway and CTD sampling on each cruise, such as analysing discrete bottle samples taken from the underway supply, sampling into glass bottles and syringes from the same Niskin bottle, and storage tests for bottle and syringe samples (Chapter 2, section 2.3.2.2; bottle/syringe data not shown).

None of those tests suggested any strong systematic bias regarding terpenes in a sampling or sample treatment method compared to others used on the same cruise, so that any differences observed in the data are likely to be caused by differences in the water samples themselves. For most compounds, the discrete samples from AMT 22 compared well with the automated underway sampling, and no consistent differences were observed for α- and β-pinene, myrcene, carene and ocimene; the same is true of ACCACIA 2 water samples (α- and β-pinene only) and the second half of AMT 23 (where data were available). However, discrepancies existed for AMT 23 for most monoterpenes during the first half of the cruise, with values from CTD samples being consistently lower than underway water by approximately 20-40 %. Exceptions were ocimene and myrcene; the former seemed to agree well throughout, while the latter was highly variable and near the DL in the first half and showed some good agreement as well as some data points below the DL where no comparison was possible. Data for β-pinene from that cruise were discarded entirely due to at least a factor of four difference between CTD and underway data (CTDs were <DL, so that the much higher underway data could not be validated). There is no obvious

reason for the inconsistent relative levels, such as a modification of sample pre-treatment or collection procedure; any changes in further sampling conditions, e.g. calibration or contamination carryover from air samples, would be expected to affect both sample types equally. Therefore, the only potential cause appears to be a conditioning of the non-toxic seawater supply throughout the cruise, removing an initially present contamination source, and the apparent step change simply being due to a period of missing data where a gradual change may have occurred.

Particularly obvious was the offset between surface CTD and underway results for limonene during AMT 22 (1.5 to 3 times higher in the underway). The high values for limonene in underway water samples during that cruise did appear unlikely given the much lower concentrations observed on AMT 23 and the fact that CTD samples were much lower (albeit still considerably above AMT 23 levels). One potential explanation for this is the regular cleaning protocol employed on AMT 22 in order to avoid biofouling of the underway supply pipes. The procedure used Decon 90, a commercial detergent with unknown ingredients. Since limonene is a common component in cleaning agents, it is possible that it is also contained in Decon 90 and the regular application resulted in a high background signal for this analyte. The relatively high concentrations (i.e. around an order of magnitude above the likely natural concentrations) that were constantly in contact with the tubing in the P&T setup may have also affected the background for CTD samples, which could explain the higher levels compared to AMT 23. Laboratory tests will be carried out as part of future work to investigate potential contamination from Decon 90 in P&T samples.

4.2.1.4 Summary of average values and trends

For large parts of all cruises, atmospheric mixing ratios after filtering for contamination as described in Chapter 2 section 2.4.2.2 were at or below the DL, while water concentrations were generally above the DL.

No obvious trends were visible for any of the compounds; concentrations were either generally stable over longer periods of time or they varied without any clear patterns and with rather different distributions compared to isoprene. Water concentrations during AMT 23 appeared to be consistently higher in the northern hemisphere, but a large gap

in the data makes it impossible to determine whether a step change or a gradual decrease occurred between the two distinct periods. The pattern in AMT 22 data for α-pinene, if considered representative of both cruises, may hint at a gradual decrease south of the equator, but no similar observations were made for any other compounds, making this only a tentative suggestion. Binning the monoterpenes by Longhurst biogeochemical provinces (Figure 4.4) as a starting point for exploring controls (see Chapter 3 section 3.2.2.2) similarly did not highlight any differences between provinces such as those observed for isoprene (Chapter 3 Figure 3.4). Apparent trends in the limonene data are unlikely to be biologically driven, which becomes clear when inspecting the timeseries. Data in the temperate and tropical biomes do not appear significantly different; the large step change compared to polar data for α- and β-pinene cannot be easily explained and may indeed be due to environmental changes, as discussed briefly in section 4.3.1. Potential biological controls of the monoterpenes are discussed in more detail in section 4.2.3.

Figure 4.5 illustrates the distribution of data (>DL only) summarised in Table 4.2, alongside sea surface temperature (SST), wind speed and Chl-*a*. Overall, levels were similar for water between the two AMT cruises (within a factor of 2-3, with the exception of limonene); for air between AMT 22 and ACCACIA 2 they were comparable insofar as they were generally below a few pptv. The picture is different when comparing the Arctic and Atlantic data more closely: seawater concentrations in the Arctic for α- and β-pinene (the only monoterpenes quantified in seawater) were around 3- to 10-fold higher, but mixing ratios in air much lower than in the Atlantic (for all monoterpenes; see Table 4.2 and Figure 4.5). Potential reasons for these differences are discussed in section 4.3.1.

Table 4.2 contains details of the means, medians and ranges of all monoterpenes observed during the three cruises as well as the ranges of the dynamic detection limit for each compound. Also given are the number of observations (n) per mean or median, and the mean and median when values below the detection limit are included as 0.5xDL. Two facts become apparent: firstly, that the median tends to be lower than the mean, which can be skewed by a few high values even though the majority of the data is lower (as can be seen in Figures 4.1 and 4.2); secondly, that excluding data <DL leads to the loss of large proportions of the dataset (which are not flagged as bad) and also to higher mean and median values.

Setting the placeholder value for data <DL as 0.5xDL gives a mid-range estimate of the

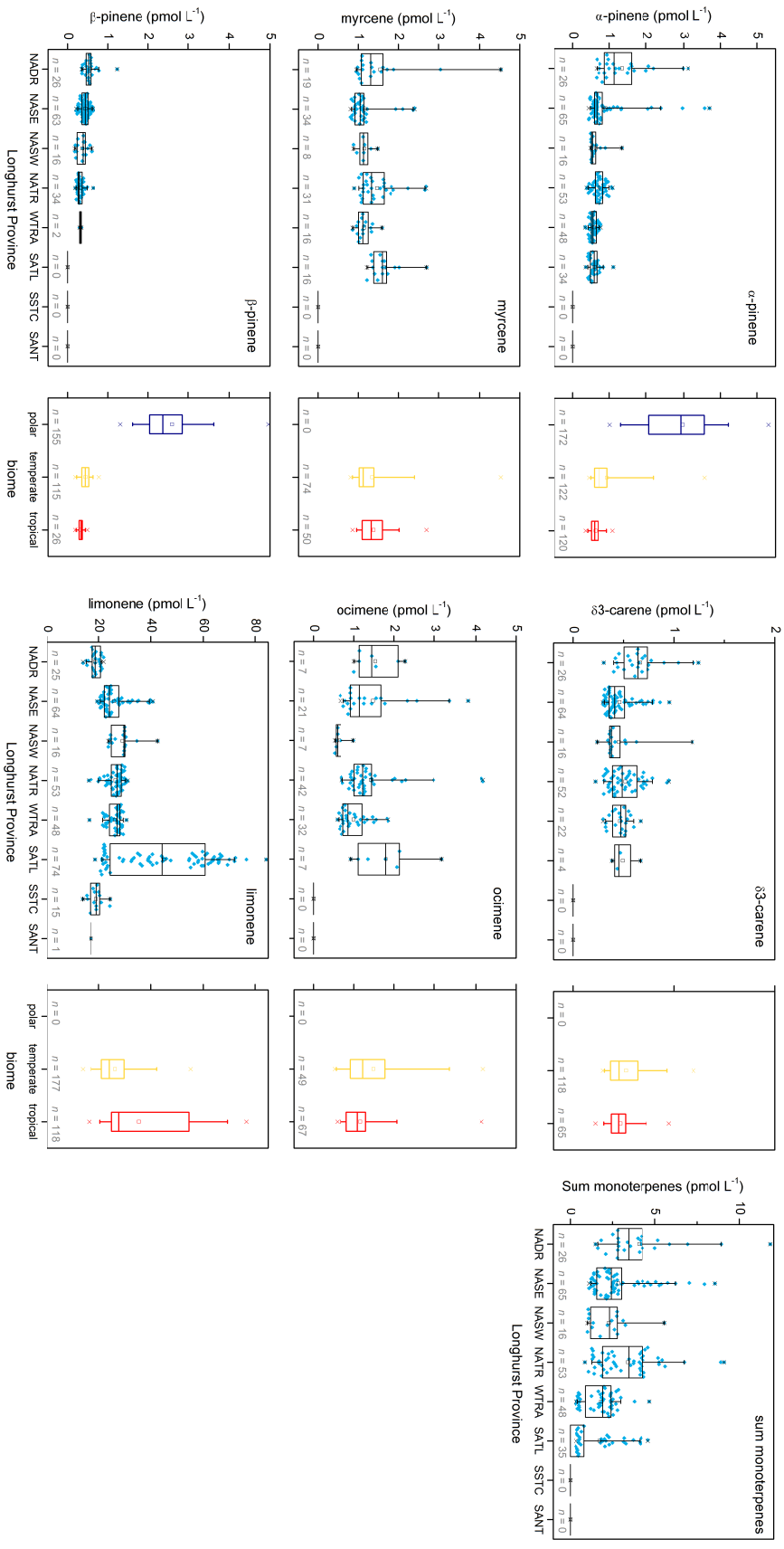

Figure 4.4 – Monoterpenes in surface water binned by Longhurst Province (NADR = North Atlantic Drift Province, NASE = N. Atl. Subtropical Gyral Province (East), NASW = N. Atl. Subtropical Gyral Province (West), NATR = N. Atl. Tropical Gyral Province, WTRA = Western Tropical Atlantic Province, SATL = South Atlantic Gyral Province, SSTC = S. Subtropical Convergence Province, SANT = Subantarctic Province) and by biome after Exton et al. (2013); mean (open square), median (line), 25-75th percentile (box); 5-95th percentile (whiskers), min./max. (cross). Sum of monoterpenes excludes limonene. AMT 22 data >DL only except polar α- and β-pinene, which is from ACCACIA 2 (>DL). *N.B.* varying y-axis scales.

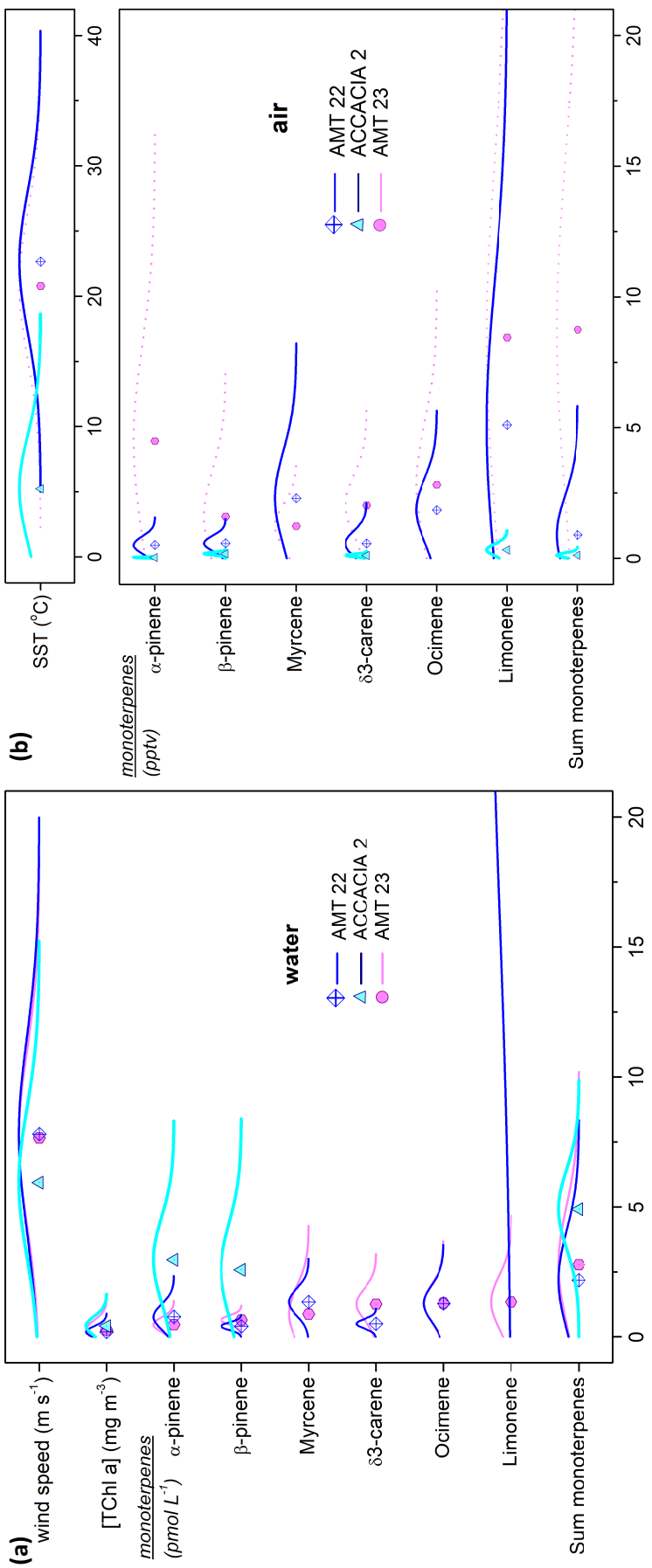

Figure 4.5 – Summary for all cruises of (a) monoterpene water concentrations, Chl-*a* concentrations and wind speed, and (b) air mixing ratios and SST; AMT 23 air data shown as dashed lines for comparison (discarded due to contamination); only data >DL (see also Table 4.2); symbol = mean; limonene and sum monoterpenes data partially off-scale to allow better presentation of valid data. Sum of monoterpenes excludes limonene (suspected contamination; see text for explanation).

potential actual value; alternatively, 1xDL or zero could be used to obtain an upper or lower limit, respectively. Since the DL was relatively well characterised in the present study, including this data (in any of the above ways) provides additional and arguably more accurate information on overall concentrations than solely using data >DL, which results in artificially high mean and median values. Disregarding such data without providing information about the DL furthermore creates the impression that analytes were not measured over large areas or data discarded following quality control – as a consequence, existing knowledge of the upper limit is not preserved.

Table 4.2 – Results for each cruise for monoterpenes in water and air; also shown are results from the ORC3 project[e]. Values calculated from only data >DL except in columns titled (0.5xDL)[b]; number of data points n applies to both mean and median (only shown with median); empty brackets indicate that no data was <DL (n is the same for both datasets).

	Cruise	Mean (range)	Mean (0.5xDL)[b]	Median (n)	Median (n) (0.5xDL)[b]	DL range[c]	surf. CTD mean (n)
α-pinene							
water	AMT 22	0.77 (<DL-3.71)	0.69	0.65 (242)	0.59 (299)	0.05-0.89	0.48 (16)
(pmol L^{-1})	AMT 23	0.47 (0.08-1.01)	()	0.33 (195)	()	0.02-0.10	0.38 (28)
	ACCACIA2	2.85 (<DL-5.31)	2.39	2.85 (172)	2.44 (172)	0.29-2.09	3.46 (41)
air	AMT 22	0.51(<DL-1.86)	0.43	0.41 (356)	0.35 (503)	0.03-0.85	
(pptv)	AMT 23[a]	-	-	-	-	-	
	ACCACIA2	0.03 (<DL-0.09)	0.02	0.03 (54)	0.03 (887)	0.01-0.12	
	ORC3	0.14 (<DL-1.03)	0.1	0.12 (572)	0.10 (876)	0.01-0.20	
β-pinene							
water	AMT 22	0.41 (<DL-1.23)	0.4	0.39 (141)	0.35 (298)	0.12-2.37	0.46 (8)
(pmol L^{-1})	AMT 23[d]	0.65 (0.24-1.00)	()	0.68 (74)	()	0.14-0.28	<DL
	ACCACIA2	2.45 (<DL-4.96)	2.08	2.35 (155)	2.09 (219)	0.66-3.83	1.40 (5)
air	AMT 22	0.57 (<DL-2.06)	0.48	0.5 (189)	0.42 (504)	0.07-2.25	
(pptv)	AMT 23[a]	-	-	-	-	-	
	ACCACIA2	0.17 (<DL-0.35)	0.13	0.17 (448)	0.13 (887)	0.03-0.57	
	ORC3	0.08 (<DL-0.57)	0.03	0.05 (104)	0.02 (873)	0.01-0.21	
Myrcene							
water	AMT 22	1.34 (<DL-4.54)	1.17	1.17 (124)	1.07 (294)	0.12-2.37	1.09 (3)
(pmol L^{-1})	AMT 23	0.88 (<DL-4.78)	0.47	0.55 (77)	0.26 (194)	0.26-0.83	1.40 (7)
air	AMT 22	2.29 (<DL-9.29)	0.9	1.70 (29)	0.70 (495)	0.42-4.31	
(pptv)	AMT 23[a]	-	-	-	-	-	
	ACCACIA2	<DL	0.19	<DL	0.17 (732)	0.18-0.89	
	ORC3	0.10 (<DL-0.55)	0.06	0.09 (448)	0.05 (786)	<0.01-0.07	

Continued...

Measured monoterpene concentrations in water and air (*continued...*)

	Cruise	Mean (range)	Mean (0.5xDL)[b]	Median (*n*)	Median (*n*) (0.5xDL)[b]	DL range[c]	surf. CTD mean (*n*)
δ3-carene							
water	AMT 22	0.50 (<DL-1.25)	0.49	0.46 (183)	0.46 (288)	0.10-2.00	0.36 (10)
(pmol L^{-1})	AMT 23	1.26 (<DL-2.93)	1.05	1.36 (137)	0.81 (174)	0.14-0.72	0.87 (19)
air	AMT 22	0.57 (<DL-2.46)	0.37	0.40 (97)	0.29 (507)	0.04-1.90	
(pptv)	AMT 23[a]	-	-	-	-	-	
	ACCACIA2	0.11 (<DL-0.26)	0.08	0.10 (33)	0.07 (868)	0.05-0.49	
	ORC3	0.09 (<DL-0.81)	0.05	0.07 (362)	0.04 (876)	0.01-0.16	
Ocimene							
water	AMT 22	1.29 (<DL-4.19)	1.1	1.12 (116)	0.88 (285)	0.41-5.18	1.39 (6)
(pmol L^{-1})	AMT 23	1.30 (<DL-3.21)	1.02	1.14 (124)	0.87 (166)	0.09-1.09	1.53 (21)
air	AMT 22	1.84 (<DL-5.72)	0.99	1.68 (29)	0.85 (496)	0.26-4.79	
(pptv)	AMT 23[a]	-	-	-	-	-	
	ACCACIA2	<DL	1.34	<DL	0.35 (878)	0.40-16.27	
	ORC3	0.23 (<DL-0.93)	0.06	0.21 (108)	0.03 (868)	0.01-0.24	
Limonene							
water	AMT 22	29.92 (13.70-84.25)	()	26.27 (296)	()	0.22-2.24	16.97 (38)
(pmol L^{-1})	AMT 23	1.34 (<DL-3.85)	1.32	1.14 (188)	1.05 (192)	0.12-0.24	1.00 (24)
air	AMT 22	5.10 (<DL-33.53)	4.15	2.92 (396)	2.35 (503)	0.12-2.12	
(pptv)	AMT 23[a]	-	-	-	-	-	
	ACCACIA2	0.32 (<DL-3.29)	0.26	0.27 (595)	0.23 (875)	0.07-0.51	
	ORC3[f]	1.08 (<DL-2.34)					

[a] discarded due to hydrocarbon contamination; [b] using a value of half the DL for points that fall below the DL but are otherwise not flagged as bad (or probably bad) data; [c] dynamic detection limit (DL), described in Chapter 2 section 2.4.1; [d] discarded, as CTD was <DL and hence underway data could not be validated; [e] results from intensive operating periods at Cape Verde Atmospheric Observatory as part of the ORC3 project (details see Chapter 5 section 5.2.1); [f] limonene during ORC3 was largely lower than a closely-eluting interference, resulting in large portions of the data being discarded.

4.2.2 Calculated fluxes

As for isoprene, sea-to-air transfer is thought to be the dominant loss term from the ocean for the monoterpenes due to their low Henry's Law constants and also since no chemical or biological losses in the water column have been identified (Palmer and Shaw, 2005; Meskhidze et al., 2015). Sea-to-air fluxes were calculated following the procedures explained in Chapter 3 section 3.2.3, assuming an air mixing ratio of zero as for isoprene, for

points where measurements above the DL existed (referred to as "actual" or "measured" flux in this chapter and summarised in Figure 4.6). As a result of high detection limits or instrument issues, large sections of data are missing for most monoterpenes and the picture obtained from the derived fluxes is incomplete.

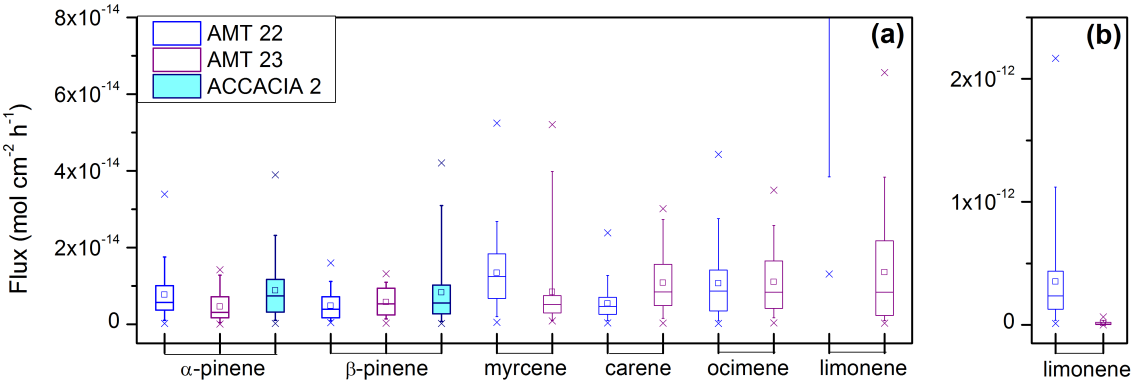

Figure 4.6 – (a) Summary of all fluxes (measured), (b) with compressed y-axis to show AMT 22 limonene; mean (open square), median (line), 25-75th percentile (box); 5-95th percentile (whiskers), min./max. (cross).

Therefore, two further emission values were estimated for the Atlantic, one based on the detection limit and the other on average oceanic concentrations of each monoterpene (underway data). Both were derived using the same calculations as the actual flux, but differed in the input water concentrations: the "maximum potential" flux used measured values where they were above the DL and 1×DL for data below the DL (and not flagged as bad), while the "constant-source" flux took a constant terpene water concentration as input for the whole transect. This single value for each analyte was chosen based on the observation that concentrations of all monoterpenes did not appear to follow a discernible trend at any time (see Figures 4.1 and 4.2), and was estimated from a period during which the underway water measurements were generally >DL (varied by cruise and analyte, specified in Table 4.2) by taking the median concentration from that period. Any data that did fall below DL for that time was replaced by a value of 1×DL. The constant-source flux was determined for the entire transect at hourly intervals (with minute-resolution surface/meteorological data averaged to the same time frame as for actual measurements, i.e. 30 or 35 minutes (AMT 22 or 23, respectively)). Results of all calculations are displayed in Figure 4.7, giving an overview of the actual fluxes as well as an expected flux if assuming constant water concentrations throughout, and, as an upper constraint based

on the experimental conditions at the time, the maximum flux that could have occurred if the water concentrations had been just below the DL.

Table 4.3 – Values (pmol L^{-1}) used for water concentrations in "constant source" flux calculations, giving in brackets the "stable" latitudinal section over which the median was taken (values <DL where included as 1×DL, see text); *Eq.* is the equator; *all* denotes entire dataset used on AMT 22, which was always the case for AMT 23.

Cruise	α-pinene	β-pinene	Myrcene	Carene	Ocimene	Limonene
AMT 22	0.65	0.37	0.91	0.42	1.05	26.27
	(50 °N-15 °S)	*(50 -10 °N)*	*(50 °N-Eq.)*	*(50 °N-Eq.)*	*(50 °N-Eq.)*	*(all)*
AMT 23	0.33	0.68	0.43	0.81	0.87	1.05

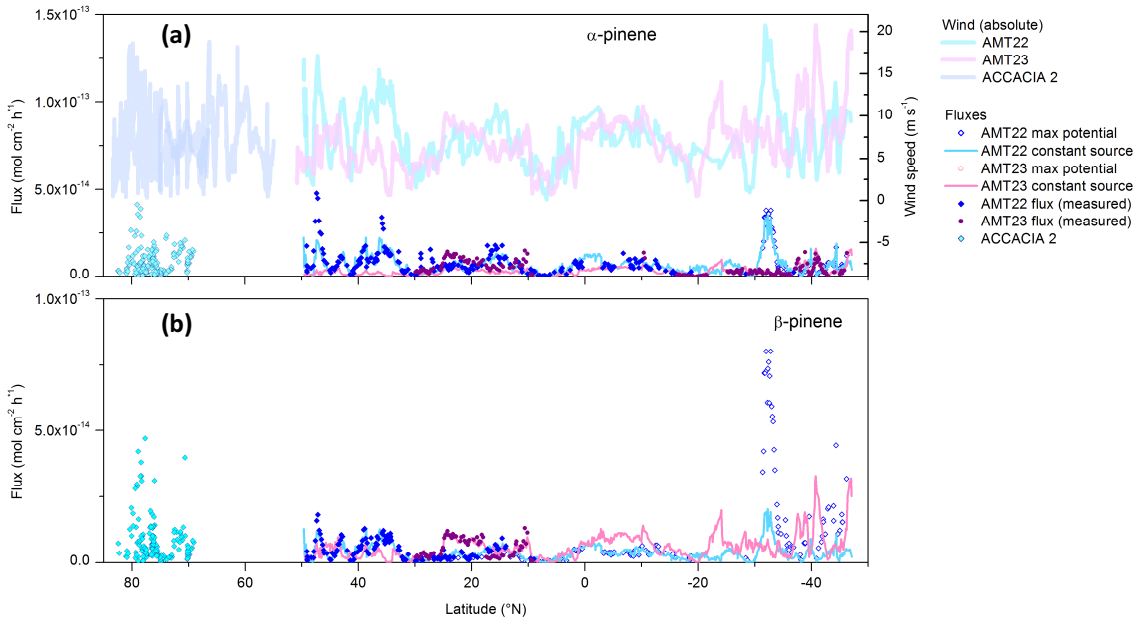

Figure 4.7 – *Continued over...*

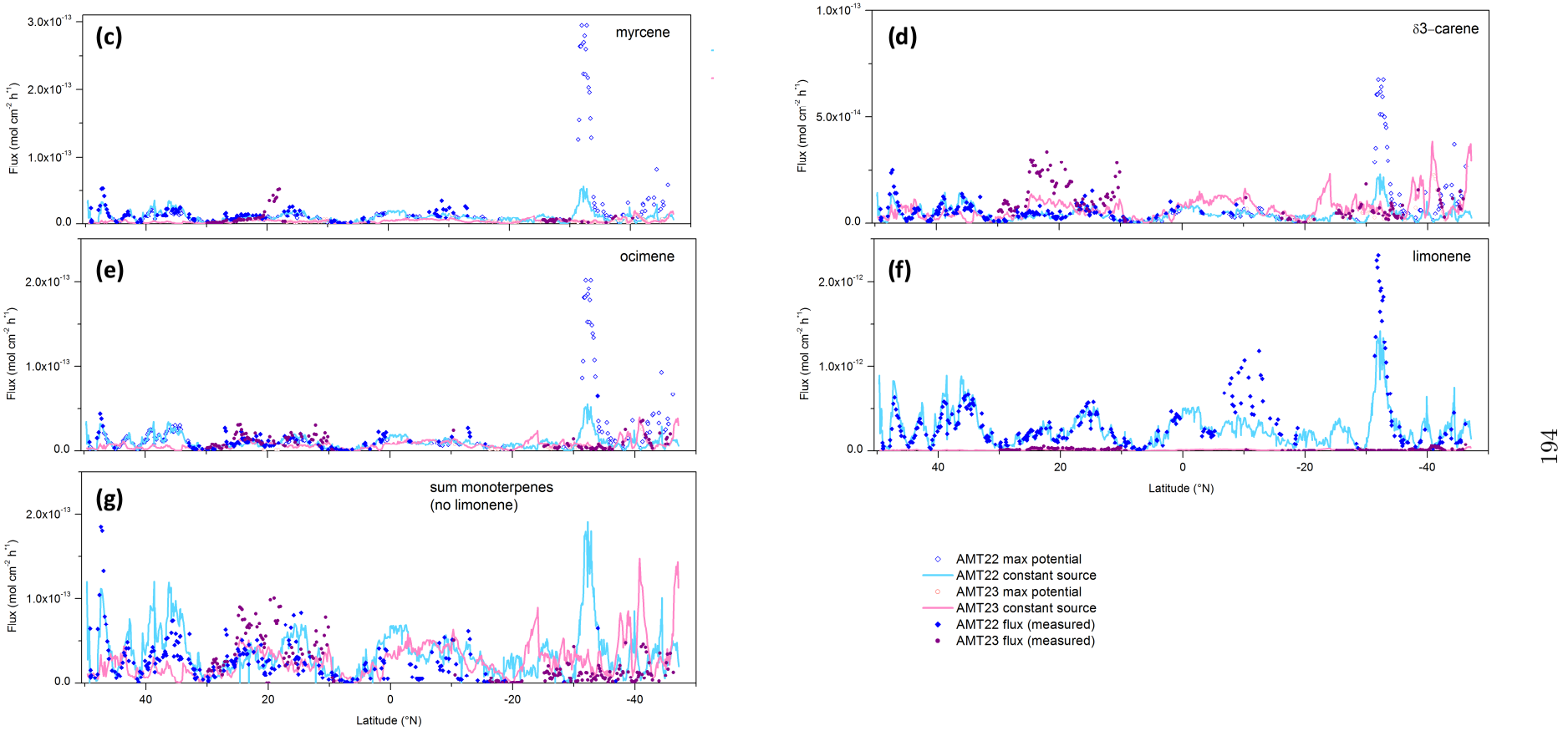

Figure 4.7 – Fluxes of monoterpenes along the AMT transects; showing actual, maximum potential and constant-source fluxes (see text); (a-b) α- and β-pinene, also including ACCACIA 2; (c-f) myrcene, δ3-carene, ocimene and limonene; (g) sum of monoterpene fluxes (actual and constant source only, no limonene); wind speed displayed in (a).

As previously mentioned, the uncertainty in Henry's Law constants for monoterpenes and their temperature dependence could substantially affect flux calculations when air mixing ratios are not assumed to be zero. Sensitivity to different approaches was explored for α-pinene, using two different published values of the Henry's Law constant (H) and temperature dependence. The results illustrate the effects of temperature dependence, of changing the value of the constant itself and of simply avoiding the use of the constant altogether by assuming an atmospheric mixing ratio of zero and only water-side limitation (discussed in Chapter 3 section 3.2.3 for isoprene). Figure 4.8b shows that the temperature dependence (using H = 7.4 x10^{-5} mol m^{-3} Pa^{-1} and $d(lnH)/d(1/T)$ = 4400 K, from Copolovici and Niinemets, 2005) has only minor effects (<0.3 %) on calculated fluxes despite using the larger of the two temperature dependence values, while a different literature value of H = 2.9 x10^{-4} mol m^{-3} Pa^{-1} (with $d(lnH)/d(1/T)$ = 1800 K, from Leng et al., 2013) results in up to 6 % lower fluxes. Fluxes determined using measured values of α-pinene in air (set as 1×DL where data <DL) and H from Copolovici and Niinemets (2005) were between 0.2-2 % lower compared to disregarding H entirely by fixing air mixing ratios at zero throughout.

This investigation suggests that assuming mixing ratios to be zero is an acceptable simplification of the flux calculation for the present datasets, and that even a 4-fold difference in H would not substantially influence fluxes. It must be highlighted that these results are only valid for situations where the analyte is supersaturated in water (500-10000 % saturation anomaly for α-pinene during AMT 22) and the air-side limitation is very small. If the water and air are nearer equilibrium (represented by a mixing ratio of 22.4 pptv in this case, with water concentrations remaining as measured; saturation anomaly is still 100-500 %), the fluxes decrease by up to 40 % compared to fluxes obtained with air = 0 pptv (Figure 4.8a). The mixing ratio of 22.4 pptv was chosen as it represents 70 % (contribution of α-pinene to sum of monoterpenes observed by Meskhidze et al., 2015) of the 32 pptv total monoterpenes measured at Chatham Rise (Lawson et al., 2015). The equilibrium α-pinene mixing ratio (based on Henry's Law parameters from Copolovici and Niinemets, 2005) would be around 50 pptv for most of AMT 22 (equilibrium conditions would lead to a flux of zero, and the effect of mixing ratio on flux becomes more pronounced the closer to equilibrium the conditions are).

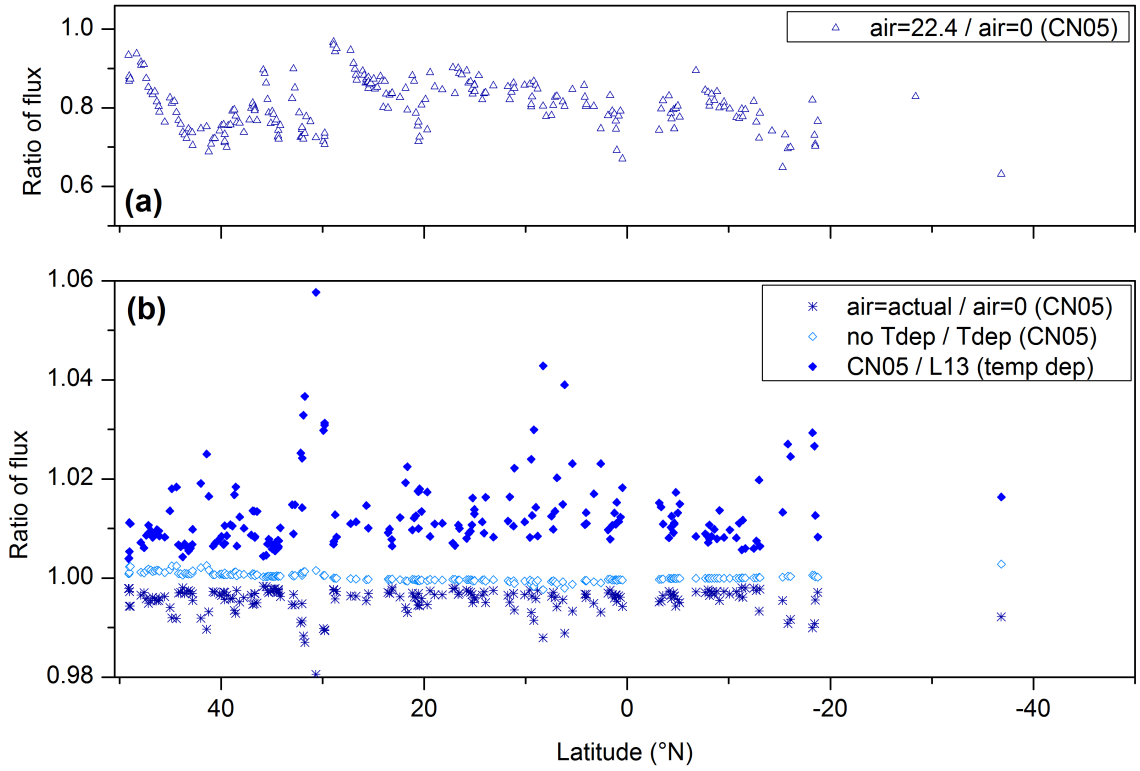

Figure 4.8 – Effects on calculated sea-to-air fluxes of α-pinene of (a) varying the analyte atmospheric mixing ratio by a large amount or (b) varying (or effectively omitting, by assuming *air=zero*) the Henry's Law constant and its temperature dependence; shown as ratio of the different results as detailed in the legend. *air=actual* using measured mixing ratios; *air=0* using mixing ratio fixed at zero and only water-side limitation; *noTdep* and *Tdep*: setting temperature dependence parameter of H to zero and to literature value, respectively; CN05 = Copolovici and Niinemets (2005); L13 = Leng et al. (2013).

4.2.3 Potential controls in the ocean

As briefly mentioned in the introduction, monoterpenes, like isoprene, have been reported to be of biogenic origin (Yassaa et al., 2008; Colomb et al., 2009; Meskhidze et al., 2015). These reports are based on laboratory studies of phytoplankton monocultures (Yassaa et al., 2008; Meskhidze et al., 2015) and field observations of positive relationships of monoterpene air mixing ratios with biological activity (Chl-*a*) or isoprene, and even observed diurnal cycles (Yassaa et al., 2008; Colomb et al., 2009), all discussed in more detail below (this section and section 4.3). From the evidence in the literature, similar correlation patterns of water concentrations with biological parameters as those found for isoprene (Chapter 3) may be expected for monoterpenes. However, an inspection of the data ((Figure 4.1/4.2) shows a lack of clear trends in the monoterpenes water measurements and certainly a lack of any trends that appear similar to observed biological patterns: examples of the biological data found to correlate with isoprene or expected to be related to monoterpenes emissions are shown in Figures 4.9 and 4.10; also see Chapter 3 for some further transect or timeseries plots of different parameters. For example, relationships could have been expected for diatoms or chlorophytes since they were found to be the strongest emitters in both laboratory studies (Yassaa et al., 2008; Meskhidze et al., 2015), but neither fucoxanthin (diatom marker pigment) nor MV-Chl-*b* (monovinyl-chlorophyll *b*; marker pigment for the division chlorophyta to which chlorophytes belong, Jeffrey et al. (2011)) or chlorophytes as determined by CHEMTAX (ACCACIA 2 only, details of this method see Chapter 3 section 3.2.4.3) showed any clear patterns that resembled those of any of the monoterpenes (Figures 4.9 and 4.10). Correlations with photoprotective pigments as seen for isoprene would have matched the observation by Meskhidze et al. (2015) that monocultures responded to light stress with enhanced terpene production, but were similarly not observed in the present datasets (Figures 4.9d, 4.10c).

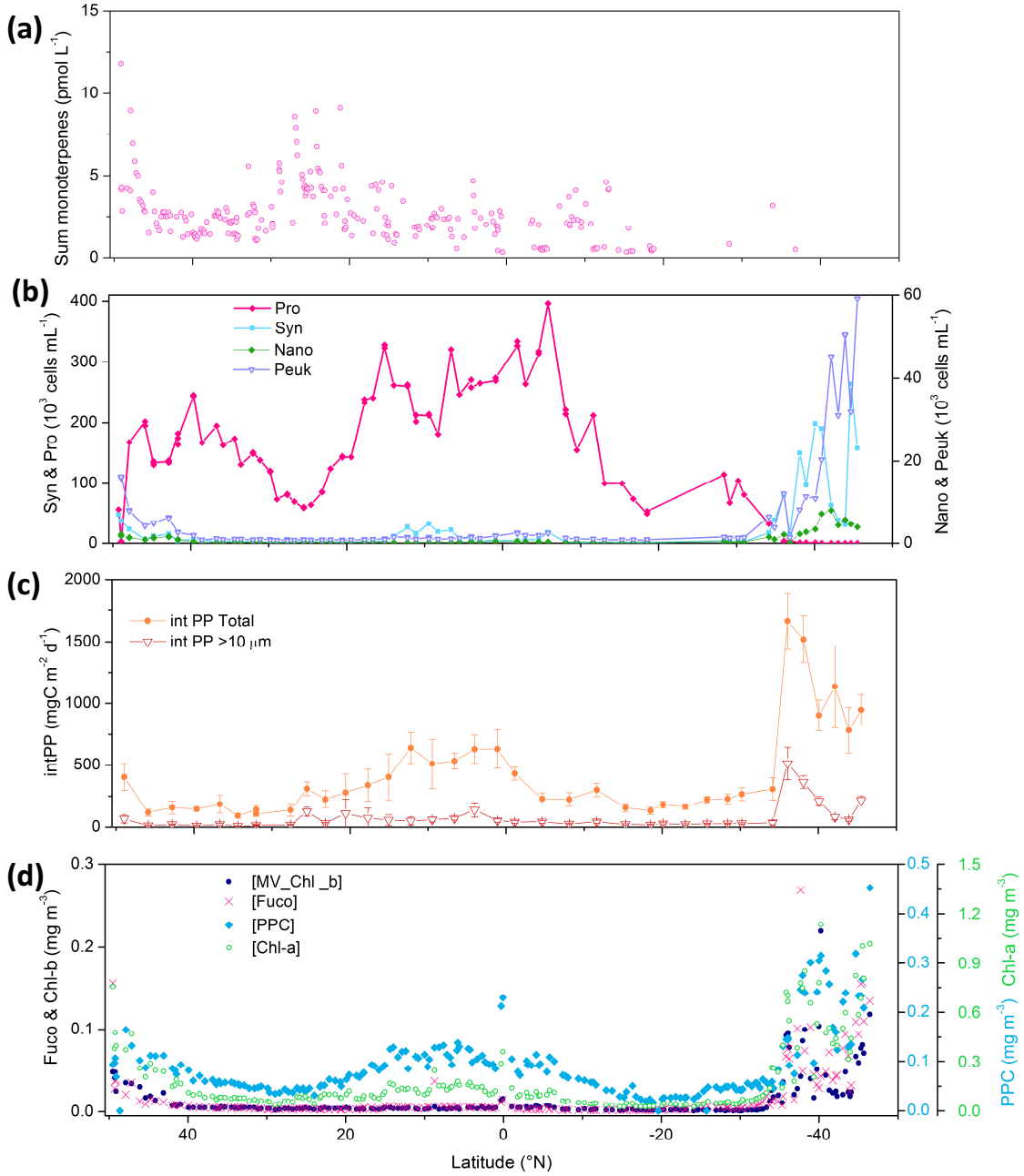

Figure 4.9 – Selected biological parameters shown alongside the monoterpene water concentrations: sum of monoterpenes excluding limonene for AMT 22, as representative of trends in both AMT cruises; *Syn, Pro*, Nano, Peuk = *Synechococcus, Prochlorococcus*, Nanoeukaryotes, Picoeukaryotes (respectively); MV-Chl *b* = monovinyl-chlorophyll *b*; intPP = integrated primary production; Fuco = Fucoxanthin, PPC = photoprotective carotenoids. Biological data from G. Tarran (PML), G. Tilstone (PML) and BODC/NERC.

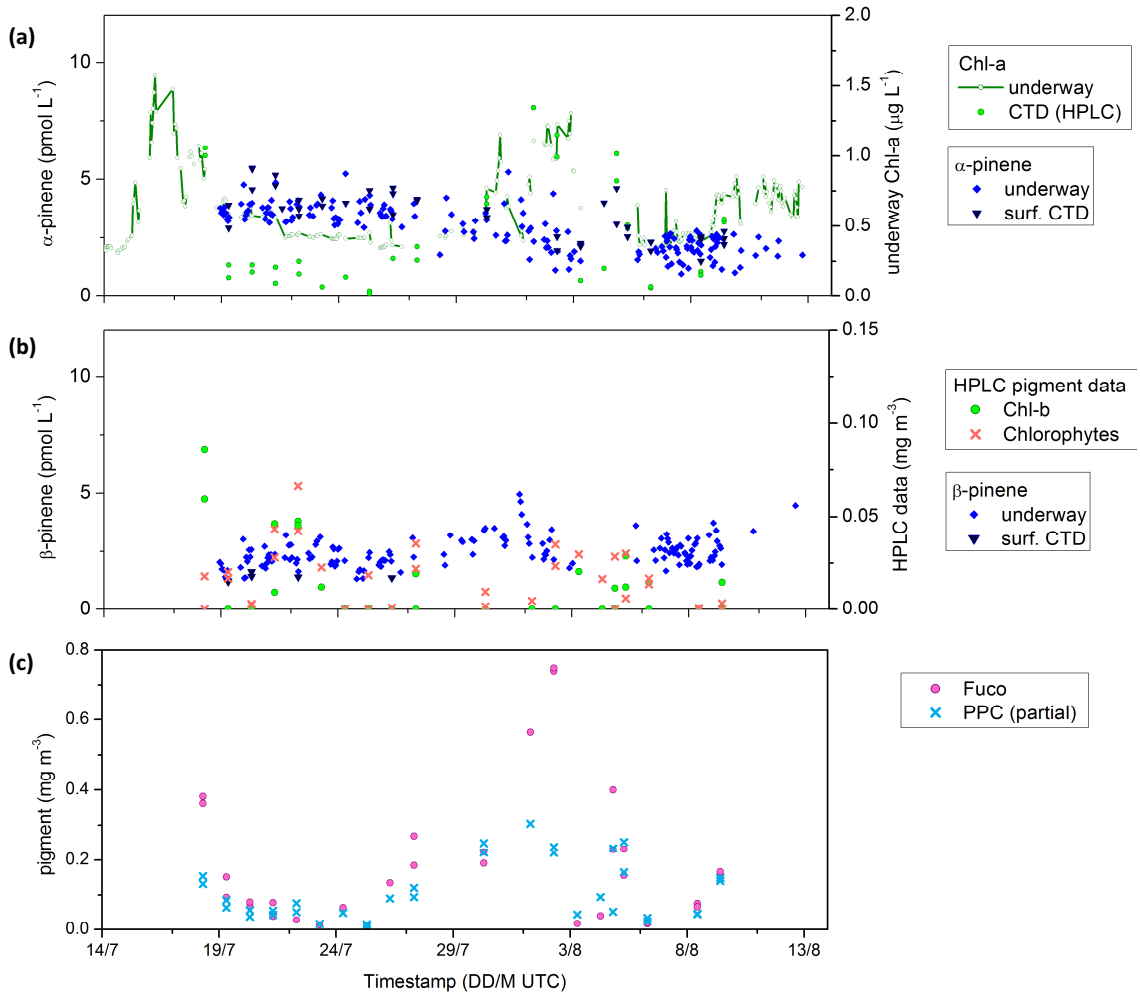

Figure 4.10 – Selected biological parameters shown alongside the monoterpene water concentrations: α- and β-pinene for ACCACIA 2; MV-Chl *b* = monovinyl-chlorophyll *b*; intPP = integrated primary production; Fuco = Fucoxanthin, PPC = photoprotective carotenoids. Biological data from A. Small and H. Bouman (University of Oxford).

As a result, no correlation analyses were performed, with the exception of a brief exploration of a numerical analysis of the relationship of β-pinene with nanoeukaryotes data from AMT 22 (Figure 4.11). The results highlight the need for careful analysis of data with expected low correlation coefficients and the importance of visual inspection of datasets before any further investigations are carried out. The R^2-value of 0.40 for the correlation suggests a reasonable linear association (supported by a p-value of <0.001), considering several of the correlation coefficients for isoprene and biological measurements were not much above this level when the datasets did show similar trends (e.g. Fucoxanthin for ACCACIA 2, Chapter 3 Figure 3.15). While the x-y correlation plot (Figure 4.11b) implies some linear relationship between the two datasets especially for lower sea surface temperature (SST), the transect plot in Figure 4.11a shows that the correlation is unlikely to be biologically meaningful - higher biological activity coincides with higher β-pinene levels at the start of the cruise (>40 °N), with a similar pattern for the first 2-3 days of sampling (>45 °N), but β-pinene remains near its initial levels while Nanoeukaryote cell counts decrease, and no increase in β-pinene was observed for elevated Nanoeukaryote counts later in the cruise (the trace gas remained below the detection limit, which may have been too high to observe an increase proportional to the Nanoeukaryote cell count). Hence, the R^2-value is mainly controlled by the low overall number of observations and a few high points, and should not be relied on to support a proposed correlation of the two parameters without prior verification of the actual trends in the datasets. The initial β-pinene concentrations could also be an artefact of the sampling system before it had been conditioned sufficiently, rather than related to the biological activity; this phenomenon was also observed on all other cruises on which the autoP&T has been deployed (Andrews et al., 2015), but cannot easily be identified as higher trace gas concentrations also do tend to occur in coastal regions than in the oligotrophic open ocean. In this case, the elevation of concentrations was neither very pronounced nor close to the coast and does appear to decrease and subsequently increase, so the observed trend is likely real and could be related to the Nanoeukaryote count. Given the small amplitude of the change compared to the noise in the subsequent section and the lack of data (none available from the other cruises for sufficiently productive regions), it is however not possible to verify this hypothesis.

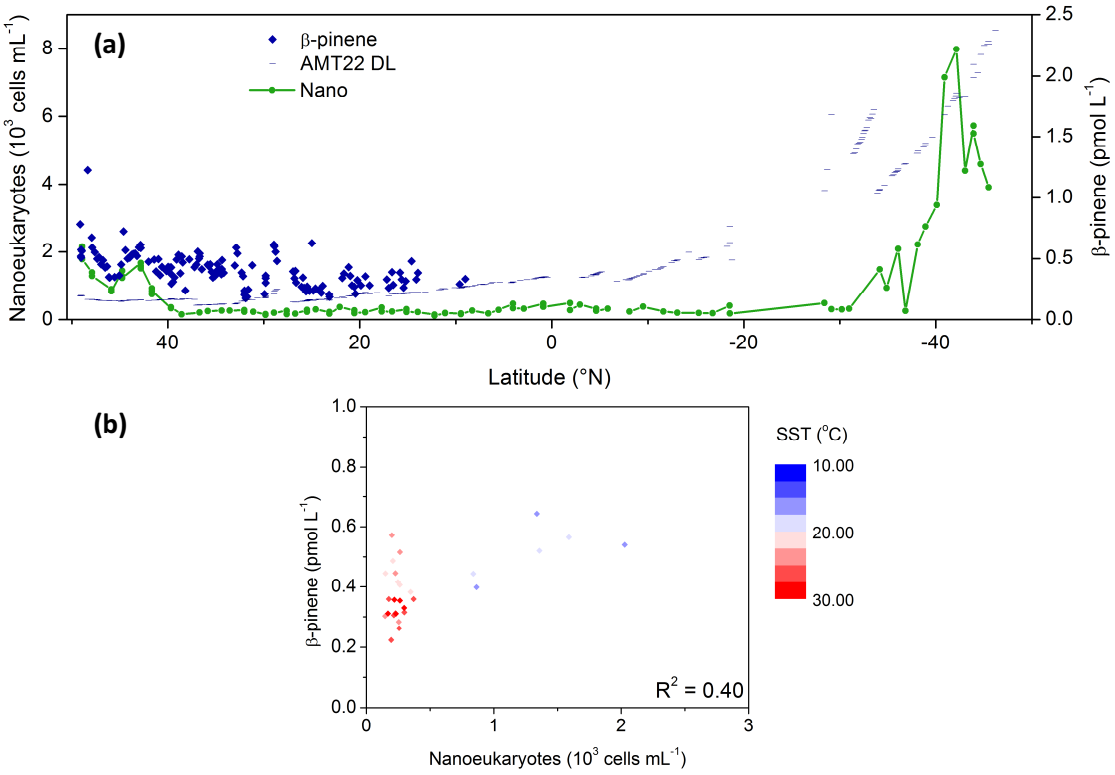

Figure 4.11 – Case study: (a) Transect plot and (b) correlation graph coloured by sea surface temperature (SST) of β-pinene with Nanoeukaryotes (Nano). DL = detection limit. Biological data provided by G. Tarran (PML).

4.3 Comparisons

4.3.1 AMT and ACCACIA

There is no immediately apparent reason why α- and β-pinene concentrations in water were substantially higher in the Arctic compared to lower latitudes. Factors affecting seawater concentations are production and consumption rates in the water column and losses to the atmosphere. Losses by sea-air gas exchange (described in section 4.2.2) were of comparable magnitude between the cruises, as a result of similar wind speeds (see Figure 4.5; mean of 6 m s^{-1} for ACCACIA 2 and *ca.* 7.5-8 m s^{-1} for both AMT cruises) and a combination of higher seawater concentrations with lower SSTs in the Arctic. The solubility increase of the gases at lower SST based on the Henry's Law temperature dependences given in Copolovici and Niinemets (2005) would only account for a 2.5-fold increase from 22 °C to 5 °C (approximate median SST for the Atlantic and Arctic cruises, respectively), and only 1.5-fold if the temperature dependence published by Leng et al. (2013) is used for α-pinene (no alternatives available for β-pinene). Additionally, no obvious or consistent relationship between SST and analyte concentrations was observed within each cruise dataset, despite the large ranges of SST encountered. As biological consumption rates are generally believed to be small (see Chapter 3 section 3.2.4), biological production remains as a potential influence. Yassaa et al. (2008) observed one of the highest production rates from a Southern Ocean diatom (*Fragilariopsis kerguelensis*), but another strain isolated from the Southern Ocean (*Chaetoceros debilis*; also responsible for open ocean blooms elsewhere) showed one of the lowest production rates. Theirs is the only published study that tested monoterpene production rates under natural growing conditions, making it difficult to draw general conclusions regarding emissions from polar phytoplankton.

Atmospheric mixing ratios were much lower during ACCACIA 2 than AMT 22, despite the similar seawater source strength. Emissions from the ocean were largely controlled by wind speed (similar to AMT); SST (lower than AMT) and seawater concentrations (higher than AMT) resulted in opposite effects of comparable magnitude, so that overall fluxes were similar for the cruises and cannot explain the difference in air mixing ratios. To test this further, observed α-pinene levels were compared with those expected based on seawater-derived fluxes. Calculations were essentially the inverse of a top-down flux

estimation, which predicts the total sea-to-air flux F as the product of the boundary layer (BL) height H_{BL} and a total production term P. This in turn is comprised of loss terms for reactions with OH and O_3 and the change in atmospheric concentrations of α-pinene (also see Chapter 5 section 5.2.2). Here, the seawater-derived flux F (in molec cm^{-2} s^{-1}) is substituted into the equation which is then solved for atmospheric concentration (assuming this to be constant throughout the day, i.e. $d[\alpha\text{-pin}]/dt = 0$):

$$P = \frac{d[\alpha\text{-pin}]}{dt} + k_{OH}[OH][\alpha\text{-pin}] + k_{O_3}[O_3][\alpha\text{-pin}] \quad (4.2)$$

$$F = P \times H_{BL} \quad (4.3)$$

$$\frac{F}{H_{BL} \times (k_{OH}[OH] + k_{O_3}[O_3])} = [\alpha\text{-pin}] \quad (4.4)$$

H_{BL} was set to 500 m as representative of the Arctic BL (1000 m for the Atlantic) and reaction rates k were taken from the literature (Chapter 5 Table 5.2). [OH] was averaged hourly over a diurnal cycle from model output (GEOS-Chem v9.2, 4x5° resolution, Sherwen et al. (2015), provided by T. Sherwen) and O_3 set to 25 ppbv (rounded value from model output). Losses due to NO_3 were not relevant to the calculation in the Arctic since it was always light (i.e. $[NO_3] = 0$), and simply reduced calculated night-time concentrations even further for AMT (not shown).

Figure 4.12 shows that observed and predicted mixing ratios agreed within a factor of three in the Arctic, while there was a discrepancy of between one and two orders of magnitude for the Atlantic, where seawater-derived fluxes could not explain the majority of the observed α-pinene in air. Potential explanations for this difference (or parts thereof) include constant low-level contamination (<1 pptv) in all AMT samples that was not obvious from any quality control criteria, or a large surface ocean source of the hydrocarbon that is emitting throughout the diurnal cycle. The relatively constant observed mixing ratios suggest that production cannot purely be photochemical such as that reported for isoprene in the surface microlayer (Ciuraru et al., 2015b, see Chapter 5), although a contribution from such a source is possible given the range of observed hydrocarbons in those experiments (Ciuraru et al., 2015a; Fu et al., 2015).

An adjustment of the BL height used in the calculations to more realistic values (as discussed in Chapter 5 section 5.2.3.2 and 5.2.4) would at most improve the agreement for AMT data by a factor of *ca.* 2-10, not by up to 300 as needed to bring the results into

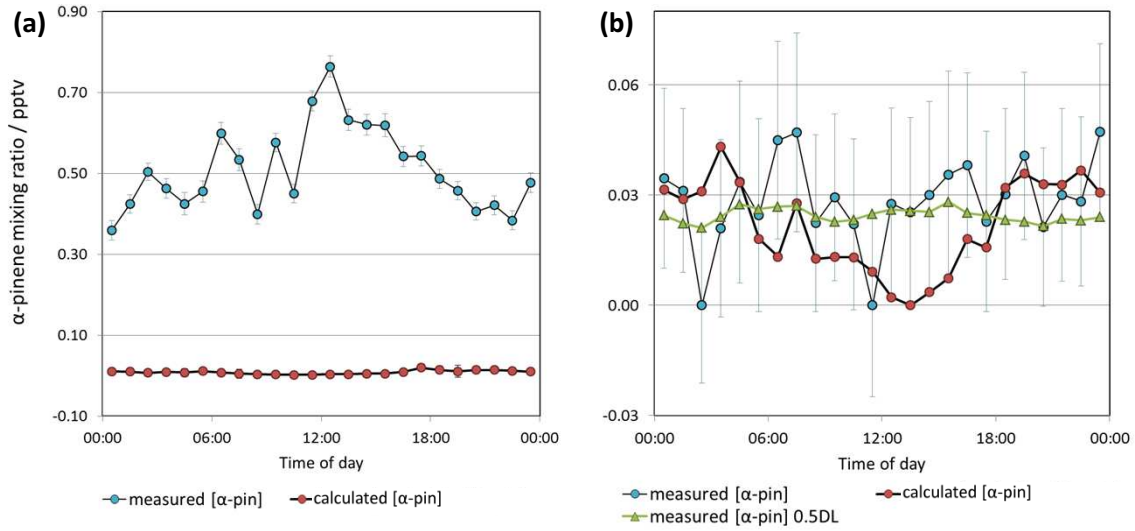

Figure 4.12 – Atmospheric α-pinene mixing ratios derived from seawater-based fluxes for (a) AMT 22 and (b) ACCACIA 2, shown alongside the respective measured values (hourly averages with standard error); error bars on calculated mixing ratios are based on the standard error of the hourly seawater-derived flux averages used in the calculation. Averages including data <DL as 0.5×DL (no error shown) are also included for ACCACIA 2 (air) as >90 % of the data were <DL.

the same range. Allowing for another potential influence, the temperature dependence of oxidation reactions for α-pinene, does not change values for AMT (mean temperature approximatey 25 °C) and increases predicted night-time air mixing ratios by up to 10 % for ACCACIA (*ca.* 0.003 pptv; not shown); i.e. this correction would not affect the results of the calculation (rounded to 2 decimal points).

4.3.2 Observations in the context of the literature

A comparison of Table 4.1 and Figure 4.1/4.2, summarised in Figure 4.13, quickly shows that the results from the current study are much lower than those reported previously (in air only), by up to two orders of magnitude. However, one important distinction between the campaigns is the biological activity, associated with the sampling region and season. While this project has not been able to find correlations of monoterpenes with biological data (see section 4.2.3), both other sets of field measurements did conclude there was a positive relationship, which is further supported by the laboratory studies, so that this discussion will be based on the assumption that biological productivity does indeed affect monoterpene levels in the environment. The AMT and ACCACIA cruises traversed

generally oligotrophic waters (median Chl-*a* for AMT 0.1-0.2 mg m^{-3}; 0.6 mg m^{-3} for ACCACIA 2 (calibration not yet quality-controlled)) that are more comparable to the "far from bloom"/background conditions described by Yassaa et al. (2008; *in-situ* Chl-*a* mean (range) of 0.355 (0.045-0.556) mg m^{-3}) and Colomb et al. (2009; Chl-*a* estimated from satellite plot 0.2-1 mg m^{-3}). If only those mixing ratio ranges are considered, the present observations were in fact within the same order of magnitude, given the large uncertainty on all measurements: 10 ± 10 pptv total monoterpenes by Colomb et al. (2009) and a mean (range) of 5 (<DL-14) pptv total α-pinene by Yassaa et al. (2008), compared to a mean (range) of 4.82 (<DL-48.16) pptv and 0.51 (0.08-1.86) pptv for AMT 22 total monoterpenes (including limonene) and total α-pinene, respectively.

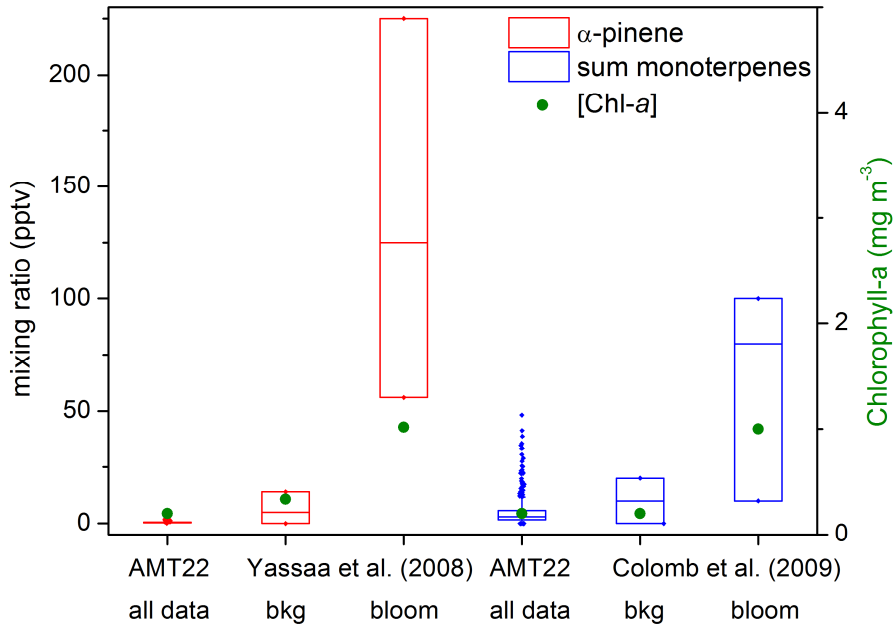

Figure 4.13 – Monoterpene atmospheric mixing ratios for AMT 22 compared to published data alongside relevant mean (literature) or median (AMT) chlorophyll-a concentrations [Chl-*a*]; bkg = background. Yassaa et al. (2008) boxes represent the range of measured values and the mean; Colomb et al. (2009) boxes show the mean and maximum/minimum calculated from mean ± standard deviation, respectively (asymmetrical for "bloom" conditions as they spanned several sections with different means and standard deviations).

Diurnal cycles of monoterpenes in air were observed by Colomb and co-workers (2009) during a period with relatively high mixing ratios (averages of 20-80 pptv for different sections); it is not clear whether this was also the case in the background regions. The present study did not establish any diurnal variation of monoterpenes, which could be

related to the low overall mixing ratios since trends may be obscured by the general noise in the distribution.

Another contributing factor to differences in mixing ratios are the different sampling methods: this project used *in-situ* GC-MS throughout all campaigns, giving speciated monoterpene measurements, while Yassaa et al. (2008) collected cartridge samples that were analysed by GC-MS in the laboratory later (also speciated), and Colomb et al. (2009) deployed a PTR-MS instrument that is limited to determining the sum of all monoterpenes (total signal at m/z 137, the protonated molecular species). All techniques have different potential artefacts and effects on the results, with PTR-MS not being able to determine contributions of individual monoterpenes, but GC-MS only quantifying those for which a calibration is available and missing contributions from unquantified isomers. The latter should only lead to minor underestimation since a number of monoterpenes was calibrated for in both of the studies discussed here, and any major additional contributions should have been noticed in the chromatogram (identifiable via library spectra if the peak is large enough) and mentioned, even if quantification was not possible. Cartridge sampling does have the potential for storage and sampling artefacts, as well as generally lower precision (e.g. Cao and Hewitt, 1995; Calogirou et al., 1996; Woolfenden, 2010), but any potential effects would typically be tested during method validation. The large relative concentrations/mixing ratios of limonene in the present study and its attribution to contamination (at least during AMT 22; see details below) highlight the benefits of speciated measurements, since they allow the distinction of potential contaminants that dominate the sum of monoterpenes. As discussed below, the relative contribution of different monoterpenes observed in the laboratory was not confirmed in the field, suggesting either different processes or species responsible for monoterpene emission or the influence of non-biogenic sources (including contamination) or sampling artefacts in the field data.

Yassaa et al. (2008) reported evidence for marine production of monoterpenes from both a laboratory study and field data. They found that all investigated cultures produced monoterpenes, albeit at different rates, with diatoms and a chlorophyte being the strongest emitters (incidentally, the chlorophyte, *Dunaliella tertiolecta* (*D. tert.*), is the species that was found by Exton et al. (2013) and Bonsang et al. (2010) to have unusually low isoprene production rates compared to other temperate species). Limonene and *p*-ocimene were the monoterpenes contributing the largest proportions to the overall emissions in the

laboratory (*ca.* 35 and 25 %, respectively), but when air measurements were made in the field, only α-pinene was quantified (*ca.* 9 % contribution to emissions in the laboratory). The other monoterpenes that had been previously identified in the culture studies were only detected at much lower levels in marine air. The authors do not state whether the relative proportions of monoterpenes varied between different monocultures; the example given is that of the strongest emitter (*D. tert.*). Meskhidze et al. (2015) observed a 70 % contribution from α-pinene and 20 % from limonene to the sum of monoterpenes in their more recently published laboratory experiments on isoprene and monoterpene emissions from four globally common algal classes (not necessarily grown at ambient conditions for each species), which seem to be consistent with the field measurements of Yassaa et al. (2008) showing α-pinene as the dominant monoterpene in air.

Measurements during the current project on AMT 22 indicated that limonene contributes around 50-90 % to the sum of monoterpenes in seawater and air, with α-pinene responsible for between 3 % (water) and 10 % (air). AMT 23 showed 10-80 % contribution of limonene (typically around 30 % in water; more scattered in air) and a relatively consistent 10 % fraction of the total attributed to α-pinene in water (around 30 % in air). During ACCACIA 2, limonene was responsible for around 50-70 % of the total monoterpenes in air, while α-pinene was largely below the DL, as were the other monoterpenes, and β-pinene alone was contributing the remaining 30-50 % to the sum. None of the above ratios are in agreement with the literature regarding the relative levels of limonene and α-pinene, or even those of α-pinene compared to the other monoterpenes (ratios not given here).

Meskhidze et al. (2015) linked VOC emissions to dual light and temperature stress, with higher emissions observed from cultures that had been exposed to light and temperature levels above those to which they had acclimated (22 °C, 90 µmol m^{-2} s^{-1}). Rates did generally reach a limit at very high light levels (light saturation) and in some cases (diatoms), production decreased again above a certain threshold. The authors found that isoprene and the monoterpenes followed the same emission patterns and suggested that temperature stress alone may not cause any visible changes in emission (none observed in their study or by Shaw et al., 2003), but that the dual temperature and light stress resulted in larger disruption than light stress alone. However, apart from lower emissions at lower temperatures and much lower emissions at temperatures higher than the species' tolerance, no clear pattern was observed for intermediate stress regimes, and tests were only conducted

on two diatom species, so that extrapolation to other species or functional types must be based on assumptions of similar behaviours in response to stress. Conclusions of the study were largely qualitative, or at least not clearly quantitatively stated, even though production rates are given. Short-term light and temperature stresses could be induced by vertical mixing in the water column (Meskhidze et al., 2015), so that a combination of the determined stress-driven rates may be representative of those in the environment, not only the light- and temperature-acclimated production rates. Since those rates vary greatly and will likely be different for species not studied and also for different temperature and light conditions during initial growth, a comparison to field measurements was not possible at this stage.

Given that field and laboratory data did not agree well beyond showing an association between phytoplankton and monoterpene emissions even in datasets collected by the same research group (Yassaa et al., 2008), a comparison of the current study and published data can only be very general. As detailed in section 4.2.3, it was not possible to establish links with biological activity like those suggested by the culture studies and also by the field measurements (Yassaa et al., 2008; Colomb et al., 2009; Meskhidze et al., 2015).

4.3.3 Investigating associations between monoterpenes and isoprene

Colomb et al. (2009) reported a linear correlation between the sum of monoterpenes (measured by PTR-MS, i.e. no speciated measurements) and isoprene in the Southern Indian Ocean (reproduced in Figure 4.14d). Yassaa et al. (2008) similarly saw a correlation of α-pinene and isoprene ($R^2 = 0.57$ in the bloom area, 0.41 for the entire cruise). Both papers suggest that this indicates similar sources and sinks of the compounds, and since the link of isoprene with biological production had already been established (Shaw et al., 2003; Milne et al., 1995; Moore et al., 1994) and a relationship with Chl-*a* or phytoplankton functional type was also observed, they conclude that both monoterpenes and isoprene must be of biogenic origin. Yassaa et al. (2008) also noted a correlation with both *in-situ* and averaged satellite back-trajectory-weighted Chl-*a*, but no correlation coefficients are given in their paper. The exact weighting of Chl-*a* along the back-trajectory is not explained, but in view of the calculations relating to the influence of air mass back-trajectories in section 4.2.1, it seems irrelevant to take into account air mass exposure to biological activity more than 24 or maybe 48 hours prior to sampling. It is unlikely that the influence of a

bloom more than a few hours away would be visible above the detection limit: assuming the highest observed mixing ratio of α-pinene from Yassaa et al. (2008) of 225 pptv and the total atmospheric lifetime during daytime of 1.7 h, the remaining mixing ratio at the point of sampling would have decreased to as little as 0.2 pptv after only 12 h, which is below their reported detection limit of 1-5 pptv and partially below that of the present campaigns (dynamic DL between 0.01-0.85 pptv). Even using the atmospheric lifetime solely with respect to OH at the mixing ratio assumed by the authors (1×10^5 molec cm^{-3}; low compared to other literature, e.g. Lee et al., 2006a), would fall below 1 pptv after less than 60 h. Considering these results, it is not clear why an association with averaged 10-day back-trajectory Chl-*a* would be observed; however the graphs only show a weak correlation, as also pointed out by the authors.

The datasets from the present study did not show a linear association of isoprene and monoterpenes, neither for the sum of all monoterpenes nor the sum of monoterpenes excluding limonene, for air or for water (Figures 4.14 and 4.16; R^2-values for correlations that were significant at the 95 % level are shown on the graphs). An investigation of only a "bloom" section (productive regions of the South Atlantic) showed no different trends for AMT 23 to the whole dataset (not shown here) and was not possible for AMT 22 due to high monoterpene detection limits. The rationale for exploring the correlation without limonene was based on its ubiquitous presence in cleaning agents and the unlikely high water concentrations during AMT 22 (see section 4.2.1) as well as generally high levels relative to the other monoterpenes that have not been observed in any of the published studies (field and laboratory), aiming to exclude potential contamination from non-oceanic sources. The patterns are in fact very similar with and without limonene in all comparisons apart from AMT 22 (water), only the absolute numbers change due to limonene contributing around 50-90 % of the total measured monoterpenes.

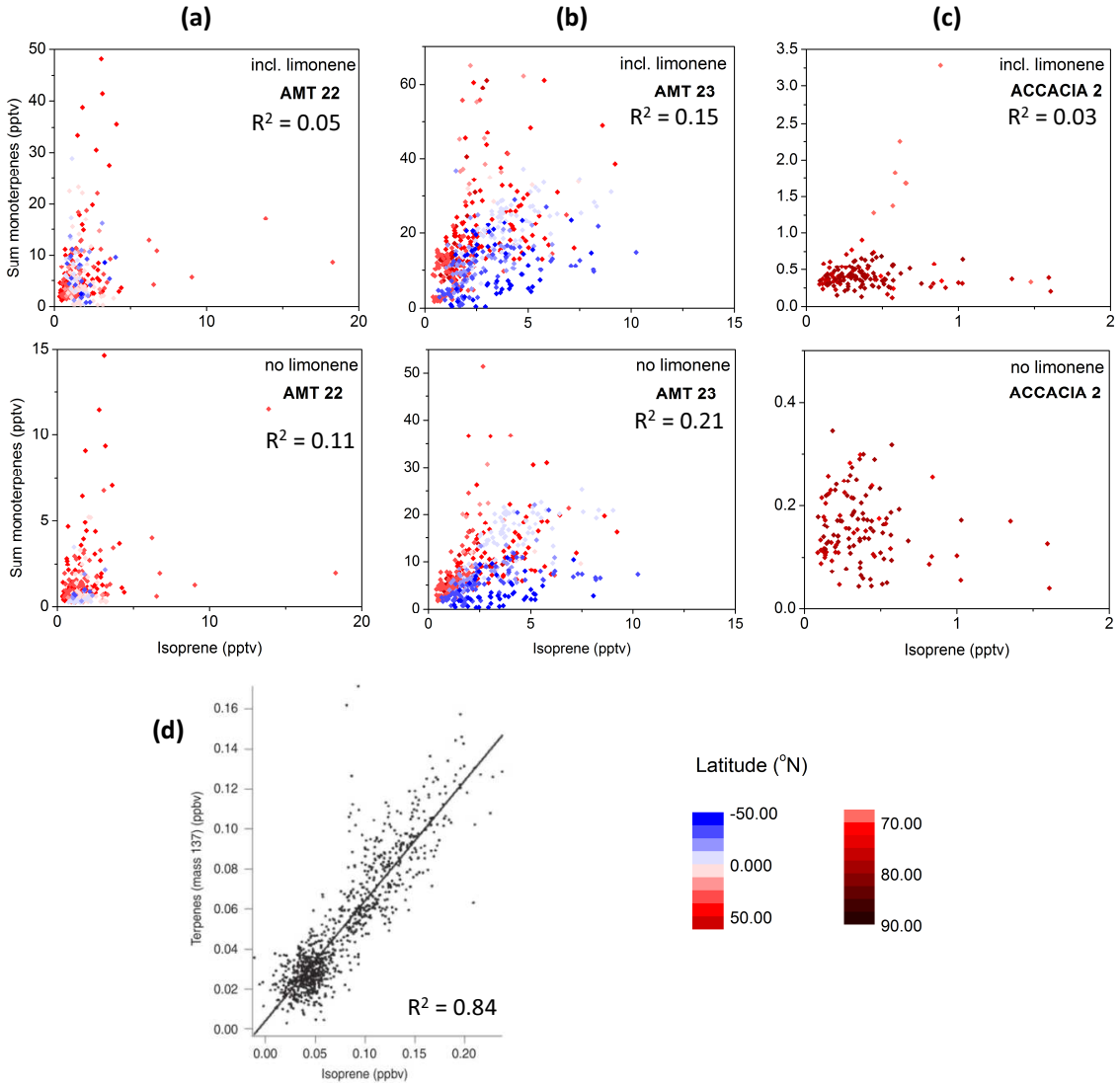

Figure 4.14 – Correlation of isoprene and sum of monoterpenes for air mixing ratios; (a) AMT 22, (b) AMT 23, (c) ACCACIA 2, (d) modified from Colomb et al. (2009; axes in ppbv). Points with zero concentration for sum of monoterpenes are the result of all concentrations being <DL but not flagged as bad (DL displayed in Figures 4.1 and 4.2). R^2-values are shown for correlations that were significant at the 95 % level (taken from Colomb et al. (2009) for (d)).

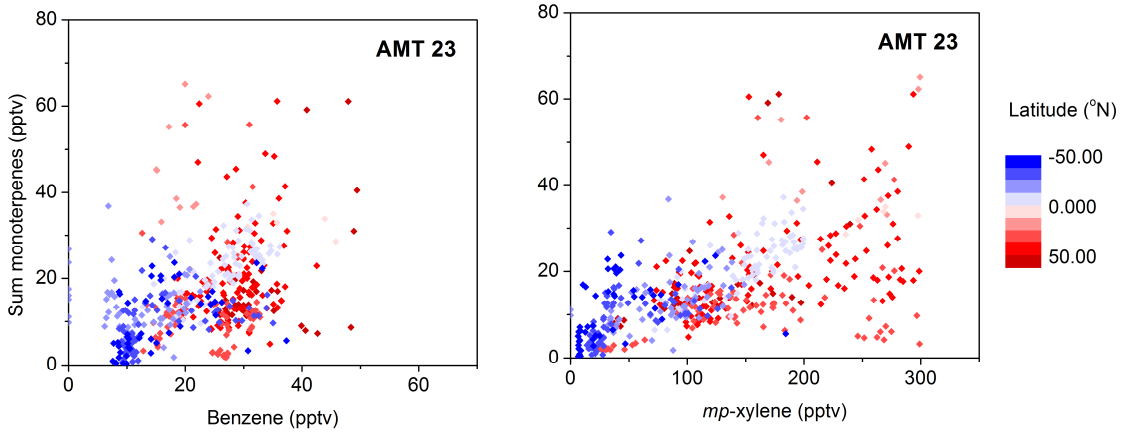

Figure 4.15 – Correlation of the sum of monoterpenes with hydrocarbon contamination markers benzene and *m*-/*p*-xylene during AMT 23.

Some correlation appeared to be present in the AMT 23 air data, but since this data was suspected to be contaminated (see section 4.2.1 and Chapter 2 section 2.4.2.2), it does not necessarily indicate common biogenic sources and rather points to a common contamination source. The latter deduction is further supported by the correlation observed for monoterpenes with the contamination markers benzene and *m*-/*p*-xylene (Figure 4.15), after data flagged as "contaminated" as described in Chapter 2 section 2.4.2.2 had already been excluded. It emphasises the benefits of concurrent measurements of hydrocarbon contamination markers for quality control purposes and in order to avoid erroneously deducing biogenic sources where they are unlikely based on the available evidence.

A distinct grouping can be seen for AMT 23 by northern/southern hemisphere, especially for the water data, however even within those groupings there is no linear relationship of isoprene and monoterpenes (Figure 4.16). There is no obvious explanation for the differences in the monoterpene concentrations that are causing this distribution, as already discussed in section 4.2.1. The (weaker) separation in the air data can be attributed to the contamination described above, which was worse in the northern hemisphere and affected the monoterpenes more than the isoprene mixing ratios. The hemispherical differences during AMT 22 were largely caused by the higher detection limits towards the end of the cruise that resulted in zero or very low total monoterpenes (without limonene; values below DL were counted as zero).

Monoterpene production rates were up to three orders of magnitude lower than those reported for isoprene in both laboratory studies, and atmospheric mixing ratios were also

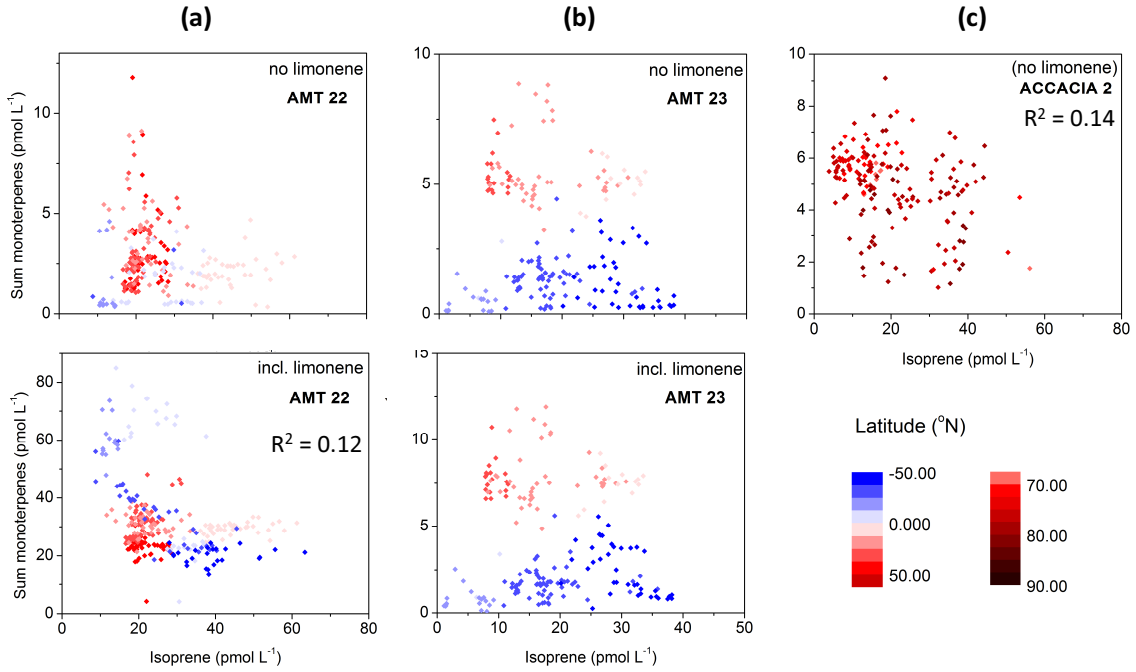

Figure 4.16 – Correlation of isoprene and sum of monoterpenes for seawater concentrations, coloured by latitude; (a) AMT 22, (b) AMT 23, (c) ACCACIA 2. Points with zero concentration for sum of monoterpenes are the result of all concentrations being <DL but not flagged as bad (DL displayed in Figures 4.1 and 4.2). R^2-values are shown for correlations that were significant at the 95 % level.

lower than those of isoprene in all previous publications. The sum of monoterpenes was around a factor of two lower than isoprene in air during the campaign by Colomb et al. (2009), while in the study by Yassaa et al. (2008), the total α-pinene was a factor of four lower in background conditions, of similar order when influenced by a "distant bloom" and around 1.5 times lower in a bloom (comparing mean concentrations). There does appear to be some discrepancy between the much lower emissions of monoterpenes than isoprene measured from monocultures and the observed air mixing ratios that seem to suggest source strengths of almost the same magnitude (or within one order of magnitude), given that their Henry's Law constants are similar (see section 4.2.2). During AMT 22, the relative levels of monoterpenes (without limonene) and isoprene in air varied between *ca.* 0.5 and 0.05 (typically 0.3-0.1), with the main influence being the detection limit, as ratios could change abruptly if one or more contributions fell to <DL and were therefore not counted in the ratio. Hence, while all datasets span large ranges and despite the overall linear relationships and mixing ratios being rather different, the analyte ratios for this cruise were in fact similar to the published data. Additional reports of surface water concentrations and water-derived fluxes, as the intermediate stages between emission by phytoplankton and atmospheric mixing ratios, could help to improve our understanding of the processes that could lead to the differences between apparent and measured (or field and laboratory) source strengths.

During this project, the ratio of total monoterpenes (without limonene) to isoprene in the surface water, and therefore similarly for the fluxes, was mostly 0.05-0.2 for AMT 22, decreased from *ca.* 0.7 to around 0.1 during AMT 23 (initial value of 1.0 with limonene included) and varied generally between >1 and 0.05 for ACCACIA 2. This large variability did not allow definite conclusions about the relative source strengths of the analytes, although it appeared that the ratios in water were closer to those in air than those reported from the culture studies. The species investigated in the laboratory are only a small subset of those encountered in the environment (albeit chosen as typical phytoplankton classes and species), and monocultures may not represent the entire biological community with respect to monoterpene emissions and losses, so that the question could now be whether additional processes produce monoterpenes in the water or the species present during the field campaigns were markedly different in their production rates from the laboratory cultures.

4.4 Conclusions

The datasets collected for this study have significantly increased the available field measurements of monoterpenes in marine air over a range of latitudes and have provided the first measurements reported to date of monoterpenes in the surface ocean. Typical concentrations (summarised in Table 4.2 and Figure 4.5) in North and South Atlantic waters were between below the detection limit (DL; sub-pmol L^{-1}) and 6 pmol L^{-1} for all monoterpenes, with mean values of around 0.5-1.3 pmol L^{-1}; an exception was limonene during AMT 22 at up to 84 pmol L^{-1} (mean 30 pmol L^{-1}; suspected contamination). Arctic seawater concentrations could only be obtained for α- and β- pinene, with a mean of 2-3 pmol L^{-1} (range <DL 5 pmol L^{-1}); no obvious explanation for this large difference to lower latitudes was found. Atmospheric mixing ratios were largely at or below the DL (sub-pptv) for AMT 22 and ACCACIA 2; all AMT 23 data was discarded due to suspected hydrocarbon contamination.

An estimate of sea-to-air fluxes for monoterpenes in the temperate and tropical Atlantic Ocean was derived based on the seawater data in this chapter, as well as for α- and β-pinene in the Arctic. These were of comparable magnitude for all compounds and cruises (see Figure 4.6). The sum of monoterpene fluxes (without limonene) was *ca.* 5-20 times lower than isoprene fluxes, largely due to the difference in seawater concentrations (all environmental parameters were the same for the different analytes). This is qualitatively consistent with the lower phytoplankton monoculture production rates for monoterpenes reported by Yassaa et al. (2008) and Meskhidze et al. (2015) compared to those published for isoprene (e.g. Shaw et al., 2003; Gantt et al., 2009; Bonsang et al., 2010; Exton et al., 2013).

Throughout this chapter, the large variability of monoterpenes in water and air has been a central theme, and comparisons with the available literature are difficult for that reason. While none of the monoterpene data collected during this project yielded any correlations with either biological activity or isoprene, it must be stressed that the overall concentrations and biological activity were low compared to other studies. Indeed, the atmospheric concentrations of total monoterpenes measured here are similar to "background" (out of bloom) data measured previously in the Southern Ocean (ranging from <DL (1-5 pptv) to 14 pptv for the sum of α-pinene enantiomers, with an average of 5 pptv). Our study

is unable to confirm or otherwise whether monoterpene levels are enhanced around highly bioactive regions of the ocean.

Nevertheless, based on large variability in atmospheric concentrations observed in different AMT cruises sampling similar waters, and evidence of elevated limonene from sample lines previously subject to a cleaning agent, we conclude that contamination is a major issue for monoterpenes, especially limonene, which can apparently add several to tens (for limonene) of ppt to the atmospheric abundance. Further, we find that even the low atmospheric mixing ratios (∼0.5 ppt) of α-pinene observed during AMT 22 could not be reconciled with the sea-air fluxes; in fact seawater concentrations would have to be around 2 orders of magnitude higher to explain the atmospheric abundances. In ACCACIA 2, much lower mixing ratios of around 0.03 ppt α-pinene were generally consistent with the observed seawater concentrations. This implies that, if a large surface ocean source of monoterpenes is the cause of elevated atmospheric abundances, in this and in previous studies, it does not appear to apply in Arctic waters. Contamination of atmospheric samples would be an alternative explanation for these results.

It is recommended that further fieldwork should be focused on measurements in seawater, ideally with gradient measurements near to the surface, to improve our understanding of the causes of the huge variability of these compounds and constrain global oceanic emission estimates, which has been previously attempted (Luo and Yu, 2010) based on only a single (atmospheric) dataset.

As already described in Chapter 2 and evident from the data presented in the current chapter, differences in experimental set-up or sampling conditions may affect measurements significantly, so that in addition to large error bars, there may be additional discrepancies that cannot be explained and could be either real variations in the samples or analytical artefacts, and further complicate comparisons with other studies. Careful method validation prior to deployment should always be combined with performance validation, and comparisons of different analytical or sampling procedures (e.g. underway *versus* CTD) during campaigns is highly recommended for any future fieldwork to minimise these effects as much as possible. A technique that is capable of speciating monoterpenes and concurrently measuring hydrocarbon contamination markers can greatly improve the reliability of a dataset compared to acquisition without such quality control measures.

The implications of the measured seawater and air concentrations for atmospheric chemistry in the remote marine boundary layer, impacts on aerosol formation and relative importance compared to isoprene emissions are discussed further in Chapter 5.

Chapter 5

Atmospheric impacts of marine isoprene and monoterpenes

This chapter explores the potential atmospheric impacts of marine isoprene and monoterpenes based on the new observations made during this project and existing knowledge of their atmospheric chemistry (formation of secondary organic aerosol via oxidation products). It investigates the trends of isoprene and monoterpenes in the remote marine boundary layer, assesses the relative importance of the compound groups in this environment and suggests some conclusions that may be drawn from the current data.

5.1 Introduction

One of the main aims of this project was to establish whether new measurements of isoprene and monoterpenes in the marine environment would agree with and support recent reports of the abundance of these compounds in the marine boundary layer and their importance for global atmospheric chemistry and climate (e.g. Meskhidze and Nenes, 2006; Gantt et al., 2009; Shaw et al., 2010 and references therein). Observations of marine isoprene made over the last 25 years and of monoterpenes over the last decade (see Chapter 3 3.1) have shown that there may be reasons to challenge the assumption that emissions from the marine environment are insignificant compared to those of terrestrial origin. While the marine source of these biogenic volatile organic compounds (BVOCs) is indeed small with respect to the global source (estimates for isoprene are 0.1-10 Tg C yr^{-1} (Shaw et al., 2010) and ~600 Tg C yr^{-1} (Guenther et al., 2006), respectively), emissions generally occur in remote locations with low aerosol loadings compared to terrestrial environments.

Arnold et al. (2009) reported that modelled isoprene secondary organic aerosol (SOA) contributed a maximum of 1-2 % to the total oceanic organic carbon loading (OC; based on a global modelled marine OC source from Spracklen et al. (2008)) in three remote locations, with lower relative contributions in summer when the Chl-*a*-dependent OC emissions were higher. Myriokefalitakis et al. (2010) similarly concluded that the sum of isoprene- and monoterpene-derived SOA only contributed around 2 % to the global marine SOA abundance. In contrast, Gantt et al. (2009) assessed the contribution of isoprene-derived SOA to total OC in the marine atmosphere using modelled emissions of isoprene and primary organic matter and found that, whilst only a minor proportion of global marine OC was derived from isoprene, isoprene did in fact contribute significantly to the sub-micron fraction of OC aerosol (which is particularly relevant for cloud formation). The contribution was especially high in the tropics (up to 30 %) and at mid-day (almost 50 %), implying that marine isoprene SOA could potentially have a significant impact on CCN (cloud condensation nuclei) activation properties of marine aerosol through its influence on the sub-micron OC aerosol loading under certain conditions. The authors also suggest that global models may need to include isoprene emissions at 1-hour temporal resolution in order to correctly represent the diurnal cycle of the effects of marine isoprene SOA.

5.2 Comparisons

5.2.1 Cruise and CVAO data

The Cape Verde Atmospheric Observatory (CVAO; www.ncas.ac.uk/index.php/en/cvao-home) is a WMO/Global Atmospheric Watch (GAW) site that provides a number of long-term measurements of trace gases and aerosols in the marine environment. The observatory is situated on the north eastern coast of the island of São Vicente (16.9 °N, 24.9 °W), providing data representative of the open ocean, as it is generally under the influence of remote marine air and has no major coastal shallows or large seaweed beds (e.g. Carpenter et al., 2010). As part of the ORC^3 project, two intensive operating periods in June/July and August/September 2014 took place at the observatory to measure speciated monoterpenes and glyoxal in addition to the long-term data (which includes isoprene) and several other parameters. The ORC^3 project is a collaboration between the Universities of Leeds and York that aims to improve our understanding of the sources and fate of marine OC aerosol precursors, specifically isoprene, monoterpenes and glyoxal (see section 5.3.2), through a combination of new measurements and global modelling approaches (Arnold et al., 2013). The current study contributes to the larger project by providing observational data for isoprene and monoterpenes.

A comparison of the atmospheric concentrations of these analytes shows that the shipboard measurements (AMT 22) and long-term/ORC^3 CVAO data are of the same order, at around 0-5 pptv typical isoprene mixing ratios at CVAO in October/November (S. Punjabi, pers. comm.) and sub-pptv levels of monoterpenes during August 2014 (data summarised in Table 4.2 (Chapter 4)).

5.2.2 Isoprene fluxes diurnal cycle

A number of studies to date have observed diurnal trends in atmospheric isoprene (Lewis et al., 2001; Matsunaga et al., 2002; Liakakou et al., 2007; Sinha et al., 2007; Lawson et al., 2011), ranging from a simple night/day difference based on a few samples (Matsunaga et al. 2002) to diurnal cycles with a peak around solar noon or early afternoon (Lewis et al., 2001; Liakakou et al., 2007; CVAO (unpublished data); Lawson et al., 2011). This trend

is perhaps unsurprising given the reported light and temperature sensitivity of isoprene production in laboratory studies (Shaw et al., 2003; Gantt et al., 2009; Bonsang et al., 2010; Exton et al., 2013; Meskhidze et al., 2015), with phytoplankton cultures emitting higher levels of isoprene when exposed to elevated light and/or temperature, similarly to terrestrial vegetation (Sharkey et al., 2008). However, it must also be taken into consideration that loss rates (mainly atmospheric, but also potentially in the water column) are higher for those conditions, primarily due to the diurnal cycle of the OH radical, the major oxidant of isoprene in the atmosphere (see Chapter 1 section 1.3 for details). Consequently, emissions during the day must be proportionally higher if a daytime maximum can be observed.

Atmospheric mixing ratios and seawater-derived fluxes (see Chapter 3 section 3.2.3) of isoprene during AMT 22 were investigated for diurnal variations by binning the data hourly, having corrected the sampling time for longitude to obtain comparable local times (adding 4 minutes per degree longitude (positive °E)). No clear trend could be seen in the binned data for mean or median values (Figure 5.1a, shown with standard error on the mean values). The atmospheric data was used to estimate hourly sea-to-air fluxes in a top-down approach by calculating hourly atmospheric loss rates and deriving the total emissions needed to sustain the observed mixing ratios (i.e. steady-state conditions).

Loss rates for reactions with OH and O_3 were included in addition to the observed change in isoprene concentration ($d([isp])/dt$; temporally smoothed to reduce the effect of random variation):

$$\text{total production } P \text{ (molec cm}^{-3}\text{ s}^{-1}\text{)} = \frac{d([isp])}{dt} + \text{loss}_{(isp+OH)} + \text{loss}_{(isp+O_3)} \quad (5.1)$$

$$\text{total flux (molec cm}^{-2}\text{ s}^{-1}\text{)} = P \times H_{BL} \quad (5.2)$$

where H_{BL} is the boundary layer (BL) height in cm (using H_{BL} = 1000 m in the initial calculations, see section 5.2.3.2) and $\text{loss}_{(isp+X)} = k_X \times [isp] \times [X]$, using reaction rates k_X from Atkinson et al. (2006) and atmospheric concentrations of O_3 and OH typical of the MBL around CVAO (Carpenter et al., 2010; Vaughan et al., 2012) which were taken to be representative of the remote marine atmosphere:

- $k_{OH} = 1.00\times10^{-10}$ cm^3 molec^{-1} s^{-1}
  and [OH] = 0 - 4.4×10^6 molec cm^{-3} (diurnal cycle, from graph)

– $k_{O_3} = 1.27\times10^{-11}$ cm^3 molec^{-1} s^{-1}
and $[O_3] = 6.25\times10^{11}$ molec cm^{-3} (25 ppbv)

Standard errors for the fluxes were calculated by substituting the standard error of the isoprene atmospheric concentrations for [isp] in equations 5.1 and 5.2, but using simply the error (not change in error) in the place of $d([isp])/dt$.

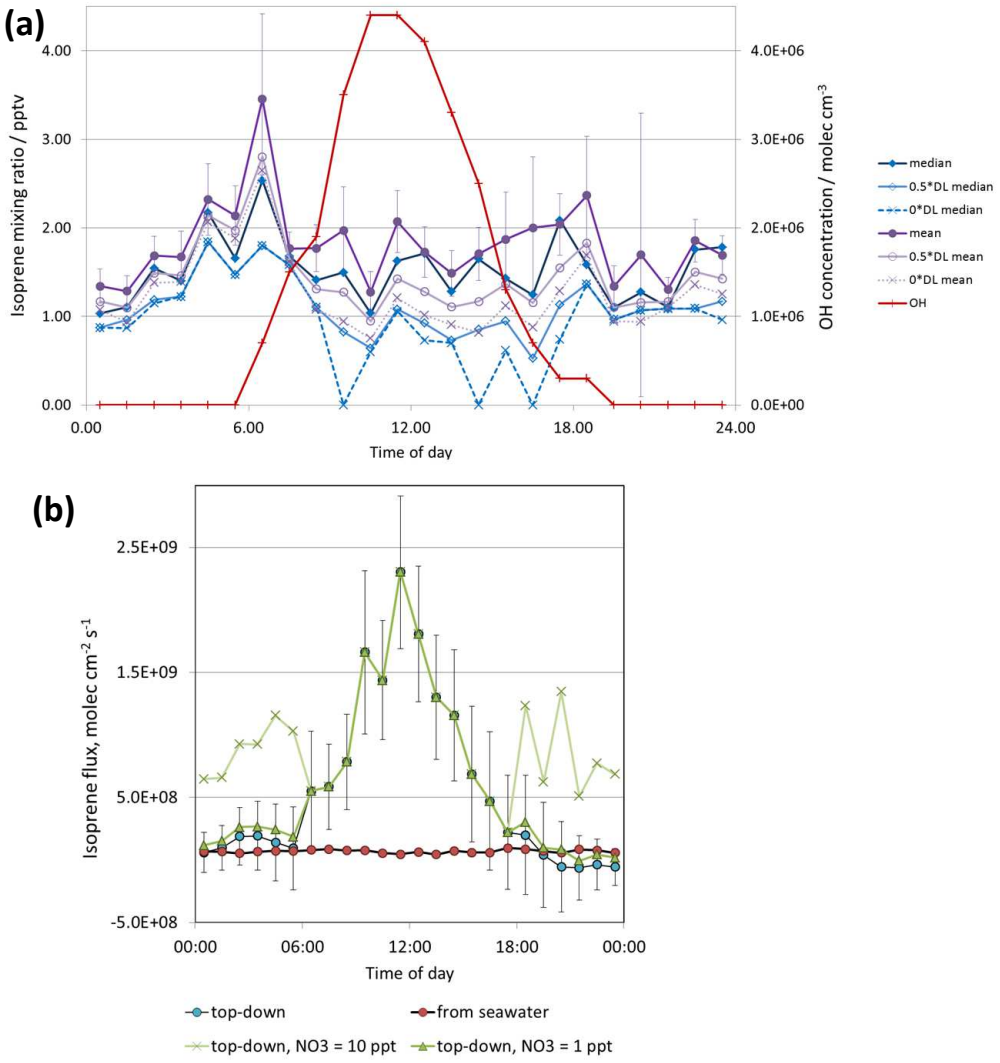

Figure 5.1 – (a) Diurnal variation of mean and median mixing ratios of isoprene in air (AMT 22), including calculations using 0.5×DL or zero for values <DL, with standard error shown for average >DL only (for clarity); also shown is [OH], the main driver of the observed diurnal cycle in top-down estimates; (b) top-down and bottom-up flux estimates for AMT 22 data, with standard error (based only on isoprene errors).

Figure 5.1b shows that the top-down and bottom-up flux estimates agree within an order of magnitude (mean value for top-down fluxes is *ca.* 5 times higher than bottom-up fluxes), but also that there is a pronounced diurnal cycle in the top-down values, which is driven by the diurnal cycle in [OH], while no trend is apparent in the seawater-derived (bottom-up) fluxes. For hourly data, the top-down values can be a factor of 2 lower at night-time and up to a factor of 50 higher during daytime than the bottom-up fluxes. Some top-down estimates fall below zero at night (due to negative $d([isp])/dt$), suggesting an air-to-sea flux of isoprene, but these are highly unlikely to be realistic numbers given the general supersaturation of the seawater with respect to the atmosphere (see Chapter 3 section 3.2.3.2) and the consistent positive seawater-derived flux; this assessment is supported by the large uncertainty associated with the averaged data – the standard error still includes above-zero values within its range.

In general, the observed discrepancies point to potentially an atmospheric loss process during the night (which would also explain the apparent negative top-down flux estimates; see section 5.2.3.1) and more importantly a large missing source of isoprene during the day that cannot be explained by fluxes driven by the bulk seawater concentrations. Recent research into processes in the sea surface microlayer (SML) has shown that it could be a source of photochemically produced functionalised and unsaturated VOCs to the atmosphere, including isoprene (Ciuraru et al., 2015a; Fu et al., 2015; Ciuraru et al., 2015b). The most recent studies investigated chemical mechanisms in laboratory simulations of these processes with artificial seawater containing a photosensitiser and a proxy or real SML sample forming the microlayer. They also quantified isoprene emissions in their experiments and extrapolated them to environmental conditions (Ciuraru et al., 2015b), showing that the actual magnitude of isoprene production in the SML in combination with the extensive presence of a SML across all oceans (Wurl et al., 2011) makes this a likely suggestion as an additional daytime source. In addition, the authors propose that these or similar reactions may take place on the surface of aerosols since sea spray aerosols generated by bubble bursting are expected to exhibit comparable characteristics to the SML (Ciuraru et al., 2015b), which would increase the magnitude of this potential additional source.

5.2.3 Sensitivity studies

5.2.3.1 NO_3

A sensitivity analysis was performed to establish the effects of night-time reaction of isoprene with the nitrate radical in equation 5.1 – the mixing ratios of NO_3 are very low in the remote MBL (e.g. 1-7 pptv observed in clean marine air by Allan et al. (2000)), so that the reaction was initially assumed to be a negligible loss term despite the fast reaction rate. However, there does appear to be a missing atmospheric loss process for the top-down estimates compared to the bottom-up values (Figure 5.1), and an additional loss term could also bring the unrealistic negative top-down estimates into a positive range. The results of the investigation using

– $k_{NO_3} = 7.0\times10^{-13}$ cm^3 molec^{-1} s^{-1}
and [NO_3] = 2.5×10^7 and 2.5×10^8 molec cm^{-3} (1 pptv and 10 pptv, respectively (night-time only))

show that the effects of NO_3 chemistry are minor at the lower concentration used for NO_3, but should be considered in locations with higher [NO_3] such as more polluted coastal environments (see Figure 5.1b).

5.2.3.2 Marine boundary layer (MBL) height

In the present calculations, a MBL height of 1000 m was used as representative of most of the Atlantic Ocean. Matsunaga et al. (2002) pointed out that it would be more reasonable to use 50-100 m as the height to which isoprene is well mixed rather than the entire BL height, given its short atmospheric lifetime compared to the time needed for mixing. The total flux calculated from equation 5.2 is directly proportional to MBL height, so that reducing H_{BL} by a factor of 10-20 would also reduce the flux by the same factor and bring the daytime top-down fluxes within a comparable range to the bottom-up values. However, while the conventional approach of assuming a constant concentration throughout the MBL is not applicable to isoprene and monoterpenes due to the very similar timescales of mixing and loss reactions, a simple reduction in H_{BL} in the calculation neglects the fact that the actual MBL height and vertical mixing within it are unchanged. A more refined

approach would be needed in order to allow for vertical mixing in addition to reactive losses, to determine a more realistic flux.

5.2.3.3 Modelled oxidant concentrations

Instead of taking oxidant mixing ratios from the literature, the top-down flux estimate was calculated using model output along the AMT 22 cruise track (OH, O_3 and NO_3, treated in the same way as the isoprene data; GEOS-Chem v9.2 (4x5° resolution, Sherwen et al., 2015), provided by T. Sherwen). The results compared well, implying that the binned model data agreed well with the literature values used for the entire Atlantic transect and that whole-cruise average model output could be a valid alternative if literature values are not available.

5.2.4 Monoterpene fluxes diurnal cycle

Monoterpene fluxes were not explored in the same way as isoprene due to the smaller number of datapoints above the detection limit that could be averaged diurnally to provide meaningful trends. Additionally, as discussed in Chapter 4, air samples are subject to large uncertainties from potential contamination in the air, and fitting top-down fluxes to potentially overestimated concentrations cannot provide useful results with respect to constraining monoterpene sea-to-air fluxes. Figure 5.2 shows α-pinene flux estimates as an example of the large discrepancy between seawater-derived and top-down fluxes (up to two orders of magnitude) which is most likely due to over-predicted fluxes using the top-down method. However, the air concentrations (AMT 22) used in these calculations were filtered carefully and although contamination cannot be fully ruled out, it is assumed to only contribute little to the measured terpene mixing ratios (unlike AMT 23, see Chapter 4). Although a comparison to ACCACIA 2 data indicates that even potential low-level contamination may result in large overpredictions (Chapter 4 section 4.3.1), these top-down fluxes are the best estimate using currently available information, which suggests that additional investigations into the basis for the difference compared to bottom-up fluxes are needed.

It is nevertheless worth noting that at an assumed [NO_3] of 1 pptv, due to the fast reaction rate, oxidation by the nitrate radical at night is responsible for a substantial proportion (up

to 80 % for α-pinene) of the predicted atmospheric losses, unlike for isoprene. Lifetimes with respect to oxidant concentrations relevant to remote environments are of the same order for all three oxidants for myrcene and ocimene and still similar (within a factor of 2-3) for α-pinene and limonene; also similar for reactions with OH and NO_3 for β-pinene and carene (but slower with O_3). As a consequence, mid-day atmospheric losses (when OH peak concentrations are around twice those used for the mean lifetime calculation) are only expected to increase by approximately a factor of two compared to night-time, and the absolute SOA yield at any point during a diurnal cycle will be determined to a large extent by the yields of each monoterpene with respect to each oxidant, which are highly uncertain (Table 5.2). For example, taking the values displayed in Table 5.2, α-pinene-derived total SOA yield would be expected to decrease at night owing to its much lower yield from oxidation by NO_3 compared to OH, while no large variations over time would be predicted for β-pinene.

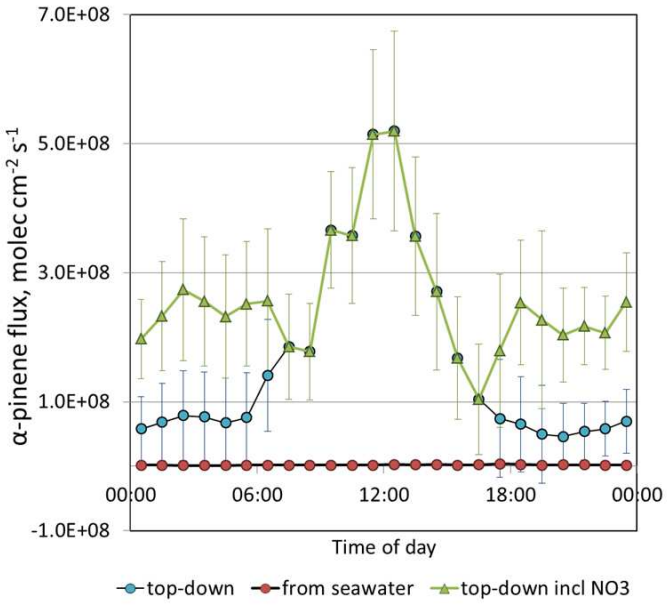

Figure 5.2 – Top-down and bottom-up flux estimates for α-pinene for AMT 22 data, using (a) H_{BL} = 1000 m.

5.2.5 Global top-down versus bottom-up emission estimates

In addition to the discrepancy between diurnal trends of fluxes estimated in two different ways, there is a large difference between global fluxes derived using these two approaches.

Bottom-up estimates typically take production rates relative to Chl-*a* reported from laboratory studies (which are inherently variable) and scale them up to a global production using satellite Chl-*a* retrievals (see also Chapter 3 section 3.1). The algorithm can also be refined by including phytoplankton functional types (PFTs) from ocean colour satellite data and PFT-specific production rates from culture studies (as in Gantt et al., 2009; Arnold et al., 2009), and may include further parameters such as light-dependence of the production (Gantt et al., 2009), or by including assumed (minor) oceanic loss terms (Palmer and Shaw, 2005; Arnold et al., 2009; main loss term is sea-air gas exchange).

Top-down estimates aim to scale emissions so that the bias of the modelled atmospheric mixing ratios compared to observed values is minimised, accounting for atmospheric losses to oxidation within the model (represented in a simplified approach by the calculations in section 5.2.2). Published top-down estimates tend to be around an order of magnitude higher than bottom-up emissions (summarised in Table 5.1), suggesting that an additional source of isoprene to the MBL is needed to reconcile these differences. As discussed in section 5.2.2 above, the SML as a source of photochemically produced isoprene could help close the gap. However, similarly to the monoterpenes, atmospheric isoprene measurements in clean environments are easily affected by contamination/pollution and the observations to which the top-down estimates are scaled may be overestimating the actual mixing ratios. Most studies report the majority of their measurements as near or below the detection limit, typically in the low pptv range. However, since population means are not very robust to outliers, a few high points that could even be from marine biogenic emissions (e.g. with an *in-situ* bloom) will increase the top-down emission values disproportionately if mean values are used, and detailed results are sometimes not published if no "interesting" events were observed (e.g. Williams et al., 2010; N. Yassaa, pers. comm. regarding data collected during the second leg of the shipboard campaign described in Yassaa et al., 2008), resulting in a potentially skewed of existing observations. Only very few studies report median values at all and it appears that none report a median (or mean) that accounts for data below the detection limit. Table 4.2 in Chapter 4 shows that for analytes such as monoterpenes that were often not detected, the number of datapoints increases substantially if values below the detection limit are included, with the mean and median values decreasing. While no absolute value can be calculated, a range of possible concentrations can be estimated based on the detection limit (in this case, 0.5×DL was used for values <DL, giving a mid-range estimate of the actual value).

The field studies chosen as representative of the whole ocean will also strongly affect flux estimates (e.g. Luo and Yu, 2010), as will the parameters for the bottom-up estimates from culture studies, which can vary widely between studies (e.g. Shaw et al., 2003; Gantt et al., 2009; Bonsang et al., 2010; see Table 3.4 in Chapter 3 for the range of reported isoprene-Chl-*a* relationships).

Table 5.1 – Published bottom-up and top-down estimates of global fluxes to date (isoprene unless specified).

Reference	Bottom-up / Tg C yr^{-1}	Top-down / Tg C yr^{-1}	Production rates reference / notes
Palmer and Shaw (2005)	0.12	-	Shaw et al. (2003)
Ito and Kawamiya (2010)	0.1	-	Broadgate et al. (1997) (isoprene/Chl-*a* relationship)
Arnold et al. (2009)	0.27	1.68	Bonsang et al. (2010)
Gantt et al. (2009)	0.31-1.09 (mean 0.92)	-	Own data and Shaw et al. (2003)
Luo and Yu (2010)	0.31	11.6	Arnold et al. (2009)
Myriokefalitakis et al. (2010)	1.1	-	Arnold et al. (2009) (not explicitly stated; no PFT dependence)
Luo and Yu (2010) (α-pinene)	0.013	29.5	Yassaa et al. (2008)
Myriokefalitakis et al. (2010) (monoterpenes)	0.2	-	Yassaa et al. (2008) (mid-range value compared to isoprene)
in-situ measurements scaled to ocean surface area			
Bonsang et al. (1992)	1.4	-	Scaled to global flux of ethanol using rel. water conc.s of isoprene and ethanol
Sinha et al. (2007)	1.4	-	mesocosm
Milne et al. (1995)	0.08-0.9		(calculated by Sinha et al., 2007; explicitly not attempted by authors themselves)
Broadgate et al. (1997)	0.22	-	coastal (calculated by Sinha et al., 2007)
Baker et al. (2000)	0.1-0.7		(calculated by Sinha et al., 2007)
Matsunaga et al. (2002)	0.26-2.7		(calculated by Sinha et al., 2007)

Both Arnold et al. (2009) and Luo and Yu (2010) suggest that the offset between the bottom-up and top-down estimates may be in part due to a lack of understanding of the phytoplankton communities *in situ* that may exhibit different emission potentials to the laboratory monocultures (e.g. different production rates during different growth phases), and to the uncertainties in the top-down approach (including the atmospheric observations and the potentially inadequate representation of sub-grid processes in models). Seawater-

based emissions could be considered an "intermediate step" since they avoid the uncertainty regarding *in-situ* production rates compared to laboratory measurements; however they still cannot account for much of the global variation in emission strength of different biological communities unless the studies sampled large extents and/or representative regions of the worlds oceans. For isoprene, this "intermediate step" has given some confidence in the model estimates based on laboratory results by agreeing in overall magnitude (see summary table in Shaw et al., 2010) – although as discussed above (section 5.2.2), a missing surface source is potentially still needed explain the top-down flux estimates. No global estimate has yet been made for monoterpenes using seawater-derived fluxes since no water measurements have been published so far. Such a bottom-up estimate for monoterpenes may help to constrain global fluxes more tightly than possible with the currently available literature data (air only).

An extrapolation of the field measurements from this project was attempted based on the *very* rough approximation that a median value of seawater-derived fluxes for AMT 22 could be seen as sufficiently representative of the global oceans (similarly to Sinha et al., 2007). This is obviously not the case; despite covering much of the Atlantic Ocean, the fact that this cruise did not sample any polar waters or much of any highly productive area is only one of the flaws in this assumption. On this basis, the fluxes can however simply be scaled globally by ocean surface area, yielding 0.03 Tg C yr^{-1} α-pinene emissions. Global isoprene emissions calculated in the same way give 0.6 Tg C yr^{-1}, which is in fact of a comparable magnitude of published estimates (see Table 5.1). SImilarly, the result for α-pinene is close to the only published global estimate by a bottom-up method (Luo and Yu, 2010), which was obtained using laboratory-derived phytoplankton functional type-specific production rates (from Yassaa et al., 2008) scaled by satellite Chl-a and climatological ocean mixed layer depth. The apparent agreement can nevertheless not be taken as a confirmation of the accuracy of either value, given the unlikely assumptions used to obtain it. It could perhaps be seen as an indication that the real source strength is likely closer to the bottom-up than the top-down estimate proposed by Luo and Yu, 2010).

A more refined approach to scale *in-situ* to global emissions using a proxy is not possible from the current dataset since no correlation with Chl-a was found for monoterpenes (or any other investigated parameter; see Chapter 4). A slightly improved estimate might be

obtained by assuming constant surface water concentrations everywhere (still a substantial approximation) and including some parameterisation for wind speed to calculate fluxes globally, similarly to the "constant source" fluxes described in Chapter 4 section 4.2.2.

5.3 Atmospheric impacts

5.3.1 Oxidative capacity of the atmosphere

The relevance of the measured isoprene and monoterpenes to atmospheric chemistry and, ultimately, climate, depends on their fate once they have been emitted from the ocean. As already discussed in section 5.2.2 (and Chapter 1 section 1.3), terpenes are oxidised mainly by the OH radical and O_3 during the day and by the NO_3 radical and O_3 at night. Therefore, if present in large enough concentrations, they can significantly affect the concentrations of oxidants in the atmosphere; e.g. Liakakou et al. (2007) reported up to 25 % decrease in night-time NO_3 and in daytime OH, but up to 25 % increase in night-time OH due to (marine) isoprene of up to 300 pptv during a seasonal study on Crete, Greece. For low levels of isoprene (<10 pptv) such as those observed during this project, the impact on OH concentrations is negligible, as shown by Lewis et al. (2001).

Table 5.2 – Reaction rates and lifetimes of isoprene and monoterpenes with respect to OH, O_3 and NO_3.

BVOC	Rate constant for reaction with... / cm^3 $molec^{-1}$ s^{-1} [a,c,e]			lifetime for reaction with ...[a]			SOA mass yield[c] / %		
	OH	O_3	NO_3	OH	O_3	NO_3[f]	photooxidation	ozonolysis[b]	oxidation by NO_3
isoprene	1.0×10^{-10} [e]	1.3×10^{-17}	7.0×10^{-13} [e]	1.4 h	1.3 day	1.6 h	2	1[i]	4-24[m]
									2-14[l]
α-pinene	5.3×10^{-11} [e]	9.0×10^{-17} [e]	6.2×10^{-12} [e]	2.6 h	4.6 h	11 min	32	41	0[n]
							38-46[d]	8-29[g]	4-16[o]
								3-18[j]	
β-pinene	7.7×10^{-11}	1.5×10^{-17}	2.5×10^{-12}	1.8 h	1.1 day	27 min	31	17	33-44[n]
								32[k]	
myrcene	2.1×10^{-10}	4.7×10^{-16}	1.1×10^{-11}	39 min	50 min	6 min	43	11	n.a.
3-carene	8.7×10^{-11}	3.7×10^{-17}	9.5×10^{-12}	1.6 h	11 h	7 min	38	54	38-65[n]
							23[k]	76[k]	
ocimene	2.5×10^{-10}	5.4×10^{-16}	2.2×10^{-11}	33 min	44 min	3 min	5.5[k]	17[k]	n.a.
limonene	1.7×10^{-10}	2.1×10^{-16}	1.3×10^{-11}	49 min	2.0 h	5 min	58	20-70[h]	20-40[o]
							36-40[k]		

"n.a." = not available; low-NOx defined by Zhang et al. (2006) as ≥10 HC:NOx ppbC:ppb.

[a] Data from Atkinson and Arey (2003), assuming [OH] = 2.0×10^6 molec cm^{-3} (12-h daytime average); [O_3] = 7×10^{11} molec cm^{-3} (24-h average); [NO_3] = 2.5×10^8 molec cm^{-3} (12-h nighttime average); [b] dark ozonolysis unless specified; [c] Lee et al. (2006a,b) (low-NOx), unless stated; [d] Ng et al. (2007) (low-NOx); [e] Atkinson et al. (2006); [f] if NO_3 = 1 pptv is assumed, lifetimes increase by a factor of 10; [g] Presto et al. (2005b), zero-NOx, not including constant 3 % reduction for effect of light; [h] Zhang et al. (2006) (atmospherically relevant concentration, low-NOx; from graph of basis-set fit); [i] Kleindienst et al. (2007); [j] Pathak et al. (2007) (atmospherically relevant concentrations; from graph); [k] Hoffmann et al. (1997) (low/medium-NOx); [l] Rollins et al. (2009); [m] Ng et al. (2008); [n] Fry et al. (2014); [o] Spittler et al. (2006).

5.3.2 SOA formation and oxidation products: glyoxal

Another impact of isoprene and terpenes on the atmosphere is through their oxidation products via the reactions with OH, O_3 and NO_3 that lead to the formation of SOA (reaction rates and lifetimes listed in Table 5.2). As detailed in Chapter 1, SOA in the marine atmosphere plays an important role in global climate through its influence on the properties of shallow marine clouds by affecting the number and composition of cloud condensation nuclei. Isoprene has recently been recognised as a source of SOA, at *ca.* 2 % mass yield for photooxidation (Lee et al., 2006b) despite the relatively high volatility of its first-generation oxidation products such as methacrolein, methyl vinyl ketone and formaldehyde, since multi-step processes can result in low- or semi-volatile compounds that can partition onto aerosol (Carlton et al., 2009). Examples of these second- or later-generation compounds include glyoxal (CHOCHO) and methylglyoxal (CH_3CHO) which are highly water-soluble (Henry's Law constants of 10^3-10^5 and around 10^2 mol m^{-3} Pa^{-1}, respectively; 5 to 10 orders of magnitude higher than isoprene (Sander, 2015)), highly reactive α-dicarbonyls (structures shown in Figure 5.3). The combined second- and third-generation molar yields for glyoxal and methylglyoxal from isoprene are 6.2 and 25 %, respectively, and 2.8 and 4.2 % respectively from monoterpenes (Fu et al., 2008). Globally, the largest single precursor of both dicarbonyls is isoprene due to its large terrestrial biogenic source: for example, Fu et al. (2008) determined that 47 % of glyoxal and 79 % of methylglyoxal are isoprene-derived, while acetylene (mostly anthropogenic) and acetone (mostly biogenic), the second most important precursors to glyoxal and methylglyoxal, respectively, contribute substantially less. A variety of further VOCs including monoterpenes and aromatics were identified as only minor sources. Nevertheless, as both acetylene and acetone are long-lived VOCs (global lifetime around 20 days), they act as dicarbonyl sources in the free troposphere or remote locations (providing around 1 pptv background, Fu et al., 2008).

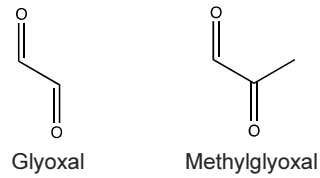

Figure 5.3 – Structures of glyoxal and methylglyoxal.

In the marine environment, glyoxal and methylglyoxal have been the focus of recent research as they are in turn believed to be precursors to SOA via the formation of low-volatility products in the aqueous phase (mainly in clouds; see Fu et al., 2008; Carlton et al., 2009 and references therein); however measurements above the ocean are scarce and their oceanic source is still poorly understood. They have recently been observed by satellite retrievals (e.g. Chan Miller et al., 2014) and by a number of field campaigns (e.g. Sinreich et al., 2010; Mahajan et al., 2014; Lawson et al., 2015) and attributed to local marine sources due to the remoteness of the measurement locations. However, the magnitude of the observations could not be explained by known precursors; e.g. Sinreich et al. (2010) measured over 100 pptv glyoxal during a study in the tropical Pacific Ocean, but calculated that the isoprene mixing ratio needed to produce that amount of glyoxal would be around 600 pptv – highly unlikely given the low isoprene measurements (note however that less isoprene would be needed if in combination with high levels of other glyoxal precursors). A more recent publication summarising glyoxal and methyl glyoxal measurements from a number of field campaigns (Mahajan et al., 2014) reported a lower mean mixing ratio of glyoxal, which would however still require unrealistic amounts of isoprene (150 pptv) or other precursors in order to explain the observations.

Monoterpenes have been suggested as at least a part of the obviously missing oceanic source, based on the fact that they are glyoxal precursors and not many oceanic observations exist to constrain them. The two published reports (Yassaa et al., 2008; Colomb et al., 2009) appeared to support a potentially significant oceanic monoterpene (and hence glyoxal) source (Lawson et al., 2015; Arnold et al., 2013). A recent study in the West Pacific measured isoprene and monoterpenes as supporting data to glyoxal and methylglyoxal samples (Lawson et al., 2015) and came to the conclusion that these BVOCs could not account for the observed concentrations of the dicarbonyls, despite the fact that their isoprene and monoterpene data was high (14 and 32 pptv, respectively, measured by PTR-MS) compared to this project (likely due to the study location being a highly productive area that could potentially support such large mixing ratios).

The sea surface microlayer (SML) has been proposed as an additional source of glyoxal and methylglyoxal based on slight correlations of concentrations of the two compounds in aerosol and SML samples and a “hint” at their photochemical formation from precursors in the SML, where they were enriched in concentration compared to the bulk seawater

(van Pinxteren and Herrmann, 2013).

5.4 Conclusions: SOA formation potential

While the isoprene SOA yield of 2 % may appear very small (Table 5.2), it has been shown to significantly impact SOA concentrations in model simulations when it was included, however with very large uncertainties regarding the magnitude of this impact (ranging from 27 % to up to 78 % of the total SOA globally, and influencing the yields of other SOA precursors; see Carlton et al., 2009, and references therein). This importance is predominantly due to the large global source of isoprene and does not necessarily translate to the marine environment where the total amount of isoprene-derived SOA remains low based on the small magnitude of oceanic emissions, estimated at around a few percent of oceanic OC (Arnold et al., 2009; Gantt et al., 2009).

5.4.1 Diurnal variations

For isoprene, the argument for a larger impact on CCN around mid-day (Gantt et al., 2009) is based on an assumed mid-day emission maximum that coincides with maximum oxidation rates (as reaction with OH is the dominant loss term). This would yield higher concentrations of SOA that could then lead to an increase in CCN numbers at the time of day with the highest irradiation when an increased cloud albedo would have the largest effect. While the results of the current study for seawater-derived fluxes, i.e. the missing mid-day maximum in isoprene emissions, call into question this enhanced impact at mid-day, the top-down flux estimates and/or additional abiotic production in the SML could still support its existence. The processes involved in SOA formation and dependence on environmental parameters are far too complex to be able to conclude how the diurnal profile would appear as a result of a less temporally variable flux; for instance, the presence of night-time isoprene emissions not included in the model would not necessarily increase the amount of isoprene-derived SOA at night compared to the model output, due to the much lower reaction rates compared to daytime oxidation by OH.

The presence of monoterpenes in the marine environment, alongside isoprene, shifts this picture of potentially higher day-time production of SOA into one of relatively constant

SOA concentrations (depending on relative SOA yields, as mentioned above) during a diurnal cycle, because of the rapid reaction of monoterpenes with the NO_3 radical. Thus, the diurnal variation in atmospheric monoterpene oxidation to SOA products is small compared to isoprene. Substantial uncertainties remain in this picture, because of the lack of determinations of SOA yields under atmospherically relevant conditions (or even any values at all for some of the currently uncharacterised monoterpene oxidation reactions) or from additional marine monoterpene sources such as the SML.

The effects of the boundary layer height on predicted diurnal flux profiles should be considered as part of further investigations for both isoprene and monoterpenes.

Recent research has shown that isoprene SOA yield may be significantly increased (up to almost 30 %) in the presence of acidic aerosol (Surratt et al., 2010), but since the exact dependence has not been established so far, the relevance of these results for the marine atmosphere cannot be known.

5.4.2 Relative importance of isoprene and monoterpenes

Monoterpenes have much higher SOA yields than isoprene for both ozonolysis and photooxidation, up to around 30-50 % (even some up to >75 %; see Table 5.2). The comparable lifetimes with respect to OH and O_3 for myrcene and ocimene, and to a lesser extent for α-pinene and limonene, imply that both loss processes are of similar importance during the day (as discussed in section 5.2.4); however when OH concentrations are at their maximum at mid-day, photooxidation still dominates as a loss process. Assuming an approximate SOA yield of 30 % (a lower estimate in many cases) and taking into account that aerosol yields are given as mass yields (i.e. only half the molar emission of monoterpenes compared to that of isoprene is required to achieve the same SOA mass), in order to be of a comparable significance to isoprene SOA (at 2-3 % yield), molar monoterpene emissions would only need to be around 3-5 % of those of isoprene (a factor of 20-30 lower). When the sum of all studied monoterpenes is considered, the total emissions (seawater-derived) are around 5-10 % of those for isoprene, i.e. of an order that may allow up to twice the amount of SOA formation relative to isoprene.

This result is perhaps surprising given the previous discussions of low water and air concentrations and fluxes of the monoterpenes, but their large potential to form SOA has been

noted in many studies (e.g. Johnson and Marston, 2008) and even at these much lower concentrations compared to previous studies (Yassaa et al., 2008; Colomb et al., 2009), the impact on marine SOA concentrations may be larger than that of isoprene. However, it must also be taken into account that published SOA mass yields vary greatly and are highly uncertain in terms of their applicability to pristine remote conditions or indeed generally to the real atmosphere, which is a complex mixture of compounds. Variations even between chamber studies have been seen for differences e.g. in VOC and oxidant concentrations, seed aerosol used (concentration and acidity), relative humidity, temperature, light and NO_x levels (or more precisely NO:NO_2 ratio) (Presto et al., 2005b,a; Pathak et al., 2007; Surratt et al., 2010; Lee et al., 2006b,a; Fry et al., 2014; reviewed generally by Hallquist et al., 2009; for isoprene by Carlton et al., 2009). Furthermore, it is obvious that treating all monoterpenes the same in a sum does not reflect their different lifetimes and yields with respect to oxidation and hence potential atmospheric impact.

Finally, it should be considered that the estimated amount of isoprene SOA was deemed negligible in the context of total marine OC (Arnold et al., 2009; Gantt et al., 2009); therefore even twice as much will still be a negligible amount. Conversely, monoterpene oxidation products have been suggested to play a role in aerosol nucleation (Laaksonen et al., 2008; Metzger et al., 2010; Kulmala et al., 2013; Riccobono et al., 2014), even if the absolute amount of SOA formed otherwise would be small, so that the role of these compounds in the remote marine boundary layer remains uncertain and potentially still significant.

Chapter 6

Summary and future perspectives

6.1 Summary of results

The importance of oceanic emissions of isoprene to global climate have been a matter of debate since they were first reported over two decades ago, and marine monoterpenes were added to this discussion following their first observations in 2008. Their proposed influence derives from the high reactivity of these species and their ability to form secondary organic aerosol (SOA), which may then affect the microphysical properties of shallow marine clouds (specifically their albedo and therefore their climate cooling effect) by modifying the number and characteristics of cloud condensation nuclei, as described in Chapter 1. However, establishing the relative importance of this mechanism for climate is largely dependent on reliable estimates of the magnitude of the actual global emissions and their distribution, in combination with a better understanding of their SOA formation potential. Both rely at least in part on model algorithms for marine volatile terpenoid fluxes which are in turn informed by observational datasets that can provide a basis for extrapolation.

As discussed in Chapter 5, the emerging consensus is that the global marine source of isoprene and monoterpenes is in fact small to negligible compared to terrestrial emissions and even to other ocean-derived organic reactive compounds (e.g. O'Dowd and de Leeuw, 2007; Arnold et al., 2009; Gantt et al., 2009). Nevertheless, it is unclear whether isoprene- and monoterpene-derived SOA or oxidation products may still be important locally and regionally (Gantt et al., 2009; Hu et al., 2013), and/or play a role in the nucleation process even at low concentrations (Laaksonen et al., 2008; Metzger et al., 2010; Kulmala et al., 2013; Riccobono et al., 2014).

The data from the present study, spanning a large range of latitudes from 80 °N to 50 °S, contributes to the growing database of isoprene measurements in water and air that help to constrain global emission estimates. Observations from the current project, with isoprene mixing ratios in air in the low pptv range and surface water concentrations in the tens of pmol L^{-1}, are similar to the recently published extensive dataset by Ooki et al. (2015) as well as the majority of previous studies in low-productivity regions. The analysis presented in Chapter 3 regarding potential controls of isoprene in the surface ocean further extends existing knowledge by exploring relationships with the widely used proxy Chl-*a* (including evaluation of previously published correlations), and by suggesting relationships with additional proxies that may be useful in expanding the data coverage

or providing an alternative approach that could validate current Chl-*a*-derived estimates. Open questions remain regarding the applicability of these predictive relationships across all oceans and seasons and also how indicative the proxies are of the actual controlling factors such as the generally proposed light or temperature. For example, the evidence for light-dependent production similar to higher plants is strong from laboratory studies, but has not been seen in the field. Measurements from the current project indicate a correlation with photoprotective pigments and generally higher production in the tropics (the latter also reported by Ooki et al., 2015), which would support the hypothesis of light stress-induced emissions. The same mechanism would not necessarily give rise to a diurnal pattern with higher surface seawater concentrations during daylight due to slow mixing in the water column, so that a lack of this trend in our observations does not contradict this potential light-related control.

Chapter 4 describes observations of monoterpenes in seawater and air made during this project. These are the first reported seawater observations, to our knowledge, and the first speciated *in-situ* measurements in air, which contribute significantly to the existing database consisting of three publications to date (including only one speciated dataset; Yassaa et al., 2008; Colomb et al., 2009; Lawson et al., 2015). Both air and water concentrations typically varied between below the detection limit (sub-pptv and sub-pmol L^{-1}, respectively) and a few pptv or pmol L^{-1}. Even at these low levels, monoterpenes are likely at least as important for marine SOA as isoprene, due to their much higher SOA yield and comparable lifetimes for both ozonolysis and photooxidation.

The importance of careful quality control and comprehensive reporting of observational data is also discussed in Chapter 4 specifically, as working close to the detection limit for these compounds results in particular challenges with respect to representing data in a meaningful way and minimising the potential for contamination of especially air samples. The newly-made measurements presented in this thesis help to establish potential marine monoterpene emissions from the datapoints above the detection limit, but also give an upper limit of the potential concentrations based on the knowledge of a dynamic detection limit and its error throughout all cruises. These values are at the low end of previously published data (Yassaa et al., 2008; Colomb et al., 2009; Lawson et al., 2015), highlighting the large spatial and temporal variability of these compounds already seen in the literature to date. It has not been possible to establish biological controls in the ocean based on the

available data despite a previously reported association with Chl-*a* (Yassaa et al., 2008), emphasising the need for further studies both in the laboratory and in the field to identify controlling factors.

6.2 Outlook: future work

Planned work on data from the current project includes evaluation of the depth profiles that were only briefly mentioned in this thesis and could give further insight into controlling factors in the water column; this will involve the use of a one-dimensional ocean mixed layer model to explore the effects of proposed controls on observed profiles. In addition, CHEMTAX analysis of AMT pigment data will be performed to compare to results from ACCACIA 2 and link data from this study to literature values of phytoplankton functional type-specific production rates. The link of isoprene to photoprotective pigments will be investigated further in view of its role in stress relief in higher plants and proposed light stress-induced emissions (Meskhidze et al., 2015).

In terms of more general future work, the collection of additional field data could contribute to more reliable and accurate predictions of global marine isoprene and monoterpene fluxes, by supporting (or helping to revise) existing model algorithms, or informing the development of new ones. This is especially true for monoterpenes, but the picture is not yet clear either for isoprene emissions. There are a number of challenges to achieving better data coverage, including the development of robust measurement systems capable of high-resolution, speciated analyses with low detection limits.

The emergence of a new potential photochemical source of functionalised and unsaturated hydrocarbons, including isoprene, from the sea surface microlayer (SML) and similarly from sea spray aerosol (Ciuraru et al., 2015b) indicates that seawater-derived (bottom-up) fluxes may not be sufficient to explain the mixing ratios of isoprene in air or predict total fluxes to the atmosphere that could act as a source of SOA; and a similar additional source could exist for monoterpenes. While the SML could possibly be enriched in these compounds and a knowledge of enrichment factors could be beneficial, it should nonetheless be remembered that SML sampling techniques are inherently unsuitable for trace gas

analysis; the extensive exposure to air during sampling will result in supersaturated volatile species like isoprene and monoterpenes being lost and undersaturated soluble gases such as glyoxal being enhanced (Carpenter and Nightingale, 2015).

Concurrent measurements of air and water concentrations could improve our understanding of the processes responsible for atmospheric mixing ratios of these reactive compounds, provided they are carefully quality controlled. As emphasised previously, the present study showed that measurements of air mixing ratios are subject to potential contamination, so that additional observations to monitor hydrocarbon contamination such as ship stack are highly recommended. The case of limonene in particular needs further attention, in order to establish whether observations in the marine boundary layer and surface ocean show a biogenic compound or a contaminant - for this, speciated measurements are essential. However, high-resolution data (e.g. from PTR-MS) can provide much information on small-scale variations and therefore potential controls, which lower-resolution observations (e.g. P&T-TD-GC-MS) are more likely to miss or average out due to their sampling methods. Diurnal variations partially fall into this category, as a greater number of data points could show trends for smaller sub-sets of data (as seen e.g. by Colomb et al., 2009), while larger-scale averaging is needed (but not necessarily useful) to evaluate trends from data with lower temporal resolution. Reducing sampling and analysis times on GC-MS systems is one potential improvement, bearing in mind that a reduction in sampling volume would also require improved detection limits to allow for the low ambient concentrations. Complementary sampling with two different systems *in situ* could increase temporal resolution while maintaining confidence in sample integrity based on the slower analysis; however this is likely to be difficult to put into practice for various reasons (e.g. logistics, expertise, operator requirements).

It is apparent that future observations of marine terpenes would be most useful in terms of establishing controlling factors if they could be conducted on cruises with a range of supporting biological, physical and chemical measurements. Following the current project, these would ideally include Chl-*a*, further pigments and primary production in order to test the relationships found so far, but further available parameters could help to identify other potential controls or proxies.

Based on this work, changes to current data analysis and reporting practices would perhaps also aid our understanding of this subject area. Literature to date often appears to include

detailed observational data only where "positive" results exist, i.e. analytes were above the detection level and/or some trend was observed that could perhaps be explained by supporting data such as Chl-*a* concentrations. It would increase the available number of data if values below the detection limit were also regarded as positive results that can be useful if reported alongside a good estimate of the detection limit (ideally reflecting any potential changes in conditions during a measurement campaign). If an averaged value is published, a consideration could be to give averages for different sections or time periods if there are differences between them; or to explicitly state where no differences in volatile terpenoid levels were observed despite for example a change in biological conditions.

Given the difficulties experienced in ensuring sample integrity, more detailed information regarding quality control procedures (prior to sampling as well as during data processing) could help to develop common approaches necessary for comparable data of consistent quality, as is generally the case in other areas such as phytoplankton pigment analysis or DMS measurements (Aiken et al., 2009; Bell et al., 2011).

Appendix A

Supplementary information

A.1 Auto Purge&Trap code

Modified Arduino code for this project (based on that written by S. Andrews and published in Andrews et al., 2015). This version was used during AMT23; different times and optional additional pressurising steps were sometimes used on other cruises.

```
//Code for auto purge & trap system. This code reads a relay trigger from the Unity2 and controls
//two valves which fill and empty the purge tube. Outputs to an LCD screen.
//it also runs isothermal heating control of the purge tube in the background.
#include <LiquidCrystal.h>

const int TDrelaypin = 7;  // Pin attatched to TD sample valve relay
const int SolenoidApin = 13; // Pin attached to solenoid via a transistor and relay
const int SolenoidBpin = 8; //same as above
const int LM35Pin = A3; //analog in with LM35 temp sensor attached
const int heaterPin = 10; //PWM output to SSR to control heating tape
const int tempsetpoint = 50; //what temp do you want the tube to be?
const int manualtriggerpin = 6;
const int omegaSSRout = 9;    //aux heater pin
const int peristaltic = 0;    //aux relay control incase other solenoid control relays break
const int floatswitch = A5;   //input for saftey float switch
const int omegatempvalue = 120;  //aux heater power setting 0-255

float tempC;
float tempdiff;
int extrapower = 4;
boolean Running = false;
boolean linespurged = false;
```

```
boolean tubefilled = false;
boolean tubepurged = false;
boolean tubepressurisedOne = false;
boolean tubeflushed = false;
boolean tubepressurised = false;
boolean tubeevacuated = false;
boolean tubepostpurged = false;
long countdownitem = 0;
long countdown = 0;
long count = 0;
long triggertime = 0;
long currenttime = 0;
long previoustemptime = 0;
int dataupdatespeed = 1000;
int previoustrigspeed = 0;
int trigspeed = 500;
long filterpurgeinterval = 30000;// 100000 no valve switch, 400um filter purge
// long filterpurgeintervalTwo = filterpurgeinterval + 5;
   // time (ms) for additional pressure release at end of prepurge before filling tube
long linepurgeinterval = filterpurgeinterval + 10000; // 210000 valve&0.7um filter purge
long fillinterval = linepurgeinterval + 420000;
   // adjust this to set the time in ms for the tube to fill for. 46.5sec =30mL
long flushinterval = fillinterval + 20000; // 1080000 time(ms) until the water is emptied to waste
long pressuriseOne = flushinterval + 5; // time(ms) to allow pressure in tube to build up before evacuating
long flushtime = pressuriseOne + 30000; // time(ms) that it empties the water for
long pressurise = flushtime + 6000;
   // time(ms) for pressure in tube to increase for effective second evacuating
long evacuate = pressurise + 10000; // second evacuation time(ms)
long postpurge = evacuate + 6000; // 60000 time(ms) to postpurge tube to waste via solenoid valve
int LM35value = 0; //value read from temp sensor
int heatervalue = 0; //PWM value to trim heater by
long POS = 0; //percentage of setpoint
int mappedLM35 = 0;
int TDtrigger = HIGH;

LiquidCrystal lcd(12, 11, 5, 4, 3, 2);

void setup() {

  lcd.begin(20, 4); // set up the LCD's number of columns and rows

  analogReference(INTERNAL);   //analog scale to 1.1V for better resolution!
  pinMode(TDrelaypin, INPUT);       //specify the pin modes
  digitalWrite(TDrelaypin, HIGH);  //pull trigger to high
  pinMode(SolenoidApin, OUTPUT);    //define inputs and outputs
  pinMode(SolenoidBpin, OUTPUT);
  pinMode(omegaSSRout, OUTPUT);
```

```
  pinMode(peristaltic, OUTPUT);
  pinMode(floatswitch, INPUT);
  pinMode(manualtriggerpin, INPUT);
  digitalWrite(SolenoidApin, LOW); //high to flush filter
  digitalWrite(SolenoidBpin, LOW); //set high to evac or fill
  digitalWrite(peristaltic, LOW); //post purge valve not peri pump
}

void loop() {

currenttime = millis();

 lcd.setCursor(0,0);
 if (tempC < (tempsetpoint-1)){
   lcd.print("Tube is below temp!!");}
else lcd.print("Automated Purge&Trap");
 LM35value = analogRead(LM35Pin); //read the value from the temp sensor
  tempC = LM35value / 9.31;
  tempdiff = tempsetpoint - tempC;
  float temppercent = tempdiff * 2.5 * extrapower;
 //mappedLM35 = map(LM35value, 0, 1023, 0, 255); //scale 1024 analoge bits to 256 digital
 //POS = mappedLM35 / tempsetpoint *100;
// if (POS < 80) {
if (tempC >= tempsetpoint) {
  heatervalue = 0;
}
//if (tempC <= 20) {
 // heatervalue = 0;
//}
if (tempC < tempsetpoint & tempC > 20) {
  heatervalue = temppercent * 2.55;
}
// }
// if (POS > 80) {
//   heatervalue = (255/100)*(100 - POS);
// }

analogWrite(omegaSSRout, heatervalue); //write the PWM value to the heater pin
analogWrite(heaterPin, omegatempvalue);

if (currenttime - previoustrigspeed > trigspeed)  {
 TDtrigger = digitalRead(TDrelaypin);
 previoustrigspeed = currenttime;} //read trigger signal from CIA8

  int manualtrigger = digitalRead(manualtriggerpin);
  if ((manualtrigger == LOW) && (Running == false)) {TDtrigger = LOW;}
   //manual trigger normally HIGH but switched LOW by button on front panel
```

```
  if (TDtrigger == LOW) {
    count = count + 1;

    if ((count == 1) && (Running == false)){
      triggertime = millis();
      lcd.setCursor(0,1);
      lcd.print("  Pre-purging Lines  ");
      countdownitem = linepurgeinterval;
      linespurged = false;
      tubefilled = false;
      tubepurged = false;
      tubepressurisedOne = false;
      tubeflushed = false;
      tubepressurised = false;
      tubeevacuated = false;
      tubepostpurged = false;
      Running = true;
    }}
  else {count = 0 ;}


  if (Running == true){

    if ((currenttime - triggertime > filterpurgeinterval) && (linespurged == false)) {
      digitalWrite(SolenoidApin, HIGH);
      digitalWrite(peristaltic, LOW);
          //useful in case peristaltic has accidentally been left at HIGH initially fte manual postpurging
      lcd.setCursor(0,1);
      lcd.print("Purging lines&filter");}

//     if ((currenttime - triggertime > filterpurgeintervalTwo) && (linespurged == false)) {
 //     digitalWrite(SolenoidApin, HIGH);
 //     digitalWrite(peristaltic, HIGH);
 //     lcd.setCursor(0,1);
 //     lcd.print("Purging lines&filter");}

    if ((currenttime - triggertime > linepurgeinterval) && (linespurged == false)) {
      digitalWrite(SolenoidApin, HIGH);
      digitalWrite(SolenoidBpin, HIGH);
      digitalWrite(peristaltic, LOW);
          //useful in case peristaltic has accidentally been left at HIGH initially fte manual postpurging
      extrapower = 8;
      lcd.setCursor(0,1);
      lcd.print(" Filling purge tube ");
      countdownitem = fillinterval;
      linespurged = true;
```

```
  }

 // if ((currenttime - triggertime > linepurgeinterval) && (linespurged == false)) {

//  }
  if ((currenttime - triggertime > fillinterval) && (tubefilled == false)) {
    digitalWrite(SolenoidApin, LOW);
    digitalWrite(SolenoidBpin, LOW);
    digitalWrite(peristaltic, LOW);
    lcd.setCursor(0,1);
    lcd.print("    Purging tube    ");
    countdownitem = flushinterval;
    tubefilled = true;
    //extrapower = 4;
  }
//  if ((currenttime - triggertime > linepurgeinterval) && (linespurged == false)) {

if ((currenttime - triggertime > flushinterval) && (tubepressurisedOne == false)){
    digitalWrite(SolenoidApin, LOW);
    digitalWrite(SolenoidBpin, LOW);
    digitalWrite(peristaltic, LOW);
    lcd.setCursor(0,1);
    lcd.print(" Pressurising 1 ");
    countdownitem = pressuriseOne;
    tubepressurisedOne = true;
    }

//  }
  if ((currenttime - triggertime > pressuriseOne) && (tubepurged == false)) {
    digitalWrite(SolenoidApin, LOW);
    digitalWrite(SolenoidBpin, HIGH);
    digitalWrite(peristaltic, LOW);
    lcd.setCursor(0,1);
    lcd.print("  Evacuating tube   ");
    countdownitem = flushtime;
    tubepurged = true;
  }

//  if ((currenttime - triggertime > linepurgeinterval) && (linespurged == false)) {

//  }
  if ((currenttime - triggertime > flushtime) && (tubeflushed == false)){
    digitalWrite(SolenoidApin, LOW);
    digitalWrite(SolenoidBpin, LOW);
    digitalWrite(peristaltic, LOW);
    lcd.setCursor(0,1);
    lcd.print(" Pressurising ");
```

```
      countdownitem = pressurise;
      tubeflushed = true;
      }

    if ((currenttime - triggertime > pressurise) && (tubepressurised == false)){
      digitalWrite(SolenoidApin, LOW);
      digitalWrite(SolenoidBpin, HIGH);
      digitalWrite(peristaltic, LOW);
      lcd.setCursor(0,1);
      lcd.print(" Evacuating again ");
      countdownitem = evacuate;
      tubepressurised = true;
      }

    if ((currenttime - triggertime > evacuate) && (tubeevacuated == false)){
      digitalWrite(SolenoidApin, LOW);
      digitalWrite(SolenoidBpin, LOW);
      digitalWrite(peristaltic, HIGH);
      lcd.setCursor(0,1);
      lcd.print("   Postpurging   ");
      countdownitem = postpurge;
      tubeevacuated = true;
      }

 if ((currenttime - triggertime > postpurge) && (tubepostpurged == false)){
      digitalWrite(peristaltic, LOW);
      Running = false;
      lcd.setCursor(0,1);
      lcd.print(" Waiting for sample ");
      tubepostpurged = true;
      }

    }

if (currenttime - previoustemptime > dataupdatespeed) {
   previoustemptime = currenttime;
   lcd.setCursor(0, 3);
   lcd.print("Tube = ");
   lcd.print(tempC,1);
   lcd.print((char)223);
   lcd.print("C  ");
  lcd.setCursor(14,3);
  lcd.print(" P=");
  lcd.print(temppercent,0);
  lcd.print("% ");

if (Running == true) {
```

```
     countdown = countdownitem - (currenttime - triggertime);
     lcd.setCursor(8,2);
     lcd.print(countdown/1000);
     lcd.print("sec ");
//      lcd.setCursor(15,3);
//   lcd.print("TRUE ");
   }
   else {lcd.setCursor(8,2);
   lcd.print("       ");
//   lcd.setCursor(15,3);
//   lcd.print("FALSE");
   }
}

  }
```

A.2 VOC scrubber code

Arduino code for the VOC scrubber used for this project, written by S. Andrews.

```
#include <Wire.h>
#include <EEPROM.h>
#include <LiquidCrystal_I2C.h>
#include <Adafruit_MCP23017.h>
#include <Adafruit_MAX31855.h>
#include <Adafruit_MCP4725.h>
#include <PID_v1.h>
#include <OneWire.h>
#include <DallasTemperature.h>

LiquidCrystal_I2C lcd(0x3F,20,4);  // set the LCD address to 0x3F for a 20 chars and 4 line display

// Data wire is plugged into port 2 on the Arduino
#define ONE_WIRE_BUS 9
OneWire oneWire(ONE_WIRE_BUS);
DallasTemperature sensors(&oneWire);

boolean running;
const int ovenSSR = 10;
const int countpin = 11;
const int valcopin =12;
int samplecounter = 0;
int samplecounter2 =0;
int samplecount;
double Temperature;
```

```
double oventemp;
double Temperature2;

// Thermocouple settings
int thermoDO = 2;
int thermoCS = 3;
int thermoCLK = 4;

int drivePin = 8;
int driveState = 0;

boolean valcoturn;
int DACoutput;
int CfingerchangeFreq = 90;
int CfingerNo = 1;
int CfingerWarning = 0;
int runTime = 1800000;
int setPoint = -17;
int ovenTempset = 50;
float current = 0.0f;
char tempString[10];
unsigned long update = 0;
unsigned long voltage = 0;
unsigned long triggeredtime = 0;

//buttons
int upbutton = 5;
int downbutton = 6;
int driveswitch = 7;
int upstate = 0;
int downstate = 0;
int driveswitchstate = 0;



Adafruit_MAX31855 thermocouple(thermoCLK, thermoCS, thermoDO);
Adafruit_MCP4725 dac;

// PID Control
// Define the aggressive and conservative Tuning Parameters
double Input;
double PIDSetPoint;
double Output;
double ovenSetpoint, ovenOutput, ovenInput;

//const double cusKp=40, cusKi=0.02, cusKd=0;
const double cusKp=25, cusKi=0.25, cusKd=0;
const double aggKp=4, aggKi=0.2, aggKd=10;
```

```
const double consKp=1, consKi=0.05, consKd=0.25;

// Specify the links and initial tuning parameters
PID pidControl(&Input, &Output, &PIDSetPoint, cusKp, cusKi, cusKd, REVERSE);
PID pidOven(&ovenInput, &ovenOutput, &ovenSetpoint, aggKp, aggKi, aggKd, DIRECT);


void setup()
{
  running = false;
  valcoturn = false;
  triggeredtime = millis();
  pinMode(countpin, INPUT_PULLUP);
  digitalWrite(countpin, HIGH);
  pinMode(valcopin, OUTPUT);
  digitalWrite(valcopin, HIGH);
  // Start up the one wire temp control library
  sensors.begin();

  pinMode(upbutton, INPUT);
  pinMode(downbutton, INPUT);
  pinMode(driveswitch, INPUT);
  digitalWrite(upbutton, HIGH);
  digitalWrite(downbutton, HIGH);
  digitalWrite(driveswitch, HIGH);


  lcd.init();                      // initialize the lcd
  lcd.init();
  // Print a message to the LCD.
  //lcd.backlight();
  //lcd.setCursor(0,2);
  //lcd.print("Hello, world!");


  Serial.begin(9600);  // Debugging output
  lcd.backlight();  //turn on the LCD light
  dac.begin(0x62); //set up the digital to analogue conversion

  pinMode(drivePin, OUTPUT);
  digitalWrite(drivePin, HIGH);

  // load the setpoint from EEROM if Stored
  if (EEPROM.read(2) == 0x55)
  {
    byte *sp = (byte *)&CfingerNo;
    sp[0] = EEPROM.read(0);
```

```
    sp[1] = EEPROM.read(1);
  }
  dac.setVoltage(0, false);

  // Set up the PID Controllers
  Input = Temperature;
  ovenInput = oventemp;
  PIDSetPoint = (double)setPoint;
  ovenSetpoint = ovenTempset;
  pidControl.SetMode(AUTOMATIC);
  pidOven.SetMode(AUTOMATIC);
  pidControl.SetOutputLimits(10, 255);
  pidOven.SetOutputLimits(0,255);

  lcd.setCursor(0, 0);
  lcd.print("Set   : ");
  lcd.print(setPoint);
  lcd.setCursor(13, 0);
  lcd.print("Off");

  lcd.setCursor(0, 1);
  lcd.print("coldzone: ");

  lcd.setCursor(0, 2);
  lcd.print("hotzone: ");

}



void loop()
{

  if (update < millis())
  {
    //Temperature = thermocouple.readCelsius();
    sensors.requestTemperatures(); // Send the command to get temperatures
    Temperature = sensors.getTempCByIndex(0);
    oventemp = sensors.getTempCByIndex(2);
    Temperature2 = sensors.getTempCByIndex(1);
    Serial.print(Temperature,1);
    Serial.print(",");
    Serial.print(setPoint);
    Serial.print(",");
    Serial.print(Output/255*100,0);
    Serial.print("%");
    Serial.print(",");
```

```
  Serial.print(oventemp,1);
  Serial.print(",");
  Serial.print(ovenTempset);
  Serial.print(",");
  Serial.print(ovenOutput/255*100,0);
  Serial.print("%");
  Serial.print(",");
  Serial.print(CfingerNo);
  Serial.print(",");
  Serial.print(samplecounter);
  Serial.print(",");
  Serial.print(triggeredtime);
  Serial.print(",");
  Serial.print(valcoturn);
  Serial.print(",");
  Serial.print(CfingerchangeFreq);
  Serial.print(",");
  Serial.print(CfingerWarning);
  Serial.print(",");
  Serial.print(Temperature2,1);
  Serial.print(",");
  Serial.print(DACoutput);
  Serial.println("");
//  Serial.print(running);
//  Serial.println("");

  if (isnan(Temperature))
  {
    lcd.setCursor(11, 1);
    lcd.print("     ");
    lcd.setCursor(11, 1);
    lcd.print("Err   ");
  }
  else
  {
    lcd.setCursor(11, 1);
    lcd.print("     ");
    lcd.setCursor(11, 1);
    lcd.print(Temperature);
    lcd.print(" ");
  }
  if (isnan(oventemp))
  {
    //lcd.setCursor(8, 1);
    //lcd.print("     ");
    //lcd.setCursor(8, 1);
    //  lcd.print("Err   ");
```

```
  }
  else
  {
    lcd.setCursor(11, 2);
    lcd.print("     ");
    lcd.setCursor(11, 2);
    lcd.print(oventemp);
    lcd.print(" ");
  }

  update = millis() + 0;
}

// delay(100);

//uint8_t buttons = lcd.readButtons();
upstate = digitalRead(upbutton);
downstate = digitalRead(downbutton);
//if (buttons)
//{
if (upstate == LOW)
{
  setPoint += 1;
  if (setPoint > 20)
    setPoint = 20;
}

if (downstate == LOW)
{
  setPoint -= 1;
  if (setPoint < -70)
    setPoint = -70;
}

driveswitchstate = digitalRead(driveswitch);
if (driveswitchstate == HIGH)
{
   if (driveState == 0)
  {
  //switch on the drive pin by setting it low
  driveState = 1;
  digitalWrite(drivePin, LOW);
  lcd.setCursor(13, 0);
  lcd.print("On ");
  // lcd.setBacklight(BLUE);
}}
else
```

```
  {
    //switch off the drive pin by setting it high
    driveState = 0;
    digitalWrite(drivePin, HIGH);
    lcd.setCursor(13, 0);
    lcd.print("Off");
    // lcd.setBacklight(GREEN);

  }

  lcd.setCursor(8, 0);
  lcd.print("    ");
  lcd.setCursor(8, 0);
  lcd.print(setPoint);



  // Set the DAC value
  //dac.setVoltage(ADCValues[abs(setPoint - 20)], false);
  //}

  //if (isnan(Temperature) == false)
  //{
    Input = Temperature;
    PIDSetPoint = (double)setPoint;
    pidControl.Compute();
    if (Output > 255.0)
      Output = 255.0;
      DACoutput = Output*16;
dac.setVoltage((int)(Output * 16.0), false);
     // dac.setVoltage(1000, false);

    ovenInput = oventemp;
    pidOven.Compute();
    if (ovenOutput > 255.0)
      ovenOutput = 255.0;
    analogWrite(ovenSSR,ovenOutput);
 // }




  samplecount = digitalRead(countpin);
 // if (samplecount == LOW){
  //  running = true;
  //  triggeredtime = millis(); }
```

```
// if (millis()-triggeredtime>10000) {
 //  running = false;
 //  samplecounter = samplecounter +1;
// }



 if ((samplecount == LOW) && (running == false)) {
   samplecounter = samplecounter +1;
   running = true;
   triggeredtime = millis();
 }
 if ((millis()-triggeredtime>1800000) && (running == true)){
   running = false;
 }

 if (samplecounter >= CfingerchangeFreq) {
   samplecounter = 0;
   valcoturn = TRUE;
   CfingerNo = CfingerNo +1;
   // Save coldfinger number in EEPROM
   byte *sp = (byte *)&CfingerNo;
   EEPROM.write(0, sp[0]);
   EEPROM.write(1, sp[1]);
   EEPROM.write(2, 0x55);
   digitalWrite(valcopin, LOW);
 }
 else {
   digitalWrite(valcopin, HIGH);
   valcoturn = FALSE;
 }

 if (CfingerNo == 10){
   CfingerWarning = 1;
 lcd.setCursor(5, 0);
 lcd.print("CHANGE SOON");
 }
 if (CfingerNo >10){
   CfingerWarning = 2;
   lcd.setCursor(5, 0);
 lcd.print("CHANGE NOW!");
 }
 if (CfingerNo <10){
   CfingerWarning = 0;}
 if (CfingerNo >11){
   CfingerNo = 1;
```

```
  // Save coldfinger number in EEPROM
    byte *sp = (byte *)&CfingerNo;
    EEPROM.write(0, sp[0]);
    EEPROM.write(1, sp[1]);
    EEPROM.write(2, 0x55);}

}
```

==========

Abbreviations

(auto)P&T	(automated) Purge and Trap
ACC	Antarctic Circumpolar Current
ACCACIA	Aerosol-Cloud Coupling And Climate Interactions in the Arctic
AFC	Automated Flow Cytometry
AMT	Atlantic Meridional Transect
BODC	British Oceanography Centre
BVOC	Biogenic Volatile Organic Compound
CCN	Cloud Condensation Nuclei (or Nucleus)
CDNC	Cloud Droplet Number Concentration
Chl-a	Chlorophyll-a
CLAW hypothesis	hypothesis named after Charlson, Lovelock, Andreae and Warren (1987)
Cocco	Coocolithophores
Cryp	Cryptophytes
CTD	Conductivity, Temperature and Depth (hydrocast)
CVAO	Cape Verde Atmospheric Observatory
DL	Detection Limit
DMAPP	Dimethylallyl pyrophosphate
dmsterps	DMS/Terpenes (standard)
E13	Exton et al. (2013)
EIC	Extracted Ion Chromatogram
Fuco	Fucoxanthin
GC	Gas Chromatograph(y)
GIN Seas	Greenland, Iceland and Norwegian Seas
GPP	Geranyl pyrophosphate or Gross Primary Production
H	Henry's Law constant
HYSPLIT	HYbrid Single-Particle Lagrangian Integrated Trajectory
ID	Internal Diameter
intPP	integrated Primary Production
IPP	Isopentenyl pyrophosphate

IS	Internal Standard
isp	isoprene
IspS, *IspS*	Isoprene synthase (enzyme and gene)
JCR	RRS James Clark Ross
MCM	Master Chemical Mechanism
MEP	3-Methylerythritol 4-phosphate
MOC	Meridional Overturning Circulation
MODIS	Moderate resolution Imaging Spectroradiometer
MRR	Molar Response Ratio
MS	Mass Spectrometer/Spectrometry
MVA	Mevalonic Acid
NAG	North Atlantic Gyre
Nano	Nanoeukaryotes
NCAS	National Centre for Atmospheric Science
NERC	Natural Environment Research Council
NPP	Net Primary Production
NHMC	Non-methane Hydrocarbon
NOAA	National Oceans and Atmospheres Administration
NOC(S)	National Oceanography Centre (Southampton)
NPL	National Physical Laboratory
NPL-MT	NPL Monoterpenes (standard)
O15	Ooki et al. (2015)
OA	Organic Aerosol
OC	Organic Carbon
OD	Outer Diameter
ORC	Organic Reactive Carbon
oVOC	oxygenated Volatile Organic Compound
PA	Peak Area
PAR	Photosynthetically Active Radiation
Peuk	Picoeukaryotes
PFT	Phytoplankton Functional Type
PML	Plymouth Marine Laboratory
POA	Primary Organic Aerosol

PP (intPP)	Primary Production (integrated PP)
PPC	Photoprotective Carotenoids
ppb (ppb)	Parts per billion (by volume)
ppt (pptv)	Parts per trillion (by volume)
Pro	*Prochlorococcus*
PT	Peak Threshold
PW	Peak Width
PTR-MS	Photon-Transfer-Reaction Mass Spectrometer
RLOC	Robust Line of Organic Correlation
ROS	Reactive Oxygen Species
RRS	Royal Research Ship
RV	Research Vessel
SA	Saturation Anomaly
S.A.	Surface Area
SAG	South Atlantic Gyre
sccm	Standard cubic centimetres per minute
SeaWiFS	Sea-Viewing Wide Field-of-View Sensor
SIM	Selected Ion Monitoring
SOA	Secondary Organic Aerosol
SSS	Sea Surface Salinity
SST	Sea Surface Temperature
std	standard
Syn	*Synechococcus*
TD	Thermal Desorption
TIC	Total Ion Chromatogram
VOC	Volatile Organic Compound
WMO	World Meteorological Organisation
Zea	Zeaxanthin

References

Acosta Navarro, J. C., Smolander, S., Struthers, H., Zorita, E., Ekman, A. M. L., Kaplan, J. O., Guenther, A., Arneth, A., and Riipinen, I.: Global emissions of terpenoid VOCs from terrestrial vegetation in the last millennium, Journal of Geophysical Research: Atmospheres, 119, 6867–6885, doi:10.1002/2013JD021238, 2014.

Aiken, J., Rees, N., Hooker, S., Holligan, P., Bale, A., Robins, D., Moore, G., Harris, R., and Pilgrim, D.: The Atlantic Meridional Transect: Overview and synthesis of data, Progress in Oceanography, 45, 257–312, doi:10.1016/S0079-6611(00)00005-7, 2000.

Aiken, J., Pradhan, Y., Barlow, R., Lavender, S., Poulton, A., Holligan, P., and Hardman-Mountford, N.: Phytoplankton pigments and functional types in the Atlantic Ocean: A decadal assessment, 1995-2005, Deep-Sea Research Part II: Topical Studies in Oceanography, 56, 899–917, doi:10.1016/j.dsr2.2008.09.017, 2009.

Allan, B. J., McFiggans, G., Plane, J. M. C., Coe, H., and McFadyen, G. G.: The nitrate radical in the remote marine boundary layer, Journal of Geophysical Research, 105, 24 191–24 204, 2000.

Allan, J. D., Williams, P. I., Najera, J., Whitehead, J. D., Flynn, M. J., Taylor, J. W., Liu, D., Darbyshire, E., Carpenter, L. J., Chance, R., Andrews, S. J., Hackenberg, S. C., and McFiggans, G.: Iodine observed in new particle formation events in the Arctic atmosphere during ACCACIA, Atmospheric Chemistry and Physics, 15, 5599–5609, doi:10.5194/acp-15-5599-2015, URL http://www.atmos-chem-phys.net/15/5599/2015/, 2015.

Alvain, S., Moulin, C., Dandonneau, Y., and Breon, F. M.: Remote sensing of phytoplankton groups in case 1 waters from global SeaWiFS imagery, Deep-Sea Research Part I: Oceanographic Research Papers, 52, 1989–2004, doi:10.1016/j.dsr.2005.06.015, 2005.

Alvain, S., Moulin, C., Dandonneau, Y., and Loisel, H.: Seasonal distribution and succession of dominant phytoplankton groups in the global ocean: A satellite view, Global Biogeochemical Cycles, 22, 1–15, doi:10.1029/2007GB003154, 2008.

Andreae, M. O.: Aerosols Before Pollution, Science, 315, 50–51, doi:10.1126/science.1136529, 2007.

Andreae, M. O. and Rosenfeld, D.: Aerosol-cloud-precipitation interactions. Part 1. The nature and sources of cloud-active aerosols, Earth-Science Reviews, 89, 13–41, doi:10.1016/j.earscirev.2008.03.001, 2008.

Andrews, S. J., Hackenberg, S. C., and Carpenter, L. J.: Technical Note: A fully automated purge and trap GC-MS system for quantification of volatile organic compound (VOC) fluxes between the ocean and atmosphere, Ocean Science, 11, 313–321, doi:10.5194/os-11-313-2015, 2015.

Anttila, T., Langmann, B., Varghese, S., and O'Dowd, C.: Contribution of Isoprene Oxidation Products to Marine Aerosol over the North-East Atlantic, Advances in Meteorology, 2010, 1–10, doi:10.1155/2010/482603, 2010.

Arneth, A., Monson, R. K., Schurgers, G., Niinemets, U., and Palmer, P. I.: Why are estimates of global terrestrial isoprene emissions so similar (and why is this not so for monoterpenes)?, Atmospheric Chemistry and Physics, 8, 4605–4620, doi:10.5194/acp-8-4605-2008, 2008.

Arnold, S., Carpenter, L. J., and Lewis, A. C.: Oceanic Reactive Carbon: Chemistry-Climate impacts (ORC^3), Grant Application Case for Support, 2013.

Arnold, S. R., Spracklen, D. V., Williams, J., Yassaa, N., Sciare, J., Bonsang, B., Gros, V., Peeken, I., Lewis, A. C., Alvain, S., and Moulin, C.: Evaluation of the global oceanic isoprene source and its impacts on marine organic carbon aerosol, Atmospheric Chemistry and Physics, 9, 1253–1262, doi:10.5194/acp-9-1253-2009, 2009.

Atkinson, R. and Arey, J.: Gas-phase tropospheric chemistry of biogenic volatile organic compounds: a review, Atmospheric Environment, 37, 197–219, doi:10.1016/S1352-2310(03)00391-1, 2003.

Atkinson, R., Baulch, D. L., Cox, R. A., Crowley, J. N., Hampson, R. F., Hynes, R. G., Jenkin, M. E., Rossi, M. J., and Troe, J.: Evaluated kinetic and photochemical data for

atmospheric chemistry: Volume II gas phase reactions of organic species, Atmospheric Chemistry and Physics, 6, 3625–4055, doi:10.5194/acp-6-3625-2006, 2006.

Ayers, G. P. and Cainey, J. M.: The CLAW hypothesis: a review of the major developments, Environmental Chemistry, 4, 366, doi:10.1071/EN07080, 2007.

Baker, A. R., Turner, S. M., Broadgate, W. J., Thompson, A., McFiggans, G. B., Vesperini, O., Nightingale, P. D., Liss, P. S., and Jickells, T. D.: Distribution and sea-air fluxes of biogenic trace gases in the eastern Atlantic Ocean, Global Biogeochemical Cycles, 14, 871–886, 2000.

Beale, R., Liss, P. S., and Nightingale, P. D.: First oceanic measurements of ethanol and propanol, Geophysical Research Letters, 37, 1–5, doi:10.1029/2010GL045534, 2010.

Beale, R., Liss, P. S., Dixon, J. L., and Nightingale, P. D.: Quantification of oxygenated volatile organic compounds in seawater by membrane inlet-proton transfer reaction/mass spectrometry, Analytica Chimica Acta, 706, 128–134, doi:10.1016/j.aca.2011.08.023, 2011.

Bell, T. G., Malin, G., Lee, G. A., Stefels, J., Archer, S., Steinke, M., and Matrai, P.: Global oceanic DMS data inter-comparability, Biogeochemistry, 110, 147–161, doi:10.1007/s10533-011-9662-3, 2011.

Bender, F. a. M., Charlson, R. J., Ekman, A. M. L., and Leahy, L. V.: Quantification of monthly mean regional-scale albedo of marine stratiform clouds in satellite observations and GCMs, Journal of Applied Meteorology and Climatology, 50, 2139–2148, doi:10.1175/JAMC-D-11-049.1, 2011.

Bidigare, R. R., Smith, R. C., Baker, K. S., and Marra, J.: Oceanic primary production estimates from measurements of spectral irradiance and pigment concentrations, Global Biogeochemical Cycles, 1, 171, doi:10.1029/GB001i003p00171, 1987.

Blomquist, B. W., Fairall, C. W., Huebert, B. J., Kieber, D. J., and Westby, G. R.: DMS sea-air transfer velocity: Direct measurements by eddy covariance and parameterization based on the NOAA/COARE gas transfer model, Geophysical Research Letters, 33, 2–5, doi:10.1029/2006GL025735, 2006.

Bonsang, B., Kanakidou, M., Lambert, G., and Monfray, P.: The marine source of C2-C6 aliphatic hydrocarbons, Journal of Atmospheric Chemistry, 6, 3–20, doi:10.1007/BF00048328, 1988.

Bonsang, B., Polle, C., and Lambert, G.: Evidence for Marine Production of Isoprene, Geophysical Research Letters, 19, 1129–1132, 1992.

Bonsang, B., Gros, V., Peeken, I., Yassaa, N., Bluhm, K., Zoellner, E., Sarda-Esteve, R., and Williams, J.: Isoprene emission from phytoplankton monocultures: the relationship with chlorophyll-a, cell volume and carbon content, Environmental Chemistry, 7, 55–563, doi:10.1071/EN09156, 2010.

Boucher, O., Randall, D., Artaxo, P., Bretherton, C., Feingold, G., Forster, P., Kerminen, V.-M., Kondo, Y., Liao, H., Lohmann, U., Rasch, P., Satheesh, S., Sherwood, S., Stevens, B., and Zhang, X.: Clouds and Aerosols, in: Climate Change 2013: The Physical Science Basis. Contribution of Working Group I to the Fifth Assessment Report of the Intergovernmental Panel on Climate Change, edited by Stocker, T. F., Qin, D., Plattner, G.-K., Tignor, M., Allen, S. K., Boschung, J., Nauels, A., Xia, Y., Bex, V., and Midgley, P. M., chap. 7, pp. 571–657, 2013.

Bravo-Linares, C. M., Mudge, S. M., and Loyola-Sepulveda, R. H.: Occurrence of volatile organic compounds (VOCs) in Liverpool Bay, Irish Sea., Marine Pollution Bulletin, 54, 1742–53, doi:10.1016/j.marpolbul.2007.07.013, 2007.

Broadgate, W. J., Liss, P. S., and Penkett, S. A.: Seasonal emissions of isoprene and other reactive hydrocarbon gases from the ocean, Geophysical Research Letters, 24, 2675–2678, doi:10.1029/97GL02736, 1997.

Bryant, C. L., Henley, S. F., Murray, C., Ganeshram, R. S., and Shanks, R.: Carbon Isotope Analysis, Proceedings of the 21st International Radiocarbon Conference, 55, 401–409, 2013.

Calogirou, A., Larsen, B. R., Brussol, C., Duane, M., and Kotzias, D.: Decomposition of Terpenes by Ozone during Sampling on Tenax, Analytical chemistry, 68, 1499–506, doi:10.1021/ac950803i, 1996.

Cao, X. L. and Hewitt, C. N.: Detection methods for the analysis of biogenic non-

methane hydrocarbons in air, Journal of Chromatography A, 710, 39–50, doi:10.1016/0021-9673(95)00427-O, 1995.

Carlton, A. G., Wiedinmyer, C., and Kroll, J. H.: A review of Secondary Organic Aerosol (SOA) formation from isoprene, Atmospheric Chemistry and Physics, 9, 4987–5005, 2009.

Carpenter, L. J. and Nightingale, P. D.: Chemistry and Release of Gases from the Surface Ocean, Chemical Reviews, p. 150326161548000, doi:10.1021/cr5007123, 2015.

Carpenter, L. J. and Reimann, S.: Update on Ozone-Depleting Substances (ODSs) and Other Gases of Interest to the Montreal Protocol [Chapter 1], in: Scientific Assessment of Ozone Depletion: 2014, edited by Engel, A. and Montzka, S. A., World Meteorological Organization, Geneva, Switzerland, URL http://hdl.handle.net/2268/175647, 2014.

Carpenter, L. J., Fleming, Z. L., Read, K. A., Lee, J. D., Moller, S. J., Hopkins, J. R., Purvis, R. M., Lewis, A. C., Müller, K., Heinold, B., Herrmann, H., Wadinga Fomba, K., van Pinxteren, D., Müller, C., Tegen, I., Wiedensohler, A., Müller, T., Niedermeier, N., Achterberg, E. P., Patey, M. D., Kozlova, E. A., Heimann, M., Heard, D. E., Plane, J. M. C., Mahajan, A., Oetjen, H., Ingham, T., Stone, D., Whalley, L. K., Evans, M. J., Pilling, M. J., Leigh, R. J., Monks, P. S., Karunaharan, A., Vaughan, S., Arnold, S. R., Tschritter, J., Pöhler, D., Frieß, U., Holla, R., Mendes, L. M., Lopez, H., Faria, B., Manning, A. J., and Wallace, D. W. R.: Seasonal characteristics of tropical marine boundary layer air measured at the Cape Verde Atmospheric Observatory, Journal of Atmospheric Chemistry, 67, 87–140, doi:10.1007/s10874-011-9206-1, 2010.

Carpenter, L. J., Archer, S. D., and Beale, R.: Ocean-atmosphere trace gas exchange, Chemical Society Reviews, 41, 6473–6506, doi:10.1039/c2cs35121h, 2012.

Carslaw, K. S., Boucher, O., Spracklen, D. V., Mann, G. W., Rae, J. G. L., Woodward, S., and Kulmala, M.: A review of natural aerosol interactions and feedbacks within the Earth system, Atmospheric Chemistry and Physics, 10, 1701–1737, doi:10.5194/acp-10-1701-2010, 2010.

Carslaw, K. S., Lee, L. a., Reddington, C. L., Pringle, K. J., Rap, A., Forster, P. M., Mann, G. W., Spracklen, D. V., Woodhouse, M. T., Regayre, L. a., and Pierce, J. R.: Large contribution of natural aerosols to uncertainty in indirect forcing., Nature, 503, 67–71, doi:10.1038/nature12674, 2013.

Chan Miller, C., Gonzalez Abad, G., Wang, H., Liu, X., Kurosu, T., Jacob, D. J., and Chance, K.: Glyoxal retrieval from the Ozone Monitoring Instrument, Atmospheric Measurement Techniques, 7, 3891–3907, doi:10.5194/amt-7-3891-2014, 2014.

Charlson, R. J., Lovelock, J. E., Andreae, M. O., and Warren, S. G.: Oceanic phytoplankton, atmospheric sulphur, cloud albedo and climate, Nature, 326, 655–661, doi:10.1038/326655a0, 1987.

Chuck, A. L., Turner, S. M., and Liss, P. S.: Oceanic distributions and air-sea fluxes of biogenic halocarbons in the open ocean, Journal of Geophysical Research C: Oceans, 110, 1–12, doi:10.1029/2004JC002741, 2005.

Ciuraru, R., Fine, L., van Pinxteren, M., DAnna, B., Herrmann, H., and George, C.: Photosensitized production of functionalized and unsaturated organic compounds at the air-sea interface, Scientific Reports, 5, 12 741, doi:10.1038/srep12741, 2015a.

Ciuraru, R., Fine, L., van Pinxteren, M., D'Anna, B., Herrmann, H., and George, C.: Unravelling new processes at interfaces: photochemical isoprene production at the sea surface, Environmental Science & Technology, p. 150910155632007, doi:10.1021/acs.est.5b02388, 2015b.

Claeys, M., Graham, B., Vas, G., Wang, W., Vermeylen, R., Pashynska, V., Cafmeyer, J., Guyon, P., Andreae, M. O., Artaxo, P., and Maenhaut, W.: Formation of secondary organic aerosols through photooxidation of isoprene., Science, 303, 1173–6, doi:10.1126/science.1092805, 2004.

Collins, W. J., Derwent, R. G., Johnson, C. E., and Stevenson, D. S.: The oxidation of organic compounds in the troposphere and their global warming potentials, Climatic Change, 52, 453–479, doi:10.1023/A:1014221225434, 2002.

Colomb, A., Yassaa, N., Williams, J., Peeken, I., and Lochte, K.: Screening volatile organic compounds (VOCs) emissions from five marine phytoplankton species by head space gas chromatography/mass spectrometry (HS-GC/MS)., Journal of Environmental Monitoring, 10, 325–30, doi:10.1039/b715312k, 2008.

Colomb, A., Gros, V., Alvain, S., Sarda-Esteve, R., Bonsang, B., Moulin, C., Klüpfel, T., and Williams, J.: Variation of atmospheric volatile organic compounds over the

Southern Indian Ocean (30 - 49 *degree*S), Environmental Chemistry, 6, 70, doi:10.1071/EN08072, 2009.

Constable, A. J., Melbourne-Thomas, J., Corney, S. P., Arrigo, K. R., Barbraud, C., Barnes, D. K. A., Bindoff, N. L., Boyd, P. W., Brandt, A., Costa, D. P., Davidson, A. T., Ducklow, H. W., Emmerson, L., Fukuchi, M., Gutt, J., Hindell, M. A., Hofmann, E. E., Hosie, G. W., Iida, T., Jacob, S., Johnston, N. M., Kawaguchi, S., Kokubun, N., Koubbi, P., Lea, M. A., Makhado, A., Massom, R. A., Meiners, K., Meredith, M. P., Murphy, E. J., Nicol, S., Reid, K., Richerson, K., Riddle, M. J., Rintoul, S. R., Smith, W. O., Southwell, C., Stark, J. S., Sumner, M., Swadling, K. M., Takahashi, K. T., Trathan, P. N., Welsford, D. C., Weimerskirch, H., Westwood, K. J., Wienecke, B. C., Wolf-Gladrow, D., Wright, S. W., Xavier, J. C., and Ziegler, P.: Climate change and Southern Ocean ecosystems I: How changes in physical habitats directly affect marine biota, Global Change Biology, pp. 3004–3025, doi:10.1111/gcb.12623, 2014.

Copolovici, L. O. and Niinemets, U.: Temperature dependencies of Henry's law constants and octanol/water partition coefficients for key plant volatile monoterpenoids., Chemosphere, 61, 1390–400, doi:10.1016/j.chemosphere.2005.05.003, 2005.

Dall'Osto, M., Ceburnis, D., Monahan, C., Worsnop, D. R., Bialek, J., Kulmala, M., Kurtén, T., Ehn, M., Wenger, J., Sodeau, J., Healy, R., and O'Dowd, C.: Nitrogenated and aliphatic organic vapors as possible drivers for marine secondary organic aerosol growth, Journal of Geophysical Research: Atmospheres, 117, 1–10, doi:10.1029/2012JD017522, 2012.

Dani, K. G. S., Jamie, I. M., Prentice, I. C., and Atwell, B. J.: Evolution of isoprene emission capacity in plants, Trends in Plant Science, 19, 439–446, doi:10.1016/j.tplants.2014.01.009, 2014.

Dettmer, K. and Engewald, W.: Adsorbent materials commonly used in air analysis for adsorptive enrichment and thermal desorption of volatile organic compounds., Analytical and bioanalytical chemistry, 373, 490–500, doi:10.1007/s00216-002-1352-5, 2002.

Doney, S. C.: The growing human footprint on coastal and open-ocean biogeochemistry., Science, 328, 1512–1516, doi:10.1126/science.1185198, 2010.

Ducklow, H. W.: Biogeochemical Provinces: Towards a JGOFS Synthesis, in: Ocean

Biogeochemistry: A New Paradigm, edited by Fasham, M. J. R., chap. 1, pp. 3–18, Springer-Verlag, New York, 2003.

Exton, D. A., Suggett, D. J., Steinke, M., and McGenity, T. J.: Spatial and temporal variability of biogenic isoprene emissions from a temperate estuary, Global Biogeochemical Cycles, 26, n/a–n/a, doi:10.1029/2011GB004210, 2012.

Exton, D. A., Suggett, D. J., McGenity, T. J., and Steinke, M.: Chlorophyll-normalized isoprene production in laboratory cultures of marine microalgae and implications for global models, Limnology and Oceanography, 58, 1301–1311, doi:10.4319/lo.2013.58.4.1301, 2013.

Fehsenfeld, F., Calvert, J., Fall, R., Goldan, P., Guenther, A. B., Hewitt, C. N., Lamb, B., Trainer, M., Westberg, H., and Zimmerman, P.: Emissions of volatile organic compounds from vegetation and the implications for atmospheric chemistry, Global Biogeochemical Cycles, 6, 389–430, 1992.

Flato, G., Marotzke, J., Abiodun, B., Braconnot, P., Chou, S., Collins, W., Cox, P., Driouech, F., Emori, S., Eyring, V., Forest, C., Gleckler, P., Guilyardi, E., Jakob, C., Kattsov, V., Reason, C., and Rummukainen, M.: Evaluation of Climate Models, in: Climate Change 2013: The Physical Science Basis. Contribution of Working Group I to the Fifth Assessment Report of the Intergovernmental Panel on Climate Change, edited by Stocker, T. F., Qin, D., Plattner, G.-K., Tignor, M., Allen, S. K., Boschung, J., Nauels, A., Xia, Y., Bex, V., and Midgley, P. M., chap. 9, pp. 741–866, doi:10.1017/CBO9781107415324.020, 2013.

Fry, J. L., Draper, D. C., Barsanti, K. C., Smith, J. N., Ortega, J., Winkler, P. M., Lawler, M. J., Brown, S. S., Edwards, P. M., Cohen, R. C., and Lee, L.: Secondary Organic Aerosol Formation and Organic Nitrate Yield from NO3 Oxidation of Biogenic Hydrocarbons, Environmental Science and Technology, 48, 11 944–11 953, doi:10.1021/es502204x, 2014.

Fu, H., Ciuraru, R., Dupart, Y., Passananti, M., Tinel, L., Rossignol, S., Perrier, S., Donaldson, D. J., Chen, J., and George, C.: Photosensitized Production of Atmospherically Reactive Organic Compounds at the Air/Aqueous Interface, Journal of the American Chemical Society, 137, 8348–8351, doi:10.1021/jacs.5b04051, 2015.

Fu, T. M., Jacob, D. J., Wittrock, F., Burrows, J. P., Vrekoussis, M., and Henze, D. K.: Global budgets of atmospheric glyoxal and methylglyoxal, and implications for formation of secondary organic aerosols, Journal of Geophysical Research: Atmospheres, 113, doi: 10.1029/2007JD009505, 2008.

Galbally, I. E., Lawson, S. J., Weeks, I. A., Bentley, S. T., Gillett, R. W., Meyer, M., and Goldstein, A. H.: Volatile organic compounds in marine air at Cape Grim, Australia, Environmental Chemistry, 4, 178, doi:10.1071/EN07024, 2007.

Gantt, B. and Meskhidze, N.: The physical and chemical characteristics of marine primary organic aerosol: A review, Atmospheric Chemistry and Physics, 13, 3979–3996, doi: 10.5194/acp-13-3979-2013, 2013.

Gantt, B., Meskhidze, N., and Kamykowski, D.: A new physically-based quantification of marine isoprene and primary organic aerosol emissions, Atmospheric Chemistry and Physics, 9, 4915–4927, doi:10.5194/acp-9-4915-2009, 2009.

Gantt, B., Glotfelty, T., Meskhidze, N., and Zhang, Y.: Simulating the Impacts of Marine Organic Emissions on Global Atmospheric Chemistry and Aerosols Using an Online-Coupled Meteorology and Chemistry Model, Atmospheric and Climate Sciences, 5, 266–274, doi:10.4236/acs.2015.53020, 2015.

Goldstein, A. H. and Galbally, I. E.: Known and unexplored organic consistuents in the Earth's atmosphere, Environ. Sci. Technol., 41, 1514, doi:10.1021/es072476p, 2007.

Groszko, W. and Moore, R. M.: A semipermeable membrane equilibrator for halomethanes in seawater, Chemosphere, 36, 3083–3092, doi:10.1016/S0045-6535(98)00019-8, 1998.

Guenther, A., Karl, T., Harley, P., Wiedinmyer, C., Palmer, P. I., and Geron, C.: Estimates of global terrestrial isoprene emissions using MEGAN (Model of Emissions of Gases and Aerosols from Nature), Atmospheric Chemistry and Physics, 6, 3181–3210, doi:10.5194/acp-6-3181-2006, 2006.

Guenther, A. B., Jiang, X., Heald, C. L., Sakulyanontvittaya, T., Duhl, T., Emmons, L. K., and Wang, X.: The model of emissions of gases and aerosols from nature version 2.1 (MEGAN2.1): An extended and updated framework for modeling biogenic emissions, Geoscientific Model Development, 5, 1471–1492, doi:10.5194/gmd-5-1471-2012, 2012.

Hakola, H., Hellén, H., Hemmilä, M., Rinne, J., and Kulmala, M.: In situ measurements of volatile organic compounds in a boreal forest, Atmospheric Chemistry and Physics, 12, 11 665–11 678, doi:10.5194/acp-12-11665-2012, 2012.

Hallquist, M., Wängberg, I., Ljungström, E., Barnes, I., and Becker, K.-H.: Aerosol and Product Yields from NO_3 Radical-Initiated Oxidation of Selected Monoterpenes, Environmental Science and Technology, 33, 553–559, doi:10.1021/es980292s, 1999.

Hallquist, M., Wenger, J. C., Baltensperger, U., Rudich, Y., Simpson, D., Claeys, M., Dommen, J., Donahue, N. M., George, C., Goldstein, A. H., Hamilton, J. F., Herrmann, H., Hoffmann, T., Iinuma, Y., Jang, M., Jenkin, M. E., Jimenez, J. L., Kiendler-Scharr, A., Maenhaut, W., McFiggans, G., Mentel, T. F., Monod, A., Prévôt, A. S. H., Seinfeld, J. H., Surratt, J. D., Szmigielski, R., and Wildt, J.: The formation, properties and impact of secondary organic aerosol: current and emerging issues, Atmospheric Chemistry and Physics, 9, 5155–5236, doi:10.5194/acp-9-5155-2009, 2009.

Harrison, S. P., Morfopoulos, C., Dani, K. G. S., Prentice, I. C., Arneth, A., Atwell, B. J., Barkley, M. P., Leishman, M. R., Loreto, F., Medlyn, B. E., Niinemets, U., Possell, M., Peñuelas, J., and Wright, I. J.: Volatile isoprenoid emissions from plastid to planet, New Phytologist, 197, 49–57, doi:10.1111/nph.12021, 2013.

Hashimoto, S., Toda, S., Suzuki, K., Kato, S., Narita, Y., Kurihara, M. K., Akatsuka, Y., Oda, H., Nagai, T., Nagao, I., Kudo, I., and Uematsu, M.: Production and air-sea flux of halomethanes in the western subarctic Pacific in relation to phytoplankton pigment concentrations during the iron fertilization experiment (SEEDS II), Deep-Sea Research Part II: Topical Studies in Oceanography, 56, 2928–2935, doi:10.1016/j.dsr2.2009.07.003, 2009.

Hays, G. C., Richardson, A. J., and Robinson, C.: Climate change and marine plankton, Trends in Ecology and Evolution, 20, 337–344, doi:10.1016/j.tree.2005.03.004, 2005.

Haywood, J. and Boucher, O.: Estimates of the direct and indirect radiative forcing due to tropospheric aerosols : a review, Reviews of Geophysics, 38, 513–543, 2000.

Heintzenberg, J., Birmili, W., Wiedensohler, A., Nowak, A., and Tuch, T.: Structure, variability and persistence of the submicrometre marine aerosol, Tellus, Series B: Chemical and Physical Meteorology, 56, 357–367, doi:10.1111/j.1600-0889.2004.00115.x, 2004.

Helmig, D.: Ozone Removal Techniques in the Sampling of Atmospheric Volatile Organic Trace Gases, Atmospheric Environment, 31, 3635–3651, 1997.

Henze, D. K. and Seinfeld, J. H.: Global secondary organic aerosol from isoprene oxidation, Geophysical Research Letters, 33, 6–9, doi:10.1029/2006GL025976, 2006.

Higgins, H. W., Wright, S. W., and Schlüter, L.: Quantitative interpretation of chemotaxonomic pigment data, in: Phytoplankton Pigments, edited by Roy, S., Llewellyn, C. A., Egeland, E. S., and Johnsen, G., chap. 6, pp. 257–313, Cambridge University Press, 2011.

Hoffmann, T. and Warnke, J.: Organic Aerosols, in: Volatile Organic Compounds in the Atmosphere, edited by Koppmann, R., chap. 9, pp. 342–387, Blackwell Publishing, 1st edn., 2007.

Hoffmann, T., Odum, J. R., Bowman, F., Collins, D., Klockow, D., Flagan, R. C., and Seinfeld, J. H.: Formation of organic aerosols from the oxidation of biogenic hydrocarbons, Journal of Atmospheric Chemistry, 26, 189–222, doi:10.1023/A:1005734301837, 1997.

Hopkins, J., Jones, I., Lewis, A. C., McQuaid, J., and Seakins, P.: Non-methane hydrocarbons in the Arctic boundary layer, Atmospheric Environment, 36, 3217–3229, doi:10.1016/S1352-2310(02)00324-2, URL http://linkinghub.elsevier.com/retrieve/pii/S1352231002003242, 2002.

Hopkins, J. R., Jones, C. E., and Lewis, A. C.: A dual channel gas chromatograph for atmospheric analysis of volatile organic compounds including oxygenated and monoterpene compounds., Journal of Environmental Monitoring, pp. 2268–2276, doi:10.1039/c1em10050e, 2011.

Hu, Q.-H., Xie, Z.-Q., Wang, X.-M., Kang, H., He, Q.-F., and Zhang, P.: Secondary organic aerosols over oceans via oxidation of isoprene and monoterpenes from Arctic to Antarctic, Scientific reports, 3, 2280, doi:10.1038/srep02280, 2013.

Ito, A. and Kawamiya, M.: Potential impact of ocean ecosystem changes due to global warming on marine organic carbon aerosols, Global Biogeochemical Cycles, 24, 1–10, doi:10.1029/2009GB003559, 2010.

Jardine, A. B., Jardine, K. J., Fuentes, J. D., Martin, S. T., Martins, G., Durgante, F., Carneiro, V., Higuchi, N., Manzi, A. O., and Chambers, J. Q.: Highly reactive light-dependent monoterpenes in the Amazon, Geophysical Research Letters, pp. 1576–1583, doi:10.1002/2014GL062573, 2015.

Jardine, K. J., Monson, R. K., Abrell, L., Saleska, S. R., Arneth, A., Jardine, A., Ishida, F. Y., Serrano, A. M. Y., Artaxo, P., Karl, T., Fares, S., Goldstein, A., Loreto, F., and Huxman, T.: Within-plant isoprene oxidation confirmed by direct emissions of oxidation products methyl vinyl ketone and methacrolein, Global Change Biology, 18, 973–984, doi:10.1111/j.1365-2486.2011.02610.x, 2012.

Jardine, K. J., Meyers, K., Abrell, L., Alves, E. G., Yanez Serrano, A. M., Kesselmeier, J., Karl, T., Guenther, A., Vickers, C., and Chambers, J. Q.: Emissions of putative isoprene oxidation products from mango branches under abiotic stress, Journal of Experimental Botany, 64, 3697–3709, doi:10.1093/jxb/ert202, 2013.

Jeffrey, S. W., Wright, S. W., and Zapata, M.: Microalgal classes and their signature pigments, in: Phytoplankton Pigments, edited by Roy, S., Llewellyn, C. A., Egeland, E. S., and Johnsen, G., chap. 1, pp. 3–77, Cambridge University Press, 2011.

Jenkin, M. E., Young, J. C., and Rickard, a. R.: The MCM v3.3 degradation scheme for isoprene, Atmospheric Chemistry and Physics Discussions, 15, 9709–9766, doi:10.5194/acpd-15-9709-2015, 2015.

Johnson, D. and Marston, G.: The gas-phase ozonolysis of unsaturated volatile organic compounds in the troposphere., Chemical Society Reviews, 37, 699–716, doi:10.1039/b704260b, 2008.

Johnson, J. E.: Evaluation of a seawater equilibrator for shipboard analysis of dissolved oceanic trace gases, Analytica Chimica Acta, 395, 119–132, doi:10.1016/S0003-2670(99)00361-X, 1999.

Johnson, M. T.: A numerical scheme to calculate temperature and salinity dependent air-water transfer velocities for any gas, Ocean Science, 6, 913–932, doi:10.5194/os-6-913-2010, 2010.

Jones, C. E., Hopkins, J. R., and Lewis, A. C.: In situ measurements of isoprene and

monoterpenes within a south-east Asian tropical rainforest, Atmospheric Chemistry and Physics, 11, 6971–6984, doi:10.5194/acp-11-6971-2011, 2011.

Kameyama, S., Tanimoto, H., Inomata, S., Tsunogai, U., Ooki, A., Takeda, S., Obata, H., Tsuda, A., and Uematsu, M.: High-resolution measurement of multiple volatile organic compounds dissolved in seawater using equilibrator inletproton transfer reaction-mass spectrometry (EIPTR-MS), Marine Chemistry, 122, 59–73, doi:10.1016/j.marchem.2010.08.003, 2010.

Kameyama, S., Yoshida, S., Tanimoto, H., Inomata, S., Suzuki, K., and Yoshikawa-Inoue, H.: High-resolution observations of dissolved isoprene in surface seawater in the Southern Ocean during austral summer 20102011, Journal of Oceanography, 70, 225–239, doi:10.1007/s10872-014-0226-8, 2014.

Karl, T., Harley, P., Emmons, L., Thornton, B., Guenther, A., Basu, C., Turnipseed, A., and Jardine, K.: Efficient Atmospheric Cleansing of Oxidized Organic Trace Gases by Vegetation, Science, 330, 816–819, doi:10.1126/science.1192534, 2010.

Kesselmeier, J. and Staudt, M.: Biogenic volatile organic compounds (VOC): An overview on emission, physiology and ecology, Journal of Atmospheric Chemistry, 33, 23–88, doi:10.1023/A:1006127516791, 1999.

Kettle, A., Rhee, T., Von Hobe, M., Poulton, A., Aiken, J., and Andreae, M.: Assessing the flux of different volatile sulfur gases from the ocean to the atmosphere, 106, doi:10.1029/2000JD900630, 2001.

Khalil, B. and Adamowski, J.: Record extension for short-gauged water quality parameters using a newly proposed robust version of the Line of Organic Correlation technique, Hydrology and Earth System Sciences, 16, 2253–2266, doi:10.5194/hess-16-2253-2012, 2012.

Kiendler-Scharr, A., Wildt, J., Dal Maso, M., Hohaus, T., Kleist, E., Mentel, T. F., Tillmann, R., Uerlings, R., Schurr, U., and Wahner, A.: New particle formation in forests inhibited by isoprene emissions., Nature, 461, 381–4, doi:10.1038/nature08292, 2009.

Kleindienst, T. E., Lewandowski, M., Offenberg, J. H., Jaoui, M., and Edney, E. O.:

Ozone-isoprene reaction: Re-examination of the formation of secondary organic aerosol, Geophysical Research Letters, 34, 1–6, doi:10.1029/2006GL027485, 2007.

Koren, I., Dagan, G., and Altaratz, O.: From aerosol-limited to invigoration of warm convective clouds, Science, 344, 1143–1146, doi:10.1126/science.1252595, 2014.

Korhonen, H., Carslaw, K. S., Forster, P. M., Mikkonen, S., Gordon, N. D., and Kokkola, H.: Aerosol climate feedback due to decadal increases in southern hemisphere wind speeds, Geophysical Research Letters, 37, 0–5, doi:10.1029/2009GL041320, 2010.

Krüger, O. and Graßl, H.: Southern Ocean phytoplankton increases cloud albedo and reduces precipitation, Geophysical Research Letters, 38, 1–5, doi:10.1029/2011GL047116, 2011.

Kulmala, M., Kontkanen, J., Junninen, H., Lehtipalo, K., Manninen, H. E., Nieminen, T., Petäjä, T., Sipilä, M., Schobesberger, S., Rantala, P., Franchin, A., Jokinen, T., Järvinen, E., Äijälä, M., Kangasluoma, J., Hakala, J., Aalto, P. P., Paasonen, P., Mikkilä, J., Vanhanen, J., Aalto, J., Hakola, H., Makkonen, U., Ruuskanen, T., Mauldin, R. L., Duplissy, J., Vehkamäki, H., Bäck, J., Kortelainen, A., Riipinen, I., Kurtén, T., Johnston, M. V., Smith, J. N., Ehn, M., Mentel, T. F., Lehtinen, K. E. J., Laaksonen, A., Kerminen, V.-M., and Worsnop, D. R.: Direct observations of atmospheric aerosol nucleation., Science, 339, 943–6, doi:10.1126/science.1227385, 2013.

Kurihara, M., Kimura, M., Iwamoto, Y., Narita, Y., Ooki, A., Eum, Y.-J., Tsuda, A., Suzuki, K., Tani, Y., Yokouchi, Y., Uematsu, M., and Hashimoto, S.: Distributions of short-lived iodocarbons and biogenic trace gases in the open ocean and atmosphere in the western North Pacific, Marine Chemistry, 118, 156–170, doi:10.1016/j.marchem.2009.12.001, 2010.

Kurihara, M., Iseda, M., Ioriya, T., Horimoto, N., Kanda, J., Ishimaru, T., Yamaguchi, Y., and Hashimoto, S.: Brominated methane compounds and isoprene in surface seawater of Sagami Bay: Concentrations, fluxes, and relationships with phytoplankton assemblages, Marine Chemistry, 134-135, 71–79, doi:10.1016/j.marchem.2012.04.001, 2012.

Laaksonen, A., Kulmala, M., O'Dowd, C. D., Joutsensaari, J., Vaattovaara, P., Mikkonen, S., Lehtinen, K. E. J., Sogacheva, L., Dal Maso, M., Aalto, P., Petäjä, T., Sogachev, A., Jun Yoon, Y., Lihavainen, H., Nilsson, D., Cristina Facchini, M., Cavalli, F., Fuzzi, S.,

Hoffmann, T., Arnold, F., Hanke, M., Sellegri, K., Umann, B., Junkermann, W., Coe, H., Allan, J. D., Rami Alfarra, M., Worsnop, D. R., Riekkola, M.-L., Hyötyläinen, T., and Viisanen, Y.: The role of VOC oxidation products in continental new particle formation, Atmospheric Chemistry and Physics, 8, 2657–2665, doi:10.5194/acp-8-2657-2008, 2008.

Law, C. S., Brévière, E., De Leeuw, G., Garçon, V., Guieu, C., Kieber, D. J., Kontradowitz, S., Paulmier, A., Quinn, P. K., Saltzman, E. S., Stefels, J., and Von Glasow, R.: Evolving research directions in Surface Ocean-Lower Atmosphere (SOLAS) science, Environmental Chemistry, 10, 1–16, doi:10.1071/EN12159, 2013.

Lawson, S. J., Galbally, I., Dunne, E., and Gras, J.: Measurement of VOCs in marine air at Cape Grim using Proton Transfer Reaction-Mass Spectrometry (PTR-MS), in: Baseline Atmospheric Program (Australia) 2007-2008 - Cape Grim, edited by Derek, N. and Krummel, P. B., pp. 23–32, 2011.

Lawson, S. J., Selleck, P. W., Galbally, I. E., Keywood, M. D., Harvey, M. J., Lerot, C., Helmig, D., and Ristovski, Z.: Seasonal in situ observations of glyoxal and methylglyoxal over the temperate oceans of the Southern Hemisphere, Atmospheric Chemistry and Physics, 15, 223–240, doi:10.5194/acp-15-223-2015, 2015.

Leck, C. and Bigg, E. K.: A modified aerosolcloudclimate feedback hypothesis, Environmental Chemistry, 4, 400, doi:10.1071/EN07061, 2007.

Lee, A., Schade, G. W., Holzinger, R., and Goldstein, A. H.: A comparison of new measurements of total monoterpene flux with improved measurements of speciated monoterpene flux, Atmospheric Chemistry and Physics, 5, 505–513, doi:10.5194/acp-5-505-2005, 2005.

Lee, A., Goldstein, A. H., Kroll, J. H., Ng, N. L., Varutbangkul, V., Flagan, R. C., and Seinfeld, J. H.: Gas-phase products and secondary aerosol yields from the ozonolysis of ten different terpenes, Journal of Geophysical Research: Atmospheres, 111, 1–18, doi:10.1029/2006JD007050, 2006a.

Lee, A., Goldstein, A. H., Kroll, J. H., Ng, N. L., Varutbangkul, V., Flagan, R. C., and Seinfeld, J. H.: Gas-phase products and secondary aerosol yields from the photooxidation of 16 different terpenes, Journal of Geophysical Research: Atmospheres, 111, 1–25, doi:10.1029/2006JD007050, 2006b.

Leng, C., Kish, J. D., Kelley, J., Mach, M., Hiltner, J., Zhang, Y., and Liu, Y.: Temperature-dependent Henry's law constants of atmospheric organics of biogenic origin, Journal of Physical Chemistry A, 117, 10 359–10 367, doi:10.1021/jp403603z, 2013.

Lewis, A. C., Bartle, K. D., Heard, D. E., McQuaid, J. B., Pilling, M. J., and Seakins, P. W.: In situ, gas chromatographic measurements of non-methane hydrocarbons and dimethyl sulfide at a remote coastal location (Mace Head, Eire) July-August 1996, J. Chem. Soc., Faraday Trans., 93, 2921–2927, doi:10.1039/A701566F, URL http://eprints.whiterose.ac.uk/48683/, 1997a.

Lewis, A. C., Bartle, K. D., and Rattner, L.: High-Speed Isothermal Analysis of Atmospheric Isoprene and DMS Using On-Line Two-Dimensional Gas Chromatography, Environmental Science & Technology, 31, 3209–3217, doi:10.1021/es970194r, 1997b.

Lewis, A. C., Carpenter, L. J., and Pilling, M. J.: Nonmethane hydrocarbons in Southern Ocean boundary layer air, Journal of Geophysical Research, 106, 4987–4994, 2001.

Liakakou, E., Vrekoussis, M., Bonsang, B., Donousis, C., Kanakidou, M., and Mihalopoulos, N.: Isoprene above the Eastern Mediterranean: Seasonal variation and contribution to the oxidation capacity of the atmosphere, Atmospheric Environment, 41, 1002–1010, doi:10.1016/j.atmosenv.2006.09.034, 2007.

Liang, Q., Newman, P. a., Daniel, J. S., Reimann, S., Hall, B. D., Dutton, G., and Kuijpers, L. J. M.: Constraining the carbon tetrachloride (CCl4) budget using its global trend and inter-hemispheric gradient, Geophysical Research Letters, 41, 5307–5315, doi:10.1002/2014GL060754, 2014.

Libes, S. M.: An Introduction to Marine Biogeochemistry, John Wiley & Sons, Inc., 1992.

Lichtenthaler, H. K.: Biosynthesis and Accumulation of Isoprenoid Carotenoids and Chlorophylls and Emission of Isoprene by Leaf Chloroplasts, Bulletin of the Georgian National Academy of Sciences, 3, 81–94, 2009.

Liss, P. S. and Merlivat, L.: Air-sea gas exchange rates: Introduction and synthesis, in: The Role of Air-Sea Exchange in Geochemical Cycling, edited by Buat-Ménard, P., pp. 113–127, Srpinger, New York, 1986.

Liss, P. S. and Slater, P. G.: Flux of Gases across the Air-Sea Interface, Nature, 247, 181–184, doi:10.1038/247181a0, 1974.

Liss, P. S., Marandino, C. A., Dahl, E. E., Helmig, D., Hintsa, E. J., Hughes, C., Johnson, M. T., Moore, R. M., Plane, J. M. C., Quack, B., Singh, H. B., Stefels, J., von Glasow, R., and Williams, J.: Short-lived Trace Gases in the Surface Ocean and the Atmosphere, in: Ocean-Atmosphere Interactions of Gases and Particles, edited by Liss, P. S. and Johnson, M. T., chap. 1, pp. 1–54, Springer Berlin Heidelberg, doi: 10.1007/978-3-642-25643-1_1, 2014.

Longhurst, A. R.: Ecological Geography of the Sea, Academic Press, Burlington, 2 edn., URL http://www.sciencedirect.com/science/book/9780124555211, 2007.

Loreto, F. and Fineschi, S.: Reconciling functions and evolution of isoprene emission in higher plants, New Phytologist, 206, 578–582, doi:10.1111/nph.13242, 2015.

Luo, G. and Yu, F.: A numerical evaluation of global oceanic emissions of α-pinene and isoprene, Atmospheric Chemistry and Physics, 10, 2007–2015, 2010.

Mackey, M. D., Mackey, D. J., Higgins, H. W., and Wright, S. W.: CHEMTAX - A program for estimating class abundances from chemical markers: Application to HPLC measurements of phytoplankton, Marine Ecology Progress Series, 144, 265–283, doi: 10.3354/meps144265, 1996.

Mahajan, A. S., Prados-Román, C., Hay, T. D., Lampel, J., Pöhler, D., Groß mann, K., Tschritter, J., Frieß, U., Platt, U., Johnston, P., Kreher, K., Wittrock, F., Burrows, J. P., Plane, J. M. C., and Saiz-Lopez, A.: Glyoxal observations in the global marine boundary layer, Journal of Geophysical Research : Atmospheres, pp. 1–10, doi:10.1002/2013JD021388, 2014.

Mather, R. L., Reynolds, S. E., Wolff, G. A., Williams, R. G., Torres-Valdes, S., Woodward, E. M. S., Landolfi, A., Pan, X., Sanders, R., and Achterberg, E. P.: Phosphorus cycling in the North and South Atlantic Ocean subtropical gyres, Nature Geoscience, 1, 439–443, doi:10.1038/ngeo232, 2008.

Matsunaga, S., Mochida, M., Saito, T., and Kawamura, K.: In situ measurement of isoprene in the marine air and surface seawater from the western North Pacific, Atmospheric Environment, 36, 6051–6057, 2002.

Meskhidze, N. and Nenes, A.: Phytoplankton and cloudiness in the Southern Ocean., Science, 314, 1419–23, doi:10.1126/science.1131779, 2006.

Meskhidze, N. and Nenes, A.: Isoprene, cloud droplets, and phytoplankton - Response, Science, 317, 42–43, URL http://www.sciencemag.org/content/317/5834/42.2, 2007.

Meskhidze, N. and Nenes, A.: Effects of Ocean Ecosystem on Marine Aerosol-Cloud Interaction, Advances in Meteorology, 2010, 1–13, doi:10.1155/2010/239808, 2010.

Meskhidze, N., Xu, J., Gantt, B., Zhang, Y., Nenes, A., Ghan, S. J., Liu, X., Easter, R., and Zaveri, R.: Global distribution and climate forcing of marine organic aerosol: 1. Model improvements and evaluation, Atmospheric Chemistry and Physics, 11, 11 689–11 705, doi:10.5194/acp-11-11689-2011, 2011.

Meskhidze, N., Sabolis, A., Reed, R., and Kamykowski, D.: Quantifying environmental stress-induced emissions of algal isoprene and monoterpenes using laboratory measurements, Biogeosciences, 12, 637–651, doi:10.5194/bg-12-637-2015, 2015.

Metzger, A., Verheggen, B., Dommen, J., Duplissy, J., Prevot, A. S. H., Weingartner, E., Riipinen, I., Kulmala, M., Spracklen, D. V., Carslaw, K. S., and Baltensperger, U.: Evidence for the role of organics in aerosol particle formation under atmospheric conditions., Proceedings of the National Academy of Sciences of the United States of America, 107, 6646–51, doi:10.1073/pnas.0911330107, 2010.

Miller, M. A. and Yuter, S. E.: Lack of correlation between chlorophyll a and cloud droplet effective radius in shallow marine clouds, Geophysical Research Letters, 35, 1–7, doi:10.1029/2008GL034354, 2008.

Milne, P. J., Riemer, D. D., Zika, R. G., and Brand, L. E.: Measurement of vertical distribution of isoprene in surface seawater, its chemical fate, and its emission from several phytoplankton monocultures, Marine Chemistry, 48, 237–244, doi:10.1016/0304-4203(94)00059-M, 1995.

Monson, R. K., Jones, R. T., Rosenstiel, T. N., and Schnitzler, J. P.: Why only some plants emit isoprene, Plant, Cell and Environment, 36, 503–516, doi:10.1111/pce.12015, 2013.

Moore, R. and Wang, L.: The influence of iron fertilization on the fluxes of methyl halides and isoprene from ocean to atmosphere in the SERIES experiment, Deep-Sea Research Part II: Topical Studies in Oceanography, 53, 2398–2409, doi:10.1016/j.dsr2.2006.05.025, 2006.

Moore, R. M., Oram, D. E., and Penkett, S. A.: Production of isoprene by marine phytoplankton cultures, Geophysical Research Letters, 21, 2507–2510, 1994.

Myhre, G., Shindell, D., Bréon, F.-M., Collins, W., Fuglestvedt, J., Huang, J., Koch, D., Lamarque, J.-F., Lee, D., Mendoza, B., Nakajima, T., Robock, A., Stephens, G., Takemura, T., and Zhang, H.: Anthropogenic and Natural Radiative Forcing, in: Climate Change 2013: The Physical Science Basis. Contribution of Working Group I to the Fifth Assessment Report of the Intergovernmental Panel on Climate Change, edited by Stocker, T., Qin, D., Plattner, G.-K., Tignor, M., Allen, S., Boschung, J., Nauels, A., Xia, Y., Bex, V., and Midgley, P., chap. 8, 2013.

Myriokefalitakis, S., Vignati, E., Tsigaridis, K., Papadimas, C., Sciare, J., Mihalopoulos, N., Facchini, M. C., Rinaldi, M., Dentener, F. J., Ceburnis, D., Hatzianastasiou, N., O'Dowd, C. D., van Weele, M., and Kanakidou, M.: Global Modeling of the Oceanic Source of Organic Aerosols, Advances in Meteorology, 2010, 1–16, doi:10.1155/2010/939171, 2010.

Ng, N. L., Chhabra, P. S., Chan, A. W. H., Surratt, J. D., Kroll, J. H., Kwan, a. J., McCabe, D. C., Wennberg, P. O., Sorooshian, A., Murphy, S. M., Dalleska, N. F., Flagan, R. C., and Seinfeld, J. H.: Effect of NOx level on secondary organic aerosol (SOA) formation from the photooxidation of terpenes, Atmospheric Chemistry and Physics, 7, 5159–5174, doi:10.5194/acp-7-5159-2007, 2007.

Ng, N. L., Kwan, A. J., Surratt, J. D., Chan, a. W. H., Chhabra, P. S., Sorooshian, A., Pye, H. O. T., Crounse, J. D., Wennberg, P. O., Flagan, R. C., and Seinfeld, J. H.: Secondary organic aerosol (SOA) formation from reaction of isoprene with nitrate radicals (NO3), Atmospheric Chemistry and Physics, 8, 4117–4140, doi:10.5194/acp-8-4117-2008, 2008.

Nightingale, P. D., Malin, G., Law, C. S., Watson, A. J., Liss, P. S., Liddicoat, M. I., Boutin, J., and Upstill-Goddard, R. C.: In situ evaluation of air-sea gas exchange parameterizations using novel conservative and volatile tracers, Global Biogeochemical Cycles, 14, 373–387, 2000.

Niinemets, U., Fares, S., Harley, P., and Jardine, K. J.: Bidirectional exchange of biogenic volatiles with vegetation: Emission sources, reactions, breakdown and deposition, Plant, Cell and Environment, 37, 1790–1809, doi:10.1111/pce.12322, 2014.

O'Dowd, C., Monahan, C., and Dall'Osto, M.: On the occurrence of open ocean particle production and growth events, Geophysical Research Letters, 37, 2–6, doi: 10.1029/2010GL044679, 2010.

O'Dowd, C. D. and de Leeuw, G.: Marine aerosol production: a review of the current knowledge., Philosophical transactions. Series A, Mathematical, physical, and engineering sciences, 365, 1753–74, doi:10.1098/rsta.2007.2043, 2007.

O'Dowd, C. D., Facchini, M. C., Cavalli, F., Ceburnis, D., Mircea, M., Decesari, S., Fuzzi, S., Yoon, Y. J., and Putaud, J.-P.: Biogenically driven organic contribution to marine aerosol., Nature, 431, 676–680, doi:10.1038/nature02959, 2004.

Omori, Y., Tanimoto, H., Inomata, S., Kameyama, S., Takao, S., and Suzuki, K.: Evaluation of using unfiltered seawater for underway measurement of dimethyl sulfide in the ocean by online mass spectrometry, Limnology and Oceanography: Methods, 11, 549–560, doi:10.4319/lom.2013.11.549, 2013.

Ooki, A. and Yokouchi, Y.: Development of a silicone membrane tube equilibrator for measuring partial pressures of volatile organic compounds in natural water, Environmental Science and Technology, 42, 5706–5711, doi:10.1021/es800912j, 2008.

Ooki, A. and Yokouchi, Y.: Determination of Henry's law constant of halocarbons in seawater and analysis of sea-to-air flux of iodoethane (C_2H_5I) in the Indian and Southern oceans based on partial pressure measurements, Geochemical Journal, 45, e1–e7, 2011.

Ooki, A., Nomura, D., Nishino, S., Kikuchi, T., and Yokouchi, Y.: A global-scale map of isoprene and volatile organic iodine in surface seawater of the Arctic, Northwest Pacific, Indian, and Southern Oceans, Journal of Geophysical Research: Oceans, pp. 1–21, doi:10.1002/2014JC010519, 2015.

Oppo, D. W. and Curry, W. B.: Deep Atlantic Circulation During the Last Glacial Maximum and Deglaciation, Nature Education Knowledge, 3, 2012.

Owen, S. M. and Peñuelas, J.: Opportunistic emissions of volatile isoprenoids., Trends in Plant Science, 10, 420–6, doi:10.1016/j.tplants.2005.07.010, 2005.

Pacifico, F., Harrison, S., Jones, C., and Sitch, S.: Isoprene emissions and climate, Atmospheric Environment, 43, 6121–6135, doi:10.1016/j.atmosenv.2009.09.002, 2009.

Palmer, P. I. and Shaw, S. L.: Quantifying global marine isoprene fluxes using MODIS chlorophyll observations, Geophysical Research Letters, 32, 1–5, doi:10.1029/2005GL022592, 2005.

Pathak, R. K., Stanier, C. O., Donahue, N. M., and Pandis, S. N.: Ozonolysis of α-pinene at atmospherically relevant concentrations: Temperature dependence of aerosol mass fractions (yields), Journal of Geophysical Research: Atmospheres, 112, 1–8, doi:10.1029/2006JD007436, 2007.

Peeters, J., Müller, J.-F., Stavrakou, T., and Nguyen, V. S.: Hydroxyl Radical Recycling in Isoprene Oxidation Driven by Hydrogen Bonding and Hydrogen Tunneling: the Upgraded LIM1 Mechanism, The Journal of Physical Chemistry A, 118, 8625–8643, doi:10.1021/jp5033146, 2014.

Pichersky, E., Sharkey, T. D., and Gershenzon, J.: Plant volatiles: a lack of function or a lack of knowledge?, Trends in Plant Science, 11, 421, doi:10.1016/j.tplants.2006.07.007, 2006.

Pirjola, L., O'Dowd, C. D., Brooks, I. M., and Kulmala, M.: Can new particle formation occur in the clean marine boundary layer?, Journal of Geophysical Research, 105, 26 531, doi:10.1029/2000JD900310, 2000.

Plass-Dülmer, C., Michl, K., Ruf, R., and Berresheim, H.: C2 - C8 Hydrocarbon measurement and quality control procedures at the Global Atmosphere Watch Observatory Hohenpeissenberg, Journal of Chromatography A, 953, 175–197, 2002.

Presto, A. A., Hartz, K. E. H., and Donahue, N. M.: Secondary organic aerosol production from terpene ozonolysis. 1. Effect of UV radiation., Environmental science & technology, 39, 7036–7045, doi:10.1021/es050174m, 2005a.

Presto, A. A., Huff Hartz, K. E., and Donahue, N. M.: Secondary organic aerosol production from terpene ozonolysis. 2. Effect of NOx concentration, Environmental Science and Technology, 39, 7046–7054, doi:10.1021/es050400s, 2005b.

Quay, P. D., Peacock, C., Bjrkman, K., and Karl, D. M.: Measuring primary production rates in the ocean: Enigmatic results between incubation and non-incubation methods at Station ALOHA, Global Biogeochemical Cycles, 24, 1–14, doi:10.1029/2009GB003665, 2010.

Quinn, P. K. and Bates, T. S.: The case against climate regulation via oceanic phytoplankton sulphur emissions, Nature, 480, 51–56, doi:10.1038/nature10580, 2011.

Quinn, P. K., Collins, D. B., Grassian, V. H., Prather, K. a., and Bates, T. S.: Chemistry and Related Properties of Freshly Emitted Sea Spray Aerosol, Chemical Reviews, p. 150406123611007, doi:10.1021/cr500713g, 2015.

Ratte, M., Plass-Dülmer, C., Koppmann, R., Rudolph, J., and Denga, J.: Production mechanism of C2-C4 hydrocarbons in seawater: Field measurements and experiments, Global Biogeochemical Cycles, 7, 369–378, doi:10.1029/93GB00054, 1993.

Reygondeau, G., Longhurst, A., Martinez, E., Beaugrand, G., Antoine, D., and Maury, O.: Dynamic biogeochemical provinces in the global ocean, Global Biogeochemical Cycles, 27, 1046–1058, doi:10.1002/gbc.20089, 2013.

Riccobono, F., Schobesberger, S., Scott, C. E., Dommen, J., Ortega, I. K., Rondo, L., Almeida, J. a., Amorim, A., Bianchi, F., Breitenlechner, M., David, A., Downard, A., Dunne, E. M., Duplissy, J., Ehrhart, S., Flagan, R. C., Franchin, A., Hansel, A., Junninen, H., Kajos, M., Keskinen, H., Kupc, A., Kürten, A., Kvashin, A. N., Laaksonen, A., Lehtipalo, K., Makhmutov, V., Mathot, S., Nieminen, T., Onnela, A., Petäjä, T., Praplan, A. P., Santos, F. D., Schallhart, S., Seinfeld, J. H., Sipilä, M., Spracklen, D. V., Stozhkov, Y., Stratmann, F., Tomé, A., Tsagkogeorgas, G., Vaattovaara, P., Viisanen, Y., Vrtala, A., Wagner, P. E., Weingartner, E., Wex, H., Wimmer, D., Carslaw, K. S., Curtius, J., Donahue, N. M., Kirkby, J., Kulmala, M., Worsnop, D. R., and Baltensperger, U.: Oxidation products of biogenic emissions contribute to nucleation of atmospheric particles, Science, 344, 717–21, doi:10.1126/science.1243527, 2014.

Robinson, C., Poulton, A. J., Holligan, P. M., Baker, A. R., Forster, G., Gist, N., Jickells, T. D., Malin, G., Upstill-Goddard, R., Williams, R. G., Woodward, E. M. S., and Zubkov, M. V.: The Atlantic Meridional Transect (AMT) Programme: A contextual view 1995-2005, Deep-Sea Research Part II: Topical Studies in Oceanography, 53, 1485–1515, doi:10.1016/j.dsr2.2006.05.015, 2006.

Robinson, C., Tilstone, G. H., Rees, A. P., Smyth, T. J., Fishwick, J. R., Tarran, G. A., Luz, B., Barkan, E., and David, E.: Comparison of in vitro and in situ plankton production determinations, Aquatic Microbial Ecology, 54, 13–34, doi:10.3354/ame01250, 2009.

Rodríguez, F., Chauton, M., Johnsen, G., Andresen, K., Olsen, L. M., and Zapata, M.: Photoacclimation in phytoplankton: Implications for biomass estimates, pigment functionality and chemotaxonomy, Marine Biology, 148, 963–971, doi:10.1007/s00227-005-0138-7, 2006.

Roelofs, G. J.: A GCM study of organic matter in marine aerosol and its potential contribution to cloud drop activation, Atmospheric Chemistry and Physics, 8, 709–719, doi:10.5194/acp-8-709-2008, 2008.

Rollins, A. W., Kiendler-Scharr, A., Fry, J., Brauers, T., Brown, S. S., Dorn, H.-P., Dubé, W. P., Fuchs, H., Mensah, A., Mentel, T. F., Rohrer, F., Tillmann, R., Wegener, R., Wooldridge, P. J., and Cohen, R. C.: Isoprene oxidation by nitrate radical: alkyl nitrate and secondary organic aerosol yields, Atmospheric Chemistry and Physics, 9, 6685–6703, doi:10.5194/acp-9-6685-2009, 2009.

Rosenfeld, D., Sherwood, S., Wood, R., and Donner, L.: Climate Effects of Aerosol-Cloud Interactions, Science, 343, 379–380, doi:10.1126/science.1247490, 2014.

Sabolis, A. W.: Quantifying Marine Emissions of Biogenic Volatile Organic Compounds Using Laboratory Measurements, Field Measurements and Remote Sensing Data, MSc thesis, North Carolina State University, 2010.

Saltzman, E. S.: Marine Aerosols, in: Surface Ocean-Lower Atmosphere Processes, edited by Le Quéré, C. and Saltzman, E. C., pp. 17–36, American Geophysical Union, Washington, 2009.

Sanadze, G. A.: Biogenic isoprene (a review), Russian Journal of Plant Physiology, 51, 729–741, doi:10.1023/B:RUPP.0000047821.63354.a4, 2004.

Sander, R.: Compilation of Henry's law constants (version 4.0) for water as solvent, Atmospheric Chemistry and Physics, 15, 4399–4981, doi:10.5194/acp-15-4399-2015, 2015.

Schlitzer, R.: Ocean Data View, URL http://odv.awi.de, 2015.

Serret, P., Robinson, C., Aranguren-Gassis, M., García-Martín, E. E., Gist, N., Kitidis, V., Lozano, J., Stephens, J., Harris, C., and Thomas, R.: Both respiration and photosynthesis determine the scaling of plankton metabolism in the oligotrophic ocean, Nature Communications, 6, 6961, doi:10.1038/ncomms7961, 2015.

Sharkey, T. D.: Is it useful to ask why plants emit isoprene?, Plant, Cell and Environment, 36, 517–520, doi:10.1111/pce.12038, 2013.

Sharkey, T. D. and Monson, R. K.: The future of isoprene emission from leaves, canopies and landscapes, Plant, Cell and Environment, 37, 1727–1740, doi:10.1111/pce.12289, 2014.

Sharkey, T. D. and Yeh, S.: Isoprene Emission from Plants, Annual Review of Plant Physiology and Plant Molecular Biology, 52, 407–36, 2001.

Sharkey, T. D., Wiberley, A. E., and Donohue, A. R.: Isoprene emission from plants: why and how., Annals of Botany, 101, 5–18, doi:10.1093/aob/mcm240, 2008.

Sharkey, T. D., Gray, D. W., Pell, H. K., Breneman, S. R., and Topper, L.: Isoprene synthase genes form a monophyletic clade of acyclic terpene synthases in the Tps-b terpene synthase family, Evolution, 67, 1026–1040, doi:10.1111/evo.12013, 2013.

Shaw, S. L.: The Production of Non-Methane Hydrocarbons by Marine Plankton, Ph.D. thesis, MIT, 2001.

Shaw, S. L., Chisholm, S. W., and Prinn, R. G.: Isoprene production by *Prochlorococcus*, a marine cyanobacterium, and other phytoplankton, Marine Chemistry, 80, 227–245, doi:10.1016/S0304-4203(02)00101-9, 2003.

Shaw, S. L., Gantt, B., and Meskhidze, N.: Production and Emissions of Marine Isoprene and Monoterpenes: A Review, Advances in Meteorology, pp. 1–24, doi:10.1155/2010/408696, 2010.

Sherwen, T., Evans, M. J., Carpenter, L. J., Andrews, S. J., Lidster, R. T., Dix, B., Koenig, T. K., Volkamer, R., Saiz-Lopez, A., Prados-Roman, C., Mahajan, A. S., and Ordóñez, C.: Iodine's impact on tropospheric oxidants: a global model study in GEOS-Chem, Atmospheric Chemistry and Physics Discussions, 15, 20 957–21 023, doi:10.5194/acpd-15-20957-2015, 2015.

Sigman, D. M. and Hain, M. P.: The Biological Productivity of the Ocean, Nature Education Knowledge, 3, URL http://www.nature.com/scitable/knowledge/library/the-biological-productivity-of-the-ocean-70631104, 2012.

Sinha, V., Williams, J., Meyerhöfer, M., Riebesell, U., Paulino, A. I., and Larsen, A.: Air-sea fluxes of methanol, acetone, acetaldehyde, isoprene and DMS from a Norwegian fjord following a phytoplankton bloom in a mesocosm experiment, Atmospheric Chemistry and Physics, 7, 739–755, doi:10.5194/acp-7-739-2007, 2007.

Sinreich, R., Coburn, S., Dix, B., and Volkamer, R.: Ship-based detection of glyoxal over the remote tropical Pacific Ocean, Atmospheric Chemistry and Physics, 10, 11 359–11 371, doi:10.5194/acp-10-11359-2010, 2010.

Skoog, D. A., West, D. M., Holler, F. J., and Crouch, S. R.: Fundamentals of Analytical Chemistry, Thomson Brooks/Cole, 8th edn., 2004.

SOLAS Scientific Steering Committee and Emilie Brévière (Editors): SOLAS 2015-2025: Science Plan and Organisation, Tech. rep., SOLAS International Project Office, Kiel, 2015.

Spittler, M., Barnes, I., Bejan, I., Brockmann, K. J., Benter, T., and Wirtz, K.: Reactions of NO_3 radicals with limonene and α-pinene: Product and SOA formation, Atmospheric Environment, 40, 116–127, doi:10.1016/j.atmosenv.2005.09.093, 2006.

Spracklen, D. V., Arnold, S. R., Sciare, J., Carslaw, K. S., and Pio, C.: Globally significant oceanic source of organic carbon aerosol, Geophysical Research Letters, 35, 1–5, doi:10.1029/2008GL033359, 2008.

Surratt, J. D., Chan, A. W. H., Eddingsaas, N. C., Chan, M., Loza, C. L., Kwan, A. J., Hersey, S. P., Flagan, R. C., Wennberg, P. O., and Seinfeld, J. H.: Reactive intermediates revealed in secondary organic aerosol formation from isoprene., Proceedings of the National Academy of Sciences of the United States of America, 107, 6640–6645, doi:10.1073/pnas.0911114107, 2010.

Tokarczyk, R. and Moore, R. M.: Production of volatile organohalogens by phytoplankton cultures, Geophysical Research Letters, 21, 285–288, doi:10.1029/94GL00009, 1994.

Tovar-Sánchez, A., Duarte, C. M., Alonso, J. C., Lacorte, S., Tauler, R., and Galbán-Malagón, C.: Impacts of metals and nutrients released from melting multiyear Arctic sea ice, Journal of Geophysical Research, 115, 1–7, doi:10.1029/2009JC005685, 2010.

Tran, S., Bonsang, B., Gros, V., Peeken, I., Sarda-Esteve, R., Bernhardt, A., and Belviso, S.: A survey of carbon monoxide and non-methane hydrocarbons in the Arctic Ocean

during summer 2010, Biogeosciences, 10, 1909–1935, doi:10.5194/bg-10-1909-2013, 2013.

Tsigaridis, K., Daskalakis, N., Kanakidou, M., Adams, P. J., Artaxo, P., Bahadur, R., Balkanski, Y., Bauer, S. E., Bellouin, N., Benedetti, A., Bergman, T., Berntsen, T. K., Beukes, J. P., Bian, H., Carslaw, K. S., Chin, M., Curci, G., Diehl, T., Easter, R. C., Ghan, S. J., Gong, S. L., Hodzic, A., Hoyle, C. R., Iversen, T., Jathar, S., Jimenez, J. L., Kaiser, J. W., Kirkevå g, A., Koch, D., Kokkola, H., Lee, Y. H., Lin, G., Liu, X., Luo, G., Ma, X., Mann, G. W., Mihalopoulos, N., Morcrette, J.-J., Müller, J.-F., Myhre, G., Myriokefalitakis, S., Ng, S., O'Donnell, D., Penner, J. E., Pozzoli, L., Pringle, K. J., Russell, L. M., Schulz, M., Sciare, J., Seland, O., Shindell, D. T., Sillman, S., Skeie, R. B., Spracklen, D., Stavrakou, T., Steenrod, S. D., Takemura, T., Tiitta, P., Tilmes, S., Tost, H., van Noije, T., van Zyl, P. G., von Salzen, K., Yu, F., Wang, Z., Zaveri, R. a., Zhang, H., Zhang, K., Zhang, Q., and Zhang, X.: The AeroCom evaluation and intercomparison of organic aerosol in global models, Atmospheric Chemistry and Physics, 14, 10 845–10 895, doi:10.5194/acp-14-10845-2014, 2014.

Twomey, S.: The Influence of Pollution on the Shortwave Albedo of Clouds, doi:10.1175/1520-0469(1977)034⟨1149:TIOPOT⟩2.0.CO;2, 1977.

UNEP: The Montreal Protocol on Substances that Deplete the Ozone Layer, URL http://ozone.unep.org/en/handbook-montreal-protocol-substances-deplete-ozone-layer/5, 1987.

van Pinxteren, M. and Herrmann, H.: Glyoxal and methylglyoxal in Atlantic seawater and marine aerosol particles: Method development and first application during the polarstern cruise ANT XXVII/4, Atmospheric Chemistry and Physics, 13, 11 791–11 802, doi:10.5194/acp-13-11791-2013, 2013.

Vaughan, S., Ingham, T., Whalley, L. K., Stone, D., Evans, M. J., Read, K. A., Lee, J. D., Moller, S. J., Carpenter, L. J., Lewis, A. C., Fleming, Z. L., and Heard, D. E.: Seasonal observations of OH and HO_2 in the remote tropical marine boundary layer, Atmospheric Chemistry and Physics, 12, 2149–2172, doi:10.5194/acp-12-2149-2012, 2012.

Velikova, V. and Loreto, F.: On the relationship between isoprene emission and thermotolerance in *Phragmites australis* leaves exposed to high temperatures and dur-

ing the recovery from a heat stress, Plant, Cell and Environment, 28, 318–327, doi: 10.1111/j.1365-3040.2004.01314.x, 2005.

Velikova, V., Sharkey, T. D., and Loreto, F.: Stabilization of thylakoid membranes in isoprene-emitting plants reduces formation of reactive oxygen species, Plant Signaling & Behavior, 7, 139–141, doi:10.4161/psb.7.1.18521, 2012.

Vichi, M., Allen, J. I., Masina, S., and Hardman-Mountford, N. J.: The emergence of ocean biogeochemical provinces: A quantitative assessment and a diagnostic for model evaluation, Global Biogeochemical Cycles, 25, 1–17, doi:10.1029/2010GB003867, 2011.

Vickers, C. E., Gershenzon, J., Lerdau, M. T., and Loreto, F.: A unified mechanism of action for volatile isoprenoids in plant abiotic stress., Nature chemical biology, 5, 283–91, doi:10.1038/nchembio.158, 2009.

Vickers, D. and Mahrt, L.: Quality control and flux sampling problems for tower and aircraft data, Journal of Atmospheric and Oceanic Technology, 14, 512–526, doi:10.1175/1520-0426(1997)014⟨0512:QCAFSP⟩2.0.CO;2, 1997.

Vignati, E., Facchini, M. C., Rinaldi, M., Scannell, C., Ceburnis, D., Sciare, J., Kanakidou, M., Myriokefalitakis, S., Dentener, F., and O'Dowd, C. D.: Global scale emission and distribution of sea-spray aerosol: Sea-salt and organic enrichment, Atmospheric Environment, 44, 670–677, doi:10.1016/j.atmosenv.2009.11.013, 2010.

von Glasow, R.: A look at the CLAW hypothesis from an atmospheric chemistry point of view, Environmental Chemistry, 4, 379, doi:10.1071/EN07064, 2007.

Wanninkhof, R.: Relationship Between Wind Speed and Gas Exchange, Journal of Geophysical Research, 97, 7373–7382, doi:10.1029/92JC00188, 1992.

Welschmeyer, N. A.: Fluorometric analysis of chlorophyll a in the presence of chlorophyll b and pheopigments, Limnology and Oceanography, 39, 1985–1992, doi:10.4319/lo.1994.39.8.1985, 1994.

Went, F. W.: Blue Hazes in the Atmosphere, Nature, 187, 641–643, doi:10.1038/187641a0, 1960.

Williams, J., Custer, T., Riede, H., Sander, R., Jöckel, P., Hoor, P., Pozzer, A., Wong-Zehnpfennig, S., Hosaynali Beygi, Z., Fischer, H., Gros, V., Colomb, A., Bonsang, B.,

Yassaa, N., Peeken, I., Atlas, E. L., Waluda, C. M., van Aardenne, J. A., and Lelieveld, J.: Assessing the effect of marine isoprene and ship emissions on ozone, using modelling and measurements from the South Atlantic Ocean, Environmental Chemistry, 7, 171, doi:10.1071/EN09154, 2010.

Wingenter, O. W.: Isoprene, Cloud Droplets, and Phytoplankton, Science, 317, 42–43, doi:10.1126/science.317.5834.42b, 2007.

Wingenter, O. W., Haase, K. B., Strutton, P., Friederich, G., Meinardi, S., Blake, D. R., and Rowland, F. S.: Changing concentrations of CO, CH_4, C_5H_8, CH_3Br, CH_3I, and dimethyl sulfide during the Southern Ocean Iron Enrichment Experiments., Proceedings of the National Academy of Sciences of the United States of America, 101, 8537–41, doi: 10.1073/pnas.0402744101, 2004.

Woolfenden, E.: Sorbent-based sampling methods for volatile and semi-volatile organic compounds in air. Part 2. Sorbent selection and other aspects of optimizing air monitoring methods, Journal of Chromatography A, 1217, 2685–2694, doi: 10.1016/j.chroma.2010.01.015, 2010.

Wu, J., Sunda, W., Boyle, E. a., and Karl, D. M.: Phosphate depletion in the western North Atlantic Ocean., Science, 289, 759–762, doi:10.1126/science.289.5480.759, 2000.

Wurl, O., Wurl, E., Miller, L., Johnson, K., and Vagle, S.: Formation and global distribution of sea-surface microlayers, Biogeosciences, 8, 121–135, doi:10.5194/bg-8-121-2011, 2011.

Yang, M., Nightingale, P. D., Beale, R., Liss, P. S., Blomquist, B., and Fairall, C.: Atmospheric deposition of methanol over the Atlantic Ocean., Proceedings of the National Academy of Sciences of the United States of America, 110, 20 034–9, doi: 10.1073/pnas.1317840110, 2013.

Yassaa, N., Peeken, I., Zöllner, E., Bluhm, K., Arnold, S., Spracklen, D., and Williams, J.: Evidence for marine production of monoterpenes, Environmental Chemistry, 5, 391, doi:10.1071/EN08047, 2008.

Yokouchi, Y., Li, H.-j., and Machida, T.: Isoprene in the marine boundary layer (Southeast Asian Sea, eastern Indian Ocean, and Southern Ocean): Comparison with dimethyl sulfide and bromoform, Journal of Geophysical Research, 104, 8067–8076, 1999.

Yuan, J. S., Himanen, S. J., Holopainen, J. K., Chen, F., and Stewart, C. N.: Smelling global climate change: mitigation of function for plant volatile organic compounds, Trends in Ecology and Evolution, 24, 323–331, doi:10.1016/j.tree.2009.01.012, 2009.

Zeng, G., Pyle, J. A., and Young, P. J.: Impact of climate change on tropospheric ozone and its global budgets, Atmospheric Chemistry and Physics, 8, 369–387, doi:10.5194/acp-8-369-2008, 2008.

Zhang, J., Huff Hartz, K. E., Pandis, S. N., and Donahue, N. M.: Secondary organic aerosol formation from limonene Ozonolysis: Homogeneous and heterogeneous influences as a function of NO x, Journal of Physical Chemistry A, 110, 11 053–11 063, doi:10.1021/jp062836f, 2006.

Zindler, C., Peeken, I., Marandino, C. a., and Bange, H. W.: Environmental control on the variability of DMS and DMSP in the Mauritanian upwelling region, Biogeosciences, 9, 1041–1051, doi:10.5194/bg-9-1041-2012, 2012.

Zindler, C., Marandino, C. A., Bange, H. W., Schütte, F., and Saltzman, E. S.: Nutrient availability determines dimethyl sulfide and isoprene distribution in the eastern Atlantic Ocean, Geophysical Research Letters, 41, 3181–3188, doi:10.1002/2014GL059547, 2014.